



TECHNISCHE UNIVERSITÄT MÜNCHEN
FAKULTÄT FÜR CHEMIE
FACHBEREICH ORGANISCHE CHEMIE

**Applications of Dehydrogenative and Borrowing Hydrogen
Catalysis and Investigation of the Menthyl Grignard Reagent for the
Synthesis of Chiral Phosphine Ligands**

Sebastian Koller

Vollständiger Abdruck der von der Fakultät für Chemie der Technischen Universität München zur Erlangung des akademischen Grades eines

Doktors der Naturwissenschaften (Dr. rer. nat.)

genehmigten Dissertation.

Vorsitzender: apl. Prof. Dr. Wolfgang Eisenreich
Prüfer der Dissertation: 1. Prof. Dr. Lukas Hintermann
2. Prof. Dr. Klaus Köhler

Die Dissertation wurde am 10.04.2019 bei der Technischen Universität München eingereicht und durch die Fakultät für Chemie am 28.05.2019 angenommen.

Die vorliegende Arbeit wurde in der Zeit von Dezember 2015 bis März 2019 unter der Leitung von Prof. Dr. Lukas Hintermann im Fachbereich Organische Chemie an der Technischen Universität München angefertigt.

Teile dieser Arbeit wurden veröffentlicht:

S. Koller, M. Blazejak, L. Hintermann, *Eur. J. Org. Chem.* **2018**, 1624–1633.

S. Koller, J. Gatzka, K. M. Wong, P. J. Altmann, A. Pöthig, L. Hintermann, *J. Org. Chem.* **2018**, 83, 15009–15028.

Danksagung

Zunächst möchte ich mich bei Prof. Dr. Lukas Hintermann für die Aufnahme in seinen Arbeitskreis, das spannende Forschungsthema und die exzellente Betreuung inklusive seiner stets nützlichen Tipps und Anregungen bedanken.

Ein großer Dank geht an meine Kollegen Matthias Schreyer, Sebastian Helmbrecht, Philippe Klein und Katja Reinhardt. Sowohl im Labor als auch außerhalb (AK Rumbles, ORCHEM Weimar und Berlin, Ibiza) war es eine unglaublich schöne Zeit mit euch, die ich nie vergessen werde. Bei Matthias möchte ich mich besonders für die vielen nützlichen Ratschläge gerade zu Beginn meiner Arbeit bedanken. Immerhin musste er mich auch lange Zeit als direkter Abzugsnachbar ertragen ;). Außerdem geht mein Dank an die im Rahmen ihrer Masterarbeit beziehungsweise eines Praktikums eher kurzfristigen Kollegen Michael Wiedemann, Corvin Lossin und Anna Gradenegger, die sich toll in unser Team eingefügt haben.

Bei Sabrina Nietsch und Verena Widhopf bedanke ich mich für die kompetente Unterstützung bei allen organisatorischen und bürokratischen Angelegenheiten.

Ein Dankeschön geht an meine Forschungspraktikanten Tim Mollner, Corvin Lossin, Jonas Meringdal, Ingrid Grøssereid und León Stopper für ihre Zusammenarbeit und den Beitrag zu meiner Forschung.

Der Hans-Fischer-Gesellschaft danke ich für den finanziellen Beitrag zu meinen Arbeiten.

Bei den zuständigen TUM-Mitarbeitern für die Kristallstrukturanalyse (inklusive Philippe Klein), Elementaranalyse, Massenspektrometrie und NMR-Routine bedanke ich mich ebenfalls für ihren geleisteten Aufwand.

Der größte Dank geht an meine Eltern Karl und Ilse, sowie den Rest meiner Familie, für ihre großartige Unterstützung. Ohne euch wäre das hier nie möglich gewesen!

Zu guter Letzt gebührt der Dank meinen Freunden – Michael (trotz des S-Bahn Lohhof-Fiaskos), Daniel (wohin geht die nächste Reise?), Dominik (darauf ein Cola-Weißbier) und allen anderen. Ihr ermöglicht es mir, auch mal von der Chemie abzuschalten.

English Abstract

In the field of catalysis research two closely related concepts, namely *acceptorless dehydrogenative coupling* and *borrowing hydrogen*, have been developed in recent years. Their advantage is high atom-economy and non-problematic or even useful byproducts (water, hydrogen), which also provides for the emerging awareness for ecological sustainability in the general public.

Within this work the *borrowing hydrogen* alkylation of pyrroles with primary alcohols as alkylation reagents has been realized by using either base at high temperature in a microwave reactor, a heterogeneous Pd/C catalyst or a homogeneous iridium PNP pincer system (**13**). Aromatic as well as aliphatic alcohols can serve as substrates and a general preference for C2/C5-alkylation was observed.

Pyrrole syntheses by *acceptorless dehydrogenative coupling* have so far been limited to alkyl- or aryl-substituted products. With a ruthenium NNP pincer complex (**10**) as catalyst, the scope could be extended onto pyrroles bearing ester or ketone functionalities. This was achieved in a one-pot procedure starting from β -keto esters or 1,3-diketones and β -amino alcohols. The initial enamine formation is followed by dehydrogenative cyclization to give the desired products. Pyridines are also obtained by this strategy by starting from γ -amino alcohols.

Another part of this thesis was concerned with the development of new chiral catalysts based on *P*-menthyl incorporating phosphorous ligands for application in (asymmetric) catalysis. An in-depth investigation of the chemistry of menthyl Grignard reagent (**30**) was performed. **30** mainly consists of two interconverting epimers (menthylmagnesium chloride (**30a**) and neomenthylmagnesium chloride (**30b**)) which can be kinetically separated by preferential reaction of **30a** with carbon dioxide at -78 °C. This allowed the determination of the epimerization kinetics of the remaining neomenthylmagnesium menthanecarboxylate (**30b'**). The reaction of **30** with various electrophiles was found to proceed either via stereoconvergence ($E^+ = R^1R^2PCl$) or stereoretention ($E^+ = CO_2, H_2O, ROH$) and always with a more or less strong kinetic preference for **30a**.

Deutsche Zusammenfassung

Auf dem Gebiet der Katalyseforschung wurden in den letzten Jahren zwei eng verwandte Konzepte entwickelt, die *akzeptorfreie dehydrierende Kupplung* und *borrowing hydrogen*. Sie sind durch eine hohe Atomökonomie und dem Anfallen unproblematischer bzw. sogar nützlicher Nebenprodukte (Wasser, Wasserstoff) gekennzeichnet und tragen dadurch auch dem in der breiten Öffentlichkeit aufkommenden Bewusstsein für ökologische Nachhaltigkeit Rechnung.

Im Rahmen dieser Arbeit wurde die Alkylierung von Pyrrolen nach dem *borrowing hydrogen* Konzept mit Alkoholen als Alkylierungsmittel realisiert. Dies geschah entweder baseninduziert bei hoher Temperatur in einem Mikrowellenreaktor, mit Palladium auf Aktivkohle als heterogenem Katalysator oder einem homogenen Iridium-PNP-Pincer System (**13**). Sowohl aromatische als auch aliphatische Alkohole sind mögliche Substrate und eine allgemeine Bevorzugung für eine Alkylierung an C2/C5-Position am Pyrrol konnte beobachtet werden.

Pyrrolynsynthesen durch *akzeptorfreie dehydrierende Kupplung* beschränkten sich bislang auf alkyl- und arylsubstituierte Produkte. Mit Hilfe eines Ruthenium-NNP-Pincer Komplexes (**10**) als Katalysator konnte die Bandbreite nun auf Pyrrole mit Ester- oder Ketonfunktionalität ausgedehnt werden. Dies gelang mittels einer Eintopfreaktion ausgehend von β -Ketoestern oder 1,3-Diketonen in Kombination mit β -Aminoalkoholen. Das gewünschte Produkt entsteht dabei über eine Enaminbildung gefolgt von einer dehydrierenden Zyklisierung. Ausgehend von γ -Aminoalkoholen ermöglicht diese Strategie auch den Zugang zu Pyridinen.

Ein weiterer Teil dieser Arbeit beschäftigte sich mit der Entwicklung neuartiger chiraler Katalysatoren auf Basis von Phosphorliganden mit einer *P*-Menthyl-Einheit für die Anwendung in der (asymmetrischen) Katalyse. Im Rahmen dessen wurde die Chemie des Menthylgrignard Reagenzes (**30**) genauer untersucht. Es besteht hauptsächlich aus zwei sich ineinander umwandelnden Epimeren (Menthylmagnesiumchlorid (**30a**) und Neomenthylmagnesiumchlorid (**30b**)), welche durch bevorzugte Reaktion von **30a** mit Kohlenstoffdioxid bei $-78\text{ }^{\circ}\text{C}$ kinetisch gespalten werden können. Dies erlaubte, die Kinetik der Epimerisierung des verbleibenden Neomenthylmagnesiummenthancarboxylats (**30b'**) zu bestimmen. Allgemein verlaufen die Reaktionen von **30** mit Elektrophilen entweder stereokonvergent ($\text{E}^+ = \text{R}^1\text{R}^2\text{PCI}$) oder stereoretentiv ($\text{E}^+ =$

CO₂, H₂O, ROH), aber stets mit einer mehr oder weniger starken kinetischen Präferenz für **30a**.

Table of Contents

Danksagung	iii
English Abstract	iv
Deutsche Zusammenfassung	v
1 Theoretical Background	1
1.1 Catalytic Acceptorless Dehydrogenation – A Contribution to Green Chemistry	1
1.2 Dehydrogenation as Substrate Activation Strategy	6
1.2.1 Catalytic Dehydrogenative Coupling of Alcohols with Nucleophiles	6
1.2.2 The Borrowing Hydrogen Principle	15
1.3 An Introduction to Asymmetric Catalysis	21
2 Aims of this thesis	24
3 Publication Summaries	26
3.1 Catalytic C-alkylation of Pyrroles with Primary Alcohols: Hans Fischer's Alkali and a New Method with Iridium P,N,P-Pincer Complexes	26
3.2 Stereochemistry of the Menthyl Grignard Reagent: Generation, Composition, Dynamics, and Reactions with Electrophiles	28
3.3 Unpublished Results (Manuscript in Preparation): Synthesis of Acceptor-Substituted Pyrroles by Ruthenium-Catalyzed Acceptorless Dehydrogenative Condensation with Amino Alcohols	31
4 Summary and Outlook	33
5 Index of Abbreviations	35
6 References	38
7 Bibliographic Data of Complete Publications	43
7.1 Catalytic C-alkylation of Pyrroles with Primary Alcohols: Hans Fischer's Alkali and a New Method with Iridium P,N,P-Pincer Complexes	43
7.2 Stereochemistry of the Menthyl Grignard Reagent: Generation, Composition, Dynamics, and Reactions with Electrophiles	44
8 Reprint Permissions	45
8.1 Wiley Article	45
8.2 ACS Article	50
9 Appendix – Publication Reprints	51

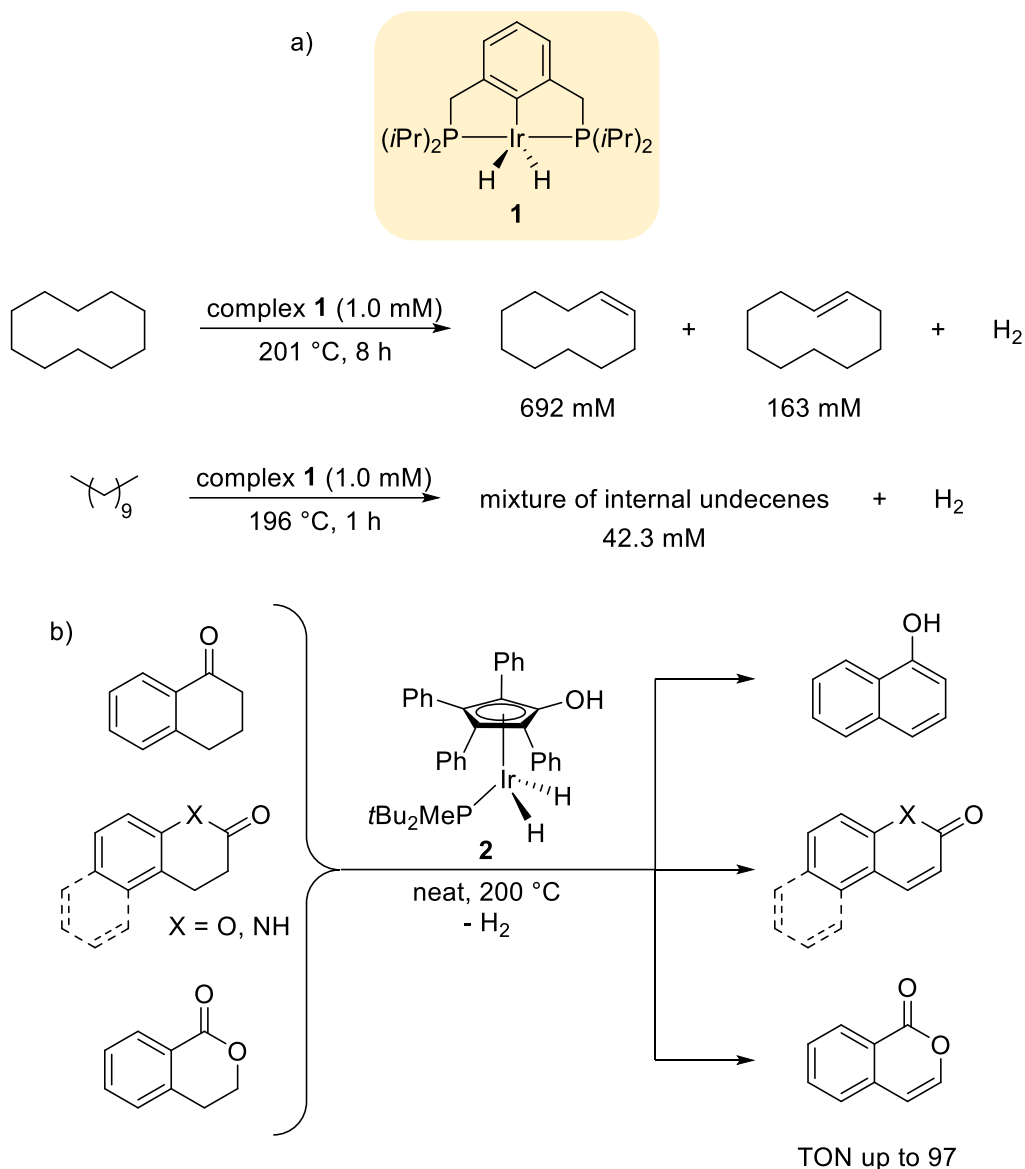
1 Theoretical Background

1.1 Catalytic Acceptorless Dehydrogenation – A Contribution to Green Chemistry

Hydrogenation, the chemical reaction of a compound with hydrogen, is a very important and basic transformation in today's time. The hydrogenation of nitrogen to give ammonia (HABER-BOSCH process), which mainly serves for the production of artificial fertilizers, is responsible for about 2% of the world's commercial energy consumption.^[1] In organic chemistry, addition of hydrogen to alkenes, alkynes, aldehydes, imines etc. is a widely used transformation. Industrial applications include the processing of vegetable oils^[2] or hydrocracking.^[3] In order to activate the otherwise unreactive molecular hydrogen under moderate conditions, the deployment of a catalyst is necessary. One may distinguish between homogeneous and heterogeneous catalysts, depending on whether the catalyst is present in the same phase as the substrate or not. WILKINSON'S $\text{RhCl}(\text{PPh}_3)_3$ ^[4] or CRABTREE'S $[\text{Ir}(\text{cod})(\text{PCy}_3)(\text{py})]\text{PF}_6$ ^[5] are used as catalysts for homogeneous hydrogenation in solution whereas the HABER-BOSCH process relies on a heterogeneous, solid iron catalyst whose substrates and products are present in the gas phase.^[6] In terms of reaction classification, a hydrogenation represents a reduction due to the lowering of the substrate's formal oxidation state. Conversely, the abstraction of hydrogen is considered an oxidation. If this conversion takes place with liberation of free hydrogen gas, it is referred to as *acceptorless dehydrogenation*.^[7] Such catalytic reactions are characterized by the lack of a stoichiometric oxidant or a sacrificial hydrogen acceptor. As a consequence, a drastic reduction of, often toxic, waste is possible. This advantageous feature makes them a valuable contribution to the development of environmentally more benign synthetic methods ('Green Chemistry').^[8] In the following, the oxidative catalytic scission of C–H, N–H and O–H bonds by applying transition metal complexes is discussed.

The endothermic dehydrogenation of alkanes is quite challenging due to their strong non-polar C–H bonds. For this reason, it is unsurprising that only few metal complexes have been reported to exhibit catalytic activity for this transformation. Considering the entropic term of the Gibbs free energy ($-T \cdot \Delta S$), the reaction is favored at high temperatures and therefore requires thermally stable catalysts. Additionally, the solubility of hydrogen in the solvent decreases with increasing temperature, which

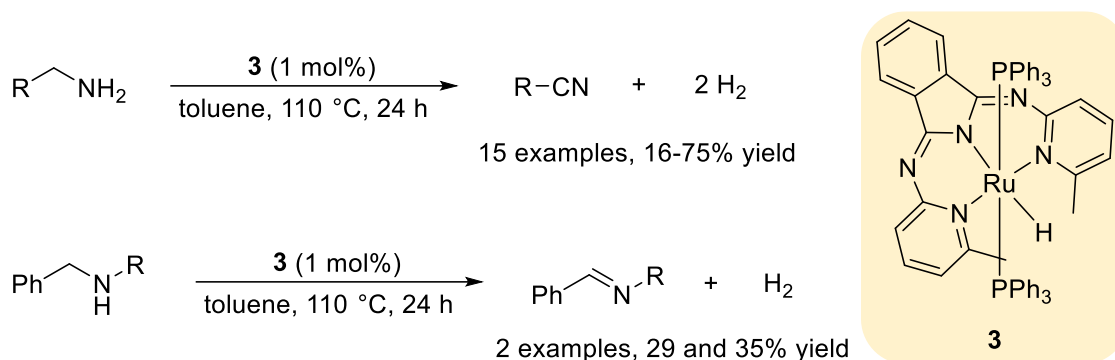
shifts the equilibrium towards the product by efficient removal of H₂ from the reaction medium.^[9] SAITO et al. showed that WILKINSON'S catalyst RhCl(PPh₃)₃ is capable of dehydrogenating cyclooctane to give cyclooctene under reflux conditions (TON = 11.9 after 48 h).^[10] This is remarkable considering that many textbooks present the reductive elimination step in the catalytic cycle for an olefin hydrogenation catalyzed by RhCl(PPh₃)₃ as irreversible. In fact, the rate of the oxidative addition is negligible under typical hydrogenation conditions at room temperature. Besides displaying superior activity than RhCl(PPh₃)₃ in the dehydrogenation of cycloalkanes, the Ir-PCP pincer complex **1** was the first homogeneous catalyst system for dehydrogenation of *n*-alkanes, though at a lower efficiency than with cyclodecane reflecting the higher dehydrogenation enthalpy of linear alkanes (Scheme 1a).^[11] The high thermal stability of **1** has to be emphasized since the reactions are conducted at up to 201 °C. An acceptorless dehydrogenation of HC–CH units adjacent to functional groups was reported by NOZAKI in 2013. He used the hydroxycyclopentadienyl iridium complex **2** as catalyst. Although the substrates in this work appear to be quite activated, the reactions had to be heated to 200 °C resulting in a maximum TON of 97 (Scheme 1b).^[12] [Cp*IrCl₂]₂ was later also found to be active in dehydrogenation of the same kind of substrates at 200 °C. The dehydrogenation of α-tetralone to 1-naphthol was achieved in 71% yield whereas other substrates did not exceed 25%.^[13]



Scheme 1. a) Alkane dehydrogenation by Ir-PCP complex **1**. Cyclodecene was obtained in a *cis/trans*-ratio of 4.2. b) Acceptorless dehydrogenation of activated HC–CH units.

Only few reports have appeared on the oxidative cleavage of N–H bonds by acceptorless dehydrogenation. This might be due to the fact that the resulting imines are good electrophiles which can easily undergo follow-up reactions with another molecule of starting amine (see chapter 1.2.2). SZYMCAK and coworkers reported the selective dehydrogenation of primary and secondary amines to the respective nitriles and imines with liberation of dihydrogen. They used a Ru-NNN hydride complex (**3**) to achieve these transformations under relatively mild conditions (Scheme 2).^[14] For this kind of oxidations, it is not always clear whether the product is formed by direct

CH–NH dehydrogenation or via CH–CH dehydrogenation followed by double-bond isomerization. JENSEN reasoned that a direct C–N dehydrogenation might take place since tertiary amines were not dehydrogenated by a slightly modified version of **3** ($P(tBu)_3$ instead of PPh_3). In addition, a secondary amine with two quaternary carbon atoms in β -position (2,2,2',2'-tetramethyldibutylamine) was successfully dehydrogenated.^[15] In contrast, GOLDMAN could show that the same Ir-complex is in fact able to dehydrogenate tertiary amines to enamines.^[16] Both groups utilized *tert*-butylethylene as sacrificial hydrogen acceptor.



Scheme 2. Acceptorless dehydrogenation of primary and secondary amines by Ru-NNN pincer complex **3**.

For the oxidation of alcohols to aldehydes or ketones, numerous methods have been developed.^[17] Chromium reagents like COLLINS reagent ($CrO_3 \cdot 2 py$) or pyridinium chlorochromate have become less important due to their toxicity. They have largely been replaced by SWERN-oxidation, IBX, Dess-Martin periodinane or catalytic variants with tetrapropyl-ammonium perruthenate (TPAP) or (2,2,6,6-tetramethylpiperidin-1-yl)oxyl (TEMPO), just to name a few. A major drawback of this type of reactions is the need for stoichiometric oxidants and therefore waste production, even in the catalytic versions. TPAP is typically combined with *N*-methylmorpholine *N*-oxide, and sodium hypochlorite is used with TEMPO in order to reoxidize the catalyst. To overcome this disadvantage, several new catalyst systems capable of oxidizing alcohols via acceptorless dehydrogenation have been developed. The ruthenium(II) hydrido borohydride complex **4** bearing a NNP-pincer ligand was synthesized in two steps from $RuCl_2(PPh_3)_3$ and was shown to successfully dehydrogenate secondary alcohols to the corresponding ketones (Figure 1a).^[18] The dehydrogenation of primary alcohols is often problematic as the formed aldehydes can undergo decarbonylation to give an

inactive carbonyl complex. FUJITA and YAMAGUCHI reported Ir-complex **5** to efficiently oxidize primary and secondary alcohols.^[19] The related complex **6** was found to catalyze the reaction in aqueous media (Figure 1b,c).^[20] Complexes **5** and **6** are both believed to act via ligand promotion. More precisely, the 2-hydroxypyridine moiety switches between the protonated species and a deprotonated 2-pyridonate ligand during the catalytic cycle.

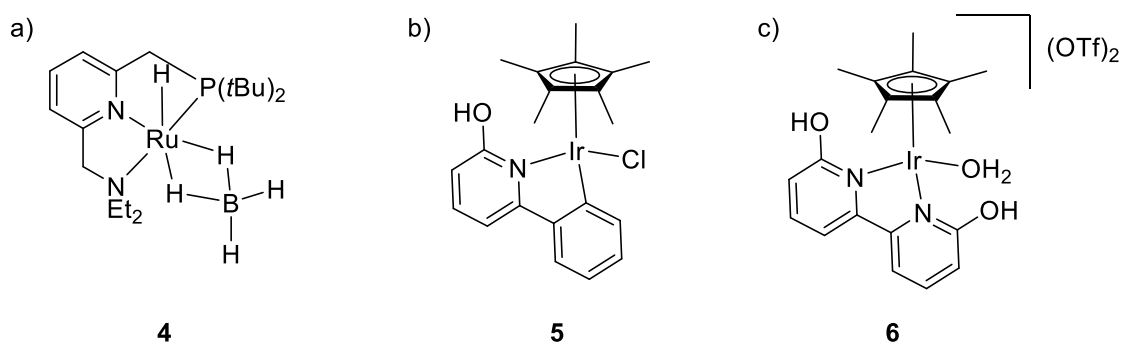
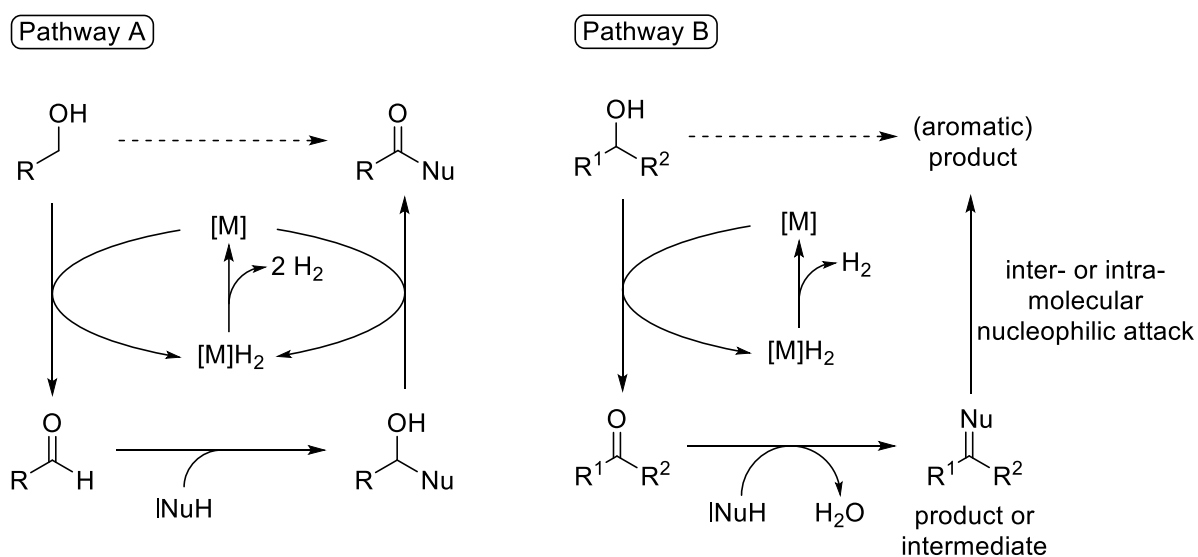


Figure 1. Catalysts for the acceptorless dehydrogenation of alcohols.

1.2 Dehydrogenation as Substrate Activation Strategy

1.2.1 Catalytic Dehydrogenative Coupling of Alcohols with Nucleophiles

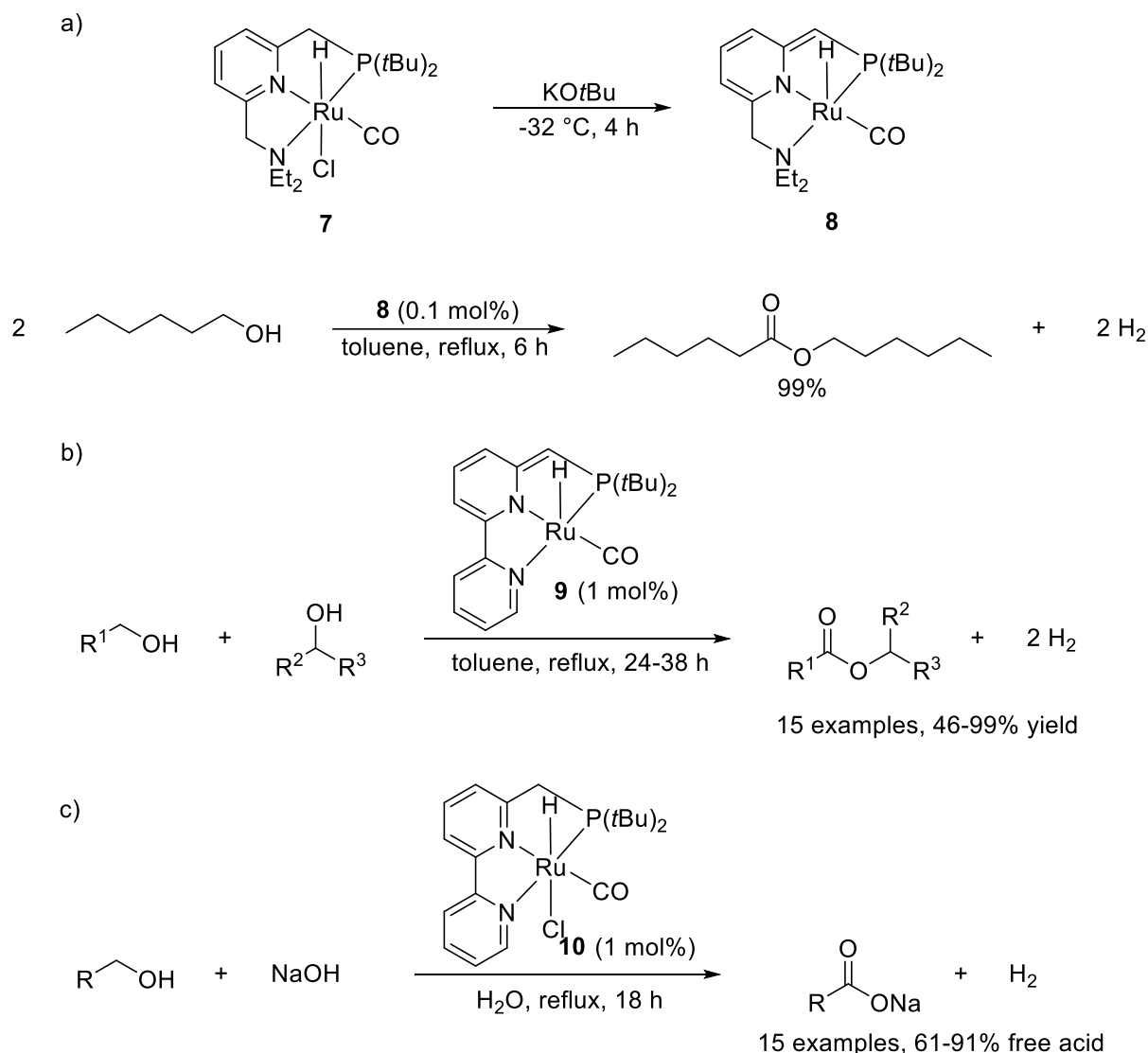
Catalytic dehydrogenative coupling is a synthetic strategy to couple alcohols to nucleophilic reaction partners. The initial alcohol dehydrogenation step yields an electrophilic carbonyl group which can undergo further reactions. The addition of a suitable nucleophile leads to numerous different target structures.^[7] After the nucleophilic attack, there are two general possibilities. Either another equivalent of hydrogen is abstracted to provide acylated nucleophile (Scheme 3, pathway A) or water is eliminated (Scheme 3, pathway B). The latter case can be followed by inter- or intramolecular nucleophilic addition. The intramolecular attack typically generates an aromatic species after further dehydrogenation (see Scheme 7a for more details). An addition of hydrogen acceptors can facilitate the dehydrogenation steps. Considering atom-economy, the abandonment of such additives is favorable.



Scheme 3. Possible pathways for the *acceptorless dehydrogenative coupling* of alcohols.

Typical nucleophiles for pathway A are alcohols (Nu = RO) or amines (Nu = RNH, R¹R²N). With alcohols, the nucleophilic attack generates a hemiacetal which is dehydrogenated to an ester. The first report on this type of reaction appeared in 1981 by MURAHASHI who used RuH₂(PPh₃)₄ (2 mol%) to obtain acyclic esters as well as lactones through intramolecular cyclization of diols. To obtain satisfying yields, a reaction temperature of 180 °C was necessary.^[21] The group of MILSTEIN found that

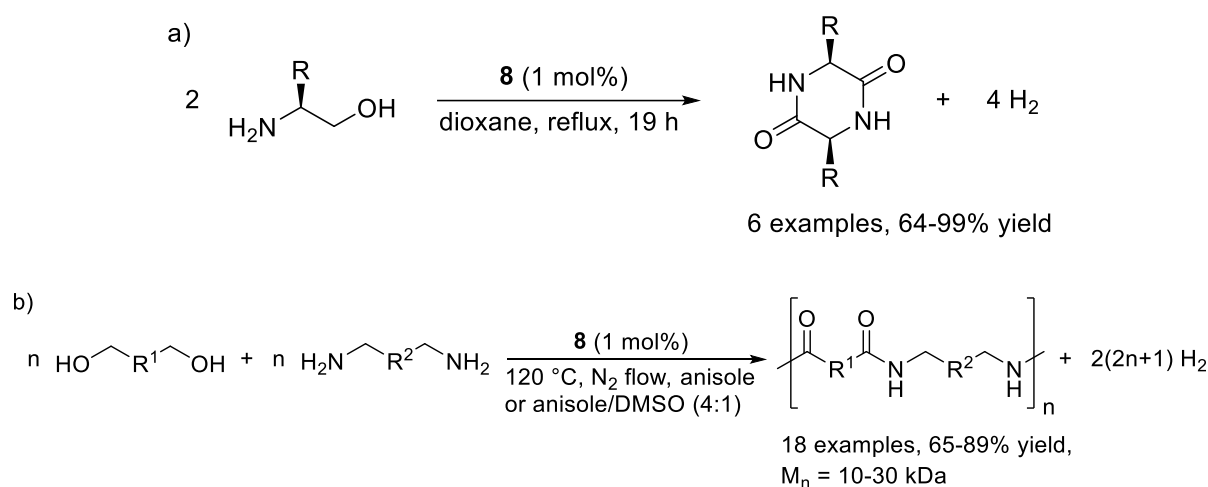
Ru-NNP pincer **7** in combination with catalytic amounts of base is a more active catalyst system. Further investigations showed that deprotonation of **7** gives **8**. **8** is able to couple alcohols without the need for additional base at very low loading. It has to be emphasized that deprotonation of **7** takes place at the benzylic position of the pincer ligand and not as might have been expected at the hydride ligand (Scheme 4a).^[22] An obvious disadvantage of this method concerns product selectivity because a combination of two different primary alcohols is expected to give a mixture of four possible products. For the case of primary plus secondary alcohol, the problem could be solved by the use of Ru-NNP complex **9** resulting in a single cross-ester product. Dehydrogenation of the primary alcohol is faster due to steric reasons and homocoupling only occurred in small amounts. Complex **9** is closely related to **8** and bears a bipyridine moiety (Scheme 4b).^[23] Similar to **8**, **9** can be prepared from **10** by reaction with strong base. The precursor **10** was found to catalyze the *acceptorless dehydrogenative coupling* of alcohols and water. The reaction is operated in basic media and yields carboxylic acid salts which upon acidification give the free carboxylic acids (Scheme 4c).^[24]



Scheme 4. a) *Dehydrogenative homocoupling* of primary alcohols to esters. This reaction can be performed with **8** or base + precursor complex **7**. b) *Dehydrogenative Coupling* of primary and secondary alcohols. c) Carboxylic acids from alcohols and hydroxide.

With amine nucleophiles, a dehydrogenative acylation following pathway A via a hemiaminal allows the synthesis of amides. Those are a very important substrate class especially for biochemical applications. This alternative approach to amide synthesis avoids the use of coupling reagents, which are usually required for carboxylic acid activation prior to reaction with an amine.^[25] Complex **8** efficiently catalyzes the process at a loading of only 0.1 mol% in refluxing toluene. The scope is limited to primary amines.^[26] Chiral β -amino alcohols react to cyclic dipeptides with retention of configuration, an attribute of the neutral reaction conditions (Scheme 5a). The

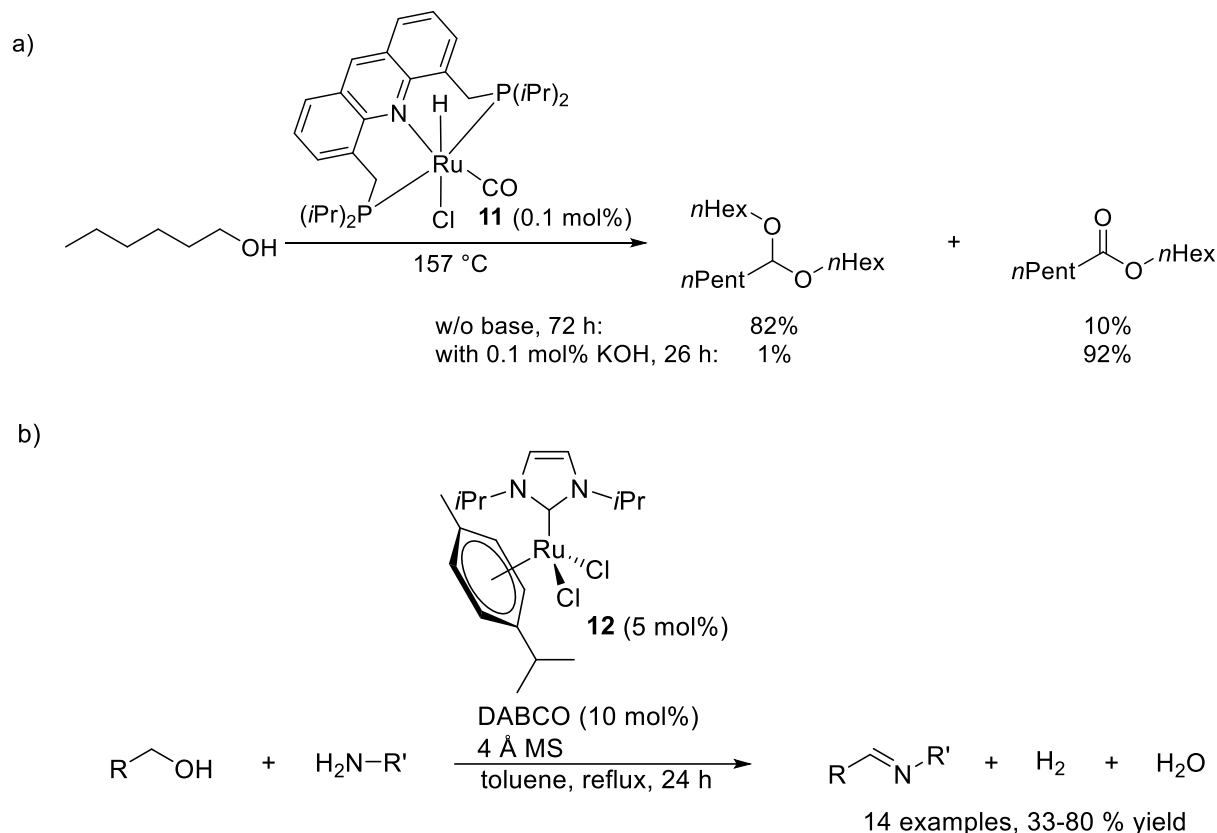
substituent in α -position to the amine has to be larger than a methyl, otherwise oligopeptides are formed.^[27] Starting from secondary amines, a modified version of **10** (Ph instead of *t*Bu at phosphorous) together with base^[28] or an Fe-PNP complex^[29] can be applied for the synthesis of tertiary amides. Methanol as the alcohol compound provides access to urea derivatives, probably via a formamide intermediate.^[30] A direct synthesis of polyamides via catalytic acceptorless dehydrogenation of diols and diamines with **8** was found to give the resulting polymers in an average molecular weight range of about 10-30 kDa (Scheme 5b).^[31]



Scheme 5. Ruthenium pincer catalyzed dehydrogenative synthesis of amides. a) Cyclic dipeptides from β -amino alcohols under retention of configuration. b) Polyamides from diols and diamines.

The two general pathways of dehydrogenative alcohol coupling (see Scheme 3) are often competing depending on the relative kinetics of a second dehydrogenation step versus dehydration of the intermediate. By tuning the reaction conditions, it is possible to switch between both possible products, even with the same catalyst. The acridine based Ru-PNP pincer complex **11** was shown to convert alcohols into esters in the presence of base. Without base, an acetal is obtained (Scheme 6a). The hemiacetal which is formed by nucleophilic attack of the alcohol on aldehyde presumably eliminates water to give an enol ether. Upon addition of another molecule of alcohol to the C–C double bond, acetal is formed.^[32] With amine nucleophiles, an even broader range of products has been obtained. The simplest ones are imines resulting from dehydration of the hemiaminal intermediate. Amongst others, the ruthenium *N*-

heterocyclic carbene complex **12** catalyzes this transformation at a loading of 5 mol% with DABCO as base (Scheme 6b).^[33]



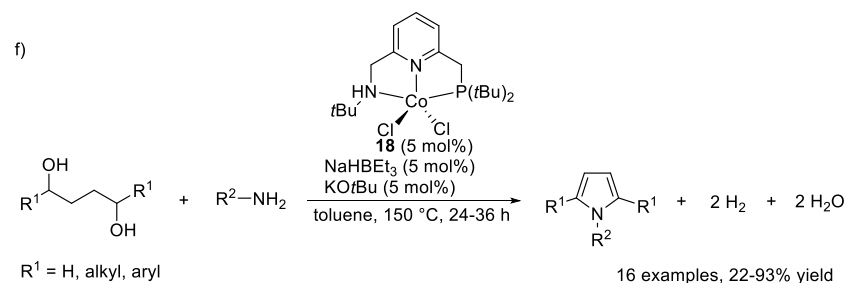
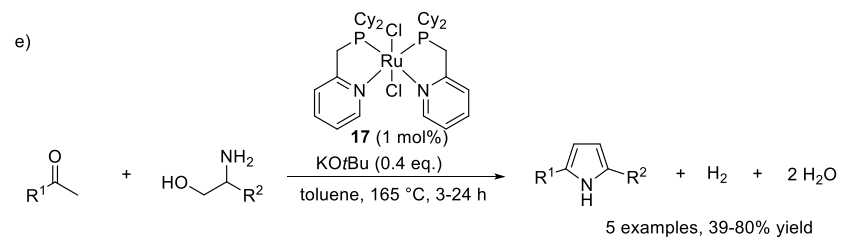
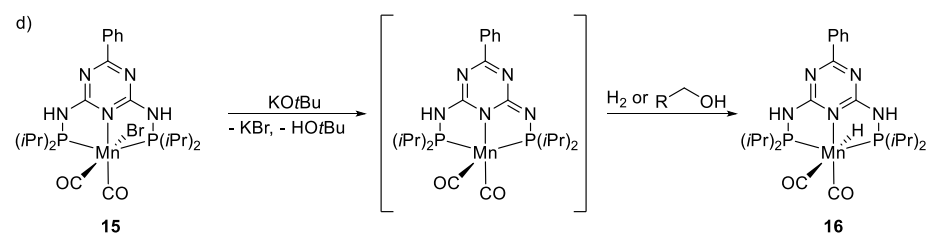
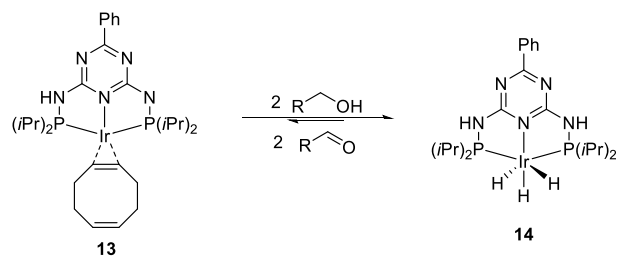
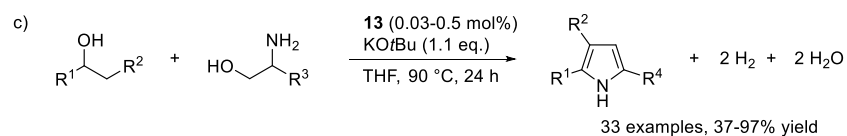
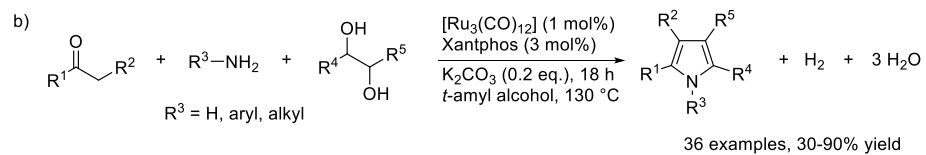
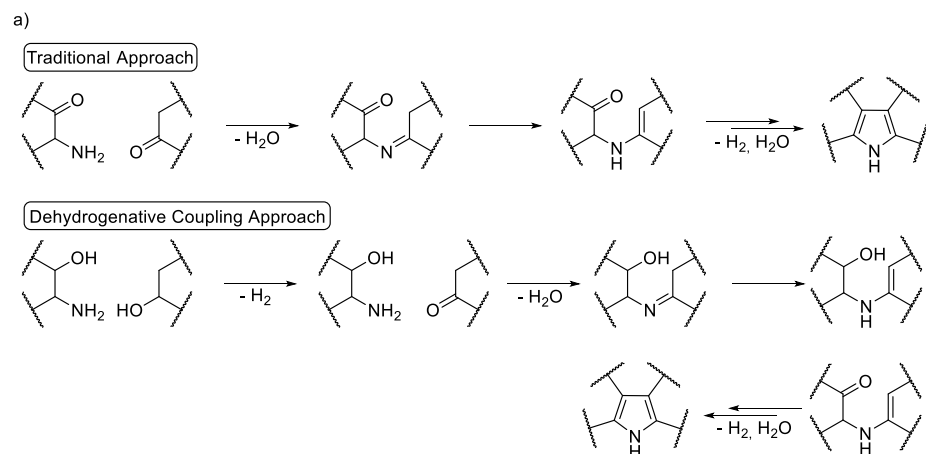
Scheme 6. a) Switch in product selectivity from acetals to esters by addition of potassium hydroxide in the *dehydrogenative coupling* of alcohols. b) Imine formation via *dehydrogenative coupling* of alcohols and amines.

Potentially more important for synthesis, the generated imines open up pathways to a large variety of *N*-heterocycles by reaction with a second functional group within the substrate. In the field of *acceptorless dehydrogenative coupling*, the synthesis of pyrroles, a structural motif found in many pharmaceuticals and natural products,^[34] has probably been the best explored. The new strategy differs from traditional approaches (e.g. Knorr pyrrole synthesis) in the oxidation level of the substrates. Carbonyl groups are replaced by alcohols that are oxidized in situ before condensation takes place (Scheme 7a). The group of BELLER described a three-component reaction with ketones, amines and diols yielding various classes of multiple substituted pyrroles. The commercially available $\text{Ru}_3(\text{CO})_{12}$ /Xantphos system efficiently catalyzed this reaction in the presence of co-catalytic amounts of weak base (K_2CO_3) (Scheme 7b). The

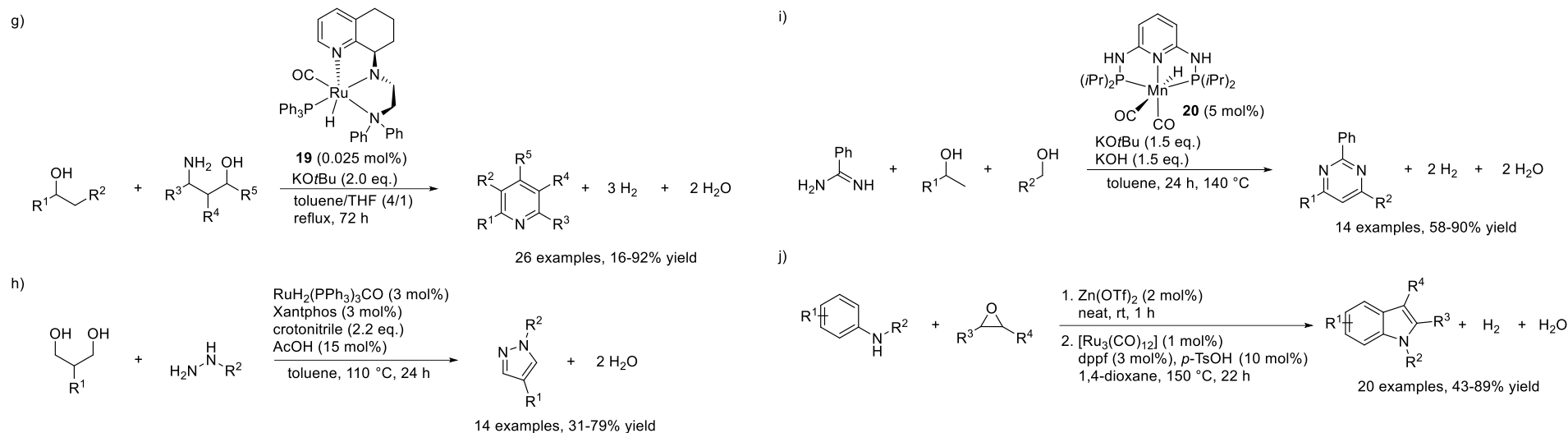
transformation also proceeds smoothly, if ammonia is used instead of amines.^[35] KEMPE reported a dehydrogenative pyrrole synthesis starting from secondary alcohols and amino alcohols using an iridium complex of an anionic PNP pincer ligand (**13**) as catalyst in the presence of stoichiometric amounts of a strong base (KO^tBu). An advantage of this procedure is the remarkably low catalyst loading, which varies between 0.03 and 0.5 mol% depending on substrates. An iridium(III) trihydride (**14**) species generated by twofold alcohol dehydrogenation was identified as catalyst resting state (Scheme 7c).^[36] Later it was found that iridium can be replaced by the more abundantly available transition metal manganese. The Mn-PNP pincer **15** is converted into its catalytically active hydride species **16** by base-induced salt elimination followed by either addition of hydrogen or alcohol dehydrogenation (Scheme 7d). Complex **16** was characterized by NMR spectroscopy and X-ray crystallography. Cobalt and iron based complexes of the same class of pincer ligands were inactive.^[37] The active role of the pincer ligand in complexes **13** and **15** is comparable to that of the ligand in the earlier mentioned Ru-NNP species (**7-10**) (see Scheme 4). A similar route to pyrroles from ketones and amino alcohols was reported by SAITO. Here, only one equivalent of dihydrogen is released in the course of the reaction. A ruthenium complex (**17**) and alkali base enable the reaction at rather high temperature (Scheme 7e).^[38] Another strategy for the dehydrogenative synthesis of *N*-substituted pyrroles is the coupling of 1,4-diols and amines. Literature reports include approaches with ruthenium,^[39] manganese^[40] and cobalt^[41] catalysts (Scheme 7f). The active cobalt species is generated from **18** with NaHBET₃ and KO^tBu, which act as hydride source and base, respectively. It is noteworthy that all of the above mentioned syntheses exclusively afford donor-substituted (alkyl, aryl) pyrroles. Complexes **13**^[42] (with a *para*-trifluoromethylphenyl group at C-4 of the triazine ligand) and **10**^[43] were also used for the annulation of secondary alcohols and γ -amino alcohols to pyridines. SUN described a highly active ruthenium catalyst (**19**) which achieved similar yields at a loading of only 0.025 mol% (Scheme 7g).^[44] A combination of 1,3-diols and alkyl hydrazines served as starting material for the synthesis of pyrazoles in the presence of RuH₂(PPh₃)₃CO, Xantphos, crotonitrile and acetic acid (Scheme 7h). Crotonitrile is a sacrificial hydrogen acceptor, rendering this approach less efficient in terms of atom economy. The role of the acid additive may lie in accelerating condensation steps.^[45] This contrasts with afore mentioned systems, which benefit from either co-catalytic or stoichiometric amounts of base. Iridium^[46] as well as manganese^[47] based pincer

complex catalysts were found to be suitable for pyrimidine syntheses from amidines and up to three different alcohols as substrates in one pot. In Scheme 7i, a three-component reaction with a hydride manganese(I) PNP pincer (**20**) introduced by KIRCHNER is depicted exemplarily.^[48] It remains unclear, why a mixture of two bases (potassium *tert*-butoxide and potassium hydroxide) is necessary to obtain good yields. BELLER and coworkers showed that indoles can be prepared from anilines and cyclohexene epoxide in the presence of a catalyst system composed of [Ru₃(CO)₁₂], dppf and catalytic amounts of *p*-toluenesulfonic acid. The reaction proceeds via acid catalyzed epoxide opening towards a β -amino alcohol, ketone formation by alcohol dehydrogenation and subsequent intramolecular cyclization. However, numerous side products were observed when other epoxides than cyclohexene epoxide were tested. An incompatibility of the epoxide opening step with the strongly acidic conditions was proved. Therefore, the aminolysis of the epoxide was performed with zinc triflate as Lewis acid prior to addition of the other reagents. The regioselectivity depends on preferential stabilization of the carbocationic character by R³ versus R⁴ in the epoxide opening step and was >90:10 (regioisomeric ratio) in most cases (Scheme 7j).^[49] Other heterocycles such as benzimidazoles,^[50] pyrazines^[27,51] or quinolines^[52] can be prepared by analogous strategies to the discussed ones.

N-Heterocycles via Acceptorless Dehydrogenative Coupling (1)



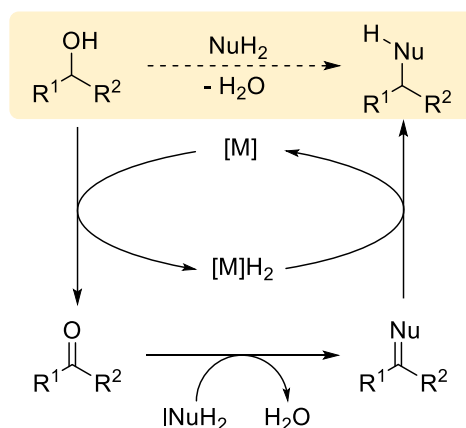
N-Heterocycles via Acceptorless Dehydrogenative Coupling (2)



Scheme 7. Overview over the construction of *N*-heterocycles via *acceptorless dehydrogenative coupling*. a) Schematic comparison between a classical approach towards *N*-heterocycles (here: pyrroles) and the new *dehydrogenative coupling* strategy. b) Three-component synthesis of pyrroles with a [Ru₃(CO)₁₂]/Xantphos system. c) Pyrrole synthesis from secondary alcohols and β -amino alcohols with Ir-PNP pincer **13** and formation of the iridium(III) trihydride resting state **14**. d) Conversion of Mn-PNP pincer **15**, which is also able to catalyze the reaction depicted in b), into its catalytically active species **16**. e) Pyrrole formation from ketones and β -amino alcohols with a ruthenium catalyst (**17**) under relatively high temperature. f) Cobalt catalyzed dehydrogenative condensation of 1,4-diols and amines to *N*-substituted pyrroles. g) Coupling of secondary alcohols and γ -amino alcohols towards pyridines with a highly active ruthenium complex (**19**) at very low catalyst loading. h) Example of a non-acceptorless dehydrogenative pyrazole synthesis from alkyl hydrazines and 1,3-diols. i) Pyrimidines by a three-component Mn-PNP pincer (**20**) catalyzed process with a combination of different bases. j) Synthesis of indoles from epoxides and arylamines. The Lewis acid catalyzed epoxide opening is followed by a ruthenium catalyzed alcohol dehydrogenation and Brønsted acid catalyzed intramolecular cyclization.

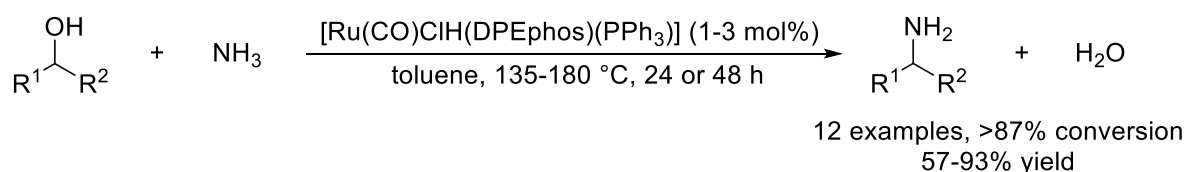
1.2.2 The Borrowing Hydrogen Principle

In the previous chapters the discussion was limited to reactions with liberation of hydrogen or its transfer onto a sacrificial acceptor. Since the metal hydride species generated in the initial dehydrogenation step may potentially hydrogenate a suitable acceptor, a new field of possible transformations is opened up. If this acceptor molecule is an intermediate in the catalytic cycle and formed from dehydrogenated starting material in a follow-up step, the whole process is called *borrowing hydrogen* reaction since the hydrogen 'borrowed' in the first step is 'returned' into the catalytic cycle later. The term *hydrogen autotransfer* (HAT) is often used as an alternative description for the same concept.^[53] Typically, the catalytic oxidation of an alcohol to the corresponding carbonyl compound is followed by spontaneous or base-mediated condensation with a suitable nucleophile. Final hydrogenation of the unsaturated species by the metal hydride gives the product and regenerates the catalyst (Scheme 8). The whole process is redox-neutral and can be described as alkylation of a nucleophile with an alcohol, whose reactivity is switched from O-nucleophile to C-electrophile. Water is the only by-product rendering this process highly atom-economic and environmentally friendly, especially in comparison to traditional alkylation methods that use toxic alkyl halides and generate inorganic halide salts as waste in stoichiometric amounts. Depending on the nucleophile, C–C or C–N bond formation is achieved. The obvious similarity of a *borrowing hydrogen* process and a *dehydrogenative coupling* (see Scheme 3) may lead to selectivity problems in the development of new transformations since the hydrogenation step competes against addition of another nucleophile.



Scheme 8. Reaction scheme (highlighted) and catalytic cycle of a *borrowing hydrogen* process.

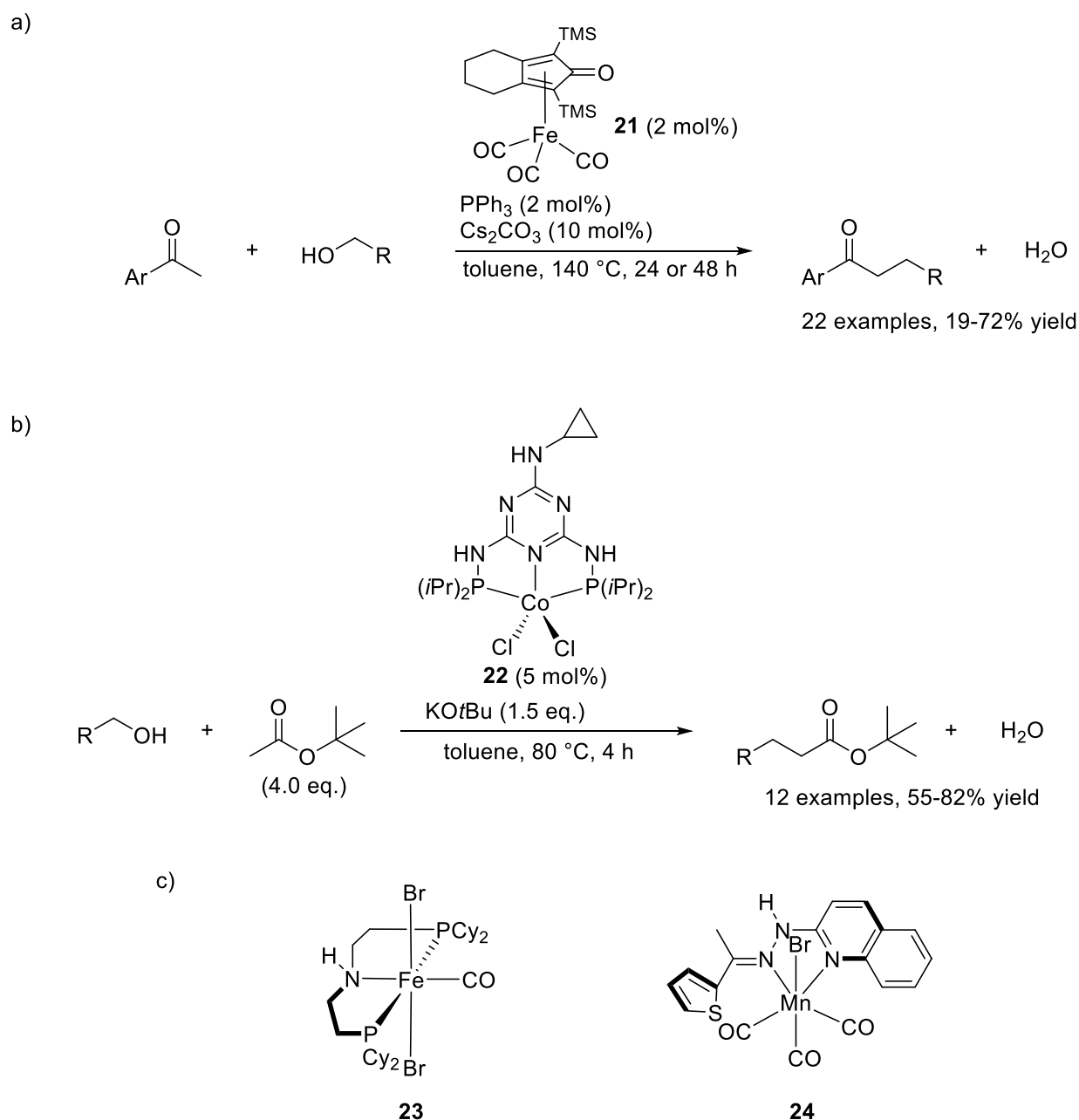
The earliest reports on alcohols as alkylating agents might go back to GUERBET in 1899, who described the synthesis of β -alkylated primary alcohols from primary or secondary alcohols in the presence of alkali hydroxides or alkoxides. The reaction proceeds via dehydrogenation, aldol dimerization and transfer hydrogenation and can be accelerated by addition of a (typically heterogeneous) hydrogen transfer catalyst.^[54] Numerous reports on the HAT-alkylation of various substrates can be found in the literature over the past 20-30 years. Already in 1984 WATANABE reported the catalytic *N*-alkylation of anilines with alcohols and $\text{RuCl}_2(\text{PPh}_3)_3$ at 150-180 °C. In most cases bisalkylation was favored.^[55] A progress in ligand design has led to more active catalyst systems: a combination of $[\text{Ru}(p\text{-cymene})\text{Cl}_2]_2$ with a bidentate phosphine (dppf or DPEphos) allows the selective and high-yielding conversion of primary amines into secondary amines, of secondary amines into tertiary amines, and the use of secondary alcohols as alkylating agent.^[56] For the challenging monoalkylation of ammonia a convenient method with $[\text{Ru}(\text{CO})\text{Cl}(\text{DPEphos})(\text{PPh}_3)]$ as catalyst was introduced by DEUTSCH. It shows reasonable selectivity for monoalkylation despite the high reaction temperatures (Scheme 9).^[57]



Scheme 9. HAT-monoalkylation of ammonia.

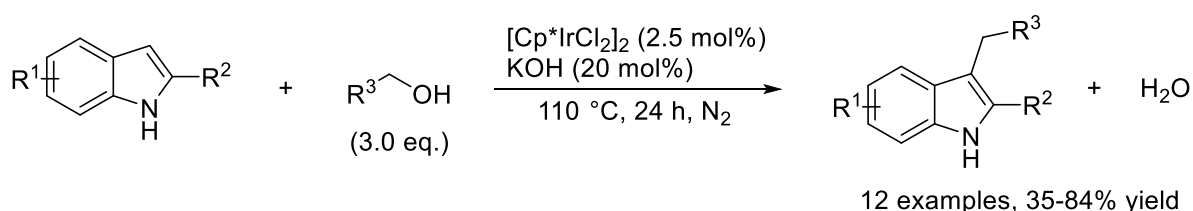
The alkylation of $\text{C}(\text{sp}^3)\text{-H}$ centers relies on the acidity of the corresponding CH -position. Therefore, activation by electron-withdrawing π -acceptor groups is required. HAT-alkylation of ketones is rather simple since its $\alpha\text{-C-H}$ bonds are strongly activated.^[58] Recently, special efforts were directed to the substitution of noble metals like iridium and ruthenium by widely-abundant first row transition metals. In 2015, a ketone α -alkylation with primary alcohols catalyzed by a KNÖLKER-type iron complex (**21**) in presence of cesium carbonate as base was published. However, the ketone scope was limited to arylalkylketones (Scheme 10a).^[59] Less activated substrates like esters or amides are *C*-alkylated by cobalt PNP pincer complex **22** as catalyst. The scope is limited to *tert*-butyl acetate and *N,N*-dialkylacetamides as CH -acidic substrates, probably due to effects of steric hindrance and to prevent

transesterifications.^[60] Scheme 10b illustrates the rather mild conditions (80 °C, short reaction time) for the ester alkylation. The α -alkylation of nitriles serves as another good example for the replacement of noble metals by first row transition metals: whereas earlier works described iridium,^[61] rhodium,^[62] palladium,^[63] ruthenium^[64] and an unusual osmium^[65] catalyst system, iron PNP pincer catalyst **23**^[66] as well as manganese complex **24**^[67] were introduced for this transformation in 2018 (Scheme 10c).



Scheme 10. First row transition metals in *borrowing hydrogen* alkylations. a) Iron catalyzed HAT-alkylation of ketones. b) Cobalt catalyzed α -alkylation of esters. c) New first row transition metal catalysts for the HAT-alkylation of nitriles.

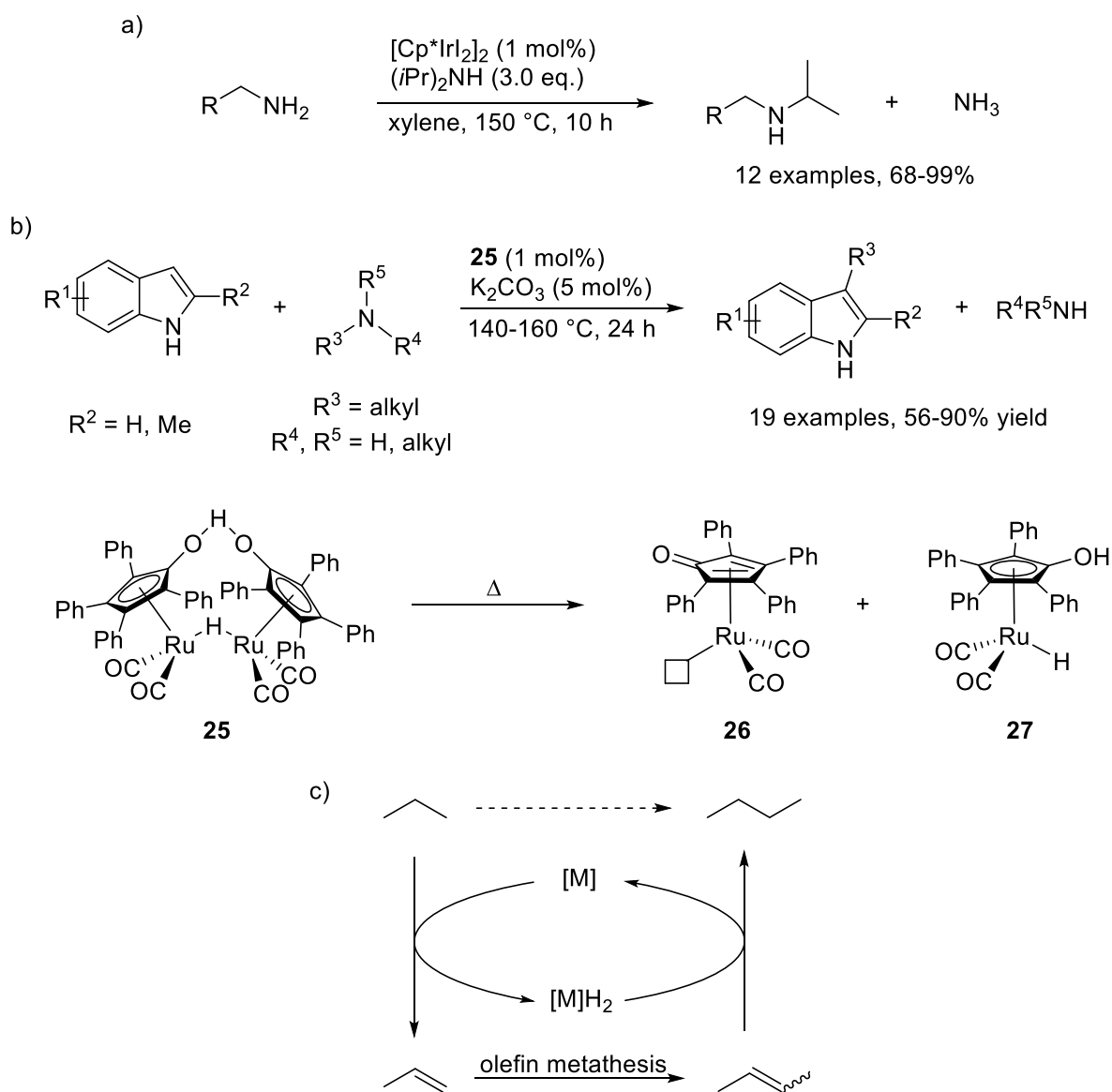
Alkylation reactions with alcohols as alkyl donors are not restricted to C(sp³) centers. They also occur at C(sp²)-H centers of electron-rich arenes. The regioselective indole C3-alkylation was achieved under basic conditions by homogeneous ([Cp*IrCl₂]₂,^[68] RuCl₂(PPh₃)₂ + DPEphos^[69]) as well as heterogeneous (Pd/C,^[69] Pt nanoclusters^[70]) catalyst systems (Scheme 11). Interestingly, RAMÓN et al. reported that this alkylation is also possible without using transition metal catalyst, under alkaline conditions at elevated levels of temperature (150 °C).^[71] The hydride transfer in this multi-step process might occur by a Cannizzaro-type mechanism. With [Cp*IrCl₂]₂ as catalyst, the regioselective C4-alkylation of phenols, more precisely of 2,6-di-*tert*-butylphenol could be performed. Subsequent removal of the *tert*-butyl groups under retro-FRIEDEL-CRAFTS conditions led to various 4-alkyl phenols.^[72]



Scheme 11. Iridium catalyzed C-3 indole alkylation via hydrogen autotransfer.

Borrowing hydrogen is not restricted to alcohols as substrates for the dehydrogenation step. Amines and alkanes are also prone to activation by dehydrogenation. Mechanistically, the *N*-alkylation of an amine by another amine is similar to the alkylation with alcohols (see Scheme 8). Initial dehydrogenation gives an imine, which after nucleophilic attack by an amine liberates ammonia (transimination). The newly generated imine is then hydrogenated to the desired product. The coupling of two oxidizable amines RNH₂ and R'NH₂ generally leads to a product mixture including R₂NH, RR'NH and R'₂NH. In 2009 WILLIAMS reported the first example for a selective amine cross-alkylation starting from two oxidizable amines. The key for success was the formation of secondary amines containing one branched and one unbranched substituent, which are sterically favored over amines with two branched substituents due to less steric strain. Additionally, dehydrogenation of secondary amines is easier. The reaction is catalyzed by [Cp*IrI₂]₂ in the absence of additional base, and diisopropylamine was used as alkyl donor (Scheme 12a).^[73] The regioselective C3-alkylation of indoles with amines was discovered by BELLER and coworkers. They found

that a combination of Shvo's catalyst (**25**) and potassium carbonate allows the reaction with a broad range of aliphatic amines including primary, secondary and even tertiary ones. The latter forms an iminium ion in the first step of the *borrowing hydrogen* mechanism. At the applied high temperature, catalyst **25** dissociates into two active species. The dehydrogenation is catalyzed by the 16 electron complex **26**, whereas the 18 electron ruthenium hydride species **27** catalyzes the hydrogenation (Scheme 12b).^[74] The application of alkane substrates in *borrowing hydrogen* processes is rather limited because of the difficult activation of their strong non-polar C–H-bonds (see chapter 1.1). One of the rare examples of homogeneous catalysis was introduced by the BROOKHART group. They realized a catalytic alkane metathesis by tandem alkane dehydrogenation–olefin metathesis (Scheme 12c). To this aim, an iridium complex for hydrogen transfer and a molybdenum based Schrock carben catalyst for olefin metathesis were combined.^[75] However, the general focus in the field of alkane metathesis is more on heterogeneous than on homogeneous systems.^[53]



Scheme 12. Amines and alkanes as alkylation reagents in *borrowing hydrogen* processes. a) Cross-coupling of two oxidizable amines. b) Regioselective C3-indole alkylation with amines and thermal activation of the Shvo catalyst **25** generating two active species **26** and **27**. c) Catalytic cycle for a *borrowing hydrogen* alkane metathesis.

1.3 An Introduction to Asymmetric Catalysis

“I call any geometrical figure, or group of points, *chiral*, and say that it has chirality, if its image in a plane mirror, ideally realized, cannot be brought to coincide with itself.”^[76] With this sentence, Lord Kelvin named a phenomenon of great importance not only, but especially in chemistry. An example for chirality in everyday life is the left and the right hand. In chemistry the most common form is point chirality. For organic molecules, it originates from an atom bearing four different substituents. However, such a stereogenic atom is not a necessary requirement. Other possible forms are axial, planar or inherent chirality (Figure 2). Stereoisomers which are mirror images of each other are called enantiomers.

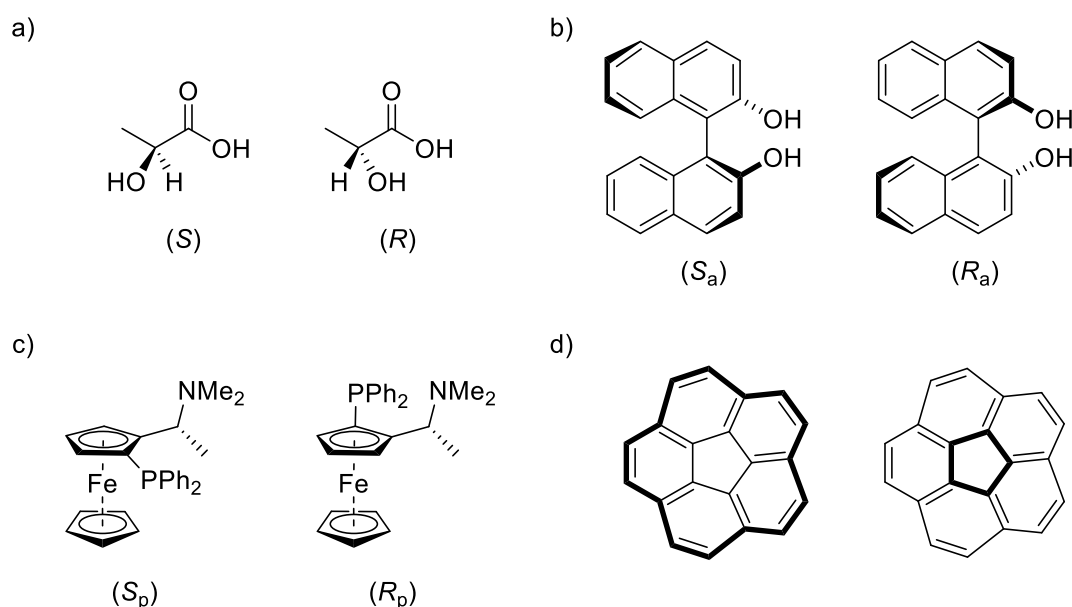
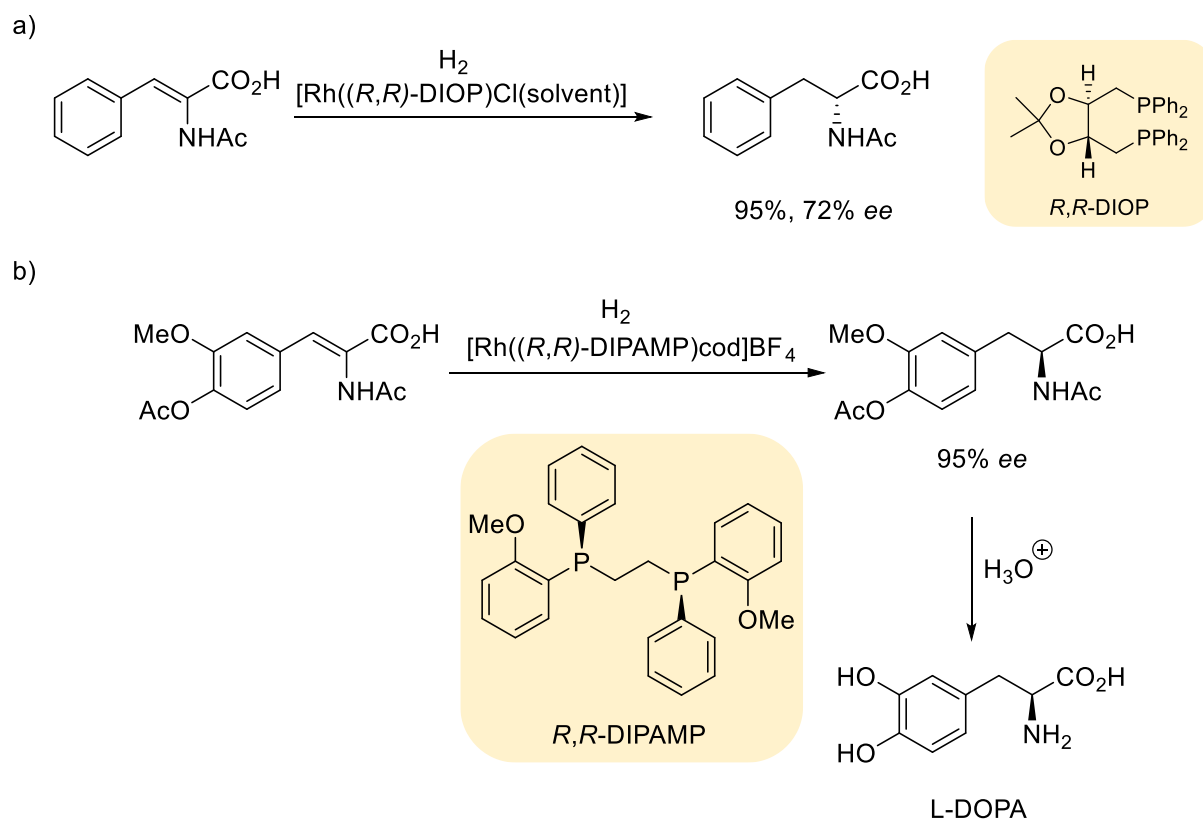


Figure 2. Different forms of chirality. a) (*S*)- and (*R*)-lactic acid as an example for point chirality. b) Axial chirality of BINOL arising from the rotation barrier around the naphthyl-naphthyl-bond. c) Planar chirality in a ferrocene system. d) Corannulene exhibits inherent chirality, but interconverts fast at room temperature.^[77]

In nature, only one of the two possible enantiomers of a molecule is usually produced by a certain organism since enantiomers can differ largely in terms of biological activity. Therefore, organic synthesis must also provide methods to selectively access single enantiomers. The first examples for asymmetric catalysis were reported in the early 20th century. In 1913 BREDIG realized a cyanohydrin formation using cinchona alkaloids as catalysts.^[78] The probably first description of an asymmetric organometallic

catalysis not related to polymer chemistry was done by NOYORI et al. in 1966. They performed the cyclopropanation of alkenes with a chiral copper chelate complex resulting in 6% enantiomeric excess.^[79] However, for broader applicability and high enantioselectivities the development of new synthetic organic ligands was crucial. A milestone in the field of hydrogenation reactions was achieved with the replacement of monodentate phosphines that were chiral at the phosphorous atom, by chelating diphosphine ligands bearing chirality in the ligand backbone. The first example for this new class of ligands was KAGAN's C₂-symmetric DIOP, which is based on enantiopure tartaric acid and is chiral in the backbone. With a rhodium(I)-DIOP system the hydrogenation of α -acetamidocinnamic acid gave the product in 72% ee (Scheme 13a).^[80] The origin of chirality does not necessarily have to be placed into the ligand backbone, as shown by the famous DIPAMP ligand, where the two chirally modified phosphorous atoms are connected by an ethylene bridge. This ligand was notably used in the industrial synthesis of L-DOPA, a non-proteinogenic amino acid used for the treatment of Parkinson's disease (Scheme 13b).^[81]



Scheme 13. a) KAGAN's Rh(I)-DIOP catalyzed hydrogenation of α -acetamidocinnamic acid. b) Asymmetric catalytic hydrogenation as key step in the synthesis of L-DOPA.

The enantioselectivity of a certain reaction is determined by the energy difference $\Delta\Delta G^\ddagger$ between its two diastereomorphous transition states. Since already fairly small energy differences lead to significant selectivity changes, finding a suitable catalyst system is mostly a trial and error approach.¹ Minor changes of the ligand structure can lead to unpredictable outcomes. To deal with this challenge, chemists have come up with a multitude of chiral ligand structures that can be tested in screenings towards more active and selective catalyst systems. It is an important requirement that the chiral ligand is provided in stereoisomerically pure form since contamination with other stereoisomers might reduce the selectivity of the resulting catalyst. Thus small molecules which are obtained from natural sources in enantiomerically pure form and in sufficient amounts are widely used feedstocks (figure 3).

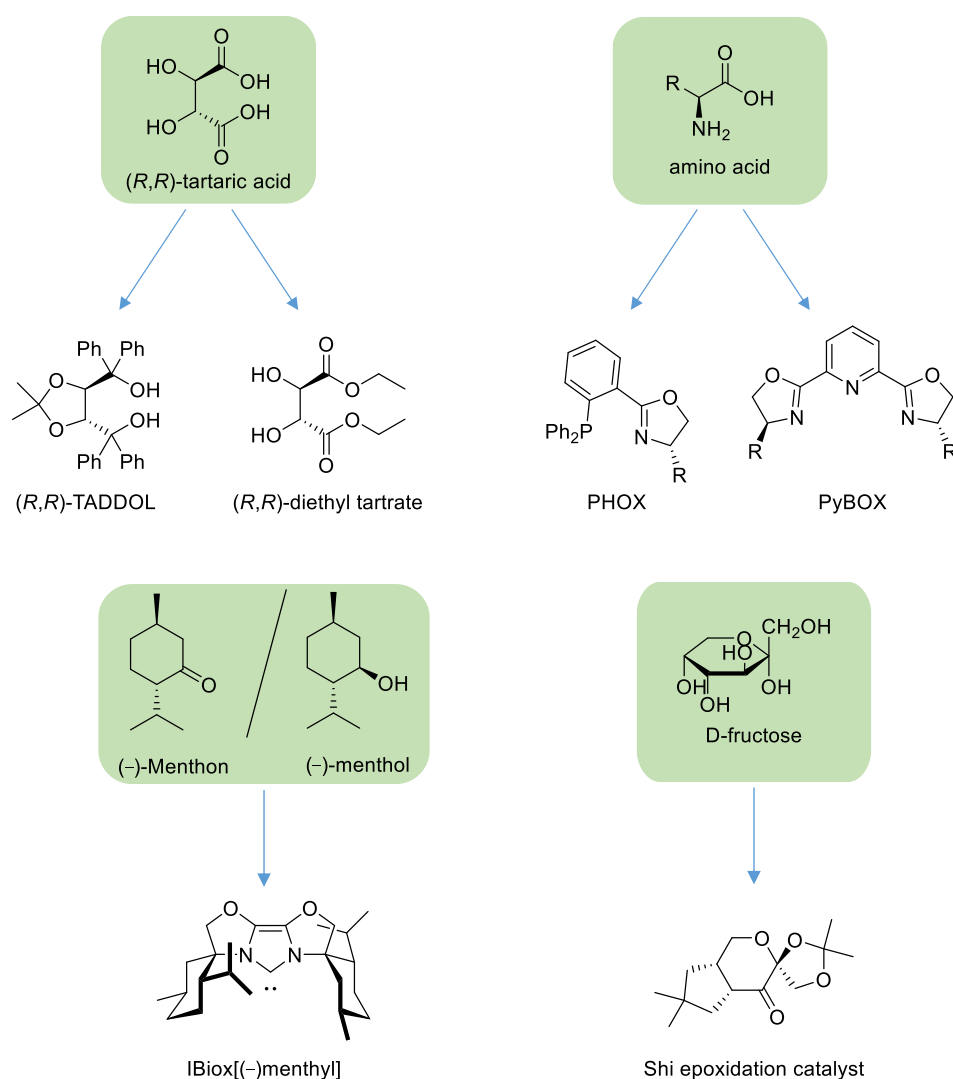


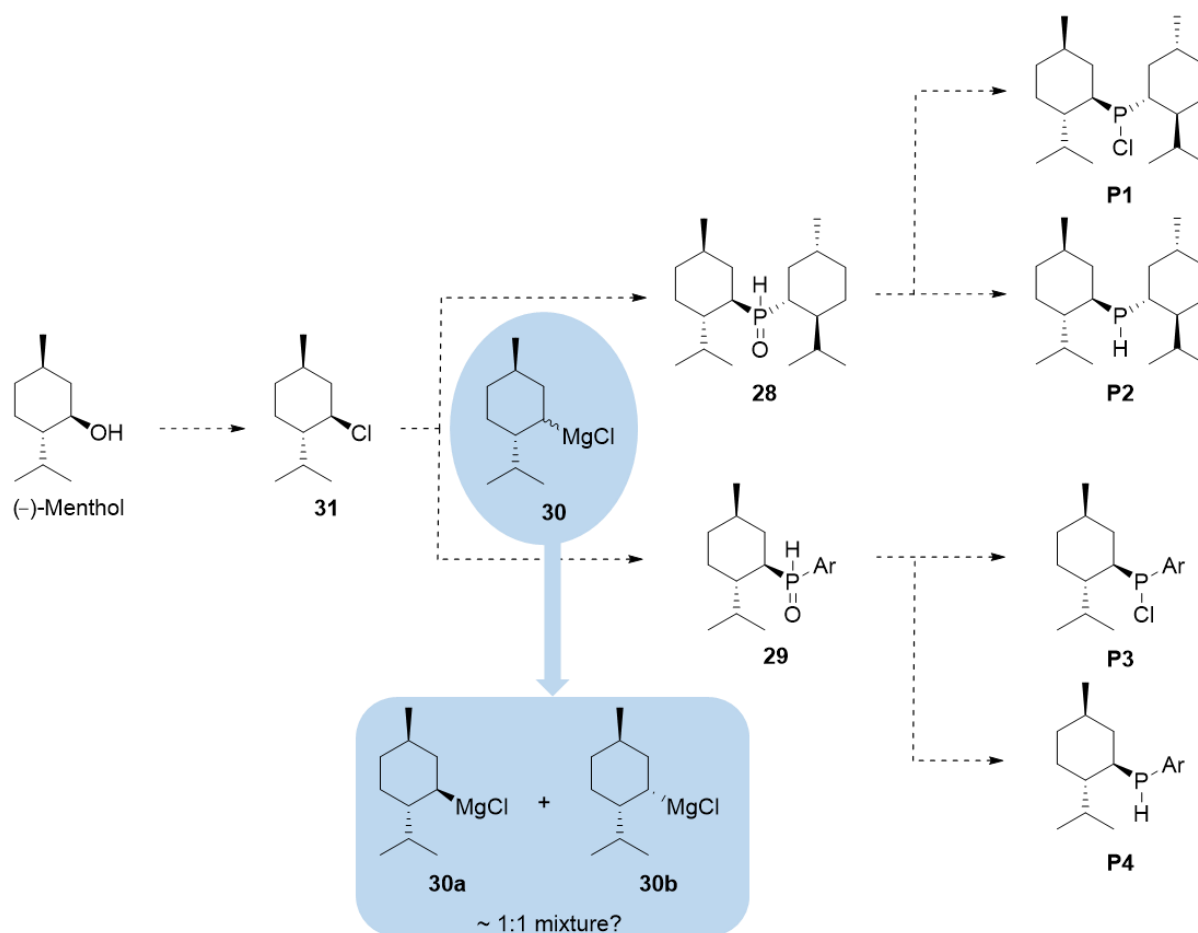
Figure 3. Examples for ligand structures derived from naturally occurring, cheap precursors.^[82]

¹ At 25 °C, a $\Delta\Delta G^\ddagger$ of 5 kJ/mol gives 76% ee whereas 7.5 kJ/mol gives 91% ee.

2 Aims of this thesis

Based on a knowledge of early work of the 1930 chemistry noble prize winner HANS FISCHER, who had described an alkoxide-mediated alkylation of pyrroles in alcoholic media,^[83] preliminary work on repetition of these experiments under microwave conditions was performed in the HINTERMANN group.^[84] We then set out to collect evidence to support our assumption that this reaction proceeds according to the *borrowing hydrogen* mechanism, which suggested itself by analogy with the reported HAT-alkylation of indoles with alcohols (see chapter 1.2.2). We also wished to study, if a catalytic version of this reaction could be developed under milder reaction conditions. Considering the interdependency between *borrowing hydrogen* and *dehydrogenative coupling*, the scope of acceptorless dehydrogenative pyrrole synthesis, which so far has been limited to donor-substituted (alkyl,aryl) pyrroles, should be extended (see chapter 1.2.1). Possible extensions of this method towards the formation of other heterocycles were to be investigated. To ensure an efficient screening procedure, the set-up of a catalyst library is necessary. Therefore, a selected number of metal complexes reported to be active in *borrowing hydrogen* catalysis as well as selected new structures, especially through variation of established ligands, should be prepared. As a readily available enantiopure precursor for the design of novel chiral catalysts for enantioselective catalysis, the terpenoid (–)-menthol was chosen. When incorporated into a phosphine ligand, the menthyl group provides good σ -donor ability and a relatively high steric demand at phosphorous. In the course of this thesis we worked out new synthetic routes to four different precursors (**P1-P4**) that can be used for accessing chiral phosphine ligands (Scheme 14). The chlorophosphines can react as electrophiles, the secondary phosphines as *P*-nucleophiles in syntheses of the ligand target structures. Furthermore, the intermediary secondary phosphine oxides (**28**, **29**) represent interesting ligands themselves with many potential applications.^[85] The key intermediate of this synthetic route is Grignard reagent **30**. Reactions of that reagent have been described with various nucleophiles, amongst others CO₂,^[86] PCl₃,^[87] GeCl₄,^[88] SnCl₄ and organotin chlorides.^[89] The products generally retain menthyl configuration in the transformation from menthol via **31** to **30** and onto **28/29**. However, DUTHIE and coworkers reported that **30** is a 1:1 mixture of configurationally stable epimers, namely menthylmagnesium chloride (**30a**) and neomenthylmagnesium chloride (**30b**). The observation of mainly menthyl

configuration in the reaction products of **30a/b** with nucleophiles was explained by the higher nucleophilicity of **30a**.^[90] Considering the need for stereoisomerically pure phosphine ligand precursors (**P1-P4**), a closer insight into the nature of **30**, its formation from **31** and its reaction with electrophiles is required.



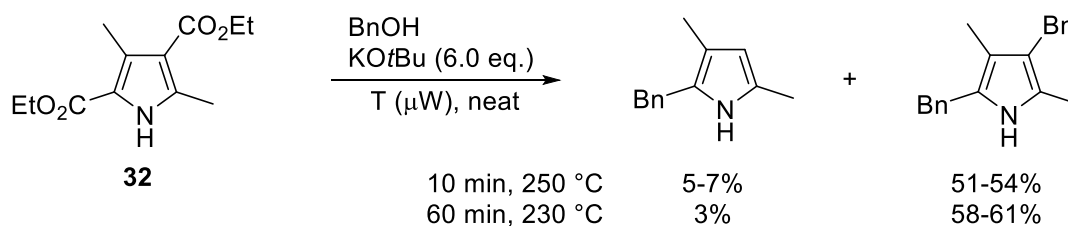
Scheme 14. Planned synthesis of menthylphosphine precursors (**P1-P4**) for chiral ligand synthesis with the crucial intermediary Grignard reagent (**30**) highlighted in blue.

3 Publication Summaries

This chapter provides brief summaries of the publications that were prepared during the course of this dissertation.

3.1 Catalytic C-alkylation of Pyrroles with Primary Alcohols: Hans Fischer's Alkali and a New Method with Iridium P,N,P-Pincer Complexes

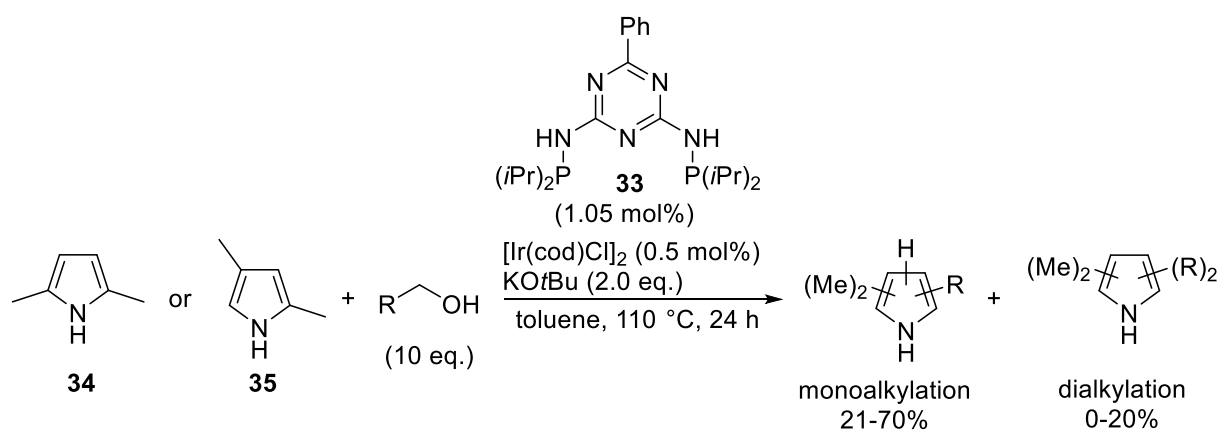
On the basis of Hans Fischer's reports on alkali alkoxide mediated pyrrole alkylation in alcoholic media, we started with a reproduction of these transformations and the collection of evidence for our assumption of a *borrowing hydrogen* mechanism.^[83] To ensure a safe and reproducible method for these high temperature reactions ($T > 200\text{ }^{\circ}\text{C}$), a microwave reactor was used. With selected model pyrroles and using benzylic alcohol as alkylating reagent, a preference for C2/C5-alkylation was observed which is in line with the higher nucleophilicity at these positions and indicating an attack of the pyrrole by an electrophile as a key step.^[91] Interestingly, when diester **32** was subjected to the reaction conditions, a de-alkoxycarbonylation preceded the alkylation (Scheme 15). Since many donor-substituted pyrroles are air-sensitive and exhibit limited shelf-life, a direct HAT-alkylation of their more stable ester-derivatives is as an attractive alternative.



Scheme 15. Microwave-assisted HAT-alkylation of diester **32**.

Next, we set out to overcome the limitations of the base-mediated pyrrole alkylation by developing a catalytic system for the reactions. A heterogenous version with Pd/C as catalyst and substoichiometric amounts of base was realized first. In a screening for a homogenous catalyst system, ruthenium and iridium complexes were tested. The best result was achieved with an iridium PNP-pincer complex (**13**) of the KEMPE type that had previously been applied to the acceptorless dehydrogenative synthesis of pyrroles

from secondary alcohols and amino alcohols.^[36] We prepared the catalyst in situ by precomplexation of $[\text{Ir}(\text{cod})\text{Cl}]_2$ with ligand **33**. Substituted benzylic alcohols as well as a model aliphatic alcohol (*n*-octyl alcohol) reacted predominantly to give monoalkylation product of **34** or **35** (Scheme 16). With 2,4-dimethyl pyrrole (**35**) a general preference for C5-alkylation over C3-alkylation was observed. With pyrrole carboxylic esters the de-alkoxycarbonylation/alkylation sequence is also possible under those conditions. Eventually, we propose mechanisms for both the base-induced and the transition metal catalyzed pyrrole alkylation based on our experimental observations and taking into account recent work on the closely related alkylation of indoles.^[68-71]

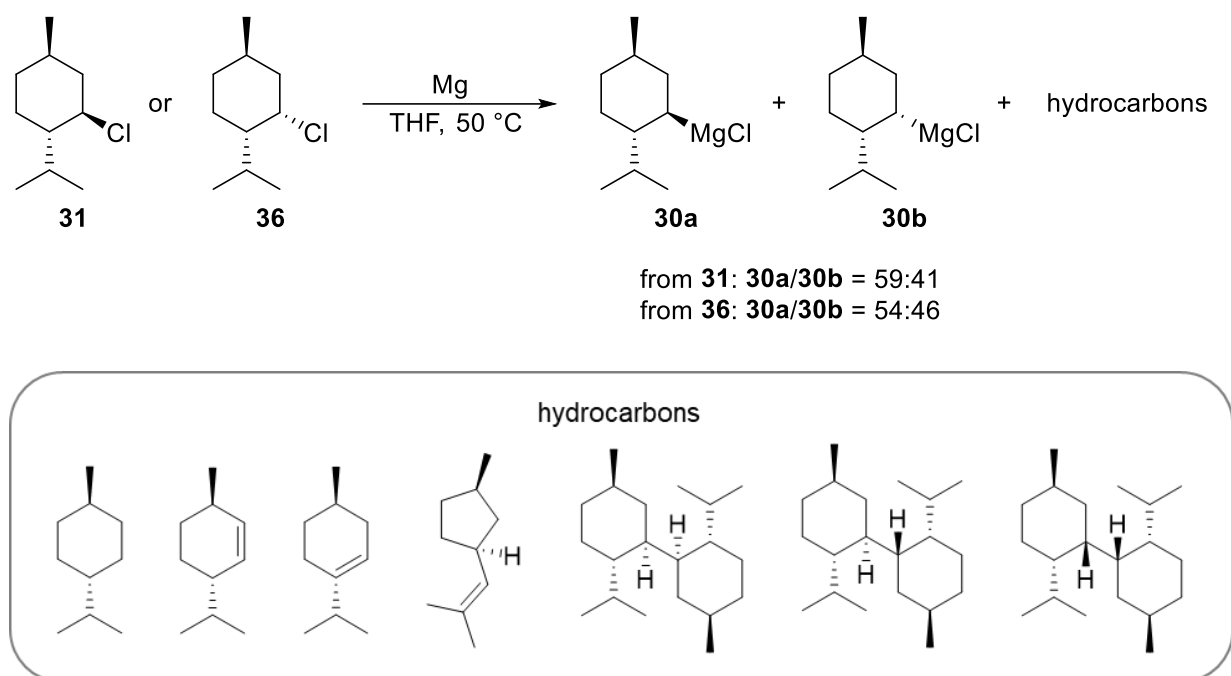


Scheme 16. Ir-PNP-pincer catalyzed HAT-alkylation of pyrroles with alcohols.

My individual contributions to this work included support of the study design, performing experimental work, analyzing analytical results and co-writing of the manuscript.

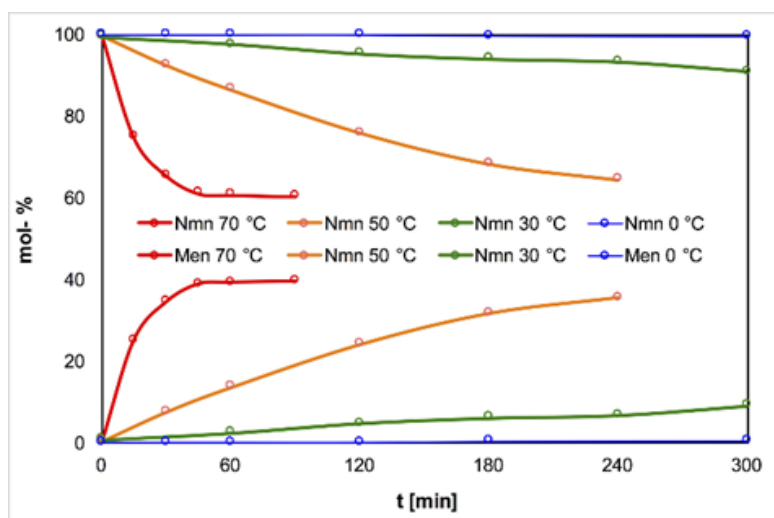
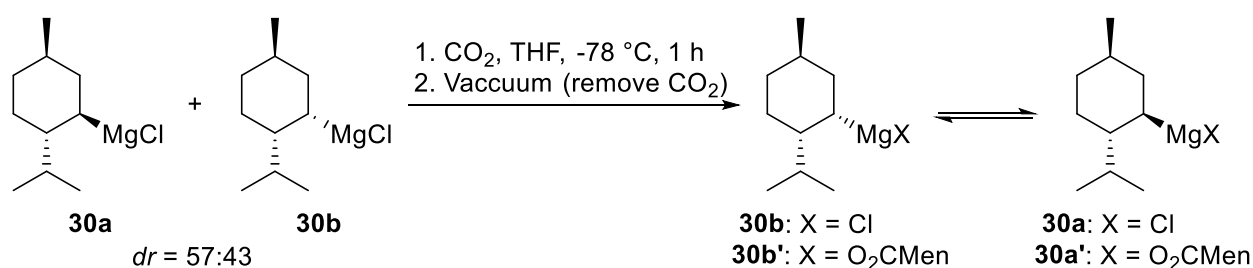
3.2 Stereochemistry of the Menthyl Grignard Reagent: Generation, Composition, Dynamics, and Reactions with Electrophiles

Our interest in the synthesis of *P,P*-dimethylphosphane based chiral phosphorous ligands urged us to gain a deeper understanding of the characteristics of the menthyl Grignard reagent **30**. At the outset, we developed suitable methods to investigate the composition of **30**. After identifying the components of this reagent by NMR and GC-MS methods (**30a**, **30b** and several hydrocarbons), we went on to quantify them by quantitative ^1H and ^{13}C NMR spectroscopy. The determination of the **30a/30b** ratio was complicated by the presence of different species due to the Schlenk and other ligand exchange equilibria, but was possible in spite of some difficulties. To avoid those problems, we established an analysis based on D_2O -quenching with subsequent ^2H NMR analysis. The kinetic ratio of **30a/30b** in the preparation of **30** from **31** at $50\text{ }^\circ\text{C}$ in THF was found to be 59:41, which is close to the thermodynamic ratio of 56:44 at $50\text{ }^\circ\text{C}$ in THF. Starting from neomenthyl chloride (**36**) under the same conditions (THF, $50\text{ }^\circ\text{C}$) almost the same ratio (54:46) was observed. This can be explained assuming that the synthesis of **30** from either **31** or **36** is a kinetically controlled and stereoconvergent process (Scheme 17).



Scheme 17. Stereoconvergent formation of menthyl Grignard reagent **30** and its composition.

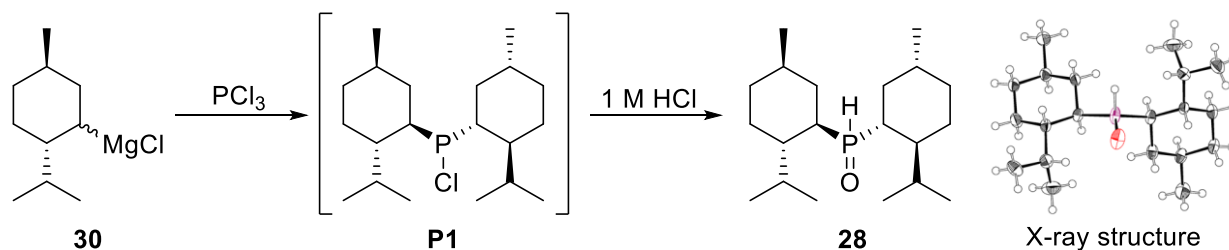
In a study of the carboxylation of **30** we found that reaction with CO₂ at -78 °C leads to a kinetic separation of diastereomers by giving the anion of menthanecarboxylic acid from **30a**. The remaining **30b** then forms the salt neomenthylmagnesium menthanecarboxylate (**30b'**) by ligand exchange at magnesium. The availability of diastereomerically pure solutions of NMnMgX allowed the investigation of the epimerization of **30** (Scheme 18). The kinetics for **30b'** → **30a'** are characterized by $\Delta H^\ddagger = 98.5$ kJ/mol and $\Delta S^\ddagger = -113$ J/mol·K. This finding rejects the assumption of Duthie who assumed that diastereomers of **30** were configurationally stable.^[90] As synthetic application of the carboxylation of **30** the physiological cooling agent **WS-5** was prepared.^[92]



Scheme 18. Kinetic resolution of **30** and temperature-dependent epimerization of neomenthylmagnesium menthanecarboxylate (**30b'**). The amounts in mol% were determined by D₂O-quenching and analysis with ²H NMR.

The stereochemistry of reactions of **30** at C1 depends on the electrophilic partner. With H₂O and D₂O, the hydro-demetalation proceeds with retention of configuration as in the reaction with CO₂ and a kinetic preference for **30a**. With alcohols, the protonation is less stereoselective. In reactions of **30** with phosphorous electrophiles

stereoconvergence from both **30a** and **30b** towards mainly menthyl-configured products occurs and allows higher yields than theoretically expected regarding the amount of menthyl epimer **30a**. These stereoconvergent reactions presumably follow a SET-mechanism as has been observed for bornyl or fenchyl Grignard reagents with phosphorous electrophiles.^[93] Dimethylphosphine oxide (**28**) was prepared via reaction of **1** with PCl_3 to chlorodimethylphosphine (**P1**), followed by hydrolysis of the intermediate during work-up (Scheme 19).

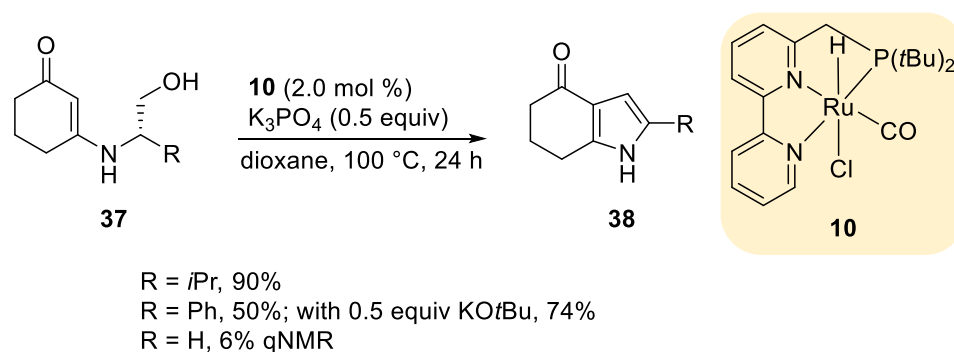


Scheme 19. Synthesis of dimethylphosphine oxide (**28**) and solid state structure of the product.

My individual contribution to this work included participation in the study designing, carrying out substantial parts of the experimental work including analytics, interpretation of experimental results and co-writing of the manuscript.

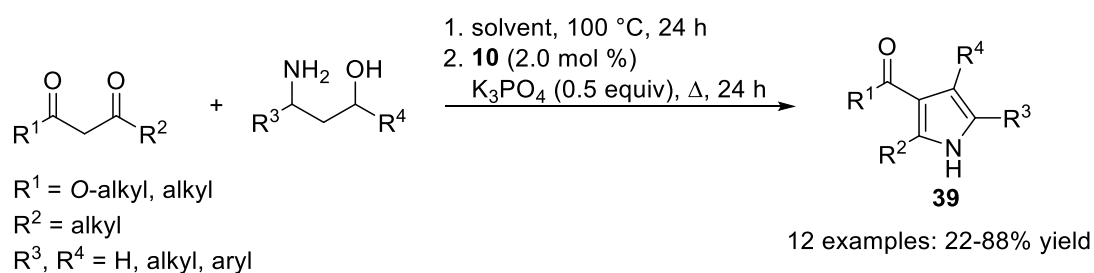
3.3 Unpublished Results (Manuscript in Preparation): Synthesis of Acceptor-Substituted Pyrroles by Ruthenium-Catalyzed Acceptorless Dehydrogenative Condensation with Amino Alcohols

The concept of *acceptorless dehydrogenative coupling* has been applied to the synthesis of pyrroles, but the range of accessible products is so far limited to donor substituted (alkyl, aryl) pyrroles.^[35-41] To overcome this drawback we chose to investigate the dehydrogenative cyclization of β -hydroxyenaminones (**37**) to 1,5,6,7-tetrahydroindol-4-ones (**38**) as a starting point. The catalyst screening included different iridium and ruthenium based systems that are known to be active in *dehydrogenative coupling* or *borrowing hydrogen* reactions. Best results were achieved with a ruthenium NNP-pincer (**10**) which was introduced by MILSTEIN (Scheme 20).^[94]



Scheme 20. Oxidative cyclization of β -hydroxyenaminones (**37**).

Starting material **37** is obtained through straightforward enamine formation that might also take place under conditions of the catalytic reaction. Starting from this hypothesis, we realized an efficient one-pot protocol from either 1,3-diketones or β -keto esters and amino alcohols to acceptor-substituted (ketone, ester) pyrroles (**39**) (Scheme 21). Reactions with γ -amino alcohols analogously lead to pyridines.



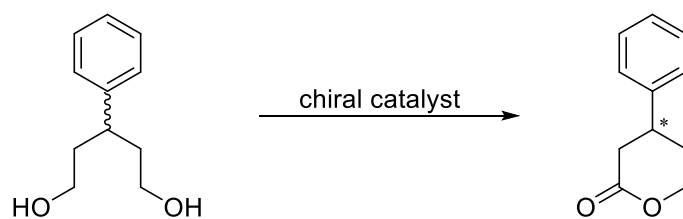
Scheme 21. Acceptorless dehydrogenative coupling of β -keto carbonyls with amino alcohols to acceptor-substituted pyrroles (**39**).

My individual contribution to this work included the study design, carrying out a substantial part of the experimental work including analytics, interpretation of the results and writing of the manuscript.

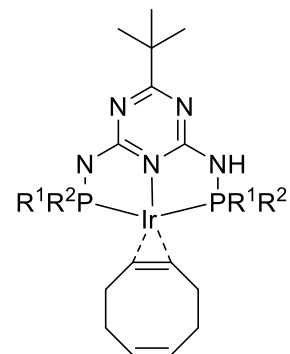
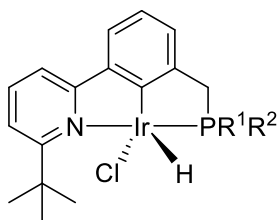
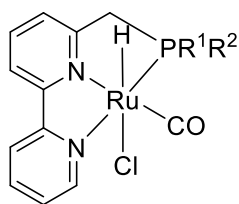
4 Summary and Outlook

The results of this thesis contribute to the development of two closely related concepts of atom-economic catalysis, namely *borrowing hydrogen* and *acceptorless dehydrogenative coupling*. Pyrroles were established as a new class of substrates for *borrowing hydrogen* alkylation with alcohols. The transformation was mediated by base under rather harsh conditions in a microwave reactor, by heterogeneous catalysis with Pd/C or by homogeneous catalysis with iridium PNP pincer complex **13**. In case of pyrrolecarboxylates, a de-alkoxycarbonylation followed by alkylation was observed. Not only the functionalization of pyrroles was investigated but also their synthesis. The scope of acceptorless dehydrogenative pyrrole synthesis was extended onto acceptor-substituted (ketone, ester) pyrroles. A simple one-pot procedure allowed the use of β -keto carbonyls and β -amino alcohols as starting materials with ruthenium NNP pincer **10** as catalyst. With γ -amino alcohols this strategy also allows the synthesis of acceptor-substituted pyridines. As part of our interest on new menthyl based chiral phosphorous ligands for asymmetric catalysis, we developed a deeper understanding of the menthyl Grignard reagent (**30**) by investigation of its generation, composition, dynamics, and reaction with electrophiles. Our findings help to describe the reaction stereochemistry of **30** which had been fairly known due to missing direct analytical studies.

Further research in the fields of *borrowing hydrogen* and *acceptorless dehydrogenative coupling* on the one hand and the synthesis of chiral *P*-menthyl ligand structures on the other hand can be characterized by two main goals. First, to further increase the sustainability of catalytic processes, the development of new catalyst systems with abundant transition metals (e.g. cobalt, iron, manganese) is necessary. Second, after preparation of the desired menthyl based ligand structures derived from **P1-P4**, they should be converted into suitable metal complexes that can be used for development of catalytic asymmetric reactions focusing on *borrowing hydrogen* and *acceptorless dehydrogenative coupling* processes. Scheme **22** provides a potential model reaction for studying asymmetric *dehydrogenative coupling* and structures of possible target metal complexes that are currently investigated in the HINTERMANN group.



Possible chiral catalysts:



with R¹ = R² = menthyl (from **P1** or **P2**)
 or R¹ = menthyl, R² = aryl (from **P3** or **P4**)

Scheme 22. Model desymmetrization reaction for the study of asymmetric *dehydrogenative coupling* and potential catalyst structures based on *P*-menthyl ligands.

5 Index of Abbreviations

Å	Ångström
Ac	acetyl
AcOH	acetic acid
Ar	aryl
BINOL	1,1'-bi-2-naphthol
Bn	benzyl
BnOH	benzyl alcohol
°C	degree Celsius
Cod	1,5-cyclooctadiene
Cp*	1,2,3,4,5-pentamethylcyclopentadienyl
Da	Dalton
DABCO	1,4-diazabicyclo[2.2.2]octane
DIOP	2,3-O-isopropylidene-2,3-dihydroxy-1,4-bis(diphenylphosphino)butane
DIPAMP	1,2-bis[(2-methoxyphenyl)(phenylphosphino)]ethane
DMSO	dimethyl sulfoxide
DPEphos	bis[(2-diphenylphosphino)phenyl] ether
dppf	1,1'-bis(diphenylphosphino)ferrocene
ee	enantiomeric excess
Et	ethyl
etc.	et cetera
GC-MS	gas chromatography-mass spectrometry
h	hour(s)

HAT	hydrogen autotransfer
HO t Bu	<i>tert</i> -butanol
IBiox	1,3'-imidazo[4,3-b:5,1-b']bis(oxazole)
IBX	2-iodoxybenzoic acid
i Pr	<i>iso</i> -propyl
J	Joule
k	kilo
KO t Bu	potassium <i>tert</i> -butoxide
L-DOPA	L-3,4-dihydroxyphenylalanine, levodopa
M	molarity, molar
[M]	metal
M $_n$	number average molecular weight
Me	methyl
Men	menthyl
mol%	mole percentage
MS	molecular sieves
Nmn	neomenthyl
NMR	nuclear magnetic resonance
Nu	nucleophile
Pd/C	palladium on carbon
Ph	phenyl
PHOX	phosphinooxazoline
p -TsOH	<i>para</i> -toluenesulfonic acid
py	pyridine
PyBOX	pyridine bis(oxazoline)

rt	room temperature
S	entropy
SET	single electron transfer
T	temperature
<i>t</i> Bu	<i>tert</i> -butyl
TEMPO	(2,2,6,6-tetramethylpiperidin-1-yl)oxyl
THF	tetrahydrofuran
TMS	trimethylsilyl
TON	turnover number
TPAP	tetrapropylammonium perruthenate
w/o	without
Xantphos	4,5-bis(diphenylphosphino)-9,9-dimethylxanthene
X-ray	Röntgen radiation
Zn(OTf) ₂	zinc triflate
Δ	delta, difference
ΔG [‡]	Gibb's energy of activation
μW	microwave irradiation

6 References

- [1] P. H. Pfromm, *J. Renew. Sustain. Ener.* **2017**, *9*, 034702.
- [2] M. Kellens, G. Calliauw, in *Edible Oil Processing* (Eds.: W. Hamm, R. J. Hamilton, G. Calliauw), John Wiley & Sons, Ltd, Chichester, **2013**, pp. 153-196.
- [3] C. Peng, X. Fang, R. Zeng, in *Catalysis, Vol. 28*, The Royal Society of Chemistry, **2016**, pp. 86-118.
- [4] J. A. Osborn, F. H. Jardine, J. F. Young, G. Wilkinson, *J. Chem. Soc. A* **1966**, 1711-1732.
- [5] R. H. Crabtree, G. E. Morris, *J. Organomet. Chem.* **1977**, *135*, 395-403.
- [6] T. Kandemir, M. E. Schuster, A. Senyshyn, M. Behrens, R. Schlögl, *Angew. Chem. Int. Ed.* **2013**, *52*, 12723-12726.
- [7] a) C. Gunanathan, D. Milstein, *Science* **2013**, *341*, 1229712; b) R. H. Crabtree, *Chem. Rev.* **2017**, *117*, 9228-9246.
- [8] P. Anastas, J. Warner, *Green Chemistry: Theory and Practice*, Oxford University Press, New York, **2000**.
- [9] K. Yukawa, T. Fujii, Y. Saito, *J. Chem. Soc., Chem. Commun.* **1991**, 1548-1549.
- [10] T. Fujii, Y. Saito, *J. Chem. Soc., Chem. Commun.* **1990**, 757-758.
- [11] F. Liu, A. S. Goldman, *Chem. Commun.* **1999**, 655-656.
- [12] S. Kusumoto, M. Akiyama, K. Nozaki, *J. Am. Chem. Soc.* **2013**, *135*, 18726-18729.
- [13] H. Ando, S. Kusumoto, W. Wu, K. Nozaki, *Organometallics* **2017**, *36*, 2317-2322.
- [14] K.-N. T. Tseng, A. M. Rizzi, N. K. Szymczak, *J. Am. Chem. Soc.* **2013**, *135*, 16352-16355.
- [15] X.-Q. Gu, W. Chen, D. Morales-Morales, C. M. Jensen, *J. Mol. Catal. A: Chem.* **2002**, *189*, 119-124.
- [16] X. Zhang, A. Fried, S. Knapp, A. S. Goldman, *Chem. Commun.* **2003**, 2060-2061.
- [17] G. Tojo, M. I. Fernandez, *Oxidation of Alcohols to Aldehydes and Ketones: A Guide to Current Common Practice*, Springer US, **2006**.
- [18] J. Zhang, E. Balaraman, G. Leitus, D. Milstein, *Organometallics* **2011**, *30*, 5716-5724.
- [19] K.-i. Fujita, T. Yoshida, Y. Imori, R. Yamaguchi, *Org. Lett.* **2011**, *13*, 2278-2281.
- [20] R. Kawahara, K.-i. Fujita, R. Yamaguchi, *J. Am. Chem. Soc.* **2012**, *134*, 3643-3646.
- [21] S.-I. Murahashi, K.-i. Ito, T. Naota, Y. Maeda, *Tetrahedron Lett.* **1981**, *22*, 5327-5330.
- [22] J. Zhang, G. Leitus, Y. Ben-David, D. Milstein, *J. Am. Chem. Soc.* **2005**, *127*, 10840-10841.
- [23] D. Srimani, E. Balaraman, B. Gnanaprakasam, Y. Ben-David, D. Milstein, *Adv. Synth. Catal.* **2012**, *354*, 2403-2406.
- [24] E. Balaraman, E. Khaskin, G. Leitus, D. Milstein, *Nature Chemistry* **2013**, *5*, 122-125.

- [25] E. Valeur, M. Bradley, *Chem. Soc. Rev.* **2009**, *38*, 606-631.
- [26] C. Gunanathan, Y. Ben-David, D. Milstein, *Science* **2007**, *317*, 790-792.
- [27] B. Gnanaprakasam, E. Balaraman, Y. Ben-David, D. Milstein, *Angew. Chem. Int. Ed.* **2011**, *50*, 12240-12244.
- [28] D. Srimani, E. Balaraman, P. Hu, Y. Ben-David, D. Milstein, *Adv. Synth. Catal.* **2013**, *355*, 2525-2530.
- [29] E. M. Lane, K. B. Uttley, N. Hazari, W. Bernskoetter, *Organometallics* **2017**, *36*, 2020-2025.
- [30] S. H. Kim, S. H. Hong, *Org. Lett.* **2016**, *18*, 212-215.
- [31] H. Zeng, Z. Guan, *J. Am. Chem. Soc.* **2011**, *133*, 1159-1161.
- [32] C. Gunanathan, L. J. W. Shimon, D. Milstein, *J. Am. Chem. Soc.* **2009**, *131*, 3146-3147.
- [33] A. Maggi, R. Madsen, *Organometallics* **2012**, *31*, 451-455.
- [34] V. Bhardwaj, D. Gumber, V. Abbot, S. Dhiman, P. Sharma, *RSC Advances* **2015**, *5*, 15233-15266.
- [35] M. Zhang, H. Neumann, M. Beller, *Angew. Chem. Int. Ed.* **2013**, *52*, 597-601.
- [36] S. Michlik, R. Kempe, *Nature Chemistry* **2013**, *5*, 140-144.
- [37] F. Kallmeier, B. Dudziec, T. Irrgang, R. Kempe, *Angew. Chem. Int. Ed.* **2017**, *56*, 7261-7265.
- [38] K. Iida, T. Miura, J. Ando, S. Saito, *Org. Lett.* **2013**, *15*, 1436-1439.
- [39] N. D. Schley, G. E. Dobereiner, R. H. Crabtree, *Organometallics* **2011**, *30*, 4174-4179.
- [40] J. C. Borghs, Y. Lebedev, M. Rueping, O. El-Sepelgy, *Org. Lett.* **2019**, *21*, 70-74.
- [41] P. Daw, S. Chakraborty, J. A. Garg, Y. Ben-David, D. Milstein, *Angew. Chem. Int. Ed.* **2016**, *55*, 14373-14377.
- [42] S. Michlik, R. Kempe, *Angew. Chem. Int. Ed.* **2013**, *52*, 6326-6329.
- [43] D. Srimani, Y. Ben-David, D. Milstein, *Chem. Commun.* **2013**, *49*, 6632-6634.
- [44] B. Pan, B. Liu, E. Yue, Q. Liu, X. Yang, Z. Wang, W.-H. Sun, *ACS Catalysis* **2016**, *6*, 1247-1253.
- [45] D. C. Schmitt, A. P. Taylor, A. C. Flick, R. E. Kyne, *Org. Lett.* **2015**, *17*, 1405-1408.
- [46] N. Deibl, K. Ament, R. Kempe, *J. Am. Chem. Soc.* **2015**, *137*, 12804-12807.
- [47] N. Deibl, R. Kempe, *Angew. Chem. Int. Ed.* **2017**, *56*, 1663-1666.
- [48] M. Mastalir, M. Glatz, E. Pittenauer, G. Allmaier, K. Kirchner, *J. Am. Chem. Soc.* **2016**, *138*, 15543-15546.
- [49] M. Peña-López, H. Neumann, M. Beller, *Chem. Eur. J.* **2014**, *20*, 1818-1824.
- [50] a) X. Sun, X.-H. Lv, L.-M. Ye, Y. Hu, Y.-Y. Chen, X.-J. Zhang, M. Yan, *Org. Biomol. Chem.* **2015**, *13*, 7381-7383; b) P. Daw, Y. Ben-David, D. Milstein, *ACS Catalysis* **2017**, *7*, 7456-7460.

- [51] a) S. P. Midya, V. G. Landge, M. K. Sahoo, J. Rana, E. Balaraman, *Chem. Commun.* **2018**, *54*, 90-93; b) P. Daw, A. Kumar, N. A. Espinosa-Jalapa, Y. Diskin-Posner, Y. Ben-David, D. Milstein, *ACS Catalysis* **2018**, *8*, 7734-7741; c) P. Daw, Y. Ben-David, D. Milstein, *J. Am. Chem. Soc.* **2018**, *140*, 11931-11934.
- [52] a) R. N. Monrad, R. Madsen, *Org. Biomol. Chem.* **2011**, *9*, 610-615; b) S. Parua, R. Sikari, S. Sinha, S. Das, G. Chakraborty, N. D. Paul, *Org. Biomol. Chem.* **2018**, *16*, 274-284.
- [53] A. Corma, J. Navas, M. J. Sabater, *Chem. Rev.* **2018**, *118*, 1410-1459.
- [54] a) M. Guerbet, *C. R. Acad. Sci. Paris* **1899**, *128*, 1002; b) A. J. O'Lenick Jr., *J. Surfact. Deterg.* **2001**, *4*, 311-315.
- [55] Y. Watanabe, Y. Tsuji, H. Ige, Y. Ohsugi, T. Ohta, *J. Org. Chem.* **1984**, *49*, 3359-3363.
- [56] M. H. S. A. Hamid, C. L. Allen, G. W. Lamb, A. C. Maxwell, H. C. Maytum, A. J. A. Watson, J. M. J. Williams, *J. Am. Chem. Soc.* **2009**, *131*, 1766-1774.
- [57] W. Baumann, A. Spannenberg, J. Pfeffer, T. Haas, A. Köckritz, A. Martin, J. Deutsch, *Chem. Eur. J.* **2013**, *19*, 17702-17706.
- [58] a) C. S. Cho, *J. Mol. Catal. A: Chem.* **2005**, *240*, 55-60; b) L. K. M. Chan, D. L. Poole, D. Shen, M. P. Healy, T. J. Donohoe, *Angew. Chem. Int. Ed.* **2014**, *53*, 761-765; c) D. Wang, K. Zhao, C. Xu, H. Miao, Y. Ding, *ACS Catalysis* **2014**, *4*, 3910-3918; d) F. Li, J. Ma, N. Wang, *J. Org. Chem.* **2014**, *79*, 10447-10455; e) X. Quan, S. Kerdphon, P. G. Andersson *Chem. Eur. J.* **2015**, *21*, 3576-3579.
- [59] S. Elangovan, J.-B. Sortais, M. Beller, C. Darcel, *Angew. Chem. Int. Ed.* **2015**, *54*, 14483-14486.
- [60] N. Deibl, R. Kempe, *J. Am. Chem. Soc.* **2016**, *138*, 10786-10789.
- [61] C. Löfberg, R. Grigg, M. A. Whittaker, A. Keep, A. Derrick, *J. Org. Chem.* **2006**, *71*, 8023-8027.
- [62] J. Li, Y. Liu, W. Tang, D. Xue, C. Li, J. Xiao, C. Wang, *Chem. Eur. J.* **2017**, *23*, 14445-14449.
- [63] A. Corma, T. Ródenas, M. J. Sabater, *J. Catal.* **2011**, *279*, 319-327.
- [64] H. W. Cheung, J. Li, W. Zheng, Z. Zhou, Y. H. Chiu, Z. Lin, C. P. Lau, *Dalton Transactions* **2010**, *39*, 265-274.
- [65] M. L. Buil, M. A. Esteruelas, J. Herrero, S. Izquierdo, I. M. Pastor, M. Yus, *ACS Catalysis* **2013**, *3*, 2072-2075.
- [66] W. Ma, S. Cui, H. Sun, W. Tang, D. Xue, C. Li, J. Fan, J. Xiao, C. Wang, *Chem. Eur. J.* **2018**, *24*, 13118-13123.
- [67] A. Jana, C. B. Reddy, B. Maji, *ACS Catalysis* **2018**, *8*, 9226-9231.
- [68] a) S. Whitney, R. Grigg, A. Derrick, A. Keep, *Org. Lett.* **2007**, *9*, 3299-3302; b) S. Bartolucci, M. Mari, A. Bedini, G. Piersanti, G. Spadoni, *J. Org. Chem.* **2015**, *80*, 3217-

- 3222; c) S. Bartolucci, M. Mari, G. Di Gregorio, G. Piersanti, *Tetrahedron* **2016**, *72*, 2233-2238.
- [69] A. E. Putra, K. Takigawa, H. Tanaka, Y. Ito, Y. Oe, T. Ohta, *Eur. J. Org. Chem.* **2013**, *2013*, 6344-6354.
- [70] S. M. A. H. Siddiki, K. Kon, K.-i. Shimizu, *Chem. Eur. J.* **2013**, *19*, 14416-14419.
- [71] R. Cano, M. Yus, D. J. Ramón, *Tetrahedron Lett.* **2013**, *54*, 3394-3397.
- [72] J. R. Frost, C. B. Cheong, T. J. Donohoe, *Synthesis* **2017**, *49*, 910-916.
- [73] O. Saidi, A. J. Blacker, M. M. Farah, S. P. Marsden, J. M. J. Williams, *Angew. Chem. Int. Ed.* **2009**, *48*, 7375-7378.
- [74] S. Imm, S. Bähn, A. Tillack, K. Mevius, L. Neubert, M. Beller, *Chem. Eur. J.* **2010**, *16*, 2705-2709.
- [75] A. S. Goldman, A. H. Roy, Z. Huang, R. Ahuja, W. Schinski, M. Brookhart, *Science* **2006**, *312*, 257-261.
- [76] W. T. B. Kelvin, *The Molecular Tactics of a Crystal*, Clarendon Press, **1894**.
- [77] L. T. Scott, M. M. Hashemi, M. S. Bratcher, *J. Am. Chem. Soc.* **1992**, *114*, 1920-1921.
- [78] G. Bredig, P. S. Fiske, *Biochem. Z.* **1913**, *46*, 7-23.
- [79] H. Nozaki, S. Moriuti, H. Takaya, R. Noyori, *Tetrahedron Lett.* **1966**, *7*, 5239-5244.
- [80] T. P. Dang, H. B. Kagan, *J. Chem. Soc. D* **1971**, 481-481.
- [81] W. S. Knowles, *Acc. Chem. Res.* **1983**, *16*, 106-112.
- [82] a) Q.-L. Zhou et al., *Privileged Chiral Ligands and Catalysts*, Wiley-VCH Verlag GmbH & Co. KGaA, **2011**; b) S. Würtz, C. Lohre, R. Fröhlich, K. Bergander, F. Glorius, *J. Am. Chem. Soc.* **2009**, *131*, 8344-8345; c) Y. Tu, Z.-X. Wang, Y. Shi, *J. Am. Chem. Soc.* **1996**, *118*, 9806-9807.
- [83] a) H. Fischer, E. Bartholomäus, *Hoppe-Seyler's Z. Physiol. Chem.* **1912**, *77*, 185-201; b) H. Fischer, E. Bartholomäus, *Ber. Dtsch. Chem. Ges.* **1912**, *45*, 466-471; c) H. Fischer, E. Bartholomäus, *Hoppe-Seyler's Z. Physiol. Chem.* **1912**, *80*, 6-16.
- [84] M. Blazejak, Dissertation, Technische Universität München **2015**.
- [85] T. Achard, *CHIMIA International Journal for Chemistry* **2016**, *70*, 8-19.
- [86] a) N. Zelinsky, *Ber. Dtsch. Chem. Ges.* **1902**, *35*, 4415-4419; b) D. Cunningham, E. T. Gallagher, D. H. Grayson, P. J. McArdle, C. B. Storey, D. J. Wilcock, *J. Chem. Soc., Perkin Trans. 1* **2002**, 2692-2698; c) S. Wu, N. Yang, L. Yang, J. Cao, J. Liu, *J. Polym. Sci., Part A: Polym. Chem.* **2010**, *48*, 1441-1448.
- [87] a) H. W. Krause, A. Kinting, *Journal für Praktische Chemie* **1980**, *322*, 485-486; b) H. Brandes, R. Goddard, P. W. Jolly, C. Krüger, R. Mynott, G. Wilke, *Z. Naturforsch., B: J. Chem. Sci.* **1984**, *39*, 1139-1150; c) G. Hägele, W. Kückelhaus, J. Seega, G. Tossing, H. Kessler, *Z. Naturforsch., B: J. Chem. Sci.* **1985**, *40*, 1053-1063.

- [88] a) L. Zeng, D. Dakternieks, A. Duthie, T. Perchyonok, C. Schiesser, *Tetrahedron: Asymmetry* **2004**, *15*, 2547-2554; b) M. B. Faraoni, V. Vetere, M. L. Casella, J. C. Podestá, *J. Organomet. Chem.* **2011**, *696*, 3440-3444.
- [89] a) J. C. Podestá, A. B. Chopra, G. E. Radivoy, C. A. Vitale, *J. Organomet. Chem.* **1995**, *494*, 11-16; b) C. Lucas, C. C. Santini, M. Prinz, M.-A. Cordonnier, J.-M. Basset, M.-F. Connil, B. Jousseau, *J. Organomet. Chem.* **1996**, *520*, 101-106.
- [90] J. Beckmann, D. Dakternieks, M. Dräger, A. Duthie, *Angew. Chem. Int. Ed.* **2006**, *45*, 6509-6512.
- [91] a) A. Gossauer, *Die Chemie der Pyrrole*, Springer, Berlin, **1974**; b) R. A. Jones, G. P. Bean, *The Chemistry of Pyrroles*, Academic Press, **1977**.
- [92] J. Leffingwell, D. G. Rowsell, *Wilkinson Sword Cooling Compounds: From the Beginning to Now, Vol. 39*, **2014**.
- [93] a) J. Beckmann, A. Schütrumpf, *Org. Biomol. Chem.* **2009**, *7*, 41-42; b) J. Beckmann, A. Schütrumpf, *Eur. J. Org. Chem.* **2010**, *2010*, 363-369.
- [94] E. Balaraman, B. Gnanaprakasam, L. J. W. Shimon, D. Milstein, *J. Am. Chem. Soc.* **2010**, *132*, 16756-16758.

7 Bibliographic Data of Complete Publications

7.1 Catalytic C-alkylation of Pyrroles with Primary Alcohols: Hans Fischer's Alkali and a New Method with Iridium P,N,P-Pincer Complexes

Sebastian Koller,^[a,b] Max Blazejak,^[a,b] and Lukas Hintermann*^[a,b]

[a] Technische Universität München, Department Chemie, Lichtenbergstr. 4, 85748 Garching bei München, Germany

[b] TUM Catalysis Research Center, Ernst-Otto-Fischer-Str. 1, 85748 Garching bei München, Germany

E-mail: lukas.hintermann@tum.de

<http://www.oca.ch.tum.de>

Eur. J. Org. Chem. **2018**, 1624-1633.

DOI: 10.1002/ejoc.201800146

7.2 Stereochemistry of the Menthyl Grignard Reagent: Generation, Composition, Dynamics, and Reactions with Electrophiles

Sebastian Koller,[†] Julia Gatzka,[†] Kit Ming Wong,[†] Philipp J. Altmann,[‡] Alexander Pöthig,[‡] and Lukas Hintermann^{*†}

[†] Technische Universität München, Department of Chemistry, and Catalysis Research Center, Lichtenbergstrasse 4, 85748 Garching bei München, Germany

[‡] Technische Universität München, Chair of Inorganic Chemistry, and Catalysis Research Center, Ernst-Otto-Fischer Strasse 1, 85747 Garching bei München, Germany

[*] Corresponding Author, Email: lukas.hintermann@tum.de

J. Org. Chem. **2018**, *83*, 15009-15028.

DOI: 10.1021/acs.joc.8b02278

8 Reprint Permissions

8.1 Wiley Article

JOHN WILEY AND SONS LICENSE TERMS AND CONDITIONS

Mar 13, 2019

This Agreement between Mr. Sebastian Koller ("You") and John Wiley and Sons ("John Wiley and Sons") consists of your license details and the terms and conditions provided by John Wiley and Sons and Copyright Clearance Center.

License Number	4546940691973
License date	Mar 13, 2019
Licensed Content Publisher	John Wiley and Sons
Licensed Content Publication	European Journal of Organic Chemistry
Licensed Content Title	Catalytic C-Alkylation of Pyrroles with Primary Alcohols: Hans Fischer's Alkali and a New Method with Iridium P,N,P-Pincer Complexes
Licensed Content Author	Sebastian Koller, Max Blazejak, Lukas Hintermann
Licensed Content Date	Mar 30, 2018
Licensed Content Volume	2018
Licensed Content Issue	14
Licensed Content Pages	10
Type of use	Dissertation/Thesis
Requestor type	Author of this Wiley article
Format	Print and electronic
Portion	Full article
Will you be translating?	No
Title of your thesis / dissertation	Applications of Dehydrogenative and Borrowing Hydrogen Catalysis and Investigation of the Menthyl Grignard Reagent for the Synthesis of Chiral Phosphine Ligands
Expected completion date	May 2019
Expected size (number of pages)	60
Requestor Location	Mr. Sebastian Koller Dietersheimer Straße 5 Eching, 85386 Germany Attn: Mr. Sebastian Koller
Publisher Tax ID	EU826007151
Total	0.00 EUR
Terms and Conditions	

TERMS AND CONDITIONS

This copyrighted material is owned by or exclusively licensed to John Wiley & Sons, Inc. or one of its group companies (each a "Wiley Company") or handled on behalf of a society with which a Wiley Company has exclusive publishing rights in relation to a particular work (collectively "WILEY"). By clicking "accept" in connection with completing this licensing transaction, you agree that the following terms and conditions apply to this transaction

(along with the billing and payment terms and conditions established by the Copyright Clearance Center Inc., ("CCC's Billing and Payment terms and conditions"), at the time that you opened your RightsLink account (these are available at any time at <http://myaccount.copyright.com>).

Terms and Conditions

- The materials you have requested permission to reproduce or reuse (the "Wiley Materials") are protected by copyright.
- You are hereby granted a personal, non-exclusive, non-sub licensable (on a stand-alone basis), non-transferable, worldwide, limited license to reproduce the Wiley Materials for the purpose specified in the licensing process. This license, and any CONTENT (PDF or image file) purchased as part of your order, is for a one-time use only and limited to any maximum distribution number specified in the license. The first instance of republication or reuse granted by this license must be completed within two years of the date of the grant of this license (although copies prepared before the end date may be distributed thereafter). The Wiley Materials shall not be used in any other manner or for any other purpose, beyond what is granted in the license. Permission is granted subject to an appropriate acknowledgement given to the author, title of the material/book/journal and the publisher. You shall also duplicate the copyright notice that appears in the Wiley publication in your use of the Wiley Material. Permission is also granted on the understanding that nowhere in the text is a previously published source acknowledged for all or part of this Wiley Material. Any third party content is expressly excluded from this permission.
- With respect to the Wiley Materials, all rights are reserved. Except as expressly granted by the terms of the license, no part of the Wiley Materials may be copied, modified, adapted (except for minor reformatting required by the new Publication), translated, reproduced, transferred or distributed, in any form or by any means, and no derivative works may be made based on the Wiley Materials without the prior permission of the respective copyright owner. For STM Signatory Publishers clearing permission under the terms of the [STM Permissions Guidelines](#) only, the terms of the license are extended to include subsequent editions and for editions in other languages, provided such editions are for the work as a whole in situ and does not involve the separate exploitation of the permitted figures or extracts, You may not alter, remove or suppress in any manner any copyright, trademark or other notices displayed by the Wiley Materials. You may not license, rent, sell, loan, lease, pledge, offer as security, transfer or assign the Wiley Materials on a stand-alone basis, or any of the rights granted to you hereunder to any other person.
- The Wiley Materials and all of the intellectual property rights therein shall at all times remain the exclusive property of John Wiley & Sons Inc, the Wiley Companies, or their respective licensors, and your interest therein is only that of having possession of and the right to reproduce the Wiley Materials pursuant to Section 2 herein during the continuance of this Agreement. You agree that you own no right, title or interest in or to the Wiley Materials or any of the intellectual property rights therein. You shall have no rights hereunder other than the license as provided for above in Section 2. No right, license or interest to any trademark, trade name, service mark or other branding ("Marks") of WILEY or its licensors is granted hereunder, and you agree that you shall not assert any such right, license or interest with respect thereto

- NEITHER WILEY NOR ITS LICENSORS MAKES ANY WARRANTY OR REPRESENTATION OF ANY KIND TO YOU OR ANY THIRD PARTY, EXPRESS, IMPLIED OR STATUTORY, WITH RESPECT TO THE MATERIALS OR THE ACCURACY OF ANY INFORMATION CONTAINED IN THE MATERIALS, INCLUDING, WITHOUT LIMITATION, ANY IMPLIED WARRANTY OF MERCHANTABILITY, ACCURACY, SATISFACTORY QUALITY, FITNESS FOR A PARTICULAR PURPOSE, USABILITY, INTEGRATION OR NON-INFRINGEMENT AND ALL SUCH WARRANTIES ARE HEREBY EXCLUDED BY WILEY AND ITS LICENSORS AND WAIVED BY YOU.
- WILEY shall have the right to terminate this Agreement immediately upon breach of this Agreement by you.
- You shall indemnify, defend and hold harmless WILEY, its Licensors and their respective directors, officers, agents and employees, from and against any actual or threatened claims, demands, causes of action or proceedings arising from any breach of this Agreement by you.
- IN NO EVENT SHALL WILEY OR ITS LICENSORS BE LIABLE TO YOU OR ANY OTHER PARTY OR ANY OTHER PERSON OR ENTITY FOR ANY SPECIAL, CONSEQUENTIAL, INCIDENTAL, INDIRECT, EXEMPLARY OR PUNITIVE DAMAGES, HOWEVER CAUSED, ARISING OUT OF OR IN CONNECTION WITH THE DOWNLOADING, PROVISIONING, VIEWING OR USE OF THE MATERIALS REGARDLESS OF THE FORM OF ACTION, WHETHER FOR BREACH OF CONTRACT, BREACH OF WARRANTY, TORT, NEGLIGENCE, INFRINGEMENT OR OTHERWISE (INCLUDING, WITHOUT LIMITATION, DAMAGES BASED ON LOSS OF PROFITS, DATA, FILES, USE, BUSINESS OPPORTUNITY OR CLAIMS OF THIRD PARTIES), AND WHETHER OR NOT THE PARTY HAS BEEN ADVISED OF THE POSSIBILITY OF SUCH DAMAGES. THIS LIMITATION SHALL APPLY NOTWITHSTANDING ANY FAILURE OF ESSENTIAL PURPOSE OF ANY LIMITED REMEDY PROVIDED HEREIN.
- Should any provision of this Agreement be held by a court of competent jurisdiction to be illegal, invalid, or unenforceable, that provision shall be deemed amended to achieve as nearly as possible the same economic effect as the original provision, and the legality, validity and enforceability of the remaining provisions of this Agreement shall not be affected or impaired thereby.
- The failure of either party to enforce any term or condition of this Agreement shall not constitute a waiver of either party's right to enforce each and every term and condition of this Agreement. No breach under this agreement shall be deemed waived or excused by either party unless such waiver or consent is in writing signed by the party granting such waiver or consent. The waiver by or consent of a party to a breach of any provision of this Agreement shall not operate or be construed as a waiver of or consent to any other or subsequent breach by such other party.
- This Agreement may not be assigned (including by operation of law or otherwise) by you without WILEY's prior written consent.
- Any fee required for this permission shall be non-refundable after thirty (30) days from receipt by the CCC.

- These terms and conditions together with CCC's Billing and Payment terms and conditions (which are incorporated herein) form the entire agreement between you and WILEY concerning this licensing transaction and (in the absence of fraud) supersedes all prior agreements and representations of the parties, oral or written. This Agreement may not be amended except in writing signed by both parties. This Agreement shall be binding upon and inure to the benefit of the parties' successors, legal representatives, and authorized assigns.
- In the event of any conflict between your obligations established by these terms and conditions and those established by CCC's Billing and Payment terms and conditions, these terms and conditions shall prevail.
- WILEY expressly reserves all rights not specifically granted in the combination of (i) the license details provided by you and accepted in the course of this licensing transaction, (ii) these terms and conditions and (iii) CCC's Billing and Payment terms and conditions.
- This Agreement will be void if the Type of Use, Format, Circulation, or Requestor Type was misrepresented during the licensing process.
- This Agreement shall be governed by and construed in accordance with the laws of the State of New York, USA, without regards to such state's conflict of law rules. Any legal action, suit or proceeding arising out of or relating to these Terms and Conditions or the breach thereof shall be instituted in a court of competent jurisdiction in New York County in the State of New York in the United States of America and each party hereby consents and submits to the personal jurisdiction of such court, waives any objection to venue in such court and consents to service of process by registered or certified mail, return receipt requested, at the last known address of such party.

WILEY OPEN ACCESS TERMS AND CONDITIONS

Wiley Publishes Open Access Articles in fully Open Access Journals and in Subscription journals offering Online Open. Although most of the fully Open Access journals publish open access articles under the terms of the Creative Commons Attribution (CC BY) License only, the subscription journals and a few of the Open Access Journals offer a choice of Creative Commons Licenses. The license type is clearly identified on the article.

The Creative Commons Attribution License

The [Creative Commons Attribution License \(CC-BY\)](#) allows users to copy, distribute and transmit an article, adapt the article and make commercial use of the article. The CC-BY license permits commercial and non-

Creative Commons Attribution Non-Commercial License

The [Creative Commons Attribution Non-Commercial \(CC-BY-NC\) License](#) permits use, distribution and reproduction in any medium, provided the original work is properly cited and is not used for commercial purposes. (see below)

Creative Commons Attribution-Non-Commercial-NoDerivs License

The [Creative Commons Attribution Non-Commercial-NoDerivs License \(CC-BY-NC-ND\)](#) permits use, distribution and reproduction in any medium, provided the original work is properly cited, is not used for commercial purposes and no modifications or adaptations are made. (see below)

Use by commercial "for-profit" organizations

Use of Wiley Open Access articles for commercial, promotional, or marketing purposes requires further explicit permission from Wiley and will be subject to a fee.

Further details can be found on Wiley Online Library
<http://olabout.wiley.com/WileyCDA/Section/id-410895.html>

Other Terms and Conditions:

v1.10 Last updated September 2015

Questions? customercare@copyright.com or +1-855-239-3415 (toll free in the US) or
+1-978-646-2777.

8.2 ACS Article



RightsLink®

Home

Account Info

Help



ACS Publications
Most Trusted. Most Cited. Most Read.

Title: Stereochemistry of the Menthyl Grignard Reagent: Generation, Composition, Dynamics, and Reactions with Electrophiles

Author: Sebastian Koller, Julia Gatzka, Kit Ming Wong, et al

Publication: The Journal of Organic Chemistry

Publisher: American Chemical Society

Date: Dec 1, 2018

Copyright © 2018, American Chemical Society

Logged in as:

Sebastian Koller

Account #:

3001397239

LOGOUT

PERMISSION/LICENSE IS GRANTED FOR YOUR ORDER AT NO CHARGE

This type of permission/license, instead of the standard Terms & Conditions, is sent to you because no fee is being charged for your order. Please note the following:

- Permission is granted for your request in both print and electronic formats, and translations.
- If figures and/or tables were requested, they may be adapted or used in part.
- Please print this page for your records and send a copy of it to your publisher/graduate school.
- Appropriate credit for the requested material should be given as follows: "Reprinted (adapted) with permission from (COMPLETE REFERENCE CITATION). Copyright (YEAR) American Chemical Society." Insert appropriate information in place of the capitalized words.
- One-time permission is granted only for the use specified in your request. No additional uses are granted (such as derivative works or other editions). For any other uses, please submit a new request.

BACK

CLOSE WINDOW

Copyright © 2019 Copyright Clearance Center, Inc. All Rights Reserved. [Privacy statement](#). [Terms and Conditions](#). Comments? We would like to hear from you. E-mail us at customercare@copyright.com

9 Appendix – Publication Reprints

Hydrogen-Autotransfer Alkylation



Catalytic C-Alkylation of Pyrroles with Primary Alcohols: Hans Fischer's Alkali and a New Method with Iridium P,N,P-Pincer Complexes

Sebastian Koller,^[a,b] Max Blazejak,^[a,b] and Lukas Hintermann*^[a,b]

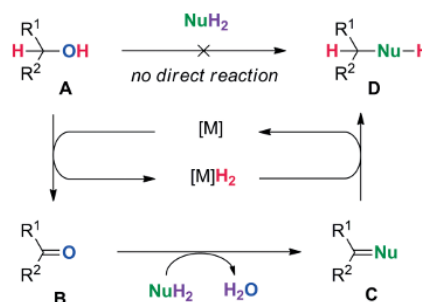
Abstract: Hydrogen-autotransfer alkylation (HAT or "borrowing-hydrogen" alkylation) of heteroaromatic compounds has been studied with a range of substrates recently, but pyrroles have been largely absent from such studies. The conditions for HAT alkylations of pyrroles were investigated under a variety of conditions and were found to take place under basic alcoholic

conditions (Hans Fischer alkylation) in the absence of transition-metal catalysts; by means of a heterogeneous Pd/C catalyst in the presence of base; and finally by means of homogeneous transition-metal catalysis combining a base and iridium pincer complexes generated in situ that have not previously been used in HAT alkylations of heterocycles.

Introduction

Catalytic reactions involving hydrogen autotransfer (HAT) from starting materials to products (i.e., following the "borrowing-hydrogen principle") have recently become a useful tool for C–C and C–N bond formation in organic chemistry.^[1,2] Such transformations generate water as the sole stoichiometric by-product and, by virtue of their high atom economy, can be important contributors to green chemistry. The principle of HAT alkylation of a nucleophile (H₂Nu; both hydrogen atoms need not be attached at the same nucleophilic center, since one may be in a tautomeric position) with alcohol **A** is illustrated in Scheme 1. Catalyst-mediated dehydrogenation of **A** gives carbonyl compound **B** and reduced catalyst [M]H₂; this is followed by spontaneous or base-catalyzed condensation of **B** with the nucleophile to give unsaturated intermediate **C**. The latter is subsequently hydrogenated by MH₂ to give product **D**, thereby regenerating catalyst [M] in the process. These reactions are typically conducted with a transition-metal catalyst (e.g., Ir, Ru) capable of hydrogen transfers, and a base co-catalyst for the condensation step. Such methodology has been applied to C-alkylation via activation of the acidified α-C(sp³)-H bonds of carbonyl compounds (ketones, esters, amides), nitriles, or other substrates.^[2] However, C-alkylation with alcohols is also possible at C(sp²)-centers of electron-rich (hetero)aromatic cores; with indoles, regioselective C-3 alkylation has been realized using a base and the catalysts [Cp*IrCl₂]₂,^[3a,b,c] RuCl₂(PPh₃)₂/DPE-Phos,^[3d] Pd/C,^[3d] and Pt nanoclusters.^[4] For the related case of

indole HAT alkylation with amines as alkylating agents, the use of Shvo's catalyst^[5a] or of a redox-active anthraquinone/amine organocatalyst has been described.^[5b,6]



Scheme 1. General mechanistic sequence for a HAT alkylation.

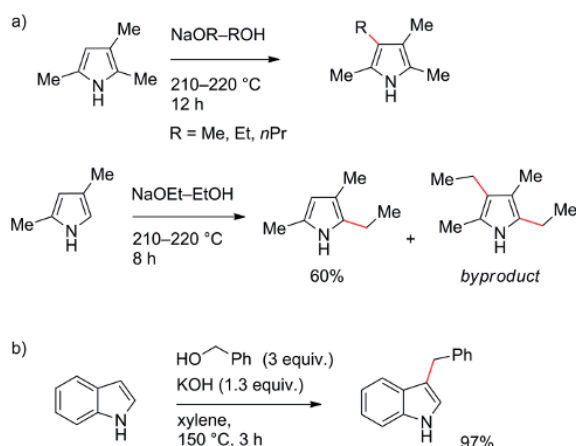
Recently, HAT C-alkylations have also been realized with phenols as examples of non-heterocyclic arenes.^[7] Notwithstanding the success of such protocols, remarkably, HAT alkylations with alcohols and alkali base as sole catalyst have been described, in which hydride transfers appear to proceed via Cannizzaro-type mechanisms.^[8] Such transition-metal-free HAT alkylations were described for ketones^[9] and electron-rich N-heterocycles including indoles.^[10,11]

In contrast to numerous studies on indoles, HAT alkylation of pyrroles has been nearly absent; while our work was in progress, an example of methylation of pyrroles by methanol (140 °C, pressure tube) using [Cp*IrCl₂]₂ as a catalyst was reported.^[12] However, we have become aware of work performed by Hans Fischer and co-workers in 1912, describing remarkable alkylations of simple pyrroles in alcoholic sodium alkoxide at elevated temperature in sealed tubes (Scheme 2, a).^[13] A Table with reaction examples reported by Fischer has been compiled in the Supporting Information (Table S-1).

[a] Technische Universität München, Department Chemie, Lichtenbergstr. 4, 85748 Garching bei München, Germany

[b] TUM Catalysis Research Center, Ernst-Otto-Fischer-Str. 1, 85748 Garching bei München, Germany
E-mail: lukas.hintermann@tum.de
http://www.oca.ch.tum.de

Supporting information and ORCID(s) from the author(s) for this article are available on the WWW under <https://doi.org/10.1002/ejoc.201800146>.



Scheme 2. a) Pyrrrole alkylations mediated by alcoholic alkoxide as performed by Hans Fischer.^[13] b) Base-induced HAT alkylation of indole.^[10]

Hans Fischer's lifework on the structure elucidation and synthesis of pyrrole pigments was highlighted by the award of the 1930 Nobel Prize of chemistry "for his researches into the constitution of haemin and chlorophyll and especially for his synthesis of haemin".^[14] He was a leading authority on the chemistry of pyrroles, and a monograph, written with H. Orth and A. Stern,^[15] remained a key reference for many years, and continues to be referenced in contemporary work.^[16,17] The alkoxide-mediated alkylation of pyrroles was among Fischer's earliest contributions to pyrrole chemistry and was immediately applied for structural proof (through synthesis) of a series of alkylated pyrroles, which had been obtained by degradation from blood pigment.^[18] The mechanism of this reaction was unknown at the time of discovery^[13a] and was still considered an unsolved riddle 60 years later.^[19,20] In view of recent developments in HAT alkylation chemistry with alkali bases, particularly the related alkylation of indoles (Scheme 2, b)^[10,11] or the base-mediated alkylation of ketones,^[9] a new interpretation of the

Hans Fischer alkylation as a hydrogen-autotransfer (HAT) reaction presented itself.

Our study aimed to address two key aspects: firstly, to collect evidence for the HAT nature of the Hans Fischer alkylation, and secondly, to take advantage of more recent knowledge of transition-metal-catalyzed HAT alkylations to establish catalytic HAT C-alkylation protocols for pyrroles that will possibly proceed under milder reaction conditions. In view of the importance of pyrroles as structural motifs in pharmacologically active compounds, an extension of the synthetic repertoire for pyrrole alkylation by simple and atom-economic methods is highly desirable.

Results and Discussion

Pyrrole alkylations according to Hans Fischer were performed in sealed tubes ("Carius bomb tubes") and had a high incidence of explosive bursts.^[21] To simulate the original reaction conditions in a reliable way we used microwave irradiation under adiabatic conditions, and with high-boiling alcohols to limit pressure buildup. Heating of 2,5-dimethylpyrrole (**1**) with benzyl alcohol (**2a**) and base to 250 °C produced mono- (**3a**) as well as dibenzylated (**4a**) products under a variety of conditions (Table 1).

KOtBu was in general superior (Table 1, entries 5–8) to sodium (entries 1, 3) or lithium (entry 4) bases. A large excess of benzyl alcohol (**2a**), which also serves as the solvent, in combination with KOtBu favors dialkylation (entries 5, 6), but a six-fold excess of alcohol in toluene favors monobenzylated product **3a** (entries 7, 8). More polar solvents (dioxane, diglyme) gave inferior results. The effect of hydrogen-transfer additives [Ph₂CO, Al(O*i*Pr)₃] on the reaction was negligible (Table S-2). However, ¹H NMR analyses of crude reaction mixtures consistently revealed the presence of benzaldehyde (in the order of 2 mol-% or more) also in the absence of such additives, which supports the importance of alcohol dehydrogenation in the process.

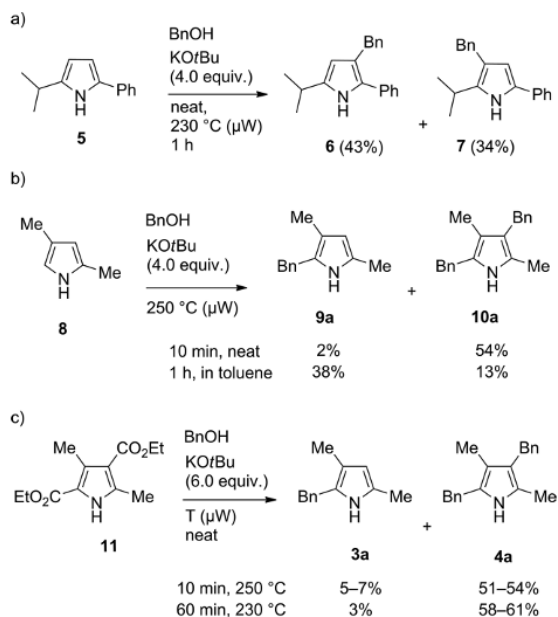
The temperature of 250 °C in the microwave experiments is higher than in Fischer's sealed-tube experiments (210–220 °C

Table 1. Base-mediated pyrrole alkylation under microwave conditions.^[a]

Entry	Base [equiv.]	BnOH [equiv.]	Solvent	T [°C]	3a ^[b] [mol-%]	4a ^[b] [mol-%]
1	NaH (2)	19	neat	250	51	19
2	KOH (2)	19	neat	250	36	18
3	NaOH (2)	19	neat	250	52	10
4	LiOBn ^[c] (2)	19	neat	250	27	0
5	KOtBu (2)	19	neat	250	31	54
6	KOtBu (4)	19	neat	250 ^[d]	8	60
7	KOtBu (4)	6	toluene	250 ^[d]	61	19
8	KOtBu (4)	6	toluene	240	48	21

[a] Reaction scale: 1.0 mmol. [b] Analytical yield determined by quantitative (q) NMR against an internal standard. [c] Base was prepared in situ by dissolving Li metal in BnOH at 70 °C. [d] Temperature was automatically reduced over the reaction time to prevent exceeding the reactor pressure limit (30 bar).

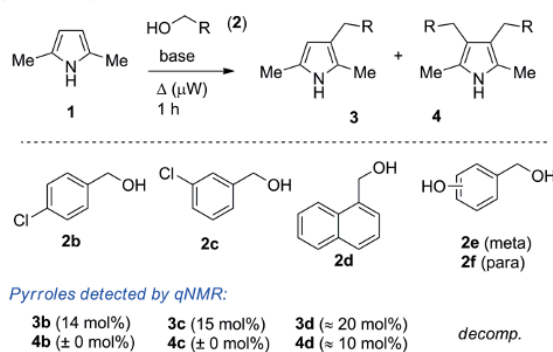
over 12–14 h), in turn the reaction time could be reduced to 1 h. In some of the screening reactions, internal overpressure (> 30 bar) built up that occasionally led to vial ruptures; the pressure is presumably caused by evolution of hydrogen. By working at or below 240 °C, and by using four or less equivalents of base, such incidents were largely prevented. With the unsymmetrical isopropyl-phenyl-pyrrole **5** (see below) as substrate, a mixture of the monoalkylated regioisomers **6/7** in similar amounts emerged (Scheme 3a).



Scheme 3. a,b) Alkylation of **5** and **8** in the presence of base; “neat” reactions use BnOH as solvent (2.0 mL per mmol), reactions in toluene use 6.0 equiv. of BnOH. c) Direct alkylation of diester **11**; analytical yield in mol-% as determined by qNMR against an internal standard.

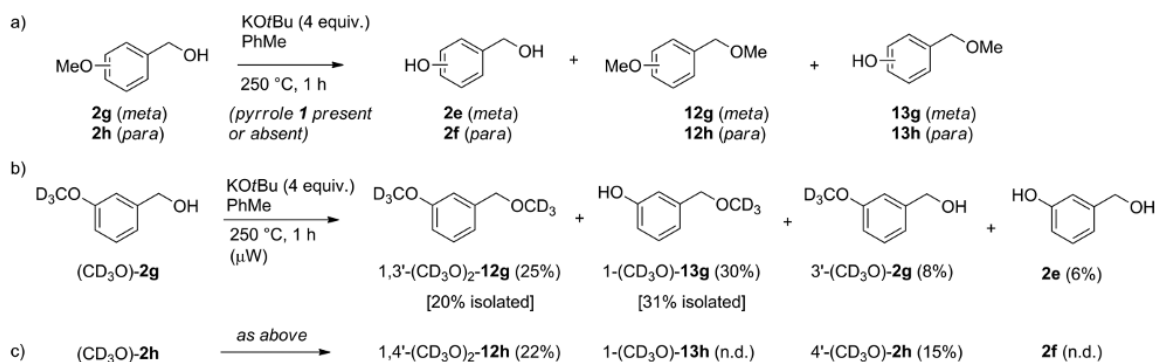
With 2,4-dimethylpyrrole (**8**), dibenylation to **10a** was achieved in a very short time in neat alcohol, but monoalkylated **9a** was the dominant product in toluene after one hour (Scheme 3b). The higher reaction rate of **8** versus that of **1** is in

line with the established higher nucleophilicity at the C-2/5 over the C-3/4 position in pyrroles.^[22] Those observations support an attack of the pyrrole (or its anion) on an electrophile as a key step. Many alkylated pyrroles including **8** are air-sensitive liquids with a limited shelf life. The standard synthesis of **8** proceeds from the air-stable diester **11** via de-alkoxycarbonylation in strong base.^[23] It would be attractive to couple this base-mediated step with a consecutive alkylation, and in fact, **11** is alkylated with **2a** under basic conditions to give **4a** in yields matching those of the reaction starting with **8** (Scheme 3c). This observation could point to a general strategy for performing HAT alkylations of electron-rich heterocycles by way of their more stable ester derivatives. The Fischer-type HAT alkylation of 2,5-dimethylpyrrole (**1**) was shortly tested with substituted benzyl alcohols, and although the alkylation products **3** and **4** were observed, it became evident that optimal results would require individual optimization of the reaction conditions (Scheme 4).



Scheme 4. Variation of benzylic alcohols in the base-mediated alkylation of **1**.

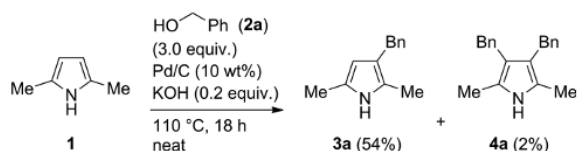
A remarkable observation in attempted alkylations of pyrroles with 3- and 4-methoxybenzyl alcohol (**2g,h**) was the generation of methyl ethers by O-methylation of the benzylic alcohol, with the methoxy group from the substrate either left intact (**12**), or dealkylated (**13**). The pyrrole was unaffected in this reaction and could be left out with no change in the result (Scheme 5a).



Scheme 5. a) Initial observation of transmethylation in attempted pyrrole alkylations. b) Base-induced alkyl transfer in deuterium-labeled 3-(CD₃O)-methoxybenzylalcohol (**2g**) at high temperature. c) Base-induced transalkylation of 4-(CD₃O)-methoxybenzyl alcohol (**2h**).

It was not immediately obvious if this alkyl transfer from an aromatic methyl ether to a benzyl alcohol was due to a direct, S_N2 -type substitution, or if a HAT-type process involving transfer of a formaldehyde equivalent and hydride might be responsible. Control experiments with deuterium-labeled alcohols (CD_3O)-**2g** and (CD_3O)-**2h** produced a mixture of di- (**12**) and mono-methylated (**13**) methyl ethers in which all methoxy groups fully retained their deuterium atoms without scrambling (Scheme 5b, Scheme 5c). An S_N2 transfer by intermolecular attack of alkoxide on the methoxy group of the aryl ether is most plausible, and although we are not aware of any literature precedent, the high reaction temperature undoubtedly facilitates this S_N2 transesterification.

Even if historically and conceptually important, the Hans Fischer alkylation of pyrroles is limited in terms of substrate range and by the harshness of reaction conditions, which can lead to unexpected side reactions such as transalkylation. Our next aim was to realize pyrrole alkylations under milder conditions taking advantage of recent developments in metal-catalyzed HAT alkylation. Very common, heterogeneous Pd/C catalysts have been applied for the HAT alkylation of amines^[24] or indole^[3d] with alcohols. Application of this catalyst system to the alkylation of dimethylpyrrole **1** with benzyl alcohol is shown in Scheme 6.



Scheme 6. Pd/C-catalyzed HAT alkylation of 2,5-dimethylpyrrole (**1**). Analytical yield in mol-% as determined by qNMR against an internal standard.

The reaction proceeds under much milder thermal conditions (110 °C) than the original Hans Fischer alkylation. A base additive is still essential, but a substoichiometric quantity is sufficient. KOH gave slightly better results than KOtBu. The reaction was extended to 1-octanol (**2i**) as aliphatic alcohol, which gave 20% of monoalkylated pyrrole (**3i**) at 160 °C. With 2,4-dimethylpyrrole (**8**) and benzyl alcohol (**2a**), a 34% yield of monoalkylated **9a** was obtained (Table S-3).

Finally, we wished to investigate the potential of HAT alkylation of pyrroles with homogeneous catalyst systems based on established ruthenium catalysts, and a few selected iridium pincer complexes (Figure 1).

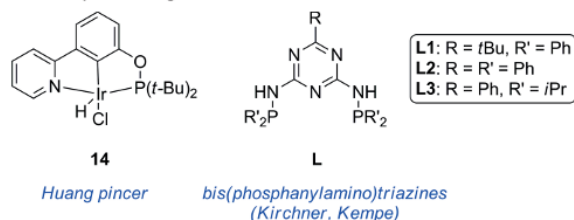
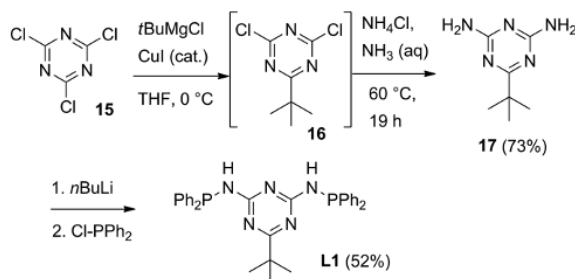


Figure 1. Structures of the Ir-NCP pincer complex (**14**) and of bis(phosphanyl)amino)triazines (**L**) as precursors for Ir-PNP pincer catalysts.

The iridium NCP-pincer complex **14** of Huang and co-workers has previously been used in HAT alkylations of esters at the

acidified α -C-H position.^[25] Iridacycles based on bis(phosphanyl)amino)triazine ligands **L**^[26] (Figure 1) were introduced by Kempe and co-workers for dehydrogenative condensation syntheses of pyrroles or pyrimidines,^[27] whereas their cobalt or iron complexes have shown activity in HAT alkylations of amines with alcohols.^[28]

Ligands **L** have the advantage of a highly modular construction principle based on a combination of 6-substituted 1,3,5-triazine-2,4-diamines and two equivalents of dialkylchlorophosphane (R_2P Cl; R = *i*Pr, *t*Bu). For the present work we extended the ligand range to 6-*tert*-butyl-substituted derivative **L1**, whose synthesis takes advantage of our selective copper-catalyzed *tert*-alkylation of multiply halogenated azines.^[29] Cyanuric chloride (**15**) was coupled with one equivalent of *t*BuMgCl to give **16**, which was aminated without isolation in the same pot by adding ammonia and ammonium chloride for solubilization of magnesium salts (Scheme 7). The new ligand **L1** was obtained by phosphonylation under basic conditions.



Scheme 7. Synthesis of a new PNP-pincer ligand (**L1**) based on selective copper-catalyzed *tert*-alkylation of cyanuric chloride.

Reaction screening started with the system Ru-DPEphos- K_3PO_4 , which had previously been successful in HAT alkylation of indoles.^[3d] The catalyst system also showed activity for pyrrole alkylation, but a stronger base was necessary for achieving conversion at 110 °C (Table 2, entries 1 vs. 2). Iridium pincer complex **14** did not show satisfactory activity in pyrrole alkylation, and mono- versus dialkylation selectivity was low (entries 3, 4). Best results were eventually obtained with Kempe-type PNP-iridium pincers, which were formed in situ from suitable iridium precursors and bis(phosphanyl)amino)triazine ligands **L1**–**L3** (Figure 1) by allowing both components to pre-complex at 50 °C for 1 h.

Up to 70% of **3a** was obtained with such a catalyst, with high selectivity over dialkylation (entries 5–16). **L3** appeared to be the most active ligand at lower catalyst loadings. Metal loading could be lowered to 1 mol-% of iridium with no loss of activity (entry 13). A sufficient excess of alcohol was required for achieving high conversion (entry 14 vs. 13). The reaction still proceeds in the absence of ligand, but the yield was lower (entry 16). In comparison to the base-catalyzed Hans Fischer alkylation, the iridium-catalyzed process is active at much lower temperature (110 vs. 240 °C). The best conditions (entry 13) were also reproduced by mixing all reaction components including the metal precursor and ligand **L3** at the outset of the reaction to obtain the products in essentially the same yield (70% **3a** + 6% **4a**), with no need for a precomplexation phase.

Table 2. Catalyst screening for the HAT alkylation of 2,5-dimethylpyrrole (**1**).^[a]

Entry	Precursor [mol-%]	Ligand [mol-%]	Base [equiv.]	BnOH [equiv.]	Solvent	T [°C]	3a ^[b] [%]	4a ^[b] [%]
1	RuCl ₂ (PPh ₃) ₃ (1.25)	DPE-Phos (1.25)	K ₃ PO ₄ (3.0)	5	neat	165	40	12
2	[Ru(<i>p</i> -cym)Cl ₂] ₂ (2.5)	DPE-Phos (5.0)	KOtBu (5.0)	10	toluene	110	53	2
3	14 (2.0)	–	–	3	neat	150	23	27
4	14 (2.0)	–	KOtBu (0.2)	3	neat	150	26	9
5 ^[c,d]	[[IrOMe(cod)] ₂] (1.5)	L3 (3.0)	KOtBu (2.0)	10	dioxane	105	26	1
6 ^[c]	[[IrOMe(cod)] ₂] (2.0)	L1 (4.2)	KOtBu (2.0)	10	toluene	110	57	3
7 ^[c]	[[Ir(cod)Cl] ₂] (2.0)	L1 (4.2)	KOtBu (2.0)	10	toluene	110	64	6
8 ^[c]	[[Ir(cod)Cl] ₂] (2.0)	L3 (4.2)	KOtBu (2.0)	10	toluene	110	70	6
9 ^[c]	[[Ir(cod)Cl] ₂] (2.0)	L2 (4.2)	KOtBu (2.0)	10	toluene	110	70	3
10 ^[c]	[[Ir(cod)Cl] ₂] (2.0)	L2 (4.2)	K ₃ PO ₄ (2.0)	10	toluene	110	44	1
11 ^[c]	[[Ir(cod)Cl] ₂] (1.0)	L2 (2.1)	KOtBu (2.0)	10	toluene	110	62	3
12 ^[c]	[[Ir(cod)Cl] ₂] (1.0)	L3 (2.1)	KOtBu (2.0)	10	toluene	110	71	7
13 ^[c,d]	[[Ir(cod)Cl] ₂] (0.5)	L3 (1.05)	KOtBu (2.0)	10	toluene	110	70 (52)	4
14 ^[c,d]	[[Ir(cod)Cl] ₂] (0.5)	L3 (1.05)	KOtBu (2.0)	5	toluene	110	51	5
15 ^[c,d]	[[Ir(cod)Cl] ₂] (0.5)	L3 (1.05)	KOtBu (1.0)	10	toluene	110	61	2
16 ^[d]	[[Ir(cod)Cl] ₂] (0.5)	–	KOtBu (2.0)	10	toluene	110	34	3

[a] All reactions were performed with 1.0 mmol pyrrole. [b] Yields were determined by qNMR against 1,1,2,2-tetrachloroethane as internal standard. Yields of isolated product are given in parenthesis. [c] Precomplexation of Ir precursor and ligand for 1 h at 50 °C in the corresponding solvent. [d] 1.5 mmol pyrrole.

Table 3. Variation of the alcohol in the catalytic HAT alkylation of pyrroles.^[a]

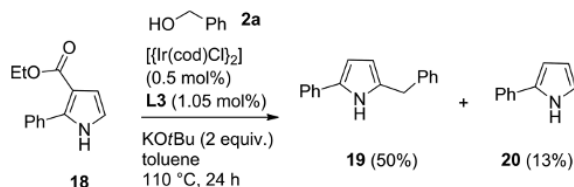
Entry	Pyrrole	Alcohol	Monoalkylation product	Yield ^[b] [%]	Dialkylation product	Yield ^[b] [%]
1	1	2g	3g	68	4g	4
2	1	2j	3j	69	4j	3
3	1	2d	3d	21	4d	3
4	1	<i>n</i> OctOH (2i)	3i	43	4i	0
5	8	BnOH (2a)	9a	49	10a	20
6	8	2g	9g	55	10g	12
7	8	<i>n</i> OctOH (2i)	9i	63	10i	10

[a] All reactions were performed with 1.5 mmol pyrrole. Precomplexation of [[Ir(cod)Cl]₂] and **L3** in toluene for 1 h at 50 °C. [b] Yields were determined by qNMR against 1,1,2,2-tetrachloroethane as an internal standard.

The optimal catalyst system from the screening successfully realized the alkylation of pyrroles **1** and **8** with some substituted benzylic alcohols (**2**) in similar yields compared to **2a** (Table 3, entries 1, 2).

The somewhat bulky 1-naphthylmethanol (**2d**) gave a low yield of monosubstituted product **3d** (entry 3). This can be attributed to steric hindrance, which may be pronounced in the presumed intermediary arylidene-azafulvene (see below). With an aliphatic alcohol, the conversion was lower (entry 4). Pyrrole **8** gave mixtures of mono- (**9**) and dialkylation (**10**) products under the catalytic alkylation conditions, with monoalkylation being favored. This underlines the higher reactivity of this substrate as a result of having available a free α -position (entries 5–7). Consequently, the C-5 position is always alkylated first, whereas products of C-3 monoalkylation have not been observed. Reactions with secondary alcohols including 2-propanol or 1-phenylethanol were not successful.

As in the case of the base-catalyzed pyrrole alkylation, the iridium-pincer-catalyzed reaction could be performed with pyrrole carboxylic esters^[30] as starting material, which undergo consecutive de-alkoxycarbonylation and alkylation (Scheme 8).

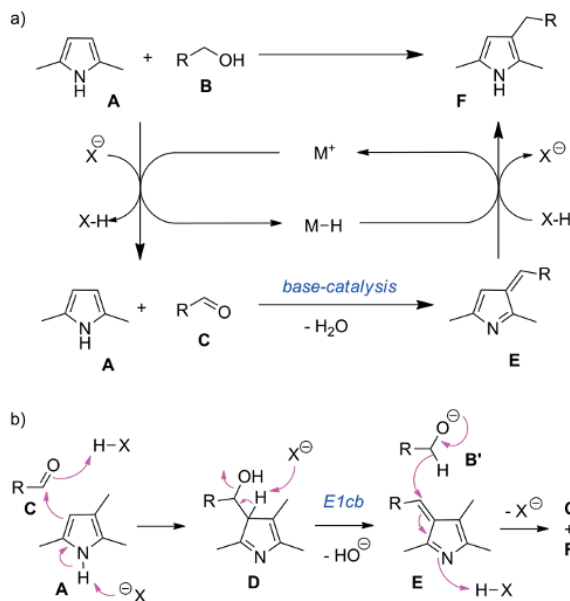


Scheme 8. Iridium pincer complex and base-catalyzed consecutive de-alkoxycarbonylation/HAT alkylation of a pyrrole ester. Yield of isolated product is given for **19**, qNMR yield for **20**.

The N-substituted substrate *N*-phenyl-2,5-dimethylpyrrole was not alkylated by benzyl alcohol under those conditions; neither did it react under the Pd/C–KOH conditions, or under the Hans Fischer alkylation conditions with base as the exclusive catalyst.

We can now propose a mechanistic scheme for this reaction and its variations (Scheme 9a).

Starting from the general mechanism of HAT alkylation (Scheme 1) and taking into account the mechanism of base-catalyzed HAT alkylation of indoles,^[10] we may assume that alcohol **B** is deprotonated by a general base (X^-) to give the alkoxide **B'**, which is oxidized by β -hydride elimination to the metal center (Ir, Ru; via their alkoxides), thereby giving aldehyde **C**. The presence of aldehyde in the final reaction mixtures (and thus also during the reaction) was proven by qNMR analysis. Next, electrophilic aldehyde **C** is attacked either by free pyrrole **A** or its N-centered anion as nucleophile, with HX acting as general acid (Scheme 9b). This step is corroborated by the regioselectivity of the overall reaction, which mirrors the known nucleophilicity pattern in pyrroles. Addition product **D** will easily eliminate water to give azafulvene **E**, which can be reduced to the final, alkylated pyrrole **F** by hydride transfer from the metal hydride. In case of the base-induced Hans Fischer alkylation, one may assume that the reduction step occurs as a conjugate 1,4-hydride transfer from alkoxide **B'** (as in the Canni-



Scheme 9. Proposed mechanisms for: a) metal-catalyzed, or; b) base-induced HAT alkylation of pyrroles with alcohols.

zarro reaction,^[8] or in hydride transfers from Hantzsch esters^[31] to azafulvene **E**, with concomitant general acid catalysis by HX, which will usually be alcohol **B** itself (Scheme 9, b). Azafulvene intermediates of pyrroles are not particularly well known in the pure state, but the related 3-benzylidene-3*H*-indole is a stable compound.^[32] Furthermore, azafulvenes related to pyrroles are postulated as intermediates in the reduction of acyl- to alkylpyrroles by sodium borohydride.^[33]

Conclusions

In this project, we have explored the possibilities of HAT alkylations of simple model pyrroles. At the outset, we were inspired by an early report from Hans Fischer, who described pyrrole alkylation by alkali alkoxides in alcohols at elevated temperature (210–220 °C, sealed-tube conditions). The mechanism of that reaction had been considered an unsolved problem for many years.^[13,19,20] By heating model pyrroles with potassium *tert*-butoxide and benzyl alcohol in a microwave reactor to 240–250 °C, we have been able to reproduce the observations of Hans Fischer in that we obtained a range of alkylated pyrroles. The similarity of the reaction conditions and regioselectivity indicate that the early Hans Fischer alkylation is mechanistically closely related to what is currently discussed as the “borrowing-hydrogen” reaction or HAT alkylation. In particular, the chemistry is also related to recent work by Yus and co-workers on the base-catalyzed HAT alkylation of indoles.^[10] The Hans Fischer alkylation of pyrroles requires harsh reaction conditions, which also induce a remarkable $\text{S}_{\text{N}}2$ transalkylation of a methyl group from aromatic methyl ethers to primary alkoxides (Scheme 5). Even if the chemoselectivity of the process is thus limited, it was possible to obtain 50–60 % of single, pure alkylation

products in suitable model reactions. Furthermore, we were able to realize the reaction starting from pyrrole esters rather than free pyrroles as substrates, because cleavage of the alkoxy-carbonyl group and C-alkylation are both induced by strong base. Considering that pyrroles tend to be quite unstable and cannot be stored for prolonged time, this approach has practical advantages.

In the second part of this work we have modernized the alkylation chemistry introduced by Hans Fischer in 1912 through application of the most recent tools from the field of transition-metal-catalyzed HAT alkylations. The most successful catalyst systems for HAT alkylation of pyrroles identified in this work are iridium-P,N,P-pincer complexes generated *in situ* based on bis(phosphinylamino)triazine ligands, which Kempe and co-workers had earlier used in dehydrogenative condensation reactions.^[27] We now find that such complexes are suitable HAT-alkylation catalysts that allow the HAT alkylation of pyrroles to be performed under fairly mild reaction conditions (110 °C, 24 h).

Experimental Section

General Remarks: Unless otherwise specified, all reagents and solvents were obtained from commercial suppliers and used without further purification. 2,5-dimethylpyrrole (**1**),^[34] 2,4-dimethylpyrrole (**8**),^[23b] 2-isopropyl-5-phenylpyrrole (**5**),^[35] diethyl 2,4-dimethylpyrrole-3,5-dicarboxylate (**11**),^[23a] and ethyl 2-phenylpyrrole-3-carboxylate (**18**)^[30] were prepared according to literature procedures. Ir-NCP pincer complex **14** and ligands **L2**, **L3** were also prepared according to literature procedures.^[35,25a,26] Solvents for water-free reactions were dried by passing through a column of Al₂O₃ and then kept over 3 Å molecular sieves under an argon atmosphere.^[36] The residual water content in dried solvents was analyzed by coulometric Karl Fischer titration.

Chromatography: Column chromatography (CC) was performed on silica gel 60 (35–70 µm particle size), usually as a flash chromatography with 0.2 bar positive air pressure. Thin layer chromatography was performed on glass plates coated with silica gel 60 F₂₅₄ and visualized with UV light (254 nm), molybdenum stain (Moston)^[37] or anisaldehyde stain.^[38]

Microwave Reactions: Reactions with microwave heating were performed in a mono-mode-type microwave reactor (Anton Paar Monowave 300) at a fixed target temperature (measured by IR sensor) with adaptive power setting under adiabatic conditions. The reaction time indicated refers to heating at target temperature without heating and cooling phases.

Analytical Data: NMR spectra were recorded at 300, 400, or 500 MHz (¹H) at ambient temperature (19–25 °C). Chemical shift δ is given in ppm. ¹H NMR spectra were internally referenced to tetramethylsilane (TMS, $\delta_{\text{H}} = 0.00$) or residual solvent peaks; in CDCl₃: $\delta_{\text{H}} = 7.26$; in (D₆)-DMSO: $\delta_{\text{H}} = 2.50$ ppm. ¹³C NMR spectra were referenced to solvent peaks. CDCl₃: $\delta_{\text{C}} = 77.16$; (D₆)-DMSO, $\delta_{\text{C}} = 39.52$ ppm.

Reaction Component Analysis by qNMR: Yield determinations by qNMR were carried out by means of suitable internal standards and appropriate pulse sequences, typically using a pulse repetition delay d1 of ≥ 20 sec, see ref. [39].

General Procedure 1 for the Microwave-Assisted, Base-Catalyzed Pyrrole Alkylation (GP 1): Into a microwave glass vessel

equipped with a stirring bar (1 cm) were added pyrrole (1.00 mmol), alcohol (2 mL if neat), base and, if indicated, additional solvent (2 mL). The reaction mixture was heated in a microwave reactor using a temperature-driven variable power setting. After the target temperature was reached, it was kept constant for the indicated reaction time. Following cooling to room temperature, a saturated solution of aq. NH₄Cl (and optionally water to dissolve solid residues) was added. The phases were separated and the aqueous phase was extracted with Et₂O (3 ×). The combined organic phase was washed with water and brine and dried with MgSO₄. Et₂O was removed in vacuo (≥ 500 mbar) and 1,1,2,2-tetrachloroethane (20 µL, 0.191 mmol) was added as an internal standard for qNMR spectroscopy.

General Procedure 2 for the Pd/C-Catalyzed Pyrrole Alkylation (GP 2): A 10 mL Schlenk tube was charged with pyrrole (1.00 mmol), Pd/C (10 wt.-% of catalyst, 5 % Pd on carbon), alcohol and base under argon. The tube was closed and the reaction mixture was heated for the indicated time in an oil bath. After cooling to room temperature, the mixture was filtered through celite; the celite was washed with Et₂O. The filtrate was evaporated in vacuo (≥ 500 mbar), and 1,1,2,2-tetrachloroethane (20 µL, 0.191 mmol) was added as internal standard for qNMR spectroscopy.

General Procedure 3 (GP 3) for the Homogenously Catalyzed Pyrrole Alkylation without Precomplexation: (Table 2, entries 1–4 and 16): A 10 mL Schlenk tube was charged with 2,5-dimethylpyrrole (**1**), metal complex, ligand, base, alcohol (**2**) and, if indicated, dry toluene (1 mL/mmol) under argon. The tube was closed and the reaction mixture was heated at the specified temperature for 24 h in an aluminum block. After cooling to room temperature, Et₂O and saturated NH₄Cl aq. were added. The phases were separated, the organic phase washed with water and brine and dried with MgSO₄. After filtration, Et₂O was removed in vacuo (≥ 500 mbar), and 1,1,2,2-tetrachloroethane was added as internal standard for qNMR spectroscopy.

General Procedure 4 (GP 4) for the Homogenously Catalyzed Pyrrole Alkylation with Precomplexation of Ligand and Metal Precursor: (Table 2, entries 5–15 and Table 3): A 10 mL Schlenk tube was charged with iridium precursor, ligand, and dry solvent under argon. The reaction mixture, which immediately turned red, was stirred at 50 °C for 1 h. The oil bath was removed and pyrrole, alcohol, base, and additional dry solvent were added. The tube was closed and the mixture was heated at the specified temperature for 24 h in a metal heating block. After cooling to room temperature, Et₂O and a saturated solution of aq. NH₄Cl were added. The phases were separated, the organic phase was washed with water and brine and dried with MgSO₄. After filtration, Et₂O was removed in vacuo (≥ 500 mbar) and 1,1,2,2-tetrachloroethane was added as an internal standard for qNMR spectroscopy.

Deuterium-Labeling Experiments on the Base-Induced Alkyl Transfer

Syntheses of Deuterated Substrates

{[3-(D₃)-Methoxy]phenyl}methanol [(CD₃O)-2g]: To a solution of 3-hydroxybenzyl alcohol (2.00 g, 16.1 mmol, 1.00 equiv.) in DMF (10 mL) was added powdered potassium carbonate (3.80 g, 27.5 mmol, 1.71 equiv.) and CD₃I (1.25 mL, 20.0 mmol, 1.24 equiv.) under vigorous stirring. The resulting suspension was stirred for 30 h at room temperature. The reaction was quenched by addition of a water/brine (1:1). After extraction with EtOAc (3 ×), the combined organic phases were washed with water/brine (1:1, 4 ×) and dried with MgSO₄. After filtration, the solvent was removed by rotary evaporation and the crude product was purified by column

chromatography (hexane/EtOAc, 3:1) to give 1.93 g (85%) of (CD₃O)-**2g** as a colorless oil. *R*_f 0.20 (hexane/EtOAc, 3:1). ¹H NMR (400 MHz, CDCl₃): δ = 7.30–7.24 (m, 1 H, Ar-H), 6.96–6.91 (m, 2 H, Ar-H), 6.86–6.80 (m, 1 H), 4.67 (s, 2 H, CH₂OH), 1.76 (br. s, 1 H, OH) ppm. ¹³C NMR (101 MHz, CDCl₃): δ = 159.98, 142.68, 129.73, 119.21, 113.40, 112.38, 65.40, 54.55 (sept, *J*_{C-D} = 22 Hz) ppm. HRMS (EI): calcd. for C₈H₇D₃O₂⁺: 141.0864, found 141.0860.

[[4-(OCD₃)-Methoxy]phenyl]methanol [(CD₃O)-2h]: To a solution of 4-hydroxybenzaldehyde (1.87 g, 15.3 mmol, 1.00 equiv.) in DMF (10 mL), powdered potassium carbonate (3.60 g, 26.0 mmol, 1.70 equiv.) and CD₃I (1.25 mL, 20.0 mmol, 1.31 equiv.) were added under vigorous stirring. The resulting suspension was stirred for 30 h at room temperature. Ethanol (10 mL) was added to the mixture, followed by sodium borohydride (0.30 g, 7.93 mmol, 0.52 equiv.) in portions. The reaction mixture was stirred for 3 h at room temperature until aldehyde was no longer detected by TLC. Ethanol was removed by rotary evaporation and the residue was partitioned between water, EtOAc, and brine. The aqueous phase was extracted with EtOAc (2 ×). The combined organic phases were washed with water/brine (1:1) and dried with MgSO₄. After filtration, the solvent was removed by rotary evaporation and the crude product was purified by column chromatography (hexane/EtOAc, 3:1) to give 1.96 g (91%) of (CD₃O)-**2h** as a colorless oil. *R*_f 0.17 (hexane/EtOAc, 3:1). ¹H NMR (400 MHz, CDCl₃): δ = 7.29 (d, *J* = 7.9 Hz, 2 H, Ar-H), 6.89 (d, *J* = 8.0 Hz, 2 H, Ar-H), 4.61 (s, 2 H, CH₂OH), 1.67 (br. s, 1 H, OH) ppm. ¹³C NMR (101 MHz, CDCl₃): δ = 159.33, 133.24, 128.77, 114.07, 65.15, 54.61 (sept, *J*_{C-D} = 22 Hz) ppm. HRMS (EI): calcd. for C₈H₇D₃O₂⁺: 141.0864, found 141.0861. Known compound, CAS 14629-71-1.

Alkyl-Transfer Experiments

Preparative Run with [3-(OCD₃)-Methoxyphenyl]methanol: A microwave vial was charged with [3-(OCD₃)-methoxyphenyl]methanol [(CD₃O)-**2g**; 706 mg, 5.00 mmol, 1.00 equiv.], potassium *tert*-butoxide (561 mg, 5.00 mmol, 1.00 equiv.), and toluene (2 mL). The reaction mixture was heated in a microwave reactor at 250 °C for 1 h. After cooling to room temperature, a saturated solution of aq. NH₄Cl (5 mL) and EtOAc (20 mL) was added. After separation of the phases, the organic layer was washed with water (5 mL) and brine (5 mL) and dried with Na₂SO₄. The solvent was evaporated and the crude product mixture was purified by column chromatography (hexane/EtOAc, 20:1 → 4:1) to afford 1-(CD₃O)-**13g** (218 mg, 31%) and 1,3'-(CD₃O)₂-**12g** (156 mg, 20%) as colorless oils.

[3-(D₃)-Methoxymethyl]phenol [1-(CD₃O)-13g]: ¹H NMR (500 MHz, CDCl₃): δ = 7.21 (t, *J* = 7.8 Hz, 1 H, Ar-H), 6.88 (d, *J* = 7.5 Hz, 1 H, Ar-H), 6.85–6.82 (m, 1 H, Ar-H), 6.76 (dd, *J* = 8.1, 2.5 Hz, 1 H, Ar-H), 5.13 (br. s, 1 H, OH), 4.43 (s, 2 H, CH₂OCD₃) ppm. ¹³C NMR (101 MHz, CDCl₃): δ = 156.21, 139.53, 129.79, 120.08, 115.08, 114.81, 74.48, 57.15 (sept, *J*_{C-D} = 22 Hz) ppm. HRMS (EI): calcd. for C₈H₇D₃O₂⁺: 141.0864, found 141.0862.

[1-(D₃)-Methoxy]-3-(OCD₃)-(methoxymethyl)benzene [1,3'-(CD₃O)₂-12g]: ¹H NMR (500 MHz, CDCl₃): δ = 7.29–7.23 (m, 1 H, Ar-H), 6.94–6.87 (m, 2 H, Ar-H), 6.83 (dd, *J* = 7.9, 1.9 Hz, 1 H, Ar-H), 4.44 (s, 2 H, CH₂OCD₃) ppm. ¹³C NMR (101 MHz, CDCl₃): δ = 159.90, 140.01, 129.53, 120.03, 113.50, 112.98, 74.63, 57.26 (sept, *J*_{C-D} = 22 Hz), 54.54 (sept, *J*_{C-D} = 22 Hz) ppm. HRMS (EI): calcd. for C₉H₆D₆O₂⁺: 158.1208, found 158.1203.

Analytical Runs with (CD₃O)-2g and (CD₃O)-2h: A microwave vial was charged with deuterium-labeled methoxybenzyl alcohol (CD₃O)-**2g** or (CD₃O)-**2h** (141 mg, 1.00 mmol, 1.00 equiv., 100 mol-%), potassium *tert*-butoxide (112 mg, 1.00 mmol, 1.00 equiv.) and toluene (2 mL). The reaction mixture was heated in a microwave

reactor at 250 °C for 1 h. After cooling to room temperature, a solution of sat. NH₄Cl aq. (3 mL) and EtOAc (15 mL) was added. After separation of the phases, the organic layer was washed with water (5 mL) and brine (5 mL) and dried with MgSO₄. After filtration, the solvent was removed in vacuo. The residue was dissolved in CDCl₃ and 1,1,2,2-tetrachloroethane (20 μL, 0.191 mmol) was added as internal standard for qNMR spectroscopy.

¹H NMR Analysis of Reaction Mixture from [3-(D₃)-Methoxyphenyl]methanol [(CD₃O)-2g]: 30 mol-% HO-C₆H₄-CH₂OCD₃ [1-(CD₃O)-**13g**] [δ_H = 4.39 (s), CH₂OCD₃], 25 mol-% D₃CO-C₆H₄-CH₂OCD₃ [1,3'-(CD₃O)₂-**12g**] [δ_H = 4.45 (s), CH₂OCD₃], 6 mol-% HO-C₆H₄-CH₂OH (**2e**) [δ_H = 4.56 (s), CH₂OH] and 8 mol-% starting material [(CD₃O)-**2g**] [δ_H = 4.63 (s), CH₂OH].

¹H NMR Analysis of Reaction Mixture from [4-(D₃)-Methoxyphenyl]methanol [(CD₃O)-2h]: 22 mol-% D₃CO-C₆H₄-CH₂OCD₃ [1,4'-(CD₃O)₂-**12h**] [δ_H = 4.39 (s), CH₂OCD₃] and 15 mol-% starting material [(CD₃O)-**2h**] [δ_H = 4.61 (s), CH₂OH].

Synthesis of Ligand L1

6-(*tert*-Butyl)-1,3,5-triazine-2,4-diamine (**17**)

Grignard-Reagent: In a Schlenk flask under argon, Mg turnings (2.67 g, 110 mmol, 1.10 equiv.) were overlaid with dry THF. A crystal of iodine and a small fraction of *tert*-butyl chloride (totally 11.0 mL, 100 mmol, 1.00 equiv.) were added. The mixture was slightly warmed until the color of iodine vanished and the reaction started. The remaining chloride and dry THF (totally 50 mL) were slowly added over 30 min, maintaining a moderate boiling. The reaction mixture was then heated to 65 °C for 1 h. The Grignard solution was titrated against salicylic aldehyde phenylhydrazone.^[40]

Coupling/Amination:^[29] In a Schlenk flask under argon atmosphere, cyanuric chloride (**15**; 7.03 g, 38.1 mmol, 1.00 equiv.) and CuI (362 mg, 1.90 mmol, 0.05 equiv.) were suspended in dry THF (25 mL) and cooled to -20 °C. A solution of *tert*-butylmagnesium chloride (93 mL; 0.43 M in THF, 40.0 mmol, 1.05 equiv.) was added dropwise over 40 min. After warming to 0 °C and stirring for 30 min, the content of the flask was poured into 25% aq. NH₃ (400 mL). The mixture was heated to 60 °C and stirred for 19 h. Saturated aq. NH₄Cl was added to dissolve magnesium salts. The mixture was basified with 25% NH₃ (aq.) and extracted with EtOAc (3 ×). The organic phases were washed with water and brine. After drying over MgSO₄ and filtration, evaporation in vacuo gave 6-(*tert*-butyl)-1,3,5-triazine-2,4-diamine (**17**; 4.67 g, 73%) as a colorless solid. The compound can be recrystallized from dichloromethane. *R*_f 0.30 (hexane/EtOAc, 1:2). M.p. 168–170 °C (lit.^[41] 169–171 °C). ¹H NMR (400 MHz, CDCl₃): δ = 5.02 (br. s, 4 H, NH₂), 1.26 (s, 9 H, CH₃) ppm. ¹³C NMR (101 MHz, CDCl₃): δ = 186.23, 167.38, 38.56, 28.70 ppm. C₇H₁₃N₅ (167.22): calcd. C 50.28, H 7.84, N 41.88; found C 50.01, H 7.80, N 41.91. Known compound, CAS 35841-84-0.

(6-*tert*-Butyl)-N²N⁴-bis(diphenylphosphanyl)-1,3,5-triazine-2,4-diamine (L1**):** Synthesis performed in analogy to literature procedures.^[26,27a] A Schlenk flask under argon atmosphere was charged with 6-(*tert*-butyl)-1,3,5-triazine-2,4-diamine (**17**; 500 mg, 2.99 mmol, 1.00 equiv.) and dry THF (20 mL). After cooling to -20 °C (NaCl/ice), *n*BuLi (4.02 mL, 1.5 M in hexane, 6.13 mmol, 2.05 equiv.) was added dropwise. The resulting white suspension was warmed to room temperature and stirred for 30 min. Chlorodiphenylphosphine (1.10 mL, 5.98 mmol, 2.00 equiv.) was added dropwise at approximately -10 °C and the resulting clear solution was warmed and stirred overnight at room temperature. The solvent was removed in vacuo and the slightly yellow, foamy residue was suspended in CH₂Cl₂. Filtration removed most of the LiCl precipitate. The solvent was removed in vacuo and the crude product was puri-

fied by column chromatography (in air, hexane/EtOAc, 10:1) to afford **L1** (828 mg, 52%) as a white, crystalline solid. R_f 0.20 (hexane/EtOAc, 10:1). $^1\text{H NMR}$ (500 MHz, C_6D_6): δ = 7.46–7.20 (m, 8 H, Ar-H), 7.09–6.89 (m, 12 H, Ar-H), 5.62 (br. s, 2 H, NH), 1.41 (s, 9 H, CH_3) ppm. $^{13}\text{C NMR}$ (126 MHz, C_6D_6): δ = 185.93, 168.23, 139.58 (d, J = 16.1 Hz), 131.59 (d, J = 22.1 Hz), 128.90, 128.39 (d, J = 6.6 Hz), 38.93, 28.65 ppm. $^{31}\text{P NMR}$ (203 MHz, C_6D_6): δ = 28.45 (br. s, 62%), 25.68 (br. s, 38%; tautomers?) ppm. HRMS (EI) calcd. for $\text{C}_{31}\text{H}_{31}\text{N}_5\text{P}_2^+$: 535.2049, found 535.2052.

Isolated Pyrrole Alkylation Products

3-Benzyl-2,5-dimethylpyrrole (3a): The product was synthesized according to GP 4. A 10 mL Schlenk tube was charged with $[\text{Ir}(\text{cod})\text{Cl}]_2$ (5.0 mg, 7.5 μmol , 0.5 mol-%), ligand **L3** (6.6 mg, 15.8 μmol , 1.05 mol-%) and dry toluene (0.2 mL) under argon. The reaction mixture, which immediately turned red, was stirred at 50 °C for 60 min. The oil bath was removed and 2,5-dimethylpyrrole (**1**; 153 μL , 1.50 mmol, 1.00 equiv.), benzyl alcohol (1.55 mL, 15.0 mmol, 10.0 equiv.), potassium *tert*-butoxide (337 mg, 3.00 mmol, 2.00 equiv.), and dry toluene (1.3 mL) were added. The tube was tightly closed and the mixture was heated at 110 °C for 24 h in an aluminum heating block. After cooling to room temperature, Et_2O (20 mL) and saturated aqueous NH_4Cl (7 mL) were added. The phases were separated; the organic phase was washed with water (5 mL) and brine (5 mL) and dried with MgSO_4 . After filtration, the solvent was removed in vacuo and the crude product was purified by Kugelrohr distillation (115 °C, 0.15 mbar) to give **3a** (144 mg, 52%) as a white crystalline solid. The compound is not very stable and slowly decomposes, even if stored under argon at 4 °C, under exclusion of light. $^1\text{H NMR}$ (400 MHz, CDCl_3): δ = 7.42 (br. s, 1 H, NH), 7.29–7.24 (m, 2 H, Ar-H), 7.23–7.19 (m, 2 H, Ar-H), 7.18–7.13 (m, 1 H, Ar-H), 5.62 (d, J = 2.7 Hz, 1 H, Ar-H), 3.72 (s, 2 H, CH_2), 2.19 (s, 3 H, CH_3), 2.17 (s, 3 H, CH_3) ppm. $^{13}\text{C NMR}$ (101 MHz, CDCl_3): δ = 142.86, 128.55, 128.37, 125.58, 125.24, 122.23, 118.25, 107.30, 32.46, 13.11, 11.20 ppm. HRMS (EI) calcd. for $\text{C}_{13}\text{H}_{15}\text{N}^+$: 185.1199, found 185.1199.

2-Benzyl-5-phenylpyrrole (19): The product was synthesized according to GP 4. A 10 mL Schlenk tube was charged with $[\text{Ir}(\text{cod})\text{Cl}]_2$ (5.0 mg, 7.5 μmol , 0.5 mol-%), ligand **L3** (6.6 mg, 15.8 μmol , 1.05 mol-%) and dry toluene (0.2 mL) under argon. The reaction mixture, which immediately turned red, was stirred at 50 °C for 60 min. The oil bath was removed and 2-phenylpyrrole-3-carboxylate (**18**; 323 mg, 1.50 mmol, 1.00 equiv.), benzyl alcohol (1.55 mL, 15.0 mmol, 10.0 equiv.), potassium *tert*-butoxide (337 mg, 3.00 mmol, 2.00 equiv.), and dry toluene (1.3 mL) were added. The tube was closed and the mixture was heated at 110 °C for 24 h in an aluminum heating block. After cooling to room temperature, Et_2O (20 mL) and a saturated solution of aq. NH_4Cl (7 mL) were added. The phases were separated, the organic one was washed with water (5 mL) and brine (5 mL) and dried with MgSO_4 . After filtration, the solvent was removed in vacuo and the crude product was purified by column chromatography (hexane/EtOAc = 20:1) to give 176 mg (50%) of **19** as a slightly pink solid. R_f 0.52 (hexane/EtOAc, 4:1). $^1\text{H NMR}$ (300 MHz, CDCl_3): δ = 8.00 (br. s, 1 H, NH), 7.40–7.20 (m, 9 H, Ar-H), 7.17–7.10 (m, 1 H, Ar-H), 6.45–6.41 (m, 1 H, Ar-H), 6.06–6.02 (m, 1 H, Ar-H), 4.01 (s, 2 H, CH_2) ppm. $^{13}\text{C NMR}$ (75 MHz, CDCl_3): δ = 139.39, 132.93, 132.12, 131.64, 128.92, 128.83, 128.80, 126.69, 125.96, 123.59, 108.76, 106.24, 34.39 ppm. Known compound, CAS 905971-72-4.

Supporting Information: Contains further information on the Hans Fischer alkylation of pyrroles with alkali alkoxide (Table S-1), additional screening experiments (Table S-2, S-3), and analytical data for alkylated pyrroles detected in reaction mixtures and NMR spectra.

Acknowledgments

We thank the Hans-Fischer-Gesellschaft for financial support.

Keywords: Alkylation · Borrowing Hydrogen · Homogeneous catalysis · Iridium · Pyrrole

- [1] a) T. D. Nixon, M. K. Whittlesey, J. M. J. Williams, *Dalton Trans.* **2009**, 753–762; b) G. Guillena, D. J. Ramón, M. Yus, *Angew. Chem. Int. Ed.* **2007**, *46*, 2358–2364; *Angew. Chem.* **2007**, *119*, 2410; c) R. Yamaguchi, K. Fujita, M. Zhu, *Heterocycles* **2010**, *81*, 1093–1140; d) Y. Obora, Y. Ishii, *Synlett* **2011**, 30–51; e) F. Alonso, F. Foubelo, J. C. González-Gómez, R. Martínez, D. J. Ramón, P. Riente, M. Yus, *Mol. Diversity* **2010**, *14*, 411–424; f) S. Bähn, S. Imm, L. Neubert, M. Zhang, H. Neumann, M. Beller, *ChemCatChem* **2011**, *3*, 1853–1864; g) G. E. Dobreiner, R. H. Crabtree, *Chem. Rev.* **2010**, *110*, 681–703; h) G. Guillena, D. J. Ramón, M. Yus, *Chem. Rev.* **2010**, *110*, 1611–1641; i) J. Leonard, A. J. Blacker, S. P. Marsden, M. F. Jones, K. R. Mulholland, R. Newton, *Org. Process Res. Dev.* **2015**, *19*, 1400–1410; j) X. Ma, C. Su, Q. Xu, *Top. Curr. Chem.* **2016**, *374*, 27.
- [2] a) F. Huang, Z. Liu, Z. Yu, *Angew. Chem. Int. Ed.* **2015**, *54*, 862–875; *Angew. Chem.* **2015**, *127*, 12860; b) Y. Obora, *Top. Curr. Chem.* **2016**, *374*, 11; c) Y. Obora, *ACS Catal.* **2014**, *4*, 3972–3981.
- [3] a) S. Whitney, R. Grigg, A. Derrick, A. Keep, *Org. Lett.* **2007**, *9*, 3299–3302; b) S. Bartolucci, M. Mari, A. Bedini, G. Piersanti, G. Spadoni, *J. Org. Chem.* **2015**, *80*, 3217–3222; c) S. Bartolucci, M. Mari, G. Di Gregorio, G. Piersanti, *Tetrahedron* **2016**, *72*, 2233–2238; d) A. E. Putra, K. Takigawa, H. Tanaka, Y. Ito, Y. Oe, T. Ohta, *Eur. J. Org. Chem.* **2013**, 6344–6354.
- [4] S. M. A. H. Siddiki, K. Kon, K. Shimizu, *Chem. Eur. J.* **2013**, *19*, 14416–14419.
- [5] a) S. Imm, S. Bähn, A. Tillack, K. Mevius, L. Neubert, M. Beller, *Chem. Eur. J.* **2010**, *16*, 2705–2709; b) S. Lerch, L.-N. Unkel, M. Brasholz, *Angew. Chem. Int. Ed.* **2014**, *53*, 6558–6562; *Angew. Chem.* **2014**, *126*, 6676.
- [6] Under acidic conditions, the HAT alkylation of indoles with alcohols takes place at nitrogen: S. Bähn, S. Imm, K. Mevius, L. Neubert, A. Tillack, J. M. J. Williams, M. Beller, *Chem. Eur. J.* **2010**, *16*, 3590–3593.
- [7] T. Donohoe, J. Frost, C. Cheong, *Synthesis* **2016**, *48*, 910–916.
- [8] C. G. Swain, A. L. Powell, W. A. Sheppard, C. R. Morgan, *J. Am. Chem. Soc.* **1979**, *101*, 3576–3583.
- [9] a) L. J. Allen, R. H. Crabtree, *Green Chem.* **2010**, *12*, 1362–1364; b) Q. Xu, J. Chen, H. Tian, X. Yuan, S. Li, C. Zhou, J. Liu, *Angew. Chem. Int. Ed.* **2014**, *53*, 225–229; *Angew. Chem.* **2014**, *126*, 229.
- [10] R. Cano, M. Yus, D. J. Ramón, *Tetrahedron Lett.* **2013**, *54*, 3394–3397.
- [11] Other base-mediated HAT-alkylation of heterocycles: a) B. Xiong, S. Zhang, H. Jiang, M. Zhang, *Org. Lett.* **2016**, *18*, 724–727; b) Y.-F. Zhu, G.-P. Lu, C. Cai, *J. Chem. Res.* **2015**, *39*, 438–441.
- [12] S.-J. Chen, G.-P. Lu, C. Cai, *RSC Adv.* **2015**, *5*, 70329–70332.
- [13] a) H. Fischer, E. Bartholomäus, *Hoppe-Seyler's Z. Physiol. Chem.* **1912**, *77*, 185–201; b) H. Fischer, E. Bartholomäus, *Ber. Dtsch. Chem. Ges.* **1912**, *45*, 466–471; c) H. Fischer, E. Bartholomäus, *Hoppe-Seyler's Z. Physiol. Chem.* **1912**, *80*, 6–16; d) H. Fischer, E. Bartholomäus, *Ber. Dtsch. Chem. Ges.* **1912**, *45*, 1979–1986; e) H. Fischer, K. Eismayer, *Ber. Dtsch. Chem. Ges.* **1914**, *47*, 1820–1828.
- [14] Official Website of the Nobel Prize, https://www.nobelprize.org/nobel_prizes/chemistry/laureates/1930/, accessed 28.4.2017.
- [15] a) H. Fischer, H. Orth, *Die Chemie des Pyrrols*, Vol. 1, Akademische Verlagsgesellschaft, Leipzig, **1934**; b) H. Fischer, A. Stern, *Die Chemie des Pyrrols*, Vol. 2, Teil 1 und 2, Akademische Verlagsgesellschaft, Leipzig, **1937**, **1940**.
- [16] A. G. Smith, M. Witty (Eds.), *Heme, chlorophyll, and bilins: methods and protocols*, Humana Press, Totowa, New Jersey, **2002**.
- [17] The book was reprinted as facsimile in **1968**, with a preface by R. B. Woodward: H. Fischer, H. Orth, A. Stern, *Die Chemie des Pyrrols*, Johnson Repr. Corp., New York, **1968**.
- [18] For a discussion of this work, see: D. A. Lightner, *Bilirubin: Jekyll and Hyde Pigment of Life*, Springer-Verlag, Wien, **2013**, p. 279 ff.
- [19] A. Treibs, *Das Leben und Wirken von Hans Fischer*, Hans-Fischer-Gesellschaft, München, **1971**. Available online at: https://www.hans-fischer-gesellschaft.de/wp-content/uploads/pdfs/Das_Leben_und_Wirken_Hans_Fischers.pdf.

- [20] Treibs (ref. [19]) wrote (p. 41): "Ein bemerkenswerter Erfolg der ersten Pyrrolarbeiten ist die Alkylierungsreaktion mit Alkoholaten zu höher substituierten, besonders Tetraalkylpyrrolen... Sie erfordert scharfe Bedingungen und steht ziemlich ohne Analogien da, ihr Mechanismus hat noch keine Erklärung gefunden." ("A remarkable success of [Fischer's]... initial work on pyrroles is the alkylation reaction with alcoholates that provides more highly substituted, especially tetraalkylpyrroles... It requires harsh conditions and is quite without analogies, its mechanism has not yet found any explanation.")
- [21] Although not mentioned in the original reports (ref. [13]), this information was conveyed by Alfred Treibs (ref. [19]), who wrote: "Die Methode war bei der Bearbeitung der Wolff-Kishner-Reaktion gefunden worden; man ließ sich nicht davon abschrecken, daß 3/4 aller Bombenröhren explodierten." ("The [pyrrole alkylation] method had been found during studies of the Wolff-Kishner reaction; one was not deterred by the fact that three out of four sealed tubes exploded.")
- [22] a) A. Gossauer, *Die Chemie der Pyrrole*, Springer, Berlin, **1974**; b) R. A. Jones, G. P. Bean, *The Chemistry of Pyrroles*, Academic Press, **1977**.
- [23] Synthesis of **8** via **11**: a) H. Fischer, *Org. Synth.* **1935**, *15*, 17–19; b) H. Fischer, *Org. Synth.* **1935**, *15*, 20–21.
- [24] a) X. Liu, P. Hermange, J. Ruiz, D. Astruc, *ChemCatChem* **2016**, *8*, 1043–1045; b) C. S. Cho, *J. Mol. Catal. A* **2005**, *240*, 55–60.
- [25] a) X. Jia, L. Zhang, C. Qin, X. Leng, Z. Huang, *Chem. Commun.* **2014**, *50*, 11056–11059; b) L. Guo, X. Ma, H. Fang, X. Jia, Z. Huang, *Angew. Chem. Int. Ed.* **2015**, *54*, 4023–4027; *Angew. Chem.* **2015**, *127*, 4095.
- [26] D. Benito-Garagorri, E. Becker, J. Wiedermann, W. Lackner, M. Pollak, K. Mereiter, J. Kisala, K. Kirchner, *Organometallics* **2006**, *25*, 1900–1913.
- [27] a) S. Michlik, R. Kempe, *Angew. Chem. Int. Ed.* **2013**, *52*, 6326–6329; *Angew. Chem.* **2013**, *125*, 6450; b) N. Deibl, K. Ament, R. Kempe, *J. Am. Chem. Soc.* **2015**, *137*, 12804–12807.
- [28] a) S. Rösler, M. Ertl, T. Irrgang, R. Kempe, *Angew. Chem. Int. Ed.* **2015**, *54*, 15046–15050; *Angew. Chem.* **2015**, *127*, 15260; b) M. Mastalir, B. Stöger, E. Pittenauer, M. Puchberger, G. Allmaier, K. Kirchner, *Adv. Synth. Catal.* **2016**, *358*, 3824–3831.
- [29] L. Hintermann, L. Xiao, A. Labonne, *Angew. Chem. Int. Ed.* **2008**, *47*, 8246–8250; *Angew. Chem.* **2008**, *120*, 8370.
- [30] J. M. Wiest, A. Pöthig, T. Bach, *Org. Lett.* **2016**, *18*, 852–855.
- [31] C. Chen, H.-X. Feng, Z.-L. Li, P.-W. Cai, Y.-K. Liu, L.-H. Shan, X.-L. Zhou, *Tetrahedron Lett.* **2014**, *55*, 3774–3776.
- [32] X.-L. Li, Y.-M. Wang, T. Matsuura, J.-B. Meng, *J. Heterocycl. Chem.* **1999**, *36*, 697–701.
- [33] R. Greenhouse, C. Ramirez, J. M. Muchowski, *J. Org. Chem.* **1985**, *50*, 2961–2965.
- [34] D. M. Young, C. F. H. Allen, *Org. Synth.* **1936**, *16*, 25–27.
- [35] S. Michlik, R. Kempe, *Nat. Chem.* **2013**, *5*, 140–144.
- [36] D. B. G. Williams, M. Lawton, *J. Org. Chem.* **2010**, *75*, 8351–8354.
- [37] Prepared from (NH₄)₆[Mo₇O₂₄]·4H₂O (10 g), Ce(SO₄)₂·4H₂O (0.2 g), H₂O (200 mL), and conc. H₂SO₄ (12 mL; added last with stirring).
- [38] Prepared from acetic acid (100 mL), conc. H₂SO₄ (2 mL), and anisaldehyde (1 mL).
- [39] a) T. Schoenberger, *Anal. Bioanal. Chem.* **2012**, *403*, 247–254; b) S. Mahajan, I. P. Singh, *Magn. Reson. Chem.* **2013**, *51*, 76–81.
- [40] B. E. Love, E. G. Jones, *J. Org. Chem.* **1999**, *64*, 3755–3756.
- [41] C. D. Bossinger, T. Enkoji (Armour Pharma), US-Patent, US3655892, **1972**.

Received: January 27, 2018

SUPPORTING INFORMATION

Title: Catalytic C-Alkylation of Pyrroles with Primary Alcohols: Hans Fischer's Alkali and a New Method with Iridium

P,N,P-Pincer Complexes

Author(s): Sebastian Koller, Max Blazejak, and Lukas Hintermann*

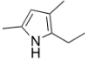
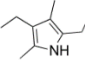
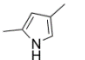
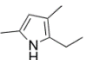
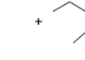
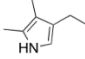
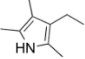
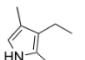
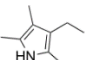
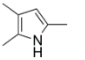
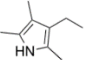
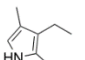
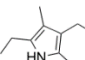
Contents

1 Hans-Fischer-alkylation of pyrroles with alkali alkoxide	2
2 HAT-alkylation of pyrroles	4
2.1 Additional screening experiments	4
2.2 Analytical data for alkylated pyrroles detected in reaction mixtures.....	6
3 NMR spectra.....	7

1 Hans-Fischer-alkylation of pyrroles with alkali alkoxide

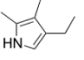
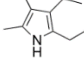
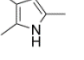
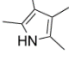
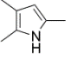
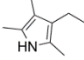
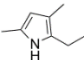
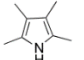
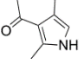
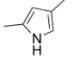
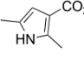
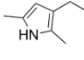
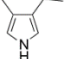
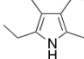
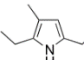
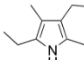
Table S-1 presents a near complete collection of the reported pyrrole alkylation reactions by means of alkali alkoxides according to the method of Hans Fischer. The data was extracted from the cited references, where it was usually only shown in text form, and is shown here in a contemporary style. Yields were calculated based on the substance amounts given in the original literature, using current molecular mass values.

Table S-1. Compilation of examples of pyrrole alkylation by Hans Fischer *et al*

Entry	Substrate	Conditions ^a	Product	Yield	Ref.
1		1 mL substrate 3 M NaOEt-EtOH (20 mL) 210–220 °C, 15 h		30% (picrate) ^b	¹
2		2.7 g substrate 3 M NaOEt-EtOH (20 mL) 210–220 °C, 8 h	 + 	60% + "very little"	¹
3		substrate: from 4 g picrate 3 M NaOMe-MeOH (20 mL) 210–220 °C, 10–12 h		57%	²
4		as above		40%	²
5		1 mL substrate 3 M NaOEt-EtOH (20 mL) 210–220 °C, 10–12 h		"yield not very good"	²
6		as above		22% (picrate) ^b	²

¹ H. Fischer, E. Bartholomäus, *Hoppe-Seyler's Z. Physiol. Chem.* **1912**, 77, 185–201.

² H. Fischer, E. Bartholomäus, *Ber. Dtsch. Chem. Ges.* **1912**, 45, 466–471.

7		as above		26% (picrate) ^b	²
8		7 g substrate 3.5 M NaOMe-MeOH 210–220 °C, ca 12 h		63% ("dampish") ³ 43% (picrate) ^b	³
9		1 mL substrate 3 M NaOPr-nPrOH (20 mL) 210–220 °C, 12 h		0% (no yield)	³
10		3.5 M NaOMe-MeOH 210–220 °C, 12 h		"mainly; not very pure"	³
11		3 M NaOMe-MeOH 200 °C, 8 h		no alkylation	³
12		1 g substrate 3 M NaOEt-EtOH (20 mL) 210–220 °C, 14 h		30% (azo-cpd) ^c	³
13		1.7 g substrate 4.3 M KOEt-EtOH (20 mL) 210 °C, 4 h		34% (picrate) ^b	⁴
14		KOEt-EtOH 210 °C, 3 h, 49 bar		26%	⁴

a) The original reactions were performed in sealed tubes; **CAUTION**: the incidence of bursting tubes was relatively high.⁵

b) "Picrate" indicates that the pyrrole was isolated as salt/complex with picric acid (2,4,6-(NO₂)₃C₆H₂OH). c) The pyrrole was coupled with diazobenzenesulfonic acid (p-N₂⁺C₆H₄SO₃⁻) and isolated as azo coupling product. Pr = propyl.

³ H. Fischer, E. Bartholomäus, *Hoppe-Seyler's Z. Physiol. Chem.* **1912**, 80, 6–16.

⁴ H. Fischer, K. Eismayer, *Chem. Ber.* **1914**, 47, 1820–1828.

⁵ A. Treibs, „Das Leben und Wirken von Hans Fischer“, Hans-Fischer-Gesellschaft e. V., München, 1971. □

2 HAT-alkylation of pyrroles

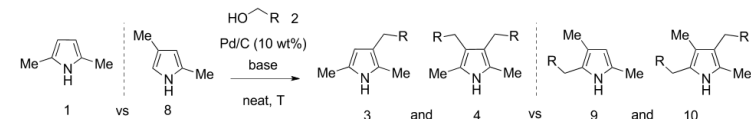
2.1 Additional screening experiments

Table S-2: Base-catalyzed HAT-alkylation of pyrroles: additional experiments^a

Entry	Pyrrole	BnOH (equiv.)	Base (equiv.)	Additive (equiv.)	Solvent (mL)	T [°C]	t [h]	3a [mol-%]	4a [mol-%]	1 [mol-%]
1 ^b	1	(3.0)	KOH (1.3)	-	neat	200	18	36	15	31
2	1	2 mL	LiOH (2.0)	-	neat	250	1	15	0	44
3 ^c	1	2 mL	Li (2.2)	-	neat	250	1	27	0	32
4 ^d	1	2 mL	Na (1.0)	-	neat	250	1	11	0	39
5	1	2 mL	KOtBu (1.0)	-	neat	250	1	40	40	0
6	1	2 mL	KOtBu (1.0)	Ph ₂ CO (0.2)	neat	250	1	37	39	10
7	1	2 mL	KOtBu (1.0)	Al(O <i>i</i> Pr) ₃ (0.2)	neat	250	1	23	18	0
8	1	(1.5)	KOtBu (2.0)	-	PhMe (2 mL)	250	1	10	1	43
9	1	(1.5)	KOtBu (2.0)	-	dioxane (2 mL)	250	1	4	0	69
10	1	(1.5)	KOtBu (2.0)	-	diglyme (2 mL)	250	1	5	<5	55
11	1	(4.0)	KOtBu (1.0)	-	PhMe (2 mL)	250	1	30	0	46
12	1	(6.0)	KOtBu (1.0)	-	PhMe (2 mL)	250	1	58	7	14
13	1	(8.0)	KOtBu (1.0)	-	PhMe (2 mL)	250	1	59	13	5
14	1	(10)	KOtBu (1.0)	-	PhMe (2 mL)	250	1	54	17	2
15	1	(6.0)	KOtBu (2.0)	-	PhMe (2 mL)	250	1	42	2	24
16	1	(6.0)	KOtBu (4.0)	-	PhMe (2 mL)	250	1	61	19	0
17	1*	2 mL	KOtBu (4.0)	-	neat	250	0.25	0	0	77 (1*)

a) Conditions: General procedure 1, with 1.00 mmol of **1**. b) Reaction conducted in an oil bath. c) Lithium metal was stirred in BnOH at 70 °C until dissolved. d) Sodium metal was stirred in BnOH at room temperature until dissolved. Diglyme = ethylene glycol dimethylether; PhMe = toluene; dioxane = 1,4-dioxane.

Table S-3: Screening of reaction conditions for Pd/C-catalyzed HAT-alkylation of pyrroles^a



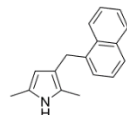
Entry	Pyrrole	Alcohol (equiv. or Vol.)	Base (equiv.)	T [°C]	t [h]	3 or 9 [mol-%]	4 or 10 [mol-%]	1 or 8 [mol-%]
1 ^b	1	BnOH (2 mL)	KOH (0.2)	110	19	29	2	3
2 ^b	1	BnOH (2 mL)	KOH (0.2)	130	16	30	1	4
3 ^b	1	BnOH (2 mL)	KOH (0.2)	150	16	31	2	8
4 ^b	1	BnOH (2 mL)	KOH (0.5)	110	19	34	3	2
5 ^b	1	BnOH (2 mL)	KOH (1.0)	110	19	27	2	11
6	1	BnOH (3.0)	KOH (0.2)	110	18	54	2	16
7	1	BnOH (3.0)	NaOH (0.2)	110	18	26	1	16
8	1	BnOH (3.0)	NaH (0.2)	110	18	13	1	30
9	1	BnOH (3.0)	KOtBu (0.2)	110	18	48	4	3
10	1	BnOH (5.0)	KOtBu (0.2)	110	18	24	2	2
11	8	BnOH (3.0)	KOtBu (0.2)	110	18	34	0	0
12 ^b	1*	BnOH (3.0)	KOtBu (0.2)	110	18	0	0	100
13	1	1-octanol (3.0)	KOH (0.2)	180	18	17	0	42
14	1	1-octanol (3.0)	KOtBu (0.2)	180	18	19	0	52
15	1	1-octanol (3.0)	-	180	18	0	0	73
16	1	1-octanol (3.0)	KOtBu (0.2)	180	41	11	0	7
17 ^c	1	1-octanol (3.0)	KOtBu (0.2)	180	18	22	0	7
18 ^c	1	1-octanol (3.0)	KOtBu (0.2)	160	18	25	0	50

a) Conditions: general procedure 2, with 1.00 mmol of pyrrole (**1/8**). b) 5 wt.-% Pd/C. c) The Schlenk tube was closed with a septum + balloon.

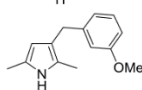
2.2 Analytical data for alkylated pyrroles detected in reaction mixtures

All products that were analyzed by qNMR in mixtures in a yield exceeding 10 mol-% are listed below. As most compounds were not known from the literature, the assignment of characteristic NMR signals is based on predicted chemical shifts and appropriate integral values. Chromatographic purification and isolation of the compounds was usually not possible due to very similar R_f values for the mono- and dialkylated pyrroles.

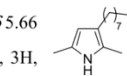
2,5-Dimethyl-3-(naphthalen-1-ylmethyl)pyrrole (3d): ^1H NMR (500 MHz, CDCl_3), selected signals: δ 5.54 (d, $J = 3.1$ Hz, 1H, Ar-H), 4.14 (s, 2H, CH_2), 2.17 (s, 3H, CH_3), 2.14 (s, 3H, CH_3).



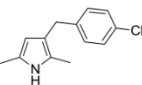
3-(3-Methoxybenzyl)-2,5-dimethylpyrrole (3g): ^1H NMR (500 MHz, CDCl_3), selected signals: δ 5.61 (d, $J = 2.8$ Hz, 1H, Ar-H), 3.67 (s, 2H, CH_2), 2.17 (s, 3H, CH_3), 2.15 (s, 3H, CH_3).



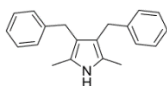
2,5-Dimethyl-3-octylpyrrole (3i): ^1H NMR (500 MHz, CDCl_3), selected signals: δ 5.66 (d, 1H, $J = 2.8$ Hz, Ar-H), 2.34–2.29 (m, 2H, CH_2), 2.20 (s, 3H, CH_3), 2.13 (s, 3H, CH_3).



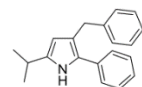
3-(4-Chlorobenzyl)-2,5-dimethylpyrrole (3j): ^1H NMR (500 MHz, CDCl_3), selected signals: δ 5.57 (d, $J = 2.9$ Hz, 1H, Ar-H), 3.66 (s, 2H, CH_2), 2.18 (s, 3H, CH_3), 2.14 (s, 3H, CH_3).



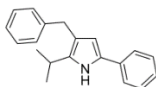
3,4-Dibenzyl-2,5-dimethylpyrrole (4a): ^1H NMR (500 MHz, CDCl_3), selected signals: δ 3.62 (s, 4H, CH_2), 2.14 (s, 6H, CH_3). HRMS (EI): calcd for $\text{C}_{20}\text{H}_{21}\text{N}^+$ (M^+): 275.1669, found 275.1667.



3-Benzyl-5-isopropyl-2-phenylpyrrole (6): ^1H NMR (400 MHz, CDCl_3), selected signals: δ 5.79 (d, $J = 2.9$ Hz, 1H, Ar-H), 2.92 (sept, $J = 6.9$ Hz, 1H, $\text{CH}(\text{CH}_3)_2$), 1.27 (d, $J = 7.0$ Hz, 6H, CH_3). HRMS (ESI): calcd for $\text{C}_{20}\text{H}_{22}\text{N}^+$ ($[\text{M}+\text{H}]^+$): 276.17468, found 276.17454.

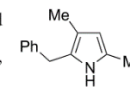


4-Benzyl-5-isopropyl-2-phenylpyrrole (7): ^1H NMR (400 MHz, CDCl_3), selected signals: δ 6.25 (d, $J = 2.8$ Hz, 1H, Ar-H), 3.19 (sept, $J = 7.0$ Hz), 1H, $\text{CH}(\text{CH}_3)_2$), 1.26 (d, $J = 7.0$ Hz, 6H, CH_3). HRMS (ESI): calcd for

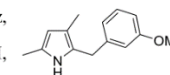


$\text{C}_{20}\text{H}_{22}\text{N}^+$ ($[\text{M}+\text{H}]^+$): 276.17468, found 276.17454.

2-Benzyl-3,5-dimethylpyrrole (9a): ^1H NMR (500 MHz, CDCl_3), selected signals: δ 5.68 (d, $J = 2.8$ Hz, 1H, Ar-H), 3.86 (s, 2H, CH_2), 2.14 (s, 3H, CH_3), 2.04 (s, 3H, CH_3). Known compound, CAS 14629-71-1 (NMR not available).



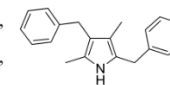
2-(3-Methoxybenzyl)-3,5-dimethylpyrrole (9g): ^1H NMR (500 MHz, CDCl_3), selected signals: δ 5.67 (d, $J = 2.8$ Hz, 1H, Ar-H), 3.83 (s, 2H, CH_2), 2.14 (s, 3H, CH_3), 2.04 (s, 3H, CH_3).



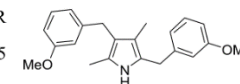
3,5-Dimethyl-2-octylpyrrole (9i): ^1H NMR (500 MHz, CDCl_3), selected signals: δ 5.63 (d, $J = 2.8$ Hz, 1H, Ar-H), 2.50–2.44 (m, 2H, CH_2), 2.20 (s, 3H, CH_3), 1.97 (s, 3H, CH_3).



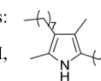
2,4-Dibenzyl-3,5-dimethylpyrrole (10a): ^1H NMR (500 MHz, CDCl_3), selected signals: δ 3.87 (s, 2H, CH_2), 3.75 (s, 2H, CH_2), 2.09 (s, 3H, CH_3), 1.90 (s, 3H, CH_3).



2,4-Bis(3-methoxybenzyl)-3,5-dimethylpyrrole (10g): ^1H NMR (500 MHz, CDCl_3), selected signals: δ 3.764 (s, 2H, CH_2), 3.755 (s, 2H, CH_2), 2.09 (s, 3H, CH_3), 1.91 (s, 3H, CH_3).



3,5-Dimethyl-2,4-dioctylpyrrole (10i): ^1H NMR (500 MHz, CDCl_3), selected signals: δ 2.50–2.44 (m, 2H, CH_2), 2.34–2.27 (m, 2H, CH_2), 2.14 (s, 3H, CH_3), 1.92 (s, 3H, CH_3).

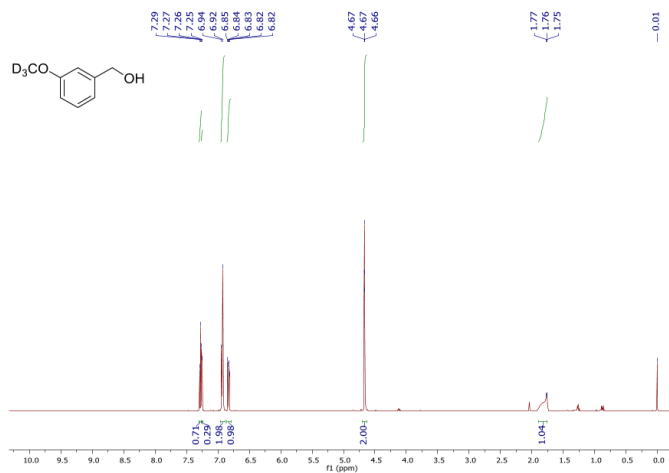


3 NMR spectra

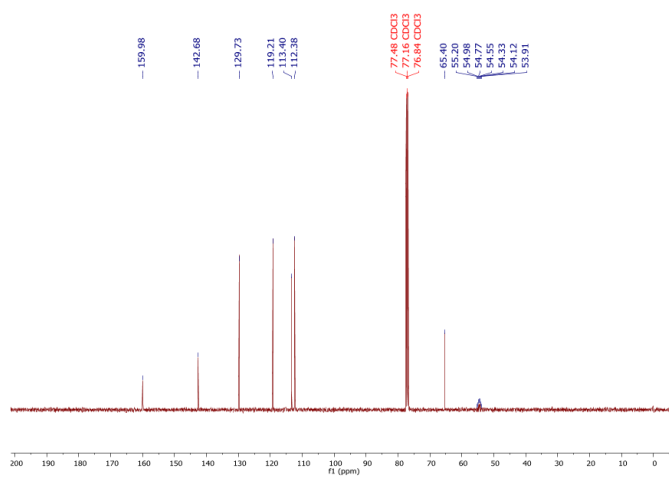
Starting from the upcoming page:

(3-(D₃-Methoxy)phenyl)methanol ((CD₃O)-2g)

¹H NMR (400 MHz, CDCl₃)

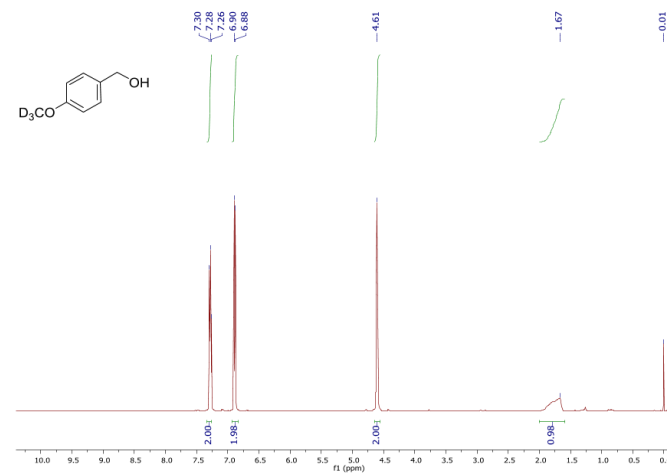


¹³C NMR (101 MHz, CDCl₃)

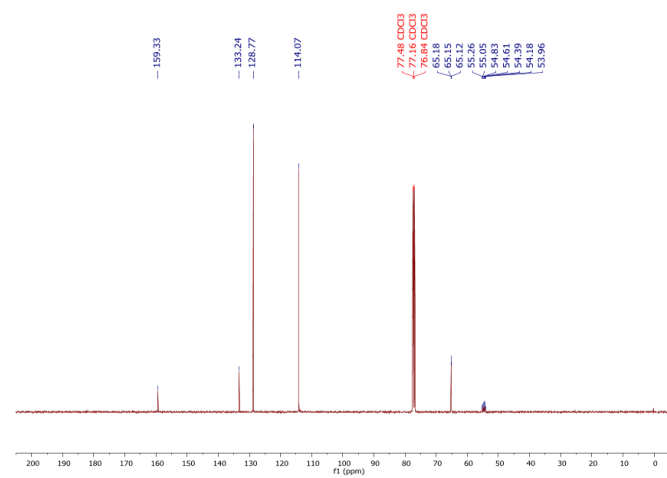


(4-(D₃-Methoxy)phenyl)methanol ((CD₃O)-2h)

¹H NMR (400 MHz, CDCl₃)

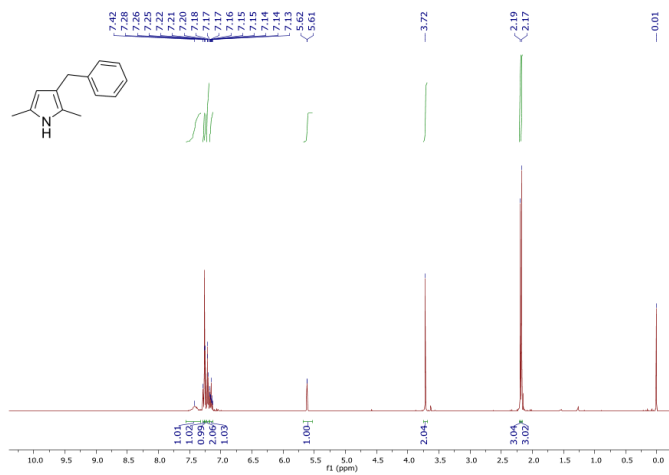


¹³C NMR (101 MHz, CDCl₃)

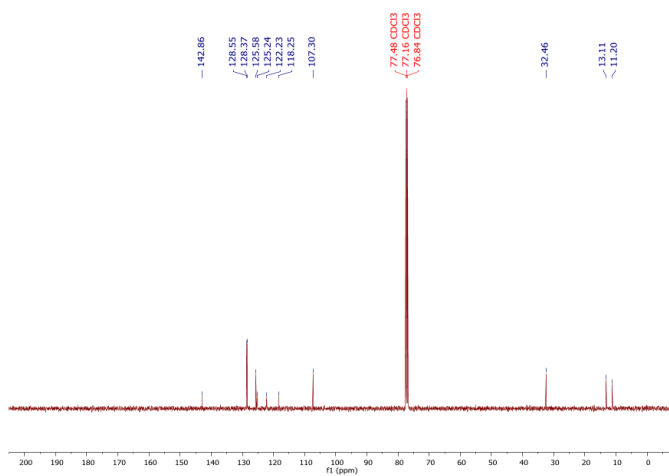


3-Benzyl-2,5-dimethylpyrrole (3a)

¹H NMR (400 MHz, CDCl₃)

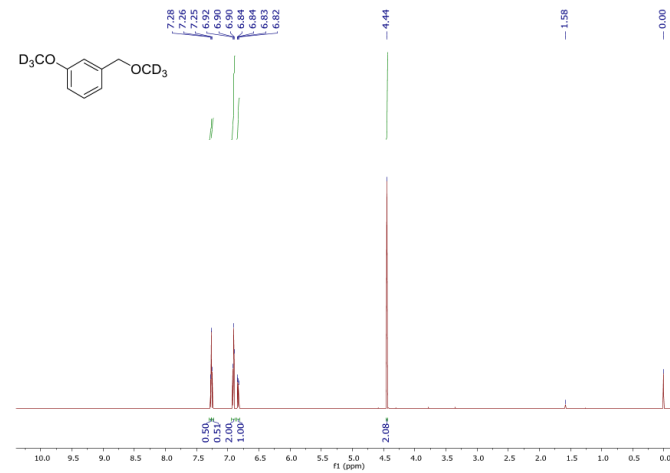


¹³C NMR (101 MHz, CDCl₃)

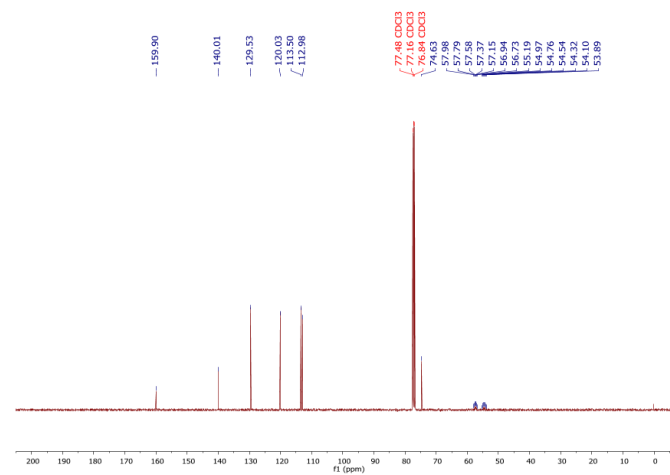


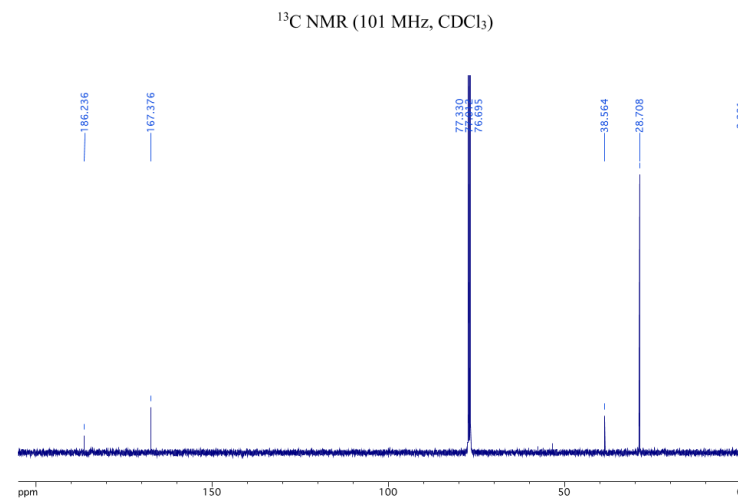
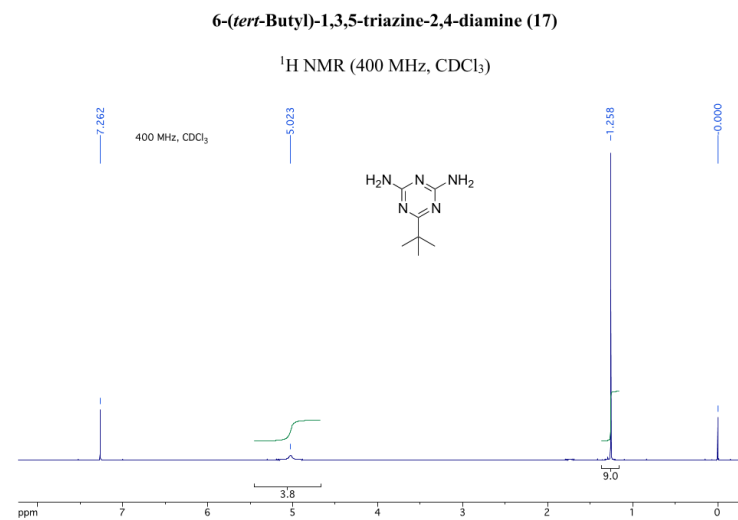
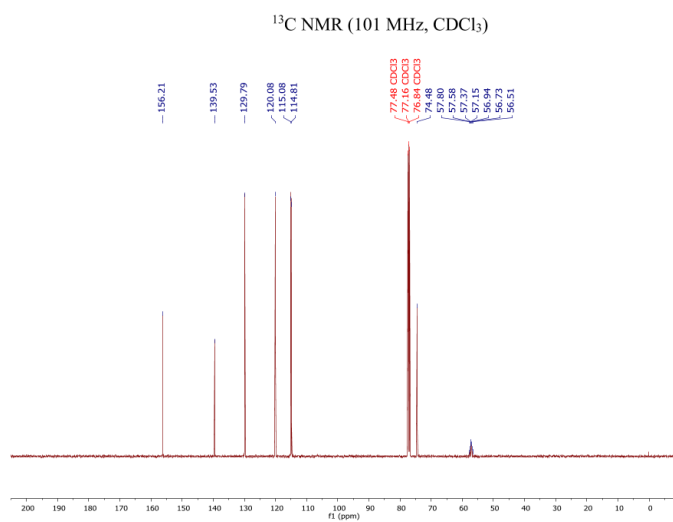
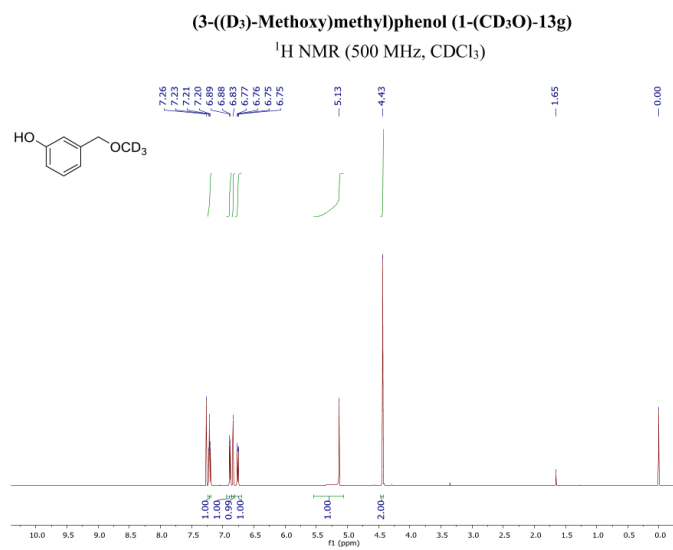
1-((D₃)-Methoxy)-3-(((D₃)-methoxy)methyl)benzene (1,3'-(CD₃O)₂-12g)

¹H NMR (500 MHz, CDCl₃)



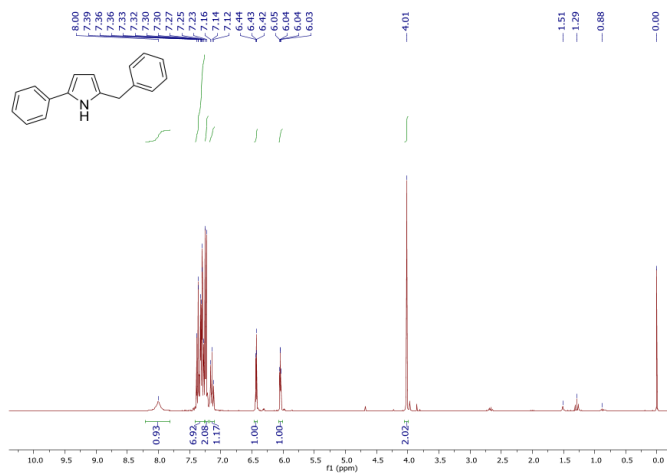
¹³C NMR (101 MHz, CDCl₃)



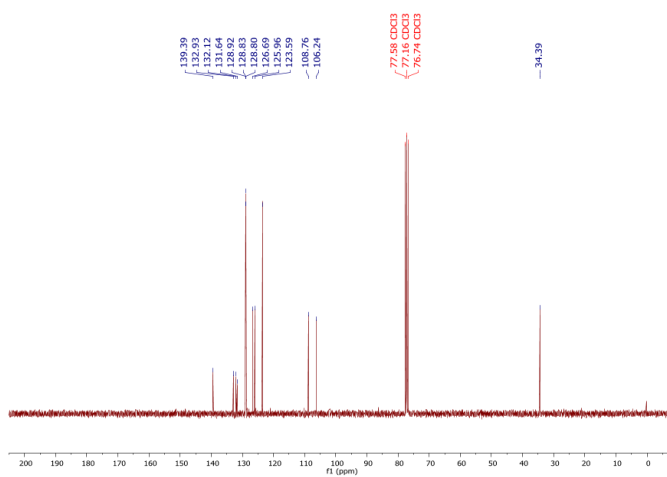


2-Benzyl-5-phenylpyrrole (19)

¹H NMR (300 MHz, CDCl₃)

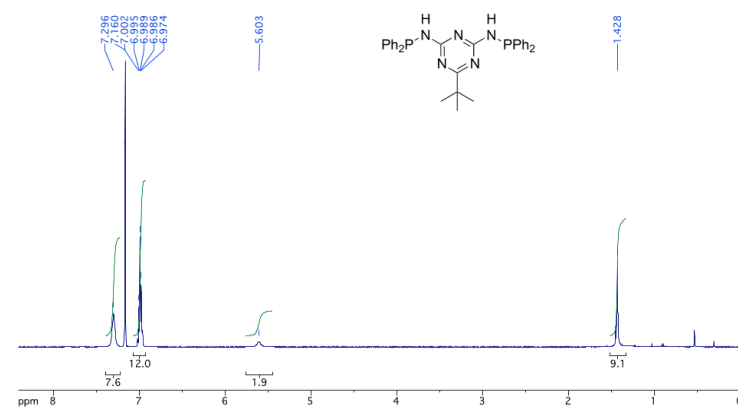


¹³C NMR (75 MHz, CDCl₃)

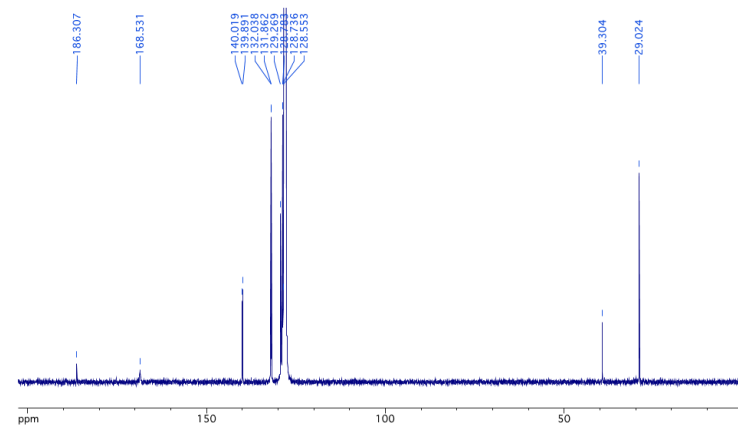


6-(*tert*-Butyl)-*N*²,*N*⁴-bis(diphenylphosphino)-1,3,5-triazine-2,4-diamine (L1)

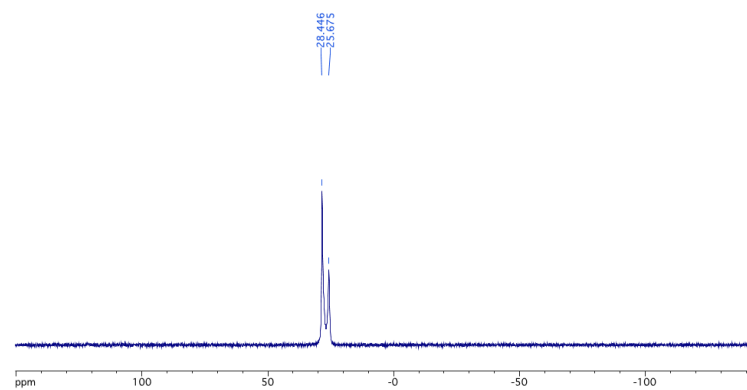
¹H NMR (500 MHz, C₆D₆)



¹³C NMR (126 MHz, C₆D₆)



^{31}P NMR (202.5 MHz, C_6D_6)



Stereochemistry of the Menthyl Grignard Reagent: Generation, Composition, Dynamics, and Reactions with Electrophiles

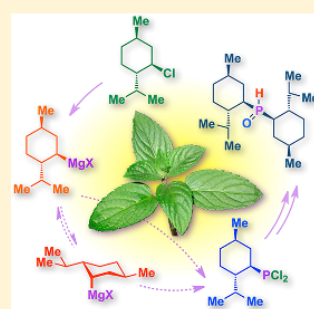
Sebastian Koller,[†] Julia Gatzka,[†] Kit Ming Wong,[†] Philipp J. Altmann,[‡] Alexander Pöthig,^{‡,†} and Lukas Hintermann^{*,†,‡}

[†]Technische Universität München, Department of Chemistry, and Catalysis Research Center, Lichtenbergstrasse 4, 85748 Garching bei München, Germany

[‡]Technische Universität München, Chair of Inorganic Chemistry, and Catalysis Research Center, Ernst-Otto-Fischer Strasse 1, 85747 Garching bei München, Germany

Supporting Information

ABSTRACT: Menthyl Grignard reagent **1** from either menthyl chloride (**2**) or neomenthyl chloride (**3**) consists of menthylmagnesium chloride (**1a**), neomenthylmagnesium chloride (**1b**), *trans-p*-menthane (**4**), 2-menthene (**8**), 3-menthene (**9**), and Wurtz coupling products including symmetrical bimenthyl **13**. The diastereomeric ratio **1a/1b** was determined in situ by ¹³C NMR or after D₂O quenching by ²H NMR analysis. Hydrolysis of the C–Mg bond proceeds with retention of configuration at C-1. The kinetic ratio **1a/1b** from Grignard reagent generation (dr 59:41 at 50 °C in THF) is close to the thermodynamic ratio (56:44 at 50 °C in THF). Carboxylation of **1** at –78 °C separates diastereomers **1a/b** to give the anion of menthane-carboxylic acid (**19**) from **1a**, which combines with unreactive **1b** to give neomenthylmagnesium menthane-carboxylate (**1b**¹). The kinetics of epimerization for the menthyl/neomenthylmagnesium system was analyzed ($\Delta H^\ddagger = 98.5$ kJ/mol, $\Delta S^\ddagger = -113$ J/mol·K for **1b**¹ → **1a**¹). Reactions of **1** with phosphorus electrophiles proceed stereoconvergently at C-1 of **1a/b** to give predominantly menthyl-configured substitution products: PCl₃ and 2 equiv of **1** give Men₂PCl (**6**), which hydrolyzes to dimethylphosphine *P*-oxide (**7**), whereas Ph₂PCl with 1 equiv of **1** gave *P*-menthyldiphenylphosphine oxide (**27**) after workup in air.



INTRODUCTION

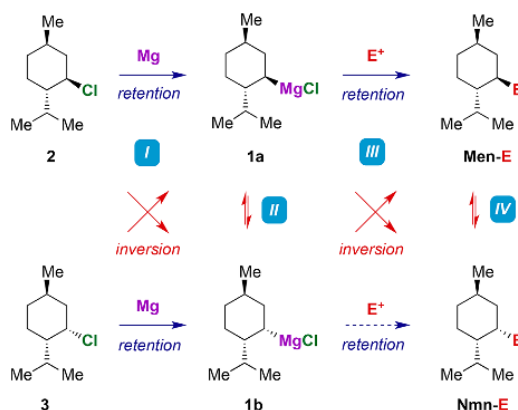
Menthyl Grignard reagent **1** is prepared in the usual way from menthyl chloride (**2**) and magnesium in etheric solution.^{1,2} This chiral organometallic reagent is widely used to attach menthyl groups to electrophilic centers. Reactions have been described, e.g., with carbon dioxide,^{3–9} formaldehyde,⁹ dichloromethane,⁴ PCl₃,^{1,10,11} PhPCl₂,¹² Ph₂PCl,^{2,13,14} GeCl₄,¹⁵ SnCl₄, or organotin chlorides.^{11a,d,16} The reagent has also been used in cross-coupling^{17,18} or transmetalation reactions.¹⁹ The products tend to retain menthyl configuration, and the sequence from **2** via **1** to various substitution products (**Men-E**) has usually been assumed to proceed with retention of configuration in all steps (Scheme 1).^{8,9,14,20,21} The occasional observation of epimeric products (**Nmn-E**) as minor components revealed that retention is not strict. It is not immediately obvious if inversion occurs at the stage of metal insertion (Scheme 1, I), by epimerization of menthyl- (**1a**) to neomenthylmagnesium chloride (**1b**) upon storage (II), during electrophilic substitution (III), by epimerization of the final product (Scheme 1, IV), or in several of those steps.²²

Duthie et al. have developed a refined picture of **1** and its reactions:² they found equal amounts of diastereomeric (3-*D*₁)-*p*-menthanes ((3-*D*₁)-**4**) by quenching **1** with D₂O and concluded that the reagent is a 1:1 mixture of configurationally stable epimers **1a/b**, which forms *stereoconvergently* from either

2 or neomenthyl chloride (**3**).² They also obtained the same product spectrum in reactions of Ph₂SnCl₂ with Grignard reagents from either **2** or **3** and proposed that the higher *nucleophilicity* of **1a** over **1b**—and thus kinetic resolution—was responsible for the usual preference of menthyl-configured substitution products. Their model implies that **1b** remains unchanged in the reaction, that a maximal yield of 50% of **Men-E** will be formed in reactions with a single equivalent of **1**, and that use of 2 equiv or more of **1** might raise yields to quantitative. This analysis (convergence in I, resolution in III) assumes that III proceeds with retention of configuration at C-1 and that **1a/b**, as well as products **Men-E/Nmn-E**, are configurationally stable under reaction conditions.^{22,23} Both assumptions are unproved; in terms of deuteration, Knochel and co-workers observed that menthylzinc iodide is an epimeric mixture with dr 65:35 but may react with MeOD to give (3-*D*₁)-**4** with dr >99:1 (**Men/Nmn**).^{18,24,25} As for epimerization of **1a/b**, no experimental data are available. A complementary, direct analysis of reagent **1** and the elucidation of its equilibration kinetics are required to benchmark the validity of the D₂O-quenching method and permit secure assignments of the stereochemistry of steps I and III.

Received: September 3, 2018

Published: October 22, 2018

Scheme 1. Stereochemical Aspects of Reactions via Menthyl Grignard Reagent to Electrophilic Substitution Products^a

^aE⁺ = electrophile. Men-E and Nmn-E represent menthyl or neomenthyl configured substitution products. Men (menthyl) is (1*R*,2*S*,5*R*)-2-isopropyl-5-methylcyclohex-1-yl, Nmn (neomenthyl) is (1*S*,2*S*,5*R*)-2-isopropyl-5-methylcyclohex-1-yl.

Statements on the composition of **1** and the stereoselectivity of **III** that are solely based on the Men/Nmn-ratio of a substitution product are insecure, in particular, if the isolated product quantities are substantially lower than the molar amount of **1** applied, meaning that kinetic resolution may have occurred.

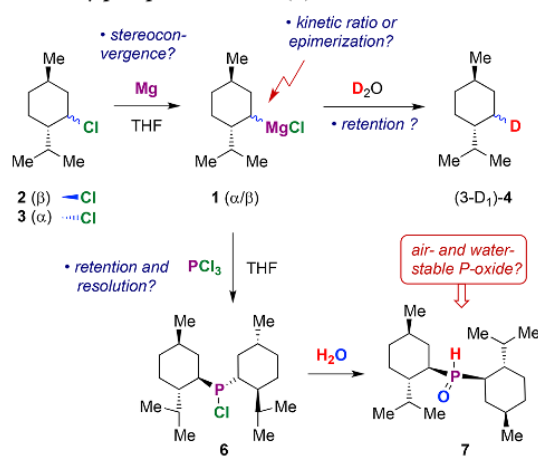
The present work emerged from an analysis of synthetic routes to *P,P*-dimenthylphosphane-based chiral phosphorus ligands.^{26,27} We have previously reported on the nucleophilic chlorination of menthol (**5**)²⁸ to menthyl chloride (**2**) and accompanying rearrangements.²⁹ In continuation of these studies, we wished to investigate the synthesis of Men₂PCl (**6**)¹ from **1** and PCl₃, which is low-yielding (13%,¹⁰ 25–35%¹) and suffers from the difficult separation of the water- and oxygen-sensitive **6** from byproducts. We anticipated that hydrolytic workup would convert **6** to dimenthylphosphine *P*-oxide (**7**),³⁰ whose expected stability toward water and air might facilitate its isolation (Scheme 2).

If so accessible, **7** might find application as a chiral secondary phosphine oxide (SPO) ligand^{31,32} or as a platform chemical for chiral phosphine and phosphine oxide synthesis.³³ Objectives of the present work were thus (a) to study the synthesis and composition of Grignard reagent **1**, (b) to determine the diastereomeric ratio **1a/1b** by NMR spectroscopy in solution and to validate D₂O quenching as quantitative analytical method for analyzing *dr*, (c) to elucidate the temperature-dependent kinetics of equilibration of **1a/b**, (d) to determine the stereochemistry of substitution of **1** with selected electrophiles, and (e) to access and isolate Men₂PHO (**7**).

RESULTS AND DISCUSSION

Synthesis and Qualitative NMR Analysis of **1**.

Menthylmagnesium bromide had been prepared within a year of Grignard's discovery³⁴ of his magnesium organometallics.⁵ The analogous chloride **1** was later obtained from **2** in Et₂O^{6,7} or THF solution.^{1,9,13} According to Duthie et al.,² reagent **1** is composed of nonpimerizing diastereomers **1a/b**

Scheme 2. In Situ Synthesis of *P*-Chlorodimenthylphosphane (**6**) and Hydrolysis to Dimenthylphosphine *P*-Oxide (**7**)

in a 1:1 ratio in THF, irrespective of its generation from **2** or **3**, which would imply kinetic control over the diastereomeric ratio. Increasing the proportion of **1a** in the mixture would then be desirable in syntheses of menthyl-configured targets since the latter were assumed to emerge from the kinetically preferred reaction of **1a** with electrophiles.² NMR spectroscopy should offer direct evidence of the composition of Grignard reagent **1** and provide structural proof of all components.

We prepared **1** from **2** (≥96% purity)²⁹ and excess magnesium, activated by iodine and 1,2-dibromoethane, in (D₈)-THF.³⁵ The majority of signals in the ¹H NMR spectrum (Figure 1) overlap in the aliphatic region (δ_H 0.5–2.5).

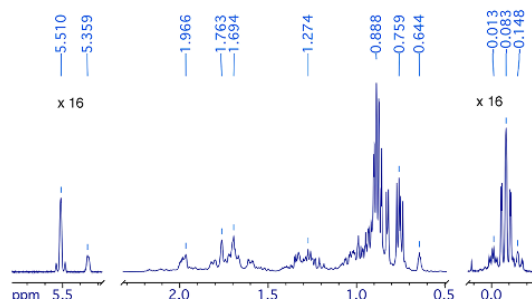


Figure 1. Excerpts from the ¹H NMR spectrum (500 MHz) of **1** in (D₈)-THF. The olefinic (δ 5.5) and high field (δ 0) regions are scaled by a vertical factor of 16.

Olefinic signals at lower field are due to 2-menthene (**8**; δ 5.51) and 3-menthene (**9**; δ 5.36), sometimes accompanied by *μ*-menthene **10**.^{36,37} A group of signals below δ_H 0, centered by a major signal (δ −0.08) with multiplicity ddd (³J_{H,H} = 13.3, 11.9, 2.9 Hz), show the typical shape of an axial H-1 in menthyl derivatives and are due to menthylmagnesium species that collectively belong to **1a**. The major signal likely represents MenMgCl(THF)_n (**1a'**). A slightly broadened signal of similar shape at lower frequency (δ −0.15) is ascribed to Men₂Mg as component of the Schlenk equilibrium

(vide infra). Minor signals at higher frequency tend to be less structured (see Figure S3 for examples) and may belong to MenMgX compounds with other coligands or counterions.^{38,39} Integration of the CHMg region against internal standard naphthalene in many experiments accounted for only 30–50 mol % of the RMgX concentration determined by titration.⁴⁰ Therefore, ¹H NMR spectroscopy gives an incomplete picture of the composition of **1**. The ¹³C NMR spectrum of **1** features a prominent signal at δ 52.8, later assigned to C-2 of **1b'**, which was set to 100 area % as reference. Approximately 80 peaks at ≥ 5 area % were detected in total, besides those of the solvent and of the internal standard naphthalene. Signal sets for 2-menthene (**8**;³⁷ 10 peaks, 19–24 area %) and 3-menthene (**9**;³⁷ 10 peaks, 10–12 area %) were assigned by reference data.⁴¹ Out of 26 major peaks (40–120 area %), six were assigned to *trans-p*-menthane (**4**)⁴² and 10 each to the predominant organomagnesium species **1a'**/**b'**.⁴³ Connectivity and peak assignments for **1a'**/**b'** and **4** were elucidated by 2D NMR methods (HSQC, HMBBC). The ¹³C NMR signals for the major organometallic species are mapped in Figure 2.

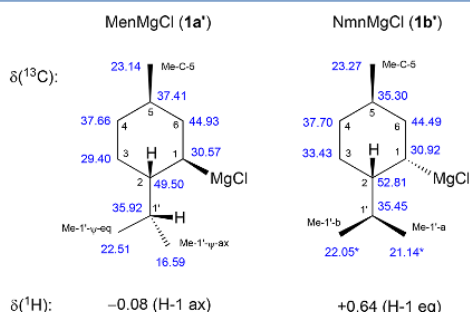


Figure 2. NMR data in (*D*₈)-THF for the major components in **1**, MenMgCl (**1a'**) and NmnMgCl (**1b'**). Solvent coordination or aggregation is not taken into consideration for simplicity. See the Supporting Information for complete ¹H NMR assignments.

The CHMg-unit of **1b'** gives rise to a poorly structured multiplet at δ_{H} 0.64 in (*D*₈)-THF (cf. Figure 1). This signal was often obscured in the more commonly analyzed THF–C₆D₆ mixtures. Assignment of signal sets to structures **1a'**/**b'** relies on the characteristic shape of the H-1-signals. Furthermore, menthyl and neomenthyl fragments are discernible by ¹³C NMR spectroscopy, where peaks for the diastereotopic methyls of C-2-isopropyl are either clearly separated with one signal at $\delta \approx 15$ –17, the other at $\delta \approx 22$ –23 (in Men-Y), or both found in close vicinity at $\delta \approx 21$ –22 (Nmn-Y).⁴⁴ These chemical shifts reflect the preferred conformation of the C-2-isopropyl group, which stands equatorial, with both methyl groups in ψ -equatorial positions relative to the cyclohexane chair in Nmn-Y derivatives (Y = variable substituent; Figure 3b), unless Y becomes sterically very demanding (Figure 3c). In most menthyl derivatives including **1a'**, repulsion of groups Y at C-1 and *i*Pr at C-2 causes the isopropyl group to rotate such that one methyl arranges ψ -axial and the other ψ -equatorial relative to the cyclohexane chair (Figure 3a).^{44,45}

At this point, 34 signals in the region δ 15–48 of the ¹³C NMR spectrum of **1** remained unassigned. GC–MS analysis (Figures S15–S17) of a D₂O-quenched sample of **1** indicated that the signals belong to three stereoisomeric hydrocarbons

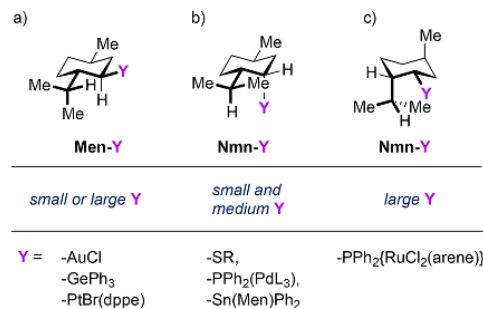


Figure 3. Preferred conformations of Men-Y and Nmn-Y derived from NMR and X-ray crystal structure data. (a) Conformation of menthyl derivatives. (b) Conformation of neomenthyl derivatives. (c) Ring-flipped conformation in neomenthyl derivatives with large Y-groups.⁴⁵

(*m/z* 278.3), namely bimenthyl (**13**), menthylneomenthyl (**14**) and bineomenthyl (**15**). A batch of **1** was quenched with aqueous acid, washed with concd H₂SO₄, and vacuum distilled. The more volatile fraction consisted of **4**, with a minor amount of ψ -menthane (1-isobutyl-3-methylcyclopentane; **16**, 96:4 ratio).⁴⁶ Distillation of the residue in high vacuum gave a bimenthyl isomer fraction (**13/14/15** = 39:45:16) as colorless oil. Its ¹H NMR spectrum covered the narrow shift range of δ 0.6–2.2 with signal overlap even at 950 MHz (Figure S18). Based on HMBBC and HSQC and the δ_{C} criterion for discerning menthyl from neomenthyl fragments, all 40 carbon and 52 proton signals in **13–15** could be assigned (Figures 4 and Figures S19, S21, and S22).

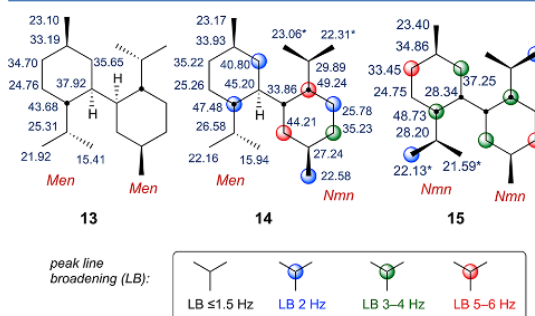


Figure 4. ¹³C NMR assignments for the Wurtz hydrocarbon byproducts Men-Men (**13**), Men-Nmn (**14**), and Nmn-Nmn (**15**). An asterisk (*) indicates interchangeable assignments.

Unlike symmetrical bimenthyl **13**, hydrocarbons **14** and **15** show δ_{C} line broadening in specific positions, indicative of a dynamic chair-flip of the neomenthyl units. The oily hydrocarbon mixture separated crystals of bimenthyl (**13**) upon standing, as revealed by NMR spectroscopy and X-ray crystal structure analysis (Figure 5). Compound **13** melts at 105–106 °C and is thus identical with a crystalline bimenthyl isomer from the Wurtz coupling of **2** described in the previous literature.⁴⁷

Quantitative Analysis of Menthyl Grignard Reagent.

Grignard reagent **1** was analyzed volumetrically for total alkylmagnesium⁴⁰ and for total magnesium by EDTA titration of acid-quenched samples.⁴⁸ Quantitative ¹H NMR spectroscopy

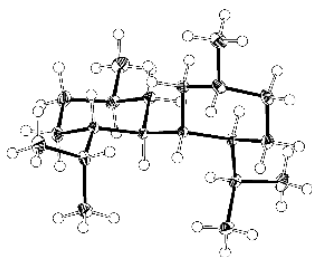


Figure 5. X-ray solid-state molecular structure of bimenthyl 13. Ellipsoids are shown at 50% probability.

copy (qNMR) with naphthalene as internal standard permitted quantification of menthenes **8/9** by integration of the well-separated olefinic signals. Since the δ 0.5–4 region did not contain well-resolved signals for integration, we usually prepared **1** in nondeuterated THF and admixed C_6D_6 for locking prior to NMR analysis. As in a previous study of the composition of crude menthyl chloride,²⁹ the high resolution and information density of ^{13}C NMR recommended use of this technique for quantitative analysis.^{49–51} Naphthalene (δ 128.6) served as internal standard under routine analysis conditions, and empirical correction factors for peaks of individual components, positions, and carbon types (CH vs CH_2 vs CH_3) were applied.⁵² Correction factors were derived from analysis of reference materials (**4**, **13–15**) against internal standard or by referencing to quantitative 1H NMR data (**8**, **9**). Since reference material is not available for **1a/b**, their correction factors were estimated from structurally similar

model compounds.⁵² Deconvolutive peak fitting was applied to reduce subjective errors and correct for peak overlap. Quantification of **1a/b** presented additional challenges due to the Schlenk and other ligand exchange equilibria. The population of Men-Mg and Nmn-Mg units is not correlated with the signal intensity of a single species (**1a'/b'**) but must be summed over various chemical forms, some of which display chemical exchange-broadened signals (Figure 6).

Figure 6a shows excerpts of the 1H and ^{13}C NMR spectra for **1**. The characteristic signal of **1a'** in the 1H NMR spectrum (H-1, δ_H 0.08) correlates (by HMBC) with C-2 at δ_C 49.5, whereas H-1 of NmnMgCl (**1b'**; δ_H 0.64, cf. Figure 1) correlates with C-2 at δ_C 52.8. The intensity ratio of the major C-2-peaks does not reflect the ratio **1a/b**: the major C-2 peak for **1a'** is accompanied by broad signals, and the total integral δ_C 48–51 (**1a**-region) surpasses that of δ_C 51–54 (**1b**-region).⁵³ Figure 6b shows spectra of **1** at high [R-Mg]/[Mg] ratio.⁵⁴ As expected, the signal at δ_H –0.19 for Men_2Mg is more intense than for a low [RMg]/[Mg] ratio.⁵⁵ The **1a**-region contains at least three broadened signals for C-2 of **1a'**, Men_2Mg , and either $MenMgBr$ ³⁸ or more complex species.⁵⁶ Satisfactory analytical results for the population and dr of **1** resulted from area integration of δ 51–54 (for **1b**) and δ 48–51 (for **1a**) after subtraction of overlapping peak signals.⁵⁷ The peak area correction factor for C-2 in **1a/b** relative to the internal standard signal was set to the value for menthol (**5**) as model compound. This introduces an unknown systematic error, which we estimate to be below 5–10% of the absolute values,⁵⁸ but will be even less important for the ratio **1a/b**, where such systematic errors cancel out.^{50a} The data thus

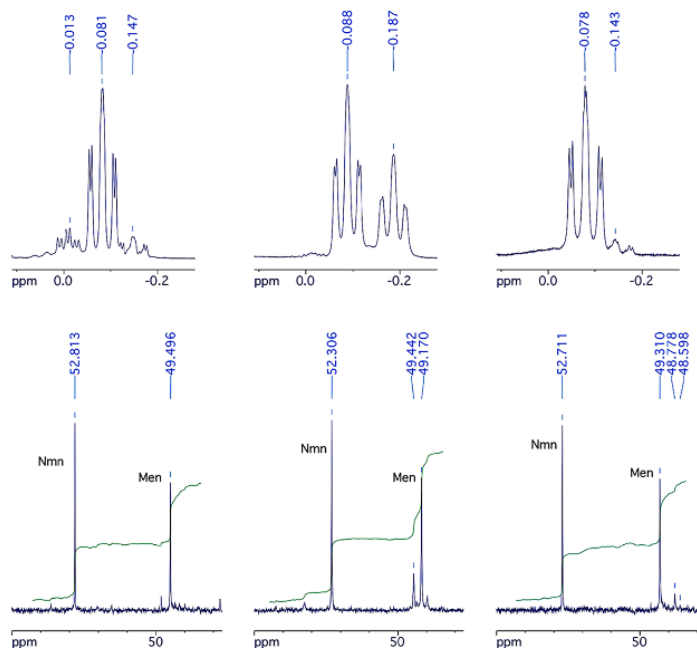


Figure 6. Excerpts from 1H (top; 500 MHz) and ^{13}C NMR (bottom; 101 MHz) spectra of Grignard reagent **1**. (a) Reagent prepared from **2** and Mg in (D_8) -THF (prepared at 70 °C, nominal concentration 0.9 M); [RMg]/[Mg] = 0.49. (b) Higher concentrated **1** in THF (50–70 °C, 1.55 M) with C_6D_6 added for locking, displaying a high content of Men_2Mg ; [RMg]/[Mg] ratio = 0.9. (c) Reagent prepared from **3** and Mg in (D_8) -THF (rt, 0.9 M); [RMg]/[Mg] ratio = 0.4; 1H NMR at 400 MHz.

Table 1. Analyses of Menthyl Grignard Reagent **1**, Prepared from **2** or **3** under Variable Reaction Conditions^a

entry	solvent	<i>t</i> (°C)	conc ^b (M)	[RMg] ^c (M)	[Mg] ^d (M)	yield ^e (%)	1 (%)	1a/1b	4 (%)	8 (%)	9 (%)	13–15 ^f (%)	13/14/15	recov ^g (%)
Reactions Starting from Menthyl Chloride (2)														
1	THF	rt	1.8	0.97	1.59	53	54.1	55:45	12.2	5.5	2.9	25.9	36:47:17	100.5
2	THF	rt	0.9	0.64	0.90	72	74.0	62:38	9.7	3.5	1.9	20.1	32:50:18	109.4
2a							(D ₂ O: 62:38)							
3	THF	50	1.8	1.44	1.88	80	72.5	59:41	6.4	2.4	1.2	11.8	32:50:18	94.5 ^h
4	THF	50	0.9	0.77	0.95	86	74.3	59:41	8.3	2.9	1.5	11.8	36:49:15	98.8
4a							(D ₂ O: 59:41)							
5	THF	50 ^f	0.9	0.76	0.85	85	76.9	58:42	7.2	2.3	1.2	11.7	31:57:12	99.4
5a							(D ₂ O: 55:45) ^f							
6	THF	70	0.9	0.74	0.92	81	87.5	55:45	6.5	1.6	0.9	8.8	38:45:17	105.3
7	Et ₂ O	RT	0.9	0.65	1.18	72 ^k	45.1	56:44	15.3	6.0	3.1	29.2	37:47:16	99.1
8	THF–PhMe	RT	1.1	0.72	1.04	67	68.6	53:47	10.6	4.4	2.3	20.5	36:48:16	106.6 ^l
9	THF–PhMe	50	1.8	1.24	1.51	70	71.4	55:45	8.4	3.5	1.7	16.2	40:44:16	101.3
10	THF–PhMe	50	1.1	0.80	1.00	75	73.0	54:46	8.2	2.4	1.4	10.8	37:45:18	96.0 ^m
11	THF–PhMe	70	1.8	1.33	1.58	75	78.4	55:45	6.7	1.6	0.9	8.5	32:54:14	96.2
11a							(D ₂ O: 56:44)							
12	THF–PhMe	70	1.1	0.95	1.10	85	85.3	58:42	4.9	1.1	0.6	5.3	44:47:9	97.2
Reactions Starting from Neomenthyl Chloride (3)														
13	THF	rt	0.9	nd	nd	nd	45.7	45:55	20.5	5.5	2.5	20.3	36:45:19	105.0 ⁿ
14	THF	30	0.9	0.55	1.39	60	44.2	48:52	9.9	5.1	2.7	20.7	35:46:19	83.7 ^o
14a							(D ₂ O: 42:58) ^p							
15	THF	50	0.9	0.66	1.37	73	63.6	54:46	13.6	3.0	2.0	16.6	35:48:17	100.2 ^q

^aSample composition in mol % of initial **2** (or **3**); concentrations in M = mol/L. ^bNominal concentration calculated from initial **2/3** and volumes of starting material and solvent, rounded to 0.1 M. ^cTotal concentration of RMg entities by titration.⁴⁰ ^dTotal Mg²⁺ concentration by EDTA titration. ^eYield of **1** calculated from [RMg]_{tot} and nominal concentration. ^fValue expressed in mol % of Men/Nmn groups; the true molarity of dimers is half this value. ^gRecovery is the sum of analytically detected Men and Nmn groups in mol %; deviations from 100% are due to undetected components and systematic errors. ^hIncluding 0.2 mol % of **10**. ⁱReagent prepared at 50 °C over 1 h, then heated to 70 °C for 2 h. ^jD₂O-quenching result **1a/1b/16** 43.3:35.5:3.0 mol % by ²H NMR against C₆D₆ as internal standard. ^kLarge deviation due to solvent loss and heterogeneity; NMR analysis performed after evaporation of Et₂O and redissolution in THF. ^lIncluding 0.2% of **10**. ^mIncluding 0.3% of **10**. ⁿIncluding 10.4% of **3**. ^oNMR analysis after ≥ 4 h, with 1.0% of remaining **3**. ^pD₂O quench performed after 2 h, at 10% of remaining **3**. ^qIncluding 1.4% of **3**.

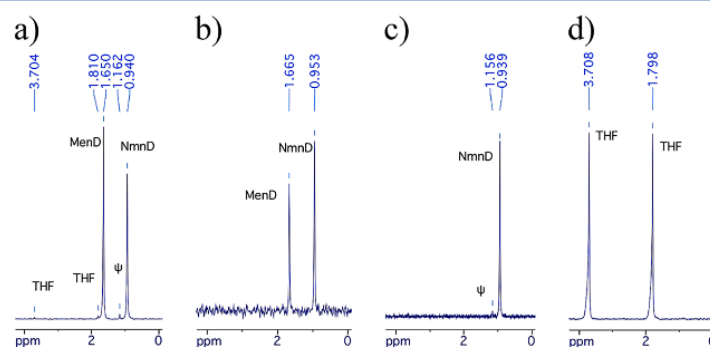


Figure 7. ²H{¹H} NMR spectra (61 MHz) of quenched samples of **1**. (a) D₂O-quenched sample of equilibrated **1**. (b) D₂O-quenched sample of the reaction **3** + Mg in THF, before completion (Table 1, entry 14a). (c) Carboxylated and D₂O-quenched **1** composed mainly of α-(3-D₁)-**4**. (d) H₂O-quenched sample of **1** generated in (D₈)-THF. Most (D₈)-THF was removed by washing with water prior to analysis; only residual (D₈)-THF is present. “ψ” marks peaks for (D₁)-**16**.

obtained for all key components in Grignard reagent **1** will be subject to additional systematic errors by variation of *T*₁ and the NOE effect with sample composition, but even if accuracy

for individual component concentrations is limited, parameter variation effects on the composition of **1** can now be systematically studied.

Effects of Reaction Conditions on the Composition of 1.

Effects of varying the solvent, reaction temperature, and total concentration in the reaction of **2** and magnesium were studied by analyzing the composition of the resulting Grignard reagent (Table 1, entries 1–12). The yield of **1** was higher at 50 or 70 °C than at ambient temperature or 30 °C and also higher in dilute (0.9–1.1 M) over concentrated (1.8 M) solution. Synthesizing the reagent in THF–toluene at 70 °C or in THF at 50–70 °C gave similar, satisfactory results with a yield of 75–85 mol %, whereas diethyl ether (entry 7) was less satisfactory. Reagent yields in THF and Et₂O agree with previously reported titration results.^{1,6} Spectroscopic yields of **1** do not correlate exactly with [RMg] from titration, since yield calculations depend on estimated reaction volumes, which are inaccurate in small-scale experiments.

In a first approximation, the diastereomeric ratio **1a**/**1b** deviates little from an average value of 57:43, irrespective of the reaction conditions. Complementary data for dr were in some cases obtained by quenching a sample with D₂O and analyzing the ratio of (3-D₁)-**4** stereoisomers by ²H NMR spectroscopy (Figure 7).^{2,59}

The signals δ_D 1.65 and 0.94 correspond to the centers of multiplets in the ¹H NMR spectrum of **4** at δ_H 1.68 and 0.97 for equatorial and axial H-3, respectively. A small peak at δ_D 1.16 corresponds to D-1' of *ψ*-menthane (**16**; δ_H 1.18) from deuterolysis of *sec-ψ*-MenMgCl (**12**).³⁹ A Grignard reagent from NmnCl (**3**; Table 1, entries 13–15) was largely identical to that from **2**, as also evident from the similar NMR spectra (Figure 6a vs c),^{2,60} at least if prepared at 50 °C (Table 1, entry 4 vs 15). The room-temperature Grignard reaction of **3** was sluggish to initiate and required several hours to reach completion (entries 13 and 14). A D₂O-quenched sample after 2 h at 30 °C gave (3-D₁)-**4** with dr 42:58 at 90% conversion (entry 14a; ²H NMR in Figure 7, b), which rose to dr 48:52 after 4 h (at 99% conversion; entry 14). Conversely, if **1** was generated from **2** at ambient temperature, a sample at 40% conversion displayed a higher dr 62:38 (Table 1, entry 2). Thus, Grignard reagent **1** is formed with a small degree of retention of configuration at ambient temperature but approaches dr 56:44 if prepared at 50 or 70 °C from either **2** or **3**, which implies that the latter is an equilibrium ratio (vide infra).

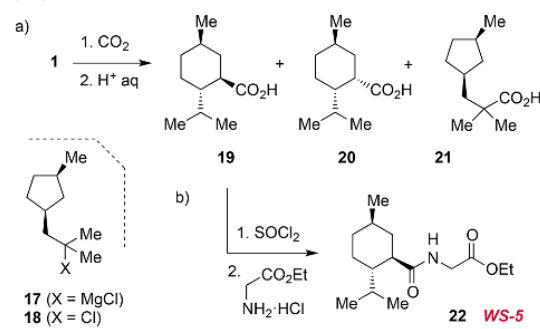
The abundance of byproduct *p*-menthane (**4**) is always higher than the sum of menthenes **8** and **9**. Radical abstraction from the solvent provides no source of **4** because when **1** was prepared in (D₈)-THF, no trace of (3-D₁)-**4** or solvent coupling-product was detected by ²H{¹H} NMR after protic workup (Figure 7, d).⁶¹ Byproducts **4**, **8**, and **9** are most abundant at room temperature (Table 1, entries 1, 2, and 13) and decrease at higher temperature (entries, 3, 6, and 12). Alkenes **8**/**9** are formed in similar amounts and isomeric ratios from both **2** and **3** (entry 15), which excludes E2-elimination (with **1** as base) as an important reaction pathway.⁶² This points to a specific mechanistic route for products **4**/**8**/**9** in addition to the obvious source of some **4** by reaction of **1** with adventitious water. We suggest that β-H elimination of surface-bound ⁵MgR (R = Men or Nmn) to surface-bound ⁵Mg–H and alkenes **8**/**9** is followed by combination of ⁵MgH and ⁵MgR to give **4**. Bimethyl isomers **13**–**15** will similarly be formed by combining two surface-bound ⁵MgR units, which agrees with the observation that the extent of Wurtz coupling and the generation of **4** + **8**/**9** are correlated. The observation of higher amounts of neutral byproducts (R–H, R–R) at

ambient temperature but higher selectivity for Grignard reagent **1** at elevated temperature might be a consequence of rate-limiting detachment of RMgCl from the metal surface. This process, involving major solvent reorganization, will have a higher activation barrier than the release of apolar hydrocarbons (RH, RR), which is likely limited by a diffusion-controlled encounter of two surface groups. The stereoconvergence from **2** and **3** to give **1a**/**b**, the generation of bimenthyls **13**–**15**, and the absence of solvent-derived products all point to a key mechanistic role of ⁵MgR units, in which R inverts at experimental time scale, much slower than a free radical, but faster than the final RMgX.^{63,64}

Conclusions on the Generation of 1. The analyses in Table 1 validate the hypothesis that menthyl Grignard reagent **1** is a diastereomeric mixture **1a**/**b** formed in a kinetically controlled and stereoconvergent process from either **2** or **3** in similar amounts.² Irrespective of reaction conditions, the ratio **1a**/**b** varies only a little around an average dr of 57:43. Presumably, this ratio is not just kinetically controlled but close to thermodynamic equilibrium. In spite of the valuable data obtained through ¹³C NMR spectroscopy, the faster and more accurate option for analyzing the dr of **1a**/**b** is ²H{¹H} NMR spectroscopy of D₂O-quenched samples. The method gives accurate results that agree with the in situ ¹³C NMR data but does not suffer from complications caused by species partitioning in the Schlenk equilibrium. Total [RMg] or individual RⁿMgX concentrations in mixtures can be quantified using the D₂O-quenching technique, if a deuterated internal standard is added for ²H{¹H} NMR analysis.⁶⁵ Given that the ratio **1a**:**1b** cannot be satisfactorily controlled by the reaction conditions used for generating the Grignard reagent, an understanding of the stereochemistry of the reactions of **1a**/**b** with electrophiles becomes even more vital.

Carboxylation of Menthyl Grignard Reagent. Carboxylation of **1** has been reported repeatedly but with inconsistent results.^{8,3,6} By pouring a THF solution of **1** over solid CO₂, Bose et al. obtained 76% of acids **19**/**20** (Scheme 3) with a dr

Scheme 3. Carboxylation of Menthyl Grignard Reagent 1 and Synthesis of Physiological Coolant Compound WS-5 (22)



of 68:32,^{3b} while Grayson et al. obtained pure **19** (dr >100:1) in 88% yield.⁸ By bubbling CO₂ into etheric **1**, Smith and Wright obtained 29% of crystalline **19** and distilled another 32% of a liquid (believed to be **20**) from the mother liquors.^{6,66} The same procedure provided Ueda et al. with 36% of **19**/**20** in a ratio of 92.6:7.4,⁹ whereas a 1975 patent found almost pure acid **19** (dr 99:1) in 53% yield.⁶⁷ Among the

highest yielding carboxylations is a patent that finds 93% of **19** by concurrent addition of CO₂ and **2** to magnesium in 2-MeTHF-cymene at 90 °C.⁶⁸

To understand the various results, we approached the problem with our own experiments. Dry ice was added to a Grignard reagent from crude **2** that contained *tert*- ψ -MenCl (**18**) as the major impurity.²⁹ Acid/base extraction gave a carboxylic acid fraction with **19**, **20**, and **21** in a ratio 77:19:4 (Scheme 3a). Coupling with ethyl glycinate gave a mixture of peptide esters (ratio 78:18:4) from which the major component **22** crystallized (Scheme 3b). Compound **22** is commercially available under the name WS-5⁶⁹ as a *physiological coolant* for inducing a cooling sensation on skin.⁷⁰ The substance has so far only been described in the patent literature; thus, we characterized it by 2D NMR methods in solution (Figure S26 and Tables S21/22) and by X-ray crystal structure analysis in the solid state (Figure 8).

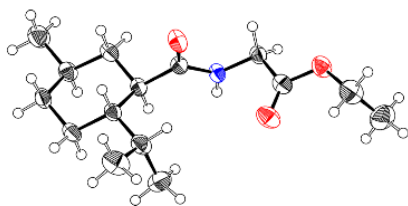
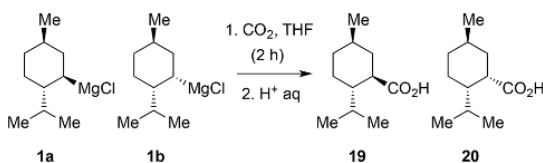


Figure 8. Solid-state molecular structure of WS-5 (**22**). Ellipsoids are shown at 50% probability. Oxygen is red, nitrogen blue. The common arrangement of the C-2 isopropyl group with ψ -axial and -equatorial methyl groups (δ_c 16.16 and 21.49) is evident. The unit cell contains six independent molecules, which differ in the conformation of the peptidic side-chain [Men-C¹(O)-NH-C²H₂-C^{1'}(O)-O-C^{1''}H₂-C^{2''}H₂], in which the torsional angles C¹(O)-N-C^{2'}-C^{1'}(O) and C^{1'}(O)-O-C^{1''}-C^{2''} are variable. The individual conformers and their angles are (a) -75/-89; (b) -87/-179; (c) +91/+96; (d) +86/+180; (e) +60/+178; (f) +58/-173. The pictured conformer is (c). See Figure S28 for depictions of all conformers.

The complexity of crude menthyl chloride had translated into regio- and stereoisomeric carboxylic acids (**19**–**21**) via metalation and carboxylation, but the ratio **1a/b** (57:43) was not retained in acids **19/20** (dr 80:20). In the ensuing carboxylation experiments, Grignard reagent **1** from purified menthyl chloride (**2** + **3** \geq 97%) was used, and the yield of **19/20** was determined by accurate qNMR methods. In one experiment, **1** was added dropwise to a saturated solution of CO₂ in THF at -20 °C, and the reaction was quenched with water at the same temperature (Scheme 4a).

A second experiment involved the addition of small pieces of CO₂ (s) into the solution of **1** at ambient temperature, which corresponds to an inverted addition mode (Scheme 4b). The outcome in (b) agrees with several literature reports that find **19** as the major and **20** as the minor component (dr \approx 8:1; Scheme 4b). Surprisingly, experiment (a) in which **1a/b** are continuously exposed to excess electrophile showed *higher* selectivity for **19** (dr 19:1) rather than approaching the ratio **1a/b** (57:43). The data in Scheme 4 suggest that dr **19/20** is not controlled by availability of (excess) electrophile but by kinetic preference of **1a** over **1b** in the reaction with electrophile. The lower yield and higher dr in (a) reflect improved kinetic resolution at lower reaction temperature. To verify this assumption, not only the reaction products **19/20** but also the unreacted Grignard reagents **1a/b** must be

Scheme 4. Carboxylation of Grignard Reagent **1** with Quantification of Carboxylic Acids **19/20**



a) Addition of **1** to CO₂ (THF) at -20 °C

1a	1b	Yield	dr	19	20
57%	43%	58.7%	95:5	55.9%	2.8%

b) Addition of CO₂ (s) to **1** at ambient temperature

1a	1b	Yield	dr	19	20
57%	43%	67.8%	89:11	60.2%	7.6%

analyzed, which was achieved by D₂O quenching in combination with use of a deuterated internal standard for ²H{¹H} NMR.⁷¹ Such experiments prove that the reaction of **1** with excess CO₂ at -78 °C is limited to epimer **1a** and proceeds with retention of configuration at C-1 to give **19** (Scheme 5, a). Neomenthyl epimer **1b** remains largely unreacted and gives rise to enriched 3 α -(D₁)-**4** after quenching with D₂O (Scheme 5, a). In repeat experiments, the kinetic resolution was consistently high to the extent where no more 3 β -(D₁)-**4** could be detected (\geq 99.5:0.5).

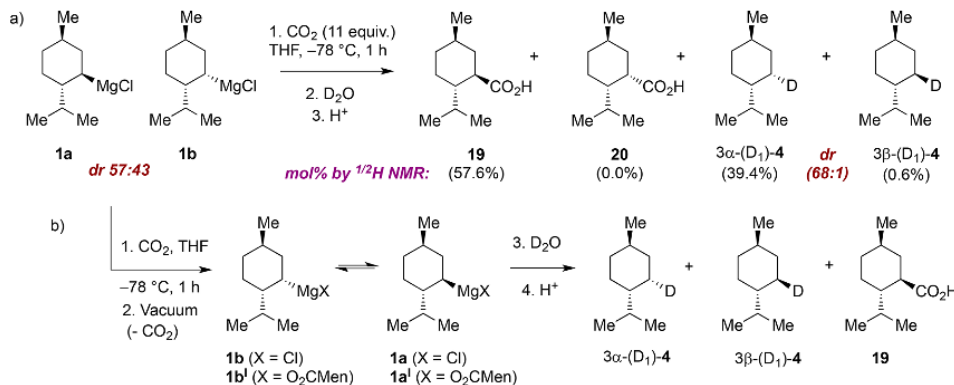
Kinetics and Equilibrium in the Epimerization of **1**.

The kinetic resolution of **1** with CO₂ gives access to highly enriched solutions of neomenthyl-configured Grignard reagent **1b**¹, from which excess electrophile can be completely removed in vacuo. The kinetics of epimerization⁷² of chiral Grignard reagent **1b**¹ could now be studied by warming to a target temperature and taking samples for D₂O quenching (Scheme 5, b). Analysis of the dr of 3-(D₁)-**4** by ²H{¹H} NMR provided consistent results as shown in Figure 9. The Mn-Grignard reagent is configurationally rather stable at 0 °C but epimerizes notably upon warming to 30 °C ($t_{1/2}$ = 14 h).⁷³

Clean first-order kinetics with $t_{1/2}$ of 62 min (50 °C) and 8 min (70 °C) operate at higher temperature. The activation energy is \sim 100 kJ/mol. The rate **1b**¹ \rightarrow **1a**¹ is characterized by ΔH^\ddagger = 98.5 kJ/mol and ΔS^\ddagger = -113 J/mol·K by Eyring analysis (ΔH^\ddagger = 96.1 kJ/mol and ΔS^\ddagger = -110 J/mol·K for **1a**¹ \rightarrow **1b**¹), with calculated epimerization half-lives of 39 h at 22 °C or 65 days at 0 °C.⁷³

Primary alkyl-Grignard reagents invert fast already below room temperature.⁷⁴ Properties of secondary alkyl-magnesium species are collected in Scheme 6. Norbornylmagnesium bromide equilibrates over a day at room temperature (Scheme 6a),^{74,78} whereas bornylmagnesium chloride is stable under the reflux conditions of its synthesis but epimerizes if refluxed in the higher boiling solvent toluene (Scheme 6b). Both the solvent and counterion differ between systems, making it difficult to assess the importance of additional methyls on configurational stability. In any case, cyclic **1b**¹ (Scheme 6c) is more inert than Hoffmann's open-chain secondary alkyl Grignard reagent, which racemizes below 0 °C (Scheme 6d).⁷⁹

The **1a**¹/**1b**¹ equilibrium ratios dr 38.3:61.7 (50 °C; after 144 h) and 39.5:60.5 (70 °C, after 1.5 h) deviate markedly from those seen in the thermal equilibration of **1a/b** (22 °C; dr 57.3:42.7 after 1 d, increased to 58.2:41.8 after 3 months; 50

Scheme 5. Kinetic Resolution of Menthyl Grignard Reagent **1** by Low-Temperature Carboxylation and Epimerization Studies

^aD₂O-quenching for analysis of unreacted Grignard reagent. ^bExperimental course for studying the epimerization of resolved neomenthylmagnesium menthanecarboxylate **1b**¹.

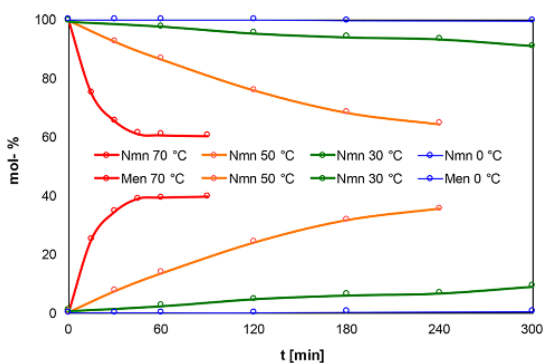
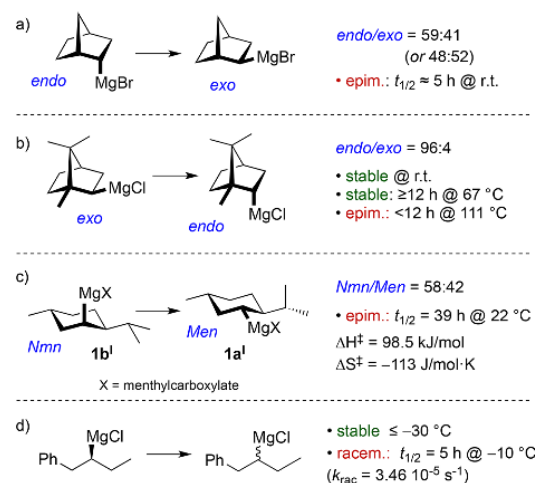


Figure 9. Temperature-dependent epimerization of NmnMg(O₂CMe) (**1b**¹) in THF solution. The 300 min data point at 0 °C was extrapolated for graphical reasons. Curves are interpolated and serve as guidelines only.

°C, dr 55.6:44.4; 70 °C, dr 54.8:45.2). This is not contradictory because the major chemical species in **1** differ from those in carboxylated reagent **1a**¹/**1b**¹ by the presence of chloride vs menthyl carboxylate as counterion (Scheme 5b). However, the carboxylated reagent shows a surprising prevalence of the axially substituted Nmn diastereomer **1b**¹, which may be a consequence of secondary dimerization and solvation equilibria⁸⁰ because MgX usually favors the equatorial position in cyclohexanes.^{81,82} Independent confirmation that the change of conformational preference is caused by the carboxylate counterion was obtained by combining **1** with lithium salts of hindered carboxylic acids and determining the composition of the in situ generated (Men/Nmn)Mg(O₂CR) species after thermal equilibration. With 2,4,6-trimethylbenzoate (mesitoate), the shift was from dr 57:43 (**1a**/**1b**, rt) to 47:53 (**1a**¹/**1b**¹, 60 °C; after 24 h). The recovery of RMgX (by quantitative ²H NMR⁷¹) was 98%, which proves that the change of composition is caused by isomerization and not kinetic ablation (e.g., by hydride elimination) of one isomer.⁷¹ In another experiment with lithium pivalate, the resulting **1a**¹/**1b**¹ was allowed to equilibrate at 70 °C, and the reaction progress was followed by sampling and D₂O quenching (Figure 10).

Scheme 6. Configurational Stability of Secondary Alkyl-Grignard Reagents



^aNorbornylmagnesium halides are known to slowly epimerize at rt. Reported data are faintly conflicting.⁷⁴ ^bBornylmagnesium chloride forms as a kinetic *endo/exo* 67:33 mixture but changes to 96:4 upon heating.^{75,76} ^cMenthylmagnesium compounds slowly epimerize at rt (this work). ^dHoffmann's open-chain chiral Grignard reagent racemizes quickly at rt.⁷⁹

The initial excess of menthyl diastereomer **1a**¹ epimerizes with a half-life of 26 min (cf. 8 min for **1a**¹/**1b**¹) to a new equilibrium at 42.9% **1a**¹, which is less than in case of mesitoate (46.8% **1a**¹) but higher than for menthanecarboxylate (39.5% of **1a**¹) as counterions. The influence of counterion X in MenMgX on Men/Nmn equilibrium composition and epimerization kinetics is substantial and contributes to the complexity of reaction systems involving reagent **1** with other ionic components.

Stereochemistry and Relative Kinetics of Electrophilic Substitution at C-1 of Menthyl Grignard Reagent. The result of the low-temperature carboxylation of **1** (Scheme 5, a) is expressed in tabular form in Table 2, entry 1. Based on

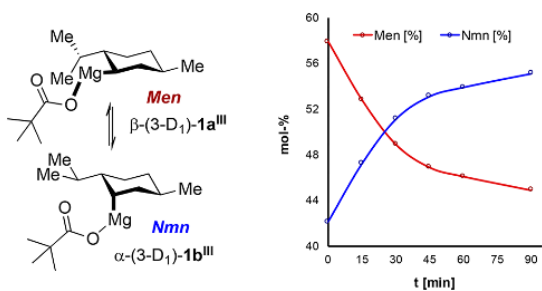


Figure 10. Equilibration of in situ prepared MenMg(OPiv)/NmnMg(OPiv) (**1a^{III}**/**1b^{III}**) in THF solution at 70 °C. A solution of **1** was mixed with LiOPiv and heated to 70 °C. Equilibrium ratio **1a^{III}**/**1b^{III}** = 42.9:57.1 (after 69 h).

the known initial amount of **1a** and **1b**, analysis of remaining Men-D (β -(3-D₁)-**4**) and Nmn-D (α -(3-D₁)-**4**) in the product mixture reveals how much of each diastereomer was converted in a reaction. This quantity is expressed as $\Delta 1a/\Delta 1b$ in mol % (−56/−3 mol %) and compared to the quantity of epimeric substitution products formed (+58/+0 mol %; Table 2, last column). Since the numbers are close, the conclusion can be reached that CO₂ reacts with **1** by a retentive mechanism. This agrees with the observation of retention of configuration at the stereogenic carbon in the carboxylation of Hoffmann's chiral Grignard reagent (cf. Scheme 6).^{79a} Reactions of other *H*- and *P*-centered electrophiles with Grignard reagent **1** were similarly investigated, and the results are collected in Table 2.

Coinciding analytical results for the dr of Grignard reagent **1** from ¹³C NMR and ²H NMR analysis (after D₂O quenching) prove that hydro-demetalation of **1a/b** proceeds with retention of configuration at C-1. This is also demonstrated in the

quenching of **1b** with D₂O to give essentially pure α -(3-D₁)-**4** (Figure 9), which implies stereospecificity. However, protonation of **1a** and **1b** could still proceed at different rates. Reaction of **1** with a limited amount of protons, followed by quenching with excess D₂O, reveals the unreacted amount and dr of **1a/b** by ²H NMR.⁷¹ In the reaction of **1** with 0.25 equiv of water, **1a** is selectively attacked while **1b** initially remains (Table 2, entry 2). With twice the amount of water (0.5 equiv), **1b** is also partially protonated, but at a lower rate than **1a**, such that the remaining **1** is depleted in the latter (Table 2, entry 3). Water is a more stereoselective acid in this reaction than alcohols are (entries 4 and 5). Kinetic resolution by protonation (or hydronation) is only relevant if the hydron source is limiting but will not play a role if excess D₂O is used to quench **1**. Neither is a dynamic kinetic resolution expected in view of the slow epimerization of **1a/b** under quenching conditions (at rt or below).

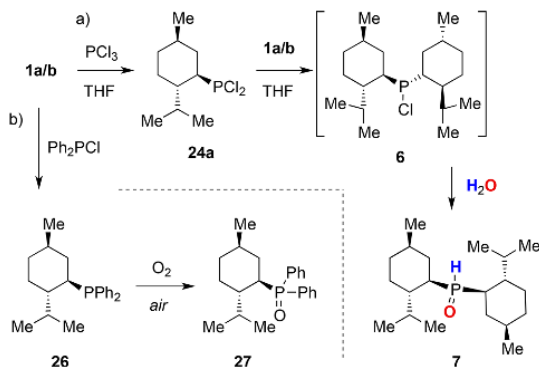
Turning to phosphorus electrophiles, reagent **1** was allowed to react with excess PCl₃ in the cold and the resulting, sensitive methyl dichlorophosphane (**24**) converted to phosphinic acid RPH(=O)(OH) (**25**) by quenching with water (Table 2, entry 6). The high yield and diastereoselectivity (dr 15:1)⁸³ prove that the reaction proceeds with a high degree of stereoconvergence from both **1a** and **1b** to **24a**. Thus, the reported high yield of 90% of **24a** from **1**,^{11a} exceeding by far the amount of available epimer **1a** in **1**, is confirmed by our experiment.

Combination of **1** with PCl₃ in a 2:1 ratio followed by heating to reflux is the standard procedure to prepare Men₂PCl (**6**).¹ The reported yield is low at 13%¹⁰ or 25–35%.¹ Analysis of the reaction mixture is considerably simplified by quenching with D₂O (**1** → (3-D₁)-**4**) and hydrolysis of **6** to phosphine oxide **7** (Scheme 7). The usual procedure (mixing at 0 °C, then heating) followed by protic, aqueous workup gave a fair

Table 2. Quantitative Investigation of the Reactions of Grignard Reagent **1** with Various Electrophiles^{a,b}

entry	RMgX (1a , 1b) ^{b,c} (mol %)	T ^d (°C)	E ^{+e} (mol %)	Men-D ($\Delta 1a$) ^f (mol %)	Nmn-D ($\Delta 1b$) ^f (mol %)	dr (D ₁)- 4	R-E ^g (mol %)
1	100 (57, 42)	−78	CO ₂ (xs)	1 (−56)	39 (−3)	1:99	MenCO ₂ H (19 ; 58%); NmnCO ₂ H (20 ; 0%)
2	100 (57, 42)	−78 → rt	H ₂ O (25)	36 (−21)	41 (−1)	47:53	
3	100 (57, 42)	−78 → rt	H ₂ O (50)	5 (−51)	28 (−13)	16:84	
4	100 (57, 42)	−78 → rt	MeOH (50)	33 (−23)	32 (−9)	51:49	
5	100 (57, 42)	−78 → rt	MenOH (50)	32 (−25)	30 (−11)	52:48	
6	100 (57, 42)	−78 → rt ^h	PCl ₃ (200)	nd	nd	nd	MenPO ₂ H ₂ (25a ; 92%); NmnPO ₂ H ₂ (25b ; 6%)
7	300 (170, 127)	0 → 50	PCl ₃ (100)	25 (−145)	34 (−93)	43:57	Men ₂ POH (7 ; 61%)
8a ⁱ	300 (170, 127)	0	PCl ₃ (100)	41 (−129)	49 (−78)	45:55	Men ₂ POH (7 ; 75%)
8b ⁱ	300 (170, 127)	0	PCl ₃ (100)	44 (−126)	48 (−79)	48:52	Men ₂ POH (7 ; 73%)
9	100 (57, 42)	0 → rt	Ph ₂ PCl (100)	8 (−49)	21 (−21)	28:72	MenPOPh ₂ (27 ; 72%)

^aGeneral conditions: **1** was added to electrophile E⁺ in THF at −78 or 0 °C. After being stirred for 1–3 h, reactions were quenched with D₂O and warmed to rt. ^bReactant quantities and analytical compositions are given in mol %, rounded to the next nearest integer number. See the Supporting Information for more precise values expressed in μ mol. ^cThe composition of **1** varies from **1a/b** = 57:43 to 58:42, with ca. 1 mol % of ψ -MenMgCl (**12**) present; the composition of starting **1** (57:42:1 mol %) represents an average value. ^dRoom temperature (rt) is ca. 22 °C. ^eE⁺ = electrophile, quantity in mol % relative to **1** in parentheses. ^fRemaining quantity of **1a/b** upon conclusion of the reaction, as determined by D₂O quenching and ²H{¹H} NMR quantification of (D₁)-**4**. The number in parentheses indicates change (loss) of organometallic reagent over the course of the reaction. ^gR-E = electrophilic substitution product. ^hReaction duration 3 h at −78 °C, followed by warming to rt with stirring overnight. ⁱ8a is a repetition experiment of 8a.

Scheme 7. Reaction of **1** with Phosphorus Electrophiles

spectral yield of **7** (Table 2, entry 7). The remaining **1** (dr 43:57; analyzed as (3- D_1)-**4**) displayed less enrichment than expected for a kinetic resolution, although this ratio might have been affected by epimerization of **1a/b** upon heating. Performing the reaction at 0 °C throughout further increased the yield of **7**, without affecting the dr of unreacted Grignard reagent (Table 2, entries 8a/b). The results show that both substitution events with nucleophile **1** along $\text{PCl}_3 \rightarrow \text{MenPCl}_2$ (**24**) $\rightarrow \text{Men}_2\text{PCl}$ (**6**) proceed stereoconvergently with respect to C-1 of **1**, with both diastereomers **1a** and **1b** contributing substantially to produce **6**, with a slight kinetic preference for **1a** in reactions with P–Cl electrophiles. Even though the generation of **7** was limited to 75 mol %, and unreacted **1** was still present, no major organophosphorus species was detected in the organic phase. Failure to detect hydrolysis product **25** (MenPO_2H_2) means that both **24** (and thus also the more reactive PCl_3) must have been spent at the conclusion of the reaction. The unaccounted loss of phosphorus in entries 7–9 is approximately half the molar quantity of unaccounted loss of RMgX , which suggests that redox processes accompanying the main reaction lead to reduced, water-soluble phosphorus species and neutral hydrocarbons as side products.

The reaction of **1** with Ph_2PCl ^{2,13,14} was also analyzed (Table 2, entry 9). A previous, qualitative report stated that quenching the reaction of equimolar **1** and Ph_2PCl with D_2O gave a mixture with half the original **1** (i.e., **1a**) converted to MenPPh_2 , with the other half (i.e., **1b**) returning Nmn-D (α -(3- D_1)-**4**). In our hands, the analytical yield of oxide **27**, which emerged from phosphane **26** during workup in air, exceeds the initially present quantity of **1a** (Table 2, entry 9; Scheme 7). Even though the kinetic preference for **1a** is marked, roughly half of epimer **1b** must have reacted with inversion of configuration at C-1 to account for the observed yield (cf. $\Delta 1\text{a/b}$ in Table 2, entry 9), which fits the pattern observed with PCl_3 ($\rightarrow 24$) and which agrees with the stereoconvergent reactions of bornyl- and fenchylmagnesium reagents with P–Cl electrophiles.^{75a} Phosphine oxide **27** was isolated and structurally characterized by X-ray crystallography (Figure 11). The conformation of the menthyl group is consistent with previous observations (Figure 3).

Synthesis and Properties of Dimethylphosphine Oxide. In the preparative study of the reaction of PCl_3 with **1** to give Men_2PCl (**6**), we were initially guided by the hypothesis that 4 equiv of **1**, corresponding to approximately 2 equiv of **1a**, might provide a higher yield if **1a** is the exclusive

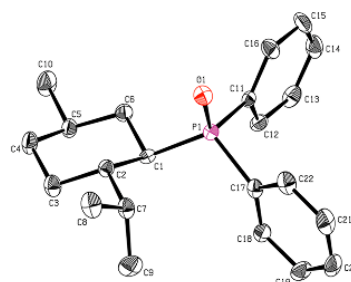


Figure 11. Solid-state X-ray molecular structure of menthlyldiphenylphosphine *P*-oxide (**27**). Ellipsoids are shown at 50% probability. Hydrogens are omitted for clarity. Oxygen is red, phosphorus purple.

nucleophile.^{2,75b} However, variation of the ratio $\text{PCl}_3/1$ over 1:1, 1:3, 1:4, and 1:6 indicated that already 1:3 was optimal and use of additional Grignard reagent had a counterproductive effect. Hydrolysis of the 1:3 reaction mixture (containing **6**) gave the expected, previously unknown dimethylphosphine *P*-oxide (**7**; Table 2, entries 7 and 8, and Scheme 7)³⁰ that was readily quantified by ^1H NMR in crude reaction mixtures. Chromatography required acetic acid as additive, with which **7** forms a hydrogen-bonded complex that must be split with base prior to solvent evaporation. The product was obtained as slowly crystallizing oil in 50% yield. Spectral properties agree with a C_1 -symmetric structure, with two signal sets for diastereotopic menthyl groups (^1H , ^{13}C NMR), a single $^{31}\text{P}\{^1\text{H}\}$ NMR resonance (δ_{P} 41.8), and a characteristic doublet of doublets at δ_{H} 6.77 with the large $^1J(^{31}\text{P},^1\text{H})$ of 435.5 Hz for the central P(O)H-unit. The identity of this material as **7** was further secured by single crystal X-ray crystallographic analysis (Figure 12).

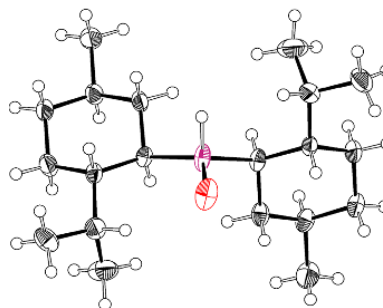


Figure 12. Solid-state molecular structure of dimethylphosphine *P*-oxide (**7**). Oxygen is colored red, phosphorus purple. Ellipsoids are shown at 50% probability. The unit cell contains three independent molecules of very similar geometry, of which one is displayed.

Based on the 2D NMR analysis (Figure S29 and Table S25), the diastereotopic menthyl groups (Men^{Re} , Men^{Si}) differ by a $^3J_{\text{P,H}}$ coupling (5.6 Hz) from H–P to H-1 in Men^{Re} , which is absent ($^3J_{\text{P,H}} \approx 0$ Hz) for H-1 in Men^{Si} . This observation is consistent with the solid-state conformation in the X-ray structure having torsional angles of -169° (to H-1 in Men^{Re}) or -50° (to H-1 in Men^{Si}). The P=O oxygen is involved in short intramolecular contacts with H-1' of the isopropyl group in Men^{Re} (237 pm) and H-2 of Men^{Si} (283 pm), and those interactions are reflected by higher frequency δ_{H} signals for the

respective nuclei, compared to their diastereotopic counterparts. The usual conformation of C-2-isopropyl in menthyl derivatives is observed (Figure 3, a).

CONCLUSIONS

Menthyl Grignard reagent (**1**) has been known and used in asymmetric synthesis for many years. However, its exact chemical composition and reaction stereochemistry have remained insecure in the absence of direct analytical studies. In the reaction sequence starting from **2** via **1** and leading to various substitution products (Scheme 1), the stereochemistry of the first and second steps were not known with certainty, and neither was the configurative stability of **1a/b** established. Methods to analyze the composition **1a/b** had relied on reactions with electrophiles (CO₂, D₂O), the results of which could have been affected by kinetic resolution effects. Even for D₂O quenching, the assumption that the dr of (3-D₁)-**4** reflects the dr of **1a/b** (i.e., retention of configuration in protodemetalation) was unproved.

In the present study, we have for the first time analyzed menthyl Grignard reagent *in situ* by combining ¹H and ¹³C NMR methods. MenMgX (**1a'**) and NmnMgX (**1b'**) were confirmed as major organometallic components of the reagent, besides hydrocarbons *trans-p*-menthane (**4**), 2-menthene (**8**), 3-menthene (**9**), and three diastereomeric Wurz products **13–15**. The Schlenk equilibrium is operative and produces considerable amounts of Men₂Mg from **1a** at low halide concentration, whereas **1b** is less notably involved in equilibria. The Schlenk equilibrium complicates quantitative NMR analysis since minor and dynamic species display exchange-broadened signals. The intensity of the characteristic ¹³C NMR signals δ_C 49.5 and 52.8 for the major components **1a'** and **1b'** does not reflect the dr **1a:1b**. Use of dibromoethane or other halogenated reagents for initiating the Grignard reaction has the beneficial effect of shifting the Schlenk equilibrium toward **1a'/b'** and giving easier to analyze NMR spectra. However, integration of defined ranges of the ¹³C NMR spectrum (δ 48–51 for C-2 of **1a**, δ 51–54 for C-2 of **1b**) led to consistent results for the **1a/b**-dr that agreed with the D₂O quenching results and confirm retention of configuration in deuterolysis of the C–Mg bond. On the basis of this benchmarking experiment, the technically simple and fast ²H{¹H} NMR analysis of **1a/b** after D₂O quenching can be carried out with confidence. Besides analyzing the peak area ratio of the α/β-(3-D₁)-**4** signals (δ_D 0.94 and 1.65), analysis in the presence of a deuterated internal standard (e.g., C₆D₆ for simplicity, or preferably less volatile, solid derivatives for weighing out⁷¹) allows the accurate quantification of **1a/b**.

NMR methods were used to investigate the effect of reaction conditions in the magnesium insertion of **2** or **3** on the composition of the resulting Grignard reagent **1**. The observed abundance of saturated and unsaturated hydrocarbon by-products agrees with their generation by a Kharasch–Reinmuth–Walborsky surface radical mechanism.⁶³ A surprising aspect is that the abundance of byproducts is inversely proportional to the reaction temperature, with reactions at 50–70 °C giving highest yields of **1** and lowest levels of byproducts. This finding opposes a comment of Kharasch and Reinmuth, “In general these [competing] reactions require (or at least are favored by) higher temperatures than the Grignard reagent formation reaction, and, in general, they are favored by relatively high halide (RX) concentrations”,⁸⁴ but agrees with

observations made during the preparation of *t*-BuMgCl in ether.⁸⁵

Epimerization in the course of Grignard reagent formation (Scheme 1, **I**) is extensive at any given reaction temperature, and both **2** and **3** give rise to comparable amounts of **1a/b** by kinetic stereoconvergence. In that aspect, the previous findings² were confirmed. However, upon closer inspection, the dr **1a/b** shows an influence of the configuration of starting materials **2/3**, if the Grignard is prepared at, or close to, ambient temperature. Walborsky has previously observed partial retention of configuration in Grignard reactions and ascribed it to a concerted oxidative addition mechanism that runs parallel to the surface-group mechanism.^{63,86}

The configurative stability of **1a/b** was formerly uncertain or had been assumed to be high at ambient temperature.² It is now clear that epimerization is fast at 50–70 °C and contributes to the generation of **1a/b** in fractions near their thermodynamic ratio (55:45 at 70 °C), although kinetic control yields similar ratios. Upon storage of reagent **1** under ambient conditions, the dr slightly rises over several days or weeks to a room temperature equilibrium value of 58:42. The closeness of kinetic and thermodynamic selectivity renders the investigation of equilibration kinetics difficult, yet such experiments have become possible through the carboxylation of **1** at low temperature, which induces a clean kinetic separation of **1b** from **1a**. Temperature-dependent kinetic equilibration studies starting with diastereomerically pure Grignard reagent **1b'** give excellent results (Figure 9) and prove that Men/Nmn-MgX are equilibrating species. The process is slow at ambient temperature but can be accelerated by heating to 70 °C without loss of reagent due to decomposition. The equilibration measurements revealed a counterion effect on the configurational equilibrium Men/NmnMgX (X = counterion) that runs against the established preference in substituted cyclohexanes of preferentially accommodating large substituents in equatorial positions. Surprisingly, we find that sterically large carboxylates X prefer NmnMgX over MenMgX. Additional steric hindrance caused by RMgX(S)_n dimerization or ligand-exchange equilibria might be responsible for this deviation from the usual steric interpretation of A values.⁸¹

Based on the newly established composition and diastereomerization kinetics of **1**, the stereochemistry of reactions with electrophiles was investigated. Determining the dr and yield of substitution product is not sufficient in such studies, since the interference of kinetic resolution effects is only recognized if absolute amounts of substitution products and unreacted **1a/b** are accurately known. This is evident from the reinvestigation of the carboxylation of **1a/b**, which had previously been reported with inconsistent results. We find that a sharp kinetic resolution of **1a/b** by reaction with CO₂ in the cold gives MenCO₂H (**19**) in a quantity that is limited by the amount of initially present **1a**, while **1b** remains unreacted. Extended reaction time or higher temperature generate variable amounts of NmnCO₂H (**20**) by slow carboxylation of **1b**. At sufficiently high temperature, dynamic kinetic asymmetric transformation of **1a/b** becomes possible, which explains the success of a patent procedure that finds a high yield of **19** by concomitant exposure of CO₂ and **2** to magnesium at 90 °C in 2-MeTHF–cymene.⁶⁸

Rather different results were obtained in reactions of **1** with phosphorus electrophiles, where all cases investigated displayed stereoconvergence, with both **1a** and **1b** contributing to

the generation of menthyl-configured substitution products, even if preferential consumption of **1a** over **1b** distinguishes the former as the better nucleophile. Kinetic product control is consistent with a common intermediate and supports the SET-mechanism²⁰ known to be operative for a range of C-electrophiles, and also established in reactions of the bornyl and fenchyl Grignard reagents with PCl_3 and other phosphorus electrophiles.⁷⁵ A consequence of the stereoconvergent SET-mechanism is the high yield of MenPCl_2 (**24**), which can be achieved in reactions of **1** with excess PCl_3 at low temperature under conditions where the interconversion of **1a/b** is frozen. Attempts to maximize the yield of Men_2PCl (**6**) from PCl_3 by using 4 or 6 equiv of **1** were counter-productive, since the spectral yields of hydrolysis product dimethylphosphine *P*-oxide (**7**) did not surpass that obtained in the reaction with 3 equiv of **1** (73–75%, Table 2). The missing 25 mol % of phosphorus in those reactions are apparently lost to redox side-reactions leading to inorganic phosphorus species. Phosphine oxide **7** is an interesting platform chemical for chiral phosphane synthesis, or may itself serve as chiral SPO (secondary phosphine oxide) ligand. Work toward both applications is currently ongoing in our laboratories.

EXPERIMENTAL SECTION

General Methods. Chemicals and solvents were obtained commercially and used without purification unless mentioned. Solvents for Grignard reactions were filtered over activated Al_2O_3 and stored under argon over molecular sieves (3 Å). The materials used in the study were all derived from menthol (**5**) of natural (1*R*)-configuration ((1*R*,2*S*,5*R*)-2-isopropyl-5-methylcyclohexanol). Menthyl chloride (**2**) and neomenthyl chloride (**3**) were obtained as previously described.²⁹ Grignard solutions were titrated against salicylaldehyde phenylhydrazone.⁴⁰ ^1H NMR measurements for quantitative analyses were performed using a relaxation recovery delay (d1) of 20 s. ESI-high-resolution mass spectra were measured using FT-ICR detection. CCDC 1499983 (**22**), 1499984 (**7**), 1519897 (**13**), and 1567948 (**27**) contain the supplementary crystallographic data for this paper. These data can be obtained free of charge from The Cambridge Crystallographic Data Centre.

Samples and Referencing. Regular NMR samples in CDCl_3 were referenced to TMS (δ_{C} and δ_{H} 0 ppm). Samples of Grignard reagent were measured in solvent mixtures of nondeuterated solvents (THF, Et_2O , toluene) with C_6D_6 added for locking or in selected cases prepared and measured in fully deuterated solvent (D_8 -THF). Naphthalene was usually added as internal standard. In view of the special media containing dissolved magnesium salts and organometallic species at high concentration, the usual practice of referencing to residual solvent signal is not advisable, since the solvent chemical shift is affected by the dissolved salts. In the majority of cases, external (machine) referencing was kept. For the key analytical samples, the chemical shift of typical components (naphthalene) and solvents is indicated to allow for comparability.

NMR Data Tables (Supporting Information) and CH Index. The substance NMR data tables list ^{13}C NMR peak chemical shifts together with peak area integration data (arbitrary units). The values were obtained by deconvolutive peak fitting. Peak area is also provided as "CH-index" value, i.e., as a dimensionless number relative to the average peak area of all CH signals (set to 1.000). The index numbers are close to 1 for CH , CH_2 and CH_3 peaks but <1 for quaternary carbons. The CH-index data is useful for assigning individual signals to peak sets of specific components (at variable abundance) in complex mixtures such as Grignard reagent **1**.

1-Methoxy-4-(D_3 -methoxy)-benzene. This deuterated compound was used as internal standard for ^2H NMR spectroscopy. Due to its volatility, applications are restricted to conditions that do not involve solvent evaporation or prolonged heating. **Synthesis:** To a solution of 4-methoxyphenol (3.29 g, 26.5 mmol, 1.00 equiv) in DMF (20 mL)

were added powdered K_2CO_3 (6.23 g, 45.1 mmol, 1.70 equiv) and CD_3I (5.00 g, 34.5 mmol, 1.30 equiv). The suspension was stirred at room temperature for 26 h. The reaction was quenched by addition of a water/brine mixture (1:1, 30 mL). After extraction with ethyl acetate (3 × 20 mL), the combined organic phases were washed with water–brine (1:1, 4 × 20 mL) and dried over MgSO_4 . After filtration, the solvent was removed by rotary evaporation, and the crude product was purified by column chromatography (hexanes– EtOAc 20:1) to give 3.20 g (86%) colorless crystalline solid. Spectral data (^1H , $^2\text{H}\{^1\text{H}\}$ and ^{13}C NMR) conformed with literature values.⁸⁷ ^1H NMR (400 MHz, CDCl_3): δ 3.76 (s, 3H), 6.83 (s, 4H). ^{13}C NMR (101 MHz, CDCl_3): δ 55.0 (sept, $J_{\text{C-D}} = 22$ Hz; CD_3), 55.9 (CH_3), 114.8 (CH), 114.8 (CH), 153.9 (2 C). $^2\text{H}\{^1\text{H}\}$ NMR (61 MHz, CH_2Cl_2 ; $\delta\{\text{CHDCl}_2\} = 5.32$): δ 3.72 (s, 3 D).

Synthesis of Menthyl Grignard Reagent in THF (1). General Procedure 1 (GP1). In a 250 mL Schlenk vessel, magnesium turnings (4.99 g, 205.5 mmol, 1.37 equiv) were covered with dry THF (35 mL) and heated to 50 °C in an oil bath. A solution of menthyl chloride (98% **2+3**; 26.74 g, 150.0 mmol, 1 equiv) in THF (65 mL) was placed into a dropping funnel and mounted on the reaction vessel. Two crystals of iodine and 1/10 of the volume of the menthyl chloride solution were added to the magnesium. After the reaction had initiated, the oil bath heating was shut off. The remaining solution of **2** was added to the stirred Mg suspension over 45 min, such that the oil bath temperature did not exceed 60 °C. After completion of the addition, the reaction mixture was stirred for 2 h at 70 °C and then cooled to room temperature. Content of active RMgX : 1.02 M by titration.

Synthesis of Menthyl Grignard Reagent (1) from Menthyl Chloride in THF–Toluene at 70 °C. In a Schlenk vessel under argon, magnesium turnings (12.5 g, 514 mmol) were covered with THF (25 mL) and toluene (50 mL). A little iodine was added and the mixture heated with stirring to 70 °C in an oil bath. A solution of menthyl chloride (**2**; 97% isomeric purity; 49.5 g, 283 mmol) in THF (25 mL) was added dropwise over 1 h with control of the external oil bath reaction temperature. After completion of the addition, the mixture was stirred for 2 h at 70 °C, cooled to rt, and stirred overnight. Titration indicated a concentration of active $[\text{RMgX}]$ of 1.43 ± 0.1 mol/L.

Analytical Scale Synthesis of Menthyl Grignard Reagent. General Procedure 2 (GP2). Menthyl chloride (**1**; 0.92–0.96 g, 5.3–5.5 mmol, 1.0 equiv) was dissolved in the solvent (1.0 mL for high concentration conditions, 2.0 mL for low concentration). Magnesium turnings (0.25 g, 1.9 equiv) and a grain of iodine were stirred in the given solvent (1.0 mL for high concentration conditions, 3.0 mL for low concentration) and heated to the required temperature. For experiments in THF–toluene, **1** was dissolved in THF (1 mL), and the reaction vessel was filled with THF (1.0 mL) and toluene (2.0 mL). An aliquot of the solution of **1** was added to initiate the reaction. After the reaction had started, the solution of **1** was added over 10 min. Reactions at room temperature were stirred overnight unless otherwise mentioned, reactions at 50 °C for 2 h, and reactions at 70 °C for 1 h. After cooling of the Grignard reagent to rt, a weighed amount of naphthalene was added as internal standard, and samples for analysis were removed.

NMR Analysis of Analytical-Scale Menthyl Grignard Samples. For recording ^1H and ^{13}C NMR spectra, a sample (ca. 0.5 mL) of the Grignard solution was filled into a septum-capped NMR tube under argon, and dry C_6D_6 (ca. 0.2 mL) was added for locking.

^2H NMR Analysis of the 1a/b Ratio (Simplified Procedure, Table 1). To record a ^2H NMR spectrum, a sample of the Grignard solution was quenched by addition of degassed D_2O . The water phase was acidified with HCl aq and extracted with CHCl_3 . The organic layer was washed with H_2O and brine and dried over MgSO_4 .

Specific Menthyl Grignard Samples for NMR Analysis. Menthyl Grignard reagent in THF for NMR analysis with C_6D_6 addition (sample A). The sample was prepared as usual from menthyl chloride (5.72 mmol, 97% purity) and Mg (6.71 mmol) in THF (2.5 mL) at rt with initial addition of iodine and ethylene bromide for activation. Naphthalene (110.1 mg, internal standard) was dissolved

in the reagent. A sample of reagent (0.30 mL) and C_6D_6 (0.30 mL) were combined in an NMR tube. External referencing placed the signals for THF at δ_C 25.300, 68.305; for C_6D_6 at δ_C 127.660; and for naphthalene at δ_C 125.699, 127.798, 133.633; the values are indicated with higher precision since they serve referencing purposes.

Menthyl Grignard reagent in (D_8)-THF (sample B). The sample was prepared following GP2, starting from menthyl chloride (5.45 mmol, 93.7% MenCl, 2.5% NmnCl), Mg (10.3 mmol) and 1,2-dibromoethane (ca. 50 μ L) in (D_8)-THF (5.0 mL) at 70 °C. Naphthalene (105.8 mg, internal standard) was dissolved in the final reagent. A sample of 0.50 mL was combined with 0.10 mL of C_6D_6 in an NMR tube. See Figure 1 for the 1H NMR spectrum. External referencing placed the residual signals of (D_7)-THF at δ_H 1.764, 3.682; silicon grease at δ_H 0.11; solvent (D_8)-THF at δ_C 24.509, 67.135, and naphthalene at δ_C 125.788, 127.847, 133.803.

Synthesis of Grignard Reagent from Neomenthyl Chloride in (D_8)-THF (Sample C). A Grignard reagent was prepared from neomenthyl chloride (5.44 mmol, 97% purity), Mg (10.3 mmol), ethylene bromide (ca. 50 μ L), and ethyl bromide (ca. 50 μ L) in (D_8)-THF (5.0 mL) at rt with overnight stirring for completion of the reaction. A sample of reagent (0.60 mL) was combined with naphthalene (34.5 mg, internal standard) in an NMR tube. External referencing placed the solvent signal of (D_8)-THF at δ_C 24.299, 67.178 and naphthalene at δ_C 125.627, 127.679, 133.585.

Synthesis of Menthyl Grignard Reagent in Ethyl Ether (Sample D). The Grignard reagent was prepared from menthyl chloride (5.34 mmol, 93.7% MenCl, 2.5% NmnCl) and Mg (10.4 mmol) in Et_2O (5.0 mL) at 40 °C. After dissolution of naphthalene (107.2 mg, internal standard), a sample (0.50 mL) was combined with C_6D_6 (0.10 mL) in an NMR tube. External referencing placed the solvent signals of Et_2O at δ_C 14.709, 65.371; of C_6D_6 at δ_C 127.518; and of naphthalene at δ_C 125.521, 127.682, 133.586.

Analysis of RMgX Content of Menthyl Grignard Reagent. By Titration against Salicylaldehyde Phenylhydrazone.⁴⁰ In a 10 mL Schlenk tube, salicylaldehyde phenylhydrazone (100 mg, 471 μ mol) was dissolved in THF (3.0 mL). Grignard solution was added dropwise from a filled syringe (1 mL, 0.01 mL graded) until the solution changed its color from yellow to orange. The titration was repeated at least once.

By Quantitative $^2H\{^1H\}$ NMR Spectroscopy. Grignard solution (0.50 mL) was added with efficient magnetic stirring to a 10 mL Schlenk tube containing D_2O (1 mL). After 15 min, aq HCl (2 M, 10 mL) was added. The mixture was extracted with $CHCl_3$ (2 \times 15 mL). The combined organic phase was washed with water (3 \times 10 mL) and satd aq NaCl (15 mL) and dried over $MgSO_4$. After filtration, the solvent was evaporated (40 °C, 450 mbar) until a few milliliters remained, C_6D_6 (10.0 μ L) or a weighed quantity of p -(CD_3O)- $C_6H_4OCH_3$ was added, and a sample was removed for $^2H\{^1H\}$ NMR analysis.

Analysis of the Mg Content of Menthyl Grignard Reagent. Total magnesium was determined by adding a known volume of the Grignard solution (0.5–1 mL) to 1 M aq HCl (ca. 5 mL) with stirring until solids were fully dissolved. After dilution to 20.00 mL, aliquots of 5.00 mL were removed for titration. Each sample was basified with 3–4 mL of pH 10 buffer (ca. 6 M, NH_3-NH_4Cl). A few milligrams of eriochrome black T (ground to a powder with solid NaCl in a 1:100 ratio) was added, and the solution was titrated against Na_2EDTA (0.1 M, 5 mL microburet).⁴⁸

Isolation of *trans-p*-Menthane (4) and Bimethyl Isomer Mixture (13/14/15) from Menthyl Grignard Reagent (1). A menthyl Grignard reagent (ca. 60 mL, 1 M) prepared from crude 2 (80% purity) was quenched with satd aq NH_4Cl (50 mL) and 1 M HCl aq (50 mL). After addition of Et_2O (50 mL) and transfer into a funnel, the phases were separated, and the organic phase washed with 1 M HCl aq (2 \times) and water (2 \times). The organic phase was evaporated and the residual oil distilled in vacuo (bath 60–70 °C, vapor 38–45 °C, vacuum 8 mbar) to remove the menthane/menthene fraction (see below for further processing). The residual yellowish oil was transferred into a separatory funnel with hexanes (40 mL) and the solution washed with concd H_2SO_4 (4 \times 10 mL); the first washing

was accompanied by warming and was completed within 20 s, immediately removing the lower acidic layer. Finally, the organic layer was washed with 10% aq NH_3 (CAUTION: exothermic reaction with H_2SO_4 residues in the funnel) and filtered over a bead of $MgSO_4$. After evaporation, a few mL of a colorless liquid remained, which was distilled in a Kugelrohr oven (170 °C, ca. 0.1 mbar) to give a colorless oil (ca. 2.0 g), consisting of 13/14/15 in a ratio of 38.6:45.1:16.3. See the Supporting Information for a complete 1H and ^{13}C NMR analysis and assignment. The menthane/menthene fraction was similarly diluted with hexanes, washed with concd H_2SO_4 , and distilled (59–60 °C, 24.3 mbar) to give a mixture of *trans-p*-menthane (4) and ψ -menthane (16) in a ratio of 96:4; see the Supporting Information for spectral analyses.

Symmetrical Bimethyl or (1*R*,1'*R*,2*S*,2'*S*,5*R*,5'*R*)-2,2'-Diisopropyl-5,5'-dimethyl-1,1'-bi(cyclohexane) (13). Upon standing of the above bimethyl diastereomer mixture, the symmetric bimethyl (13) crystallized over several days (Figure S20); one crystal was used for the X-ray crystal structure analysis. The liquid fraction was removed with a pipet (1.60 g; 13/14/15 = 23.5:56.1:20.4) and the solid was pressed between tissue paper to remove liquid. Recrystallization from hot $EtOH$ with addition of toluene for solubilization, followed by standing at rt gave colorless crystals (240 mg). Mp: 105.6–106.2 °C. ^{13}C NMR (100 MHz, $CDCl_3$): δ 15.4, 21.9, 23.1, 24.8, 25.3, 33.2, 34.7, 35.6, 37.9, 43.7; see the Supporting Information for comprehensive 1H and ^{13}C NMR data and assignments. HR-ESI-MS: calcd for $C_{20}H_{38}^+$ ($[M]^+$) 278.2968, found 278.2972.

Carboxylation of 1 under Different Addition Modes (Scheme 4). **Addition of Solid CO_2 to Grignard Solution at Ambient Temperature.** Preparation of the Grignard reagent: Menthyl chloride (3.68 g, 21.1 mmol) in THF (4 mL) was added dropwise over 10 min to iodine-activated magnesium turnings (1.05 g, 43.2 mmol) in THF (4 mL) at 50 °C. After being stirred for 2 h at 50 °C, the reaction mixture was stirred overnight at ambient temperature. Titration against salicylaldehyde phenylhydrazone indicated a concentration of active reagent of 1.36 mol/L. A Schlenk vessel was charged with Grignard reagent (4 mL, 5.44 mmol) under argon and placed in a room-temperature water bath. Pieces of dry ice (CO_2 (s)) were added consecutively to the stirred solution such that a constant CO_2 evolution was notable (silicon oil bubbler). The reaction mixture became viscous over time. After 2 h, the reaction was quenched by addition of aq 1 M HCl (10 mL). The organic phase was collected, and the aqueous phase was extracted with Et_2O (10 mL). The combined organic phase was extracted three times with aq 2 M NaOH (3 \times 30 mL). The aqueous extract was acidified with aq 6 M HCl to pH 2 and the mixture extracted three times with Et_2O (3 \times 30 mL). The combined organic extracts were washed with satd NaCl aq (40 mL) and dried over $MgSO_4$. Filtration and evaporation in vacuo gave colorless oil (724 mg, 72.4% crude yield). The composition was determined by adding 1,1,2,2-tetrachloroethane (317 mg, 1.89 mmol) and $CDCl_3$ (1.4 mL) to the mixture, followed by recording of a quantitative 1H NMR ($d_1 = 20$ s). Analysis: 60.24 mol % of 19, 7.57 mol % of 20, combined = 67.8% (see Figure S23 for the spectrum).

Addition of Grignard Solution to Excess CO_2 in THF Solution at Low Temperature. In a Schlenk vessel under argon, THF (6 mL) was cooled to -72 °C in an $EtOH-CO_2$ (s) bath. Pieces of dry ice (CO_2 (s); ca. 4 g) were added to the THF, and the bath temperature was increased to -20 °C. Menthyl Grignard reagent (as above; 5 mL, 6.80 mmol) was added dropwise to the CO_2 solution over 20 min. The reaction was stirred for 2 h at -20 °C, with some more additions of CO_2 (s) to ascertain a constant gas evolution through the silicon oil bubbler vent. The reaction was then quenched at -20 °C by addition of aq 1 M HCl (15 mL). Workup as above gave a colorless oil (783 mg, 62.6% crude yield), which was analyzed by 1H NMR after addition of 1,1,2,2-tetrachloroethane (300 mg, 1.79 mmol) and $CDCl_3$ (1.4 mL). Analysis: 55.9 mol % of 19, 2.8 mol % of 20, combined: 58.7% (see Figure S24 for the spectrum).

Selected Analytical ^{13}C NMR Data for Carboxylic Acids. Complete NMR data assignments for menthyl- and neomenthylcarboxylic acids 19/20 have been published.⁸⁸ The ^{13}C NMR chemical

shifts for stereo- and regioisomeric carboxylic acids from the current work are listed below. The data sets have been extracted from carboxylation mixtures, and acids **21** and **23** were only detected as minor components.

Menthylcarboxylic acid (19). ^{13}C NMR (100 MHz, CDCl_3): δ 16.0, 21.3, 22.3, 23.8, 29.3, 32.0, 34.5, 38.8, 44.2, 47.7, 183.3.

Neomenthylcarboxylic Acid (20). ^{13}C NMR (100 MHz, CDCl_3): δ 21.3 (overl.), 21.5, 22.4, 25.5, 27.5, 30.3, 35.3, 38.0, 42.0, 46.4, 182.2. The following acids have been detected as minor components in the carboxylation products of Grignard reagents from crude menthyl chloride isomer mixtures. **tert- ψ -Menthancarboxylic Acid (21).** ^{13}C NMR (75.5 MHz, CDCl_3): δ 21.0, 25.7* (or $2 \times \text{CH}_3$?), (29.1*?), 33.0, 33.5, 34.2, 37.5, 42.3, 43.8, 47.3, 184.7*. Due to signal overlap, it is not clear if δ 25.7 corresponds to $2 \times \text{CH}_3$, and δ 29.1 might be an artifact. **sec- ψ -Menthancarboxylic Acid (23).** ^{13}C NMR (100 MHz, CDCl_3), two diastereomers: δ 18.3/18.1, 20.84/20.78, 21.51 (overl.)/21.47, 29.1/29.0, 29.62/29.60, 33.3/33.2, 34.3/34.0, 40.1/39.9, 40.5/40.3, 57.54/57.49, 181.8/181.7.

Ethyl 2-((1R,2S,5R)-2-isopropyl-5-methylcyclohexane-carboxamido)acetate (22). **Carboxylation of Grignard Reagent 1.** A ca. 1 M Grignard reagent **1** derived from 75% pure menthyl chloride isomer mixture (containing regioisomeric chloromethanes, see ref 29) and magnesium in THF (70 mL, ≥ 70 mmol) was combined with a piece of dry CO_2 (s) (ca. 4 g) with stirring. The mixture first warmed, and then cooled again. After the CO_2 (g) evolution had ceased, the mixture was carefully quenched with 2 M HCl aq (100 mL) in small portions and Et_2O (200 mL). The organic phase was washed with 2 M HCl aq (50 mL) and water (3×50 mL). The organic phase was extracted with 1 M Na_2CO_3 aq (100 mL + 2×50 mL). The combined basic aqueous phase was extracted with Et_2O (2×50 mL) and acidified with concd HCl aq (25 mL; CO_2 evolution). Extraction with Et_2O (3×50 mL), drying of the organic extract (Na_2SO_4), filtration, and evaporation gave 8.34 g of crude viscous oil, which was used in the next step. According to ^1H NMR analysis, the crude product contained the carboxylic acids **19/20/21** in a molar ratio of 100:5.2:24.2.

Coupling with Ethyl Glycinate (Adapted from ref 69b). The crude carboxylic acid mixture (8.34 g, ca. 45 mmol) in CH_2Cl_2 (25 mL) was combined with SOCl_2 (5.0 mL, 69 mmol) and DMF (5 drops) and stirred for 2 h at 50°C , while developing acidic exhaust gases were absorbed into water. Volatiles were then removed at 50°C into a cooling trap using water aspiration vacuum (12 mbar). The residue was taken up in toluene (5 mL), and volatiles were again evaporated at 75°C in vacuo (12 mbar). The residual crude acid chloride was taken up in Et_2O (80 mL) and this solution was added to a solution of ethyl glycinate hydrochloride (10.0 g, 71.6 mmol) in water (100 mL). Solid NaHCO_3 (16.0 g, 190 mmol) was added in portions (CO_2 evolution) to the two-phase mixture, which was further stirred overnight (15 h) at rt. The aqueous phase was deployed, and the organic phase washed with satd aq NaHCO_3 and satd aq NaCl. After drying (Na_2SO_4), filtration, and evaporation, the oily residue, which had an amine smell, was taken up in EtOAc and washed with 2 M HCl aq ($2 \times$) and water ($2 \times$). After evaporation to dryness, a viscous oil was obtained, which crystallized over the course of 2 days and consisted of a mixture of product together with the neomenthyl and *tert- ψ* -menthyl isomers (78.3:3.9:17.8, by ^1H NMR). The material was dissolved in hot hexanes (50 mL) and stored at -20°C to produce colorless crystals of pure material (3.0 g, 25%) also suitable for X-ray crystal structure analysis. Mp: $80.5\text{--}81.4^\circ\text{C}$. ^1H NMR (400 MHz, CDCl_3): δ 0.79 (d, $^3J(\text{H,H}) = 6.9$ Hz, 3 H; Me of 2'-iPr), 0.89 (d, $^3J(\text{H,H}) = 6.5$ Hz, 3 H; Me-C5'), 0.90 (d, $^3J(\text{H,H}) = 6.9$ Hz, 3 H; Me' of 2'-iPr), 0.96 (m, 1 H; H-4'), 1.02 (m, 1 H; H-3'), 1.23 (q, $^2/3J(\text{H,H}) \approx 12.4$ Hz, 1 H; H-6' ax), 1.29 (t, $^3J(\text{H,H}) = 7.2$ Hz, 3 H; Me of OEt), 1.31–1.42 (m, H-5'), 1.54 (tt, $^3J(\text{H,H}) = 11.5$, 2.9 Hz, H-2') 1.65–1.77 (m, 3 H; H-3' at δ 1.68, H-4' at δ 1.73, CH of 2-iPr at δ 1.74), 1.81 (dq, $^2J(\text{H,H}) = 12.7$, $^3J(\text{H,H}) = 2.3$ Hz, 1H; H-6' eq), 2.10 (td, $^3J(\text{H,H}) = 11.6$, 3.4 Hz, 1 H; H-1'), 4.04 (ψ -d, $^2J(\text{H,H}) = 5.2$ Hz, 2 H; H-2 of Gly), 4.22 (q, $^2J(\text{H,H}) = 7.2$ Hz, 2 H; CH₂ of OEt), 5.97 (br. t, $^3J(\text{H,H}) = 5.2$ Hz, 1 NH). ^{13}C NMR (100 MHz, CDCl_3): δ 14.2, 16.2, 21.5, 22.4, 23.9, 28.7, 32.4, 34.7, 39.5,

41.3, 44.4, 49.6, 61.5, 170.3, 176.1; see the Supporting Information for comprehensive assignments. HR-ESI-MS: calcd for $\text{C}_{15}\text{H}_{28}\text{NO}_3^+$ ($[\text{M} + \text{H}]^+$) 270.2064, found 270.2063.

Equilibration Studies with Menthyl Grignard Reagent. **Equilibrium Composition of Menthyl Grignard Reagent at Various Temperatures.** A 10 mL Schlenk tube was charged with Grignard reagent (2.94 mL, 1.02 M in THF, 3.00 mmol). The solution was stirred for 3 h at 50°C and another 3 h at 70°C . Samples (ca. 0.5 mL) were taken at the outset, after 3 h at 50°C , and after 3 h at 70°C . The D_2O quenching analysis was performed according to GP 4 (see below). A room-temperature sample was measured after storing reagent **1** for several weeks at ambient temperature. Recovery may be measured by adding *p*- $\text{C}_6\text{H}_4(\text{OMe})(\text{OCD}_3)$ to the thermally equilibrated Grignard solution prior to quenching. Erratic results (overly high recovery) were obtained if the internal standard was added to hot Grignard solutions for kinetic measurements. Thus, the latter had to rely on the ratio **1a/1b** (i.e., (D_1)-**4a/4b**).

Kinetic Resolution of 1a/b with Carbon Dioxide. **General Procedure 3 (GP3).** A 20 mL Schlenk tube was charged with THF (2 mL) and cooled to -78°C . CO_2 (ca. 2.0 g) was added, and the tube was closed with a septum and balloon. Then Grignard solution (5.88 mL, 1.02 M in THF, 6.00 mmol) was added dropwise over 10 min, and the resulting mixture was stirred for 1 h at -78°C . Unreacted CO_2 was removed by applying a high vacuum (15 min at -78°C) to give a solution of neomenthylmagnesium carboxylate **1b**¹ (>99:1 neomenthyl/menthyl-Mg) as indicated by ^2H NMR after D_2O quench (GP4).

D_2O Quenching of Grignard Carboxylate Solutions. **General Procedure 4 (GP4).** A sample (~ 0.5 mL) of the Grignard solution (GP3) was mixed with D_2O (1 mL) and stirred vigorously for 15 min at room temperature under argon. Then 2 M HCl (10 mL) was added followed by extraction with CH_2Cl_2 (2×15 mL). The combined organic phases were washed with satd Na_2CO_3 (3×15 mL) and brine (10 mL) and dried over MgSO_4 . After filtration, the solvent was evaporated until a few milliliters remained (750 mbar, 40°C), which were analyzed by $^2\text{H}\{^1\text{H}\}$ NMR analysis.

Kinetic Equilibration Studies of Neomenthylmagnesium Menthylcarboxylate. Solutions of neomenthylmagnesium menthylcarboxylate (**1b**¹) were prepared by the GP3 as described above. The reaction vessel was placed into an oil-bath at the desired temperature. In regular intervals, samples (~ 0.5 mL) were removed and quenched according to the GP4 to determine the diastereomeric ratio. For data points and plots, see Tables S18 and S19 and Figure S25.

Menthyl/Neomenthyl Epimerization of 1 after Addition of Lithium Carboxylates. **Equilibrium Epimer Distribution in the Presence of Carboxylates.** The procedure is exemplified with mesitoic acid (2,4,6-trimethylbenzoic acid): Lithium mesitoate was generated from mesitoic acid (82.1 mg, 0.50 mmol; 1 equiv) in the presence of a trace amount of phenanthroline (basicity indicator) in THF (3 mL) by titration with *n*-BuLi in hexanes (1.6 M; ca. 0.33 mL required). Grignard solution **1** (0.49 mL; 1.02 M in THF, 0.50 mmol, 1 equiv) was added at rt. The mixture was heated to 60°C and stirred for 24 h. Internal standard (*p*- $\text{MeOC}_6\text{H}_4\text{OCD}_3$; 35.3 mg) was added and the mixture quenched with D_2O (5 mL) and stirred for 15 min under argon. The mixture was acidified with 2 M HCl aq (10 mL) and extracted with CH_2Cl_2 (2×15 mL). The combined organic phase was washed with water (15 mL) and brine (15 mL) and dried over MgSO_4 . After filtration, the solvent was carefully concentrated in vacuo (750 mbar, 40°C) to a few milliliters, which were used for $^2\text{H}\{^1\text{H}\}$ NMR analysis. The ratio Men/Mnm was 46.8/53.2, and the recovery of [RMg] (as sum of (D_1)-**4** and (D_1)-**16**) was 489 μmol (= 98%).

Kinetic Experiment with Lithium Pivalate. Pivalic acid (112.3 mg, 1.10 mmol) and a few crystals of phenanthroline (basicity indicator) in dry THF (3.0 mL) were titrated with *n*-BuLi solution (1.6 M in hexane; ca. 0.74 mL) until the color turned from yellow to brownish. Additional THF (2.0 mL) and a solution of menthyl Grignard reagent **1** (0.98 mL, 1 mmol; equilibrated at rt) were added at rt. The vessel was placed into an oil bath at 70°C , and samples were removed after

the indicated time for quenching with D₂O (GP4). See Figure S25 and Tables S19 and 20 for the kinetic data and analysis.

Analytical Studies of Reactions of 1 with Electrophiles (Table 2). *Reaction of 1 with CO₂ (Table 2, Entry 1).* A 20 mL Schlenk tube was charged with THF (1 mL) and cooled to -78 °C. CO₂ (ca. 1.5 g) was added, and the tube was closed with a septum and balloon. Then Grignard solution (2.94 mL, 1.02 M in THF, 3.00 mmol) was added dropwise over 7 min, and the resulting mixture was stirred for 1 h at -78 °C. The cooling bath was removed, and D₂O (4 mL) was added carefully in portions. After the solution was stirred for 15 min at room temperature, 2 M HCl (10 mL) was added followed by extraction with CH₂Cl₂ (2 × 15 mL). The combined organic phases were washed with satd NaHCO₃ (3 × 15 mL, removal of carboxylic acids) and brine (10 mL) and dried over MgSO₄. After filtration, the solvent was evaporated until few milliliters remained, C₆D₆ (20.0 μL) was added, and a sample was taken for the ²H NMR (no NMR solvent). The combined NaHCO₃ phases were acidified with 2 M HCl and extracted with ethyl acetate (4 × 20 mL). After drying over Na₂SO₄ and filtration, the solvent was evaporated to give a colorless oil. It was dissolved in CHCl₃ (1.5 mL), and 1,1,2,2-tetrachloroethane was added as internal standard for ¹H qNMR.

Reactions of 1 with protic Acids H₂O or ROH (Table 2, Entries 2–5). A 10 mL Schlenk tube was charged with Grignard solution (1; 0.98 mL, 1.02 M in THF, 1.00 mmol) and cooled to -78 °C (if the mixture gets too viscous, dilution with a little THF is recommended). In reactions with water, H₂O was added as 1 M stem solution in THF (250/500 μL); in reactions with alcohols, a solution of the alcohol (500 μmol) in THF (0.5 mL) was added. The mixture was stirred for 1 h at -78 °C, the cooling bath was removed, and the reaction was stirred for 30 min at room temperature. The mixture was placed in an ice bath, quenched by addition of D₂O (2 mL), and stirred vigorously for 15 min at room temperature. A weighed amount of internal standard 1-methoxy-4-(D₃-methoxy)benzene and aq HCl (2 M, 10 mL) was added. After extraction with CH₂Cl₂ (2 × 15 mL), the combined organic phases were washed with water (15 mL) and satd aq NaCl (15 mL) and dried over MgSO₄. The solvent was evaporated (40 °C, 750 mbar) until few milliliters remained, and a sample was removed for ²H{¹H} NMR analysis.

Reaction of 1 with Phosphorus Electrophiles (Table 2, Entries 6–9). A solution of the corresponding phosphorus electrophile in THF was cooled (0 or -78 °C) and the Grignard solution (1.02 M) added dropwise over 10 min. The resulting suspension was stirred for the specified time at the indicated temperature followed by appropriate workup.

Reaction of 1 with Ph₂PCl and Isolation of MenPOPh₂ (27). The mixture was placed in an ice bath, quenched by addition of D₂O (2 mL), and stirred vigorously for 15 min at room temperature. After addition of aq HCl (2 M, 10 mL) and extraction with CH₂Cl₂ (2 × 15 mL), the combined organic phases were washed with water (15 mL) and satd aq NaCl (15 mL) and dried over Na₂SO₄. The solvent was evaporated (40 °C, 750 mbar) until few mL remained, a weighed amount of internal standard 1-methoxy-4-(D₃-methoxy)benzene was added, and a sample was removed for ²H{¹H} NMR and ¹H qNMR analysis, which revealed the presence of 72% of MenP(O)Ph₂ (27). Isolation of the main product was performed by column chromatography (CH₂Cl₂-MeOH 50:1) and subsequent recrystallization of the combined product fractions from hexanes-EtOAc (5:1) to give colorless solid (121 mg, 36%; not optimized).

Data for P-Menthylidiphenylphosphine P-Oxide (27). Crystals suitable for X-ray crystal structure analysis were grown by slow evaporation (open flask) of solvent from the mother liquor. ¹H NMR (400 MHz, CDCl₃): δ 0.48 (d, J = 6.7 Hz, 3 H), 0.77 (d, J = 6.4 Hz, 3 H), 0.78 (d, J = 6.8, 3 H), 0.84–0.96 (m, 1 H), 1.04–1.16 (m, 2 H), 1.26–1.39 (m, 1 H), 1.48–1.55 (m, 1 H), 1.66–1.82 (m, 3 H), 1.99 (sept, J ≈ 6.1 Hz, 1 H), 2.31–2.40 (m, 1 H), 7.41–7.50 (m, 6 H), 7.74–7.89 (m, 4 H). ¹³C NMR (101 MHz, C₆D₆): δ 16.0 (CH₃), 21.9 (CH₃), 22.7 (CH₃), 25.2 (d, J(P,C) = 12.0 Hz), 28.5 (d, J(P,C) = 3.4 Hz), 33.7 (d, J(P,C) = 13.5 Hz), 34.7 (d, J(P,C) = 1.5 Hz), 36.6 (d, J(P,C) = 2.0 Hz), 39.6 (d, J(P,C) = 70.6 Hz), 43.8 (d, J(P,C) = 3.1 Hz), 128.5 (d, J(P,C) = 0.5 Hz), 128.6 (d, J(P,C) = 0.5 Hz),

130.7 (d, J(P,C) = 8.5 Hz), 130.81 (d, J(P,C) = 2.7 Hz), 130.82 (d, J(P,C) = 2.7 Hz), 131.4 (d, J(P,C) = 8.1 Hz), 135.3 (d, J(P,C) = 92.4 Hz), 137.3 (d, J(P,C) = 90.0 Hz). ³¹P NMR (126 MHz, CDCl₃): δ 33.7.

Reaction of 1 with Excess PCl₃. The reaction was quenched by addition of 1 M HCl (5 mL) at 0 °C (ice bath) followed by vigorous stirring for 30 min at 0 °C. The mixture was extracted with EtOAc (2 × 15 mL), and the organic phase washed with brine (2 × 5 mL) and evaporated. The residue was dissolved in CDCl₃; 1,1,2,2-tetrachloroethane was added as internal standard for ¹H qNMR.

Data for Menthylphosphinic Acid (25). ¹H NMR (400 MHz, CDCl₃): δ 0.78–1.11 (m, 3 H), 0.84 (d, J = 6.8 Hz, 3 H), 0.93 (d, J = 6.7 Hz, 3 H), 0.95 (d, J = 7.1 Hz, 3 H), 1.28–1.41 (m, 1 H), 1.53–1.64 (m, 1 H), 1.67–1.80 (m, 3 H), 1.92–2.01 (m, 1 H), 2.21 (sept × d, J = 6.8, 2.8 Hz, 1 H), 7.12 (d, ¹J(P,H) = 536.7 Hz, 1 H), 11.51 (br. s, 1 H, OH). ¹³C NMR (126 MHz, CDCl₃): δ 15.5, 21.5, 22.5, 24.3 (d, J(P,C) = 14.2 Hz), 28.2 (br), 32.0, 32.7 (d, J(P,C) = 15.4 Hz), 34.4, 39.5 (d, J(P,C) = 95.5 Hz), 42.3. ³¹P NMR (162 MHz, CDCl₃): δ 41.0 (MenPO₂H₂), 36.5 (NmnPO₂H₂).

Reaction with Limiting PCl₃. The mixture was quenched by addition of D₂O (4 mL) at rt, followed by vigorous stirring for 15 min. Then 2 M HCl (3 mL, degassed by bubbling with argon for 1 min) was added. After stirring for 3 h at room temperature, the mixture was extracted with diethyl ether (2 × 15 mL), the organic phase washed with 1 M HCl (3 × 10 mL) and brine (15 mL) and dried over MgSO₄. After filtration, the solvent was evaporated (40 °C, 500 mbar) and the residue dissolved in a little CH₂Cl₂ (ca. 3 mL). After addition of naphthalene and C₆D₆ as internal standards, a sample for ²H NMR was removed; from the remainder, CH₂Cl₂ was carefully removed (40 °C, 500 mbar), and a ¹H qNMR spectrum was measured in CDCl₃.

Dimethylphosphine Oxide or Bis((1R,2S,5R)-2-isopropyl-5-methylcyclohexyl)phosphine Oxide (7). *Synthesis from Purified 97% Menthyl Chloride.* All steps prior to hydrolytic workup were performed under argon. A Grignard reagent was prepared from menthyl chloride (2; 97% isomeric purity; 49.5 g, 283 mmol) in THF (25 mL) by dropwise addition at 70 °C over 1 h to iodine activated magnesium turnings (12.5 g, 514 mmol) in THF (25 mL) and toluene (50 mL). The mixture was stirred for another 2 h at 70 °C, cooled to rt, and stirred overnight. Titration indicated a concentration of active RMgX of 1.43 ± 0.1 mol/L. The Grignard solution was transferred through PTFE tubing and dropped into a stirred solution of PCl₃ (8.12 mL, 93.1 mmol) in THF (40 mL) cooled to 0–10 °C (ice–water bath) in a 500 mL round-bottom Schlenk flask. The rate of addition was regulated to prevent overheating and intense stirring was applied to keep the developing slurry homogeneous and in a state of constant movement. A brownish crystalline residue of the Grignard solution was dissolved in THF (10 mL) and also added to the PCl₃ suspension. After completion of the additions (1.5 h), the reaction mixture was allowed to warm to 20–30 °C (0.5 h) and further heated to 60 °C (3 h) with intense stirring. The fine, thick gray-greenish slurry was allowed to cool to rt. After being placed into an ice bath, the mixture was quenched by addition of Et₂O (100 mL) and 1 M HCl aq (200 mL) in portions. After overnight stirring, two homogeneous phases had formed. The mixture was transferred (in air) into a separatory funnel. The aqueous phase was extracted with Et₂O (1×). The combined, slightly yellow organic phase was washed with 1 M HCl aq (2×) and sat NaCl aq (1×). The organic phase was evaporated (10 mbar, 50 °C) to leave a viscous oil, which was absorbed on 30 g of silica. The crude product was purified by dry column chromatography⁸⁹ in two batches, using 100 mL solvent fractions of *t*-BuOMe–hexane (1:5) with increasing percentage of HOAc from 0–3 vol % for elution (Table S23). Product fractions of differing purity were collected separately, washed with 2 M NaOH aq (3 × 30–100 mL), and washed with brine (1×). The organic phase was evaporated to give the product as a colorless solid (15.2 g, 50%) in five fractions of 90–97% purity (Table S24). A sample for analysis was recrystallized by dissolving in a small volume of hexane and cooling to -70 °C. Mp: 90.2–90.5 °C. IR (film): 1158, 1167 (P=O), 1454 (CH₂ bend), 2304 (br, P–H), 2868, 2923, 2952 (C–H st).

¹H NMR (CDCl₃, 500 MHz): δ 0.81 (d, ³J(H,H) = 6.9 Hz, 3 H), 0.85 (d, ³J(H,H) = 6.8 Hz, 3 H), 0.93 (d, ³J(H,H) = 6.6 Hz, 3 H), 0.94 (d, ³J(H,H) = 7.0 Hz, 3 H), 0.95 (d, ³J(H,H) = 6.1 Hz, 3 H), 0.97 (d, ³J(H,H) = 6.8 Hz, 3 H), 0.8–1.2 (m, 5 H), 1.33–1.46 (m, 3 H), 1.53 (m, 1 H), 1.61–1.82 (m, 8 H), 1.96 (m, 1 H), 2.22 (sept × d, ³J(H,H) = 6.9, 2.5 Hz, 1 H), 2.64 (sept × d, ³J(H,H) = 6.9, 2.8 Hz, 1 H), 6.77 (dd, ¹J(P,H) = 435.5 Hz, ³J(H,H) = 5.6 Hz, 1 H, P–H). ¹³C{¹H} NMR (CDCl₃, 126 MHz): δ 15.5, 15.7, 21.5, 21.6, 22.6, 22.7, 24.2 (d, J(P,C) = 11.1 Hz), 24.7 (d, J(P,C) = 12.6 Hz), 27.4 (d, J(P,C) = 5.1 Hz), 28.3 (d, J(P,C) = 2.4 Hz), 32.3 (d, J(P,C) = 3.8 Hz), 32.7 (d, J(P,C) = 14.4 Hz), 32.7 (d, J(P,C) = 12.5 Hz), 34.33 (d, J(P,C) = 1.7 Hz), 34.34, 34.4 (d, J(P,C) = 1.2 Hz), 36.5 (d, J(P,C) = 62.0 Hz), 37.0 (d, J(P,C) = 64.6 Hz), 41.4 (d, J(P,C) = 3.5 Hz), 44.6 (d, J(P,C) = 3.0 Hz). ³¹P{¹H} NMR (CDCl₃, 162 MHz): δ 41.8. HR-ESI-MS: calcd for C₂₀H₄₀OP⁺ 327.2811 ([M + H]⁺), found 327.2811.

■ ASSOCIATED CONTENT

Supporting Information

The Supporting Information is available free of charge on the ACS Publications website at DOI: 10.1021/acs.joc.8b02278.

Detailed NMR spectral illustrations, data and assignments, copies of NMR spectra of isolated compounds, kinetic data points and details of the data-analysis, photographs of crystals, additional ORTEP and ball and stick illustrations, and general crystallographic information (PDF)

X-ray data for compound **7** (CIF)

X-ray data for compound **13** (CIF)

X-ray data for compound **22** (CIF)

X-ray data for compound **27** (CIF)

■ AUTHOR INFORMATION

Corresponding Author

*E-mail: lukas.hintermann@tum.de

ORCID

Alexander Pöthig: 0000-0003-4663-3949

Lukas Hintermann: 0000-0003-2622-8663

Notes

The authors declare no competing financial interest.

■ ACKNOWLEDGMENTS

We thank Prof. Dr. Wolfgang Eisenreich (TU München), for assistance with setting up two-dimensional NMR spectra, Dr. Gerd Gemmecker and M. Sc. Johannes Günther from the Chair of Biomolecular NMR Spectroscopy (TU München) for recording 950 MHz spectra, and the Hans-Fischer-Gesellschaft for financial support.

■ REFERENCES

- (1) Krause, H. W.; Kinting, A. Herstellung von *P*-Chlordimethylphosphin. *J. Prakt. Chem.* **1980**, 322 (3), 485–486.
- (2) Beckmann, J.; Dakternieks, D.; Dräger, M.; Duthie, A. New Insights into the Classic Chiral Grignard Reagent (1*R*,2*S*,5*R*)-Menthylmagnesium Chloride. *Angew. Chem., Int. Ed.* **2006**, 45 (39), 6509–6512.
- (3) (a) Dallacker, F.; Alroggen, I.; Krings, H.; Laurs, B.; Lipp, M. Neue Verbindungen der Terpenreihe und verwandter Systeme. *Justus Liebigs Annalen der Chemie* **1961**, 647 (1), 23–36. (b) Bose, A. K.; Harrison, S.; Farber, L. Stereochemistry of Terpenes. IV. The Configuration of Some Amines. *J. Org. Chem.* **1963**, 28 (5), 1223–1225. (c) Pfeiffer, H.-P.; Sander, H.; Breitmaier, E. Chirale Lattenzaun-Porphyrine. *Liebigs Annalen der Chemie* **1987**, 1987 (8), 725–726.

(4) Wu, S.; Yang, N.; Yang, L.; Cao, J.; Liu, J. A novel type of optically active helical polymers: Synthesis and characterization of poly(α,β -unsaturated ketone). *J. Polym. Sci., Part A: Polym. Chem.* **2010**, 48 (6), 1441–1448.

(5) Zelinsky, N. Ueber die Synthese der Menthancarbonsäure und der Camphancarbonsäure. *Ber. Dtsch. Chem. Ges.* **1902**, 35 (4), 4415–4419.

(6) Smith, J. G.; Wright, G. F. The Diastereomeric Menthyl Chlorides Obtained from (–) Menthol. *J. Org. Chem.* **1952**, 17 (8), 1116–1121.

(7) (a) Kurssanow, N. Über Menthol und Mentholderivate. *Chem. Zentralbl.* **1915**, 86, 893–895. (b) Kurssanow, N. Über Menthancarbonsäure. *Chem. Zentralbl.* **1923**, 94, 1275–1276.

(8) Cunningham, D.; Gallagher, E. T.; Grayson, D. H.; McArdle, P. J.; Storey, C. B.; Wilcock, D. J. Synthesis and characterization of a suite of four chiral pyridyl alcohols derived from (–)-menthol. *J. Chem. Soc., Perkin Trans.* **2002**, 1 (23), 2692–2698.

(9) Kato, A.; Ueda, H.; Hashimoto, Y. Studies on Menthol Derivatives. *Agric. Biol. Chem.* **1970**, 34 (1), 28–31.

(10) Hägele, G.; Kückelhaus, W.; Seega, J.; Tossing, G.; Kessler, H.; Schuck, R. Menthylsubstituierte Phosphorverbindungen, II. L-Men-(R)P(X)Cl (R = Cl, L-Men, D-Men; X = –, S). Charakterisierung singularer, diastereotoper und enantiotoper Menthylgruppen durch ¹H-, ¹³C- und ³¹P-NMR-Techniken/ Menthyl-Substituted Phosphorus Compounds, II L-M en(R)P(X)Cl (R = Cl, L-Men, D-Men; X = –, S). Characterization of Singular, Diastereotopic and Enantiotopic Menthyl-Groups by ¹H, ¹³C and ³¹P NMR Techniques. *Z. Naturforsch., B: J. Chem. Sci.* **1985**, 40 (8), 1053–1063.

(11) (a) Brandes, H.; Goddard, R.; Jolly, P. W.; Krüger, C.; Mynott, R.; Wilke, G. Transition Metal Allyls, V. The Preparation and Structure of [NiX(PmenthylR₁R₂)(η^3 -allyl)] Complexes. *Z. Naturforsch., B: J. Chem. Sci.* **1984**, 39 (8), 1139–1150. (b) Gruber, M.; Schmutzler, R.; Ackermann, M.; Seega, J.; Hägele, G. Menthyl-Substituted Organo-Phosphorus-Compounds. VII: Fluorinated Compounds and Derivatives. *Phosphorus, Sulfur Silicon Relat. Elem.* **1989**, 44 (1–2), 109–122. (c) Hidai, M.; Mizuta, H.; Yagi, H.; Nagai, Y.; Hata, K.; Uchida, Y. Palladium-catalyzed asymmetric telomerization of isoprene. Preparation of optically active citronellol. *J. Organomet. Chem.* **1982**, 232 (1), 89–98. (d) Hinke, A.; Kuchen, W. Zur Kenntnis der Organophosphorverbindungen, XXI. Darstellung von Organobromphosphanen aus RPCL₂ und R₂PCl durch Halogenaustausch. *Phosphorus Sulfur Silicon Relat. Elem.* **1983**, 15 (1), 93–98.

(12) Wang, J.-P.; Nie, S.-Z.; Zhou, Z.-Y.; Ye, J.-J.; Wen, J.-H.; Zhao, C.-Q. Preparation of Optically Pure Tertiary Phosphine Oxide via the Addition of *P*-Stereoogenic Secondary Phosphine Oxide to Activated Alkenes. *J. Org. Chem.* **2016**, 81 (17), 7644–7653.

(13) Tanaka, M.; Ogata, I. A Novel Route to Menthylidiphenylphosphine. *Bull. Chem. Soc. Jpn.* **1975**, 48 (3), 1094–1094.

(14) Dakternieks, D.; Dunn, K.; Henry, D. J.; Schiesser, C. H.; Tiekink, E. R. T. Organostannanes Derived from (–)-Menthol: Controlling Stereochemistry during the Preparation of (1*R*,2*S*,5*R*)-Menthylidiphenyltin Hydride and Bis((1*R*,2*S*,5*R*)-menthyl)phenyltin Hydride. *Organometallics* **1999**, 18 (17), 3342–3347.

(15) (a) Zeng, L.; Dakternieks, D.; Duthie, A.; Perchyonok, T.; Schiesser, C. Synthesis, characterization and enantioselective free radical reductions of (1*R*,2*S*,5*R*)-menthylidiphenylgermane and its enantiomer. *Tetrahedron: Asymmetry* **2004**, 15 (16), 2547–2554. (b) Faraoni, M. B.; Vetere, V.; Casella, M. L.; Podestá, J. C. Synthesis of new (–)-menthylgermanium derivatives and its use in heterogeneous bimetallic catalysis. *J. Organomet. Chem.* **2011**, 696 (21), 3440–3444.

(16) (a) Lucas, C.; Santini, C. C.; Prinz, M.; Cordonnier, M.-A.; Basset, J.-M.; Connil, M.-F.; Jousseau, B. New optically active organotin compounds for heterogeneous bimetallic catalysis. *J. Organomet. Chem.* **1996**, 520 (1–2), 101–106. (b) Podestá, J. C.; Chopra, A. B.; Radivoy, G. E.; Vitale, C. A. Synthesis and some reactions of mixed (–)-menthyltin hydrides. *J. Organomet. Chem.* **1995**, 494 (1–2), 11–16. (c) Podestá, J. C.; Radivoy, G. E. Synthesis and Physical Properties of Hexa(–)-menthyltin and Its Derivatives.

- Organometallics* **1994**, *13* (8), 3364–3365. (d) Vitale, C. A.; Podestá, J. C. Synthesis and some properties of mixed alkyl-di-(–)-menthyltin hydrides. *J. Chem. Soc., Perkin Trans. 1* **1996**, No. 19, 2407–2410. (e) Schumann, H.; Wassermann, B. C. Novel asymmetric triorganotin hydrides containing the (–)-menthyl ligand. *J. Organomet. Chem.* **1989**, *365* (1–2), C1–C5.
- (17) Schumann, H.; Stenzel, O.; Dechert, S.; Girgsdies, F.; Halterman, R. L. Menthyl-Functionalized Chiral Nonracemic Monoindenyl Complexes of Rhodium, Iridium, Cobalt, and Molybdenum. *Organometallics* **2001**, *20* (11), 2215–2225.
- (18) (a) Thaler, T.; Haag, B.; Gavryushin, A.; Schober, K.; Hartmann, E.; Gschwind, R. M.; Zipse, H.; Mayer, P.; Knochel, P. Highly diastereoselective Csp^3 – Csp^2 Negishi cross-coupling with 1,2-, 1,3- and 1,4-substituted cycloalkylzinc compounds. *Nat. Chem.* **2010**, *2* (2), 125–130. (b) Thaler, T.; Guo, L.-N.; Mayer, P.; Knochel, P. Highly Diastereoselective $C(sp^3)$ – $C(sp)$ Cross-Coupling Reactions between 1,3- and 1,4-Substituted Cyclohexylzinc Reagents and Bromoalkynes through Remote Stereocontrol. *Angew. Chem., Int. Ed.* **2011**, *50* (9), 2174–2177. (c) Moriya, K.; Knochel, P. Diastereoconvergent Negishi Cross-Coupling Using Functionalized Cyclohexylzinc Reagents. *Org. Lett.* **2014**, *16* (3), 924–927.
- (19) Zuzek, A. A.; Reynolds, S. C.; Glueck, D. S.; Golen, J. A.; Rheingold, A. L. Synthesis and Structure of Gold and Platinum Menthyl Complexes. *Organometallics* **2011**, *30* (7), 1812–1817.
- (20) Hoffmann, R. W. The quest for chiral Grignard reagents. *Chem. Soc. Rev.* **2003**, *32* (4), 225–230.
- (21) (a) Bethell, D.; Bulman Page, P. C.; Vahedi, H. Catalytic Asymmetric Oxidation of Sulfides to Sulfoxides Mediated by Chiral 3-Substituted-1,2-benzisothiazole 1,1-Dioxides. *J. Org. Chem.* **2000**, *65* (20), 6756–6760. (b) De Mallmann, A.; Lot, O.; Perrier, N.; Lefebvre, F.; Santini, C. C.; Basset, J. M. Surface Organometallic Chemistry of Tin: Reactivity of Two Chiral Organostannic, ((–)-menthyl) Me_3Sn and ((–)-menthyl) Me_2SnH , toward Silica. *Organometallics* **1998**, *17* (6), 1031–1043. (c) Hofmann, M.; Clark, T.; Heinemann, F. W.; Zenneck, U. Rock around the Ring: An Experimental and Theoretical Study of the Molecular Dynamics of Stannyltriphospholes with Chiral Tin Substituents. *Eur. J. Inorg. Chem.* **2008**, *2008* (13), 2225–2237.
- (22) For related questions in reactions of lithium reagents, see: Basu, A.; Thayumanavan, S. Configurational Stability and Transfer of Stereochemical Information in the Reactions of Enantioenriched Organolithium Reagents. *Angew. Chem., Int. Ed.* **2002**, *41*, 716–738.
- (23) Configurational stability tests for organometallics: (a) Hoffmann, R. W. (2010). *Test on the Configurational Stability/Lability of Organolithium Compounds. In Stereochemical Aspects of Organolithium Compounds*; Gawley, R. E., Ed.; Verlag Helvetica Chimica Acta: Zürich, 165–188. doi: DOI: 10.1002/9783906390628.ch5. (b) Hoffmann, R. W.; Julius, M.; Chemla, F.; Ruhland, T.; Frenzen, G. Configurational stability of chiral organolithium compounds on the time scale of their addition to aldehydes. *Tetrahedron* **1994**, *50* (20), 6049–6060.
- (24) Seel, S. (2013). Stereoselective Preparation and Stereochemical Behaviour of Organozinc and Organolithium Reagents. PhD Thesis, Ludwig-Maximilian-Universität, München, URN: urn:nbn:de:bvb:19-165998.
- (25) Menthylzinc iodide with CF_3CO_2D at rt gave (D_1)-4 with dr 65:35, but dr > 99:1 at –78 °C; with MeOD at rt, the dr was also > 99:1. Since the reagent is configurationally stable on the time-scale of the quenching experiment, the results were explained by kinetically controlled co-occurrence of retentive (MenZnI) and invertive (NmnZnI) pathways of proto-demetalation, see reference 24. An alternative explanation involving kinetic resolution (incomplete deuteration prior to protic workup of the reaction mixture) might also be considered.
- (26) *P*-Menthyl- and *P*-neomenthyl-incorporating phosphane ligands: (a) Landert, H.; Spindler, F.; Wyss, A.; Blaser, H.-U.; Pugin, B.; Ribourdouille, Y.; Gschwend, B.; Ramalingam, B.; Pfaltz, A. Chiral Mixed Secondary Phosphine-Oxide-Phosphines: High-Performing and Easily Accessible Ligands for Asymmetric Hydrogenation. *Angew. Chem., Int. Ed.* **2010**, *49* (38), 6873–6876. (b) Marinetti, A.; Mathey, F.; Ricard, L. Synthesis of optically active phosphiranes and their use as ligands in rhodium(I) complexes. *Organometallics* **1993**, *12* (4), 1207–1212. (c) Brunner, H.; Ziegler, J. Enantioselective Katalysen LXII. 1,2-Bis(dimethylphosphino)ethan. *J. Organomet. Chem.* **1990**, *397* (2), C25–C27. (d) King, R. B.; Bakos, J.; Hoff, C. D.; Marko, L. Poly(tertiary phosphines and arsines). 17. Poly(tertiary phosphines) containing terminal neomenthyl groups as ligands in asymmetric homogeneous hydrogenation catalysts. *J. Org. Chem.* **1979**, *44* (18), 3095–3100. (e) Fisher, C.; Mosher, H. S. Asymmetric homogeneous hydrogenation with phosphine-rhodium complexes chiral both at phosphorus and carbon. *Tetrahedron Lett.* **1977**, *18* (29), 2487–2490. (f) Tanaka, M.; Ogata, I. A Novel Route to Menthylidiphenylphosphine. *Bull. Chem. Soc. Jpn.* **1975**, *48* (3), 1094–1094. (g) Morrison, J. D.; Burnett, R. E.; Aguiar, A. M.; Morrow, C. J.; Phillips, C. Asymmetric homogeneous hydrogenation with rhodium(I) complexes of chiral phosphines. *J. Am. Chem. Soc.* **1971**, *93* (5), 1301–1303.
- (27) *P,P*-Dimethylphosphanyl-based ligands and compounds: (a) Ota, Y.; Ito, S.; Kobayashi, M.; Kitade, S.; Sakata, K.; Tayano, T.; Nozaki, K. Crystalline Isotactic Polar Polypropylene from the Palladium-Catalyzed Copolymerization of Propylene and Polar Monomers. *Angew. Chem., Int. Ed.* **2016**, *55* (26), 7505–7509. (b) Ota, Y.; Ito, S.; Kuroda, J.; Okumura, Y.; Nozaki, K. Quantification of the Steric Influence of Alkylphosphine–Sulfonate Ligands on Polymerization, Leading to High-Molecular-Weight Copolymers of Ethylene and Polar Monomers. *J. Am. Chem. Soc.* **2014**, *136* (34), 11898–11901. (c) Fries, G.; Wolf, J.; Ilg, K.; Walfort, B.; Stalke, D.; Werner, H. A new route to achiral and chiral 1,2-bis(phosphino)ethanes, 1-arsino-2-phosphinoethanes, and 1,3-bis(phosphino)propanes and the molecular structure and catalytic activity of some rhodium(I) complexes derived thereof. *Dalton Transactions* **2004**, *12*, 1873–1881. (d) Wolf, J.; Manger, M.; Schmidt, U.; Fries, G.; Barth, D.; Weberndörfer, B.; Vicio, D. A.; Jones, W. D.; Werner, H. A new synthetic route to ligands of the general composition $R_2PCH_2ER'_2$ ($E = P, As$) and some rhodium complexes derived thereof. *J. Chem. Soc., Dalton Trans.* **1999**, No. 11, 1867–1876. (e) Brunner, H.; Janura, M. Enantioselective Catalysis 113: New Menthylphosphane Ligands Differing in Steric and Electronic Properties. *Synthesis* **1998**, *1998* (01), 45–55. (f) Bogdanović, B.; Henc, B.; Meister, B.; Pauling, H.; Wilke, G. A Catalyzed Asymmetric Synthesis. *Angew. Chem., Int. Ed. Engl.* **1972**, *11* (11), 1023–1024.
- (28) (a) Oertling, H.; Reckziegel, A.; Surburg, H.; Bertram, H.-J. Applications of Menthol in Synthetic Chemistry. *Chem. Rev.* **2007**, *107* (5), 2136–2164. (b) Ager, D., Ed. *Handbook of Chiral Chemicals*, 2nd ed.; Taylor & Francis: Boca Raton, 2005; DOI: 10.1201/9781420027303. (c) Seyden-Penne, J. *Chiral Auxiliaries and Ligands in Asymmetric Synthesis*; John Wiley: New York, 1995. (d) Grabulosa, A. *P-Stereogenic Ligands in Enantioselective Catalysis*; RSC Publishing: Cambridge, 2010; DOI: 10.1039/9781849732703. (e) Talapatra, S. K.; Talapatra, B. Monoterpenoids (C10). In *Chemistry of Plant Natural Products*; Springer: Heidelberg, 2014; pp 345–401; DOI: 10.1007/978-3-642-45410-3_6.
- (29) Hintermann, L.; Wong, K. M. Rearrangement in Stereoretentive Syntheses of Menthyl Chloride from Menthol: Insight into Competing Reaction Pathways through Component Quantification Analysis. *Eur. J. Org. Chem.* **2017**, *2017* (37), 5527–5536.
- (30) Dimethylphosphine oxide itself was unknown at the outset of this work but was described in a report that appeared while our manuscript was being prepared: Black, R. E.; Jordan, R. F. Synthesis and Reactivity of Palladium(II) Alkyl Complexes that Contain Phosphine-cyclopentanesulfonate Ligands. *Organometallics* **2017**, *36* (17), 3415–3428.
- (31) (a) Achard, T. Advances in Homogeneous Catalysis Using Secondary Phosphine Oxides (SPOs): Pre-ligands for Metal Complexes. *Chimia* **2016**, *70* (1), 8–19. (b) Shaikh, T. M.; Weng, C.-M.; Hong, F.-E. Secondary phosphine oxides: Versatile ligands in

transition metal-catalyzed cross-coupling reactions. *Coord. Chem. Rev.* **2012**, *256* (9–10), 771–803.

(32) Phosphine oxides incorporating a single menthyl group: (a) Wang, J.-P.; Nie, S.-Z.; Zhou, Z.-Y.; Ye, J.-J.; Wen, J.-H.; Zhao, C.-Q. Preparation of Optically Pure Tertiary Phosphine Oxides via the Addition of *P*-Stereogenic Secondary Phosphine Oxide to Activated Alkenes. *J. Org. Chem.* **2016**, *81* (17), 7644–7653. (b) Zhang, H.; Sun, Y.-M.; Zhao, Y.; Zhou, Z.-Y.; Wang, J.-P.; Xin, N.; Nie, S.-Z.; Zhao, C.-Q.; Han, L.-B. One-Pot Process That Efficiently Generates Single Stereoisomers of 1,3-Bisphosphinylpropanes Having Five Chiral Centers. *Org. Lett.* **2015**, *17* (1), 142–145.

(33) The mixed (*R_p*)-*P*-phenyl-menthyl-phosphine-*P*-oxide has recently been exposed to a range of stereoselective reactions: (a) Zhang, H.; Sun, Y.-M.; Zhao, Y.; Zhou, Z.-Y.; Wang, J.-P.; Xin, N.; Nie, S.-Z.; Zhao, C.-Q.; Han, L.-B. One-Pot Process That Efficiently Generates Single Stereoisomers of 1,3-Bisphosphinylpropanes Having Five Chiral Centers. *Org. Lett.* **2015**, *17* (1), 142–145. (b) Wang, J.-P.; Nie, S.-Z.; Zhou, Z.-Y.; Ye, J.-J.; Wen, J.-H.; Zhao, C.-Q. Preparation of Optically Pure Tertiary Phosphine Oxides via the Addition of *P*-Stereogenic Secondary Phosphine Oxide to Activated Alkenes. *J. Org. Chem.* **2016**, *81* (17), 7644–7653. (c) Nie, S.-Z.; Zhou, Z.-Y.; Wang, J.-P.; Yan, H.; Wen, J.-H.; Ye, J.-J.; Cui, Y.-Y.; Zhao, C.-Q. Nonpimerizing Alkylation of H–P Species to Stereospecifically Generate *P*-Stereogenic Phosphine Oxides: A Shortcut to Bidentate Tertiary Phosphine Ligands. *J. Org. Chem.* **2017**, *82* (18), 9425–9434. (d) Ye, J.-J.; Nie, S.-Z.; Wang, J.-P.; Wen, J.-H.; Zhang, Y.; Qiu, M.-R.; Zhao, C.-Q. Nucleophilic Substitution of *P*-Stereogenic Chlorophosphines: Mechanism, Stereochemistry, and Stereoselective Conversions of Diastereomeric Secondary Phosphine Oxides to Tertiary Phosphines. *Org. Lett.* **2017**, *19* (19), 5384–5387. (e) Du, J.-Y.; Ma, Y.-H.; Yuan, R.-Q.; Xin, N.; Nie, S.-Z.; Ma, C.-L.; Li, C.-Z.; Zhao, C.-Q. Metal-Free One-Pot Synthesis of 3-Phosphinoylbenzofurans via Phospha-Michael Addition/Cyclization of H-Phosphine Oxides and in Situ Generated ortho-Quinone Methides. *Org. Lett.* **2018**, *20* (2), 477–480.

(34) Grignard, V. Sur les combinaisons organomagnésiennes mixtes et leur application à des synthèses d'acides, d'alcools et d'hydrocarbures. *Annal. Chim. Phys., Septième Ser.* **1901**, *24*, 433–490.

(35) With pure solvent and **2**, the reaction starts without initiation at rt. Activation with 1,2-dibromoethane alone was not very efficient. Bromoethane provides efficient initiation but introduces EtMg signals in the low-frequency region of the ¹H NMR spectrum.

(36) Traces of *ψ*-menthene **10** (1-methyl-3-(2-methylprop-1-en-1-yl)cyclopentane; δ 5.05) result from a small amount of *sec-ψ*-menthyl chloride (**11**; 1-(1-chloro-2-methylpropyl)-3-methylcyclopentane) which was present as an impurity (ca. 2 mol %) in **2**.

(37) See Table 1 or the Supporting Information for structure formulas of all components.

(38) Bromide is present due to activation of Mg with ethylene bromide.

(39) The impurity *sec-ψ*-menthyl chloride (**11**) in **2** produced signals for *sec-ψ*-MenMgCl (**12**). Two CHMg signals (δ_{C} 45.38, 45.63) were detected by HSQC correlation to signals at δ_{H} –0.02 (dd, $J = 7.7, 4.2$ Hz) and 0.00 (dd, $J = 8.2, 4.0$ Hz). Compound **12** is thus present in diastereomeric forms (1:1) at C-1'. See the Supporting Information.

(40) Love, B. E.; Jones, E. G. The Use of Salicylaldehyde Phenylhydrazone as an Indicator for the Titration of Organometallic Reagents. *J. Org. Chem.* **1999**, *64* (10), 3755–3756.

(41) (a) Gorobetz, E. V.; Kasatkin, A. N.; Kutchin, A. V.; Tolstikov, G. A. Anomalous hydroalumination of methyl nopol ether with a LiAlH₄-3AlBr₃ system. *Russ. Chem. Bull.* **1994**, *43* (3), 466–470. (b) Quast, H.; Dietz, T. Dehydration of Secondary Alcohols via Thermolysis of In Situ Generated Alkyl Diphenyl Phosphates: An Inexpensive and Environmentally Compatible Method for the Preparation of Alkenes. *Synthesis* **1995**, *1995* (10), 1300–1304.

(42) *p*-Menthane (**4**) gives rise to seven peaks, but signals C-1/8 often overlap by chance, depending on solvent and sample concentration. (a) Senda, Y.; Imaizumi, S. ¹³C Pulse Fourier Transform NMR of menthol stereoisomers and related compounds. *Tetrahedron*

1975, *31* (23), 2905–2908. (b) Bazyl'chik, V. V.; Samitov, Y. Y.; Ryabushkina, N. M. Application of ¹H NMR and ¹³C NMR for establishing the spatial structure of stereoisomeric *o*- and *p*-menthane, *o*- and *p*-menthene, and isopropylcyclohexane. *J. Appl. Spectrosc.* **1980**, *32* (5), 543–548. (c) Reference 41a.

(43) Numeral **1a** encompasses all chemical forms of MenMg (including, e.g., Men₂Mg), whereas **1a'** denotes the major species RMgCl detected by NMR.

(44) (a) Firl, J.; Kresze, G.; Bosch, T.; Arndt, V. Die Isopropylgruppe als stereochemische Sonde; ¹³C-NMR-Untersuchungen an Menthan- und Isomenthanderivaten. *Justus Liebigs Annalen der Chemie* **1978**, No. 1, 87–97. (b) Härtner, J.; Reinscheid, U. M. Conformational analysis of menthol diastereomers by NMR and DFT computation. *J. Mol. Struct.* **2008**, *872* (2–3), 145–149.

(45) The conformational preferences of Men and Nmn compounds are supported by X-ray crystallography data (CSD search, 12.9.2016): All 24 Men-metal derivatives, 2 Men-carboxylic acid derivatives, and 58 *P*-Men-phosphorus compounds follow the general rules. For Nmn compounds, all 15 *S*-Nmn-sulfur compounds had *iPr* equatorial, and 13 out of 21 *P*-Nmn-phosphorus compounds with large substituents at phosphorus show a ring-flip with equatorial *P* and axial *iPr*. In the latter cases, the ¹³C NMR prediction of Men vs Nmn configuration may fail.

(46) The *ψ*-menthane component **16** results from protonation of *sec-ψ*-MenMgCl (**12**) and *tert-ψ*-MenMgCl (**17**), both of which emerge from regioisomeric impurities in crude menthyl chloride (**2**), cf. ref 29. Thus, **16** is an artifact from impure **2**. See Figure S1 for formulas.

(47) (a) Kursanoff, N. Ueber Halogenderivate des Menthols und einiger daraus erhaltenen Kohlenwasserstoffe. *Justus Liebigs Ann. Chem.* **1901**, *318* (2–3), 327–344. (b) Pryde, A. W. H.; Rule, H. G. 71. Solvent effects with optically active saturated hydrocarbons. *J. Chem. Soc.* **1940**, 345–347.

(48) Schwarzenbach, G., Flaschka, H.; *Die komplexometrische Titration, 5. Auflage*; Ferdinand Enke Verlag: Stuttgart, 1965.

(49) (a) Pieters, L. A. C.; Vlietinck, A. J. Applications of quantitative ¹H- and ¹³C-NMR spectroscopy in drug analysis. *J. Pharm. Biomed. Anal.* **1989**, *7* (12), 1405–1417. (b) Shoolery, J. N. Some quantitative applications of ¹³C NMR spectroscopy. *Prog. Nucl. Magn. Reson. Spectrosc.* **1977**, *11* (2), 79–93. (c) El-Shahed, F.; Doerffel, K.; Radeaglia, R. Anwendung von Relaxationsreagenzien in der quantitativen ¹³C-NMR-Spektroskopie. *J. Prakt. Chem.* **1979**, *321* (5), 859–864.

(50) (a) Otte, D. A. L.; Borchmann, D. E.; Lin, C.; Weck, M.; Woerpel, K. A. ¹³C NMR Spectroscopy for the Quantitative Determination of Compound Ratios and Polymer End Groups. *Org. Lett.* **2014**, *16* (6), 1566–1569. (b) Mareci, T. H.; Scott, K. N. Quantitative analysis of mixtures by carbon-13 nuclear magnetic resonance spectrometry. *Anal. Chem.* **1977**, *49* (14), 2130–2136.

(51) (a) Formacek, V.; Kubezcka, K.-H. ¹³C-NMR Analysis of Essential Oils. In *Aromatic Plants*; Margaris, N., Koedam, A., Vokou, D., Eds.; Martinus Nijhoff Publishers: The Hague 1982; pp 177–181; DOI: 10.1007/978-94-009-7642-9_13. (b) Kubezcka, K.-H.; Formacek, V. Application of Direct Carbon-13 NMR Spectroscopy in the Analysis of Volatiles. In *Analysis of Volatiles*; Schreyer, P., Ed.; De Gruyter: Berlin, 1984; pp 219–230; DOI: 10.1515/9783110855944.219.

(52) Both substance- and position-specific correction factors are empirical and will vary with measurement conditions and spectrometers. Typical values in our case were: sp²-CH (0.95), sp³-CH₂ (1.06), and CH₃ (1.094), relative to sp³-CH (1.00).

(53) For precedence of ¹³C NMR area integration in the case of a Schlenk equilibrium, see: Gawley, R. E.; Zhang, P. 1-Magnesiote-tetrahydroisoquinoloxazolines as Chiral Nucleophiles in Stereoselective Additions to Aldehydes: Auxiliary Optimization, Asymmetric Synthesis of (+)-Corlumine, (+)-Bicuculline, (+)-Egenine, and (+)-Corytensine, and Preliminary ¹³C NMR Studies of 1-Lithio- and 1-Magnesiote-tetrahydroisoquinoloxazolines. *J. Org. Chem.* **1996**, *61* (23), 8103–8112.

- (54) The ratio $[R-Mg]/[Mg]$ is derived from volumetric titration results. It varied from 0.25–0.88 over many samples. The theoretical value ($RCl + Mg = RMgCl$) is 1, but Wurtz coupling and use of activating agents (ethylene bromide, iodine) lowers the value.
- (55) (a) Heard, P. J. NMR of Organomagnesium Compounds, *PATAI'S Chemistry of Functional Groups*; John Wiley & Sons: Chichester, 2009; DOI: 10.1002/9780470682531.pat0402. (b) Bonesteel, J.-A. Nuclear Magnetic Resonance Analyses of Grignard Reagents. In *Handbook of Grignard Reagents*; Silverman, G. S., Rakita, P. E., Eds.; Dekker: New York, 1996; Chapter 8, pp 103–116; DOI: 10.1201/b16932-9.
- (56) (a) Jastrzebski, J. T. B. H.; Boersma, J.; Koten, G. V. Structural Organomagnesium Chemistry. In *PATAI'S Chemistry of Functional Groups*; Rappoport, Z., Marek, I., Eds.; John Wiley & Sons: Chichester, 2009; Chapter 1; DOI: 10.1002/9780470682531.pat0400. (b) Sakamoto, S.; Imamoto, T.; Yamaguchi, K. Constitution of Grignard Reagent $RMgCl$ in Tetrahydrofuran. *Org. Lett.* **2001**, 3 (12), 1793–1795.
- (57) The overlapping peaks in the C-2-region of **1a** are δ 49.24 (broad, C-2' of **14**) and δ 48.73 (broad, C-2 of **15**); their area was estimated from better discernible peak signals of **14/15** by applying empirical correction factors derived from spectra of pure samples.
- (58) The error estimate is based on many correlations between 1H and ^{13}C NMR quantifications performed during this and a previous study²⁹ and a satisfactory correlation of 1H NMR of $\delta_{H1} -0.3$ to 0.1 (total **1a** population) with the ^{13}C NMR derived value for **1a**.
- (59) Use of D_2O -quenching for determining the configuration of menthyl-lithium: Maercker, A.; Schuhmacher, R.; Buchmeier, W.; Lutz, H. D. Studien zur enantio- und diastereoselektiven α -Metallierung prochiraler Sulfoxide mit (+)-Menthylolithium. *Chem. Ber.* **1991**, 124 (11), 2489–2498.
- (60) The signal for **12** at $\delta -0.02$ is absent in Figure 8c, since impurity **11** is absent from **3**.
- (61) Solvent-derived products are partially but not completely suppressed in deuterated solvents: (a) Garst, J. F.; Ungváry, F.; Baxter, J. T. Definitive Evidence of Diffusing Radicals in Grignard Reagent Formation. *J. Am. Chem. Soc.* **1997**, 119 (1), 253–254. (b) Walborsky, H. M. Mechanism of Grignard reagent formation. The surface nature of the reaction. *Acc. Chem. Res.* **1990**, 23 (9), 286–293.
- (62) Studies by Hüchel et al. and Ingold et al. have established that **2** or **3** give rather different ratios **8/9** in E2-elimination. (a) Hüchel, W.; Tappe, W.; Legutke, G. Abspaltungsreaktionen und ihr sterischer Verlauf. *Justus Liebigs Ann. Chem.* **1940**, 543 (1), 191–230. (b) Hughes, E. D.; Ingold, C. K.; Rose, J. B. 785. Mechanism of elimination reactions. Part XIX. Kinetics and steric course of elimination from isomeric menthyl chlorides. *J. Chem. Soc.* **1953**, 3839–3845.
- (63) (a) Hamdouchi, C.; Walborsky, H. Mechanism of Grignard Reagent Formation. *Handbook of Grignard Reagents*; Silverman, G. S., Rakita, P. E., Eds.; Dekker: New York, 1996; Chapter 10, pp 145–218; DOI: 10.1201/b16932-11. (b) Hazimeh, H.; Mattalia, J.-M.; Attolini, M.; Bodineau, N.; Handoo, K.; Marchi Delapierre, C.; Peralez, E.; Chanon, M. Grignard reagent and Green Chemistry: Mechanistic studies to understand the molecular origins of selectivity in the formation of $RMgX$. *Indian J. Chem.* **2006**, 45B, 2270–2280. (c) Garst, J. F.; Ungváry, F. In *Mechanisms of Grignard Reagent Formation*. In *Grignard Reagents: New Developments*; Richey, H. G., Ed.; Wiley: Chichester, 2000; Chapter 7, pp 185–275. (d) Garst, J. F.; Soriaga, M. P. Grignard reagent formation. *Coord. Chem. Rev.* **2004**, 248 (7–8), 623–652.
- (64) Our results are well accommodated by the qualitative Kharasch–Reinmuth–Walborsky (KRW) mechanism; see ref 63a.
- (65) The technique may be unsuitable in case of highly volatile RH.
- (66) Neomenthyl acid **20** has more recently been described as a solid melting at 65–67 °C; thus, the liquid acid may have been an eutectic mixture **19/20** Dillner, D. K. Syntheses of C-1 Axial Derivatives of *l*-Menthol. *Org. Prep. Proced. Int.* **2009**, 41 (2), 147–152.
- (67) Rowsell, D. G. Preparation of p-menthane carboxylic acid. GB Patent 1392907A, 1975.
- (68) Johnson, W. E. Process for preparing alicyclic carboxylic acid compounds. US Patent 7868200 B2, 2011.
- (69) The WS compound family was developed at Wilkinson Sword: (a) Watson, H. R.; Rowsell, D. G.; Spring, D. J. Substituted p-menthane carboxamides and compositions containing them. GB Patent 1351761, 1971. (b) Watson, H. R.; Rowsell, D. G.; Spring, D. J. N-Substituted p-Menthan-3-carboxamide and deren Verwendung. DE Patent 2205255 (A1), 1972. (c) Watson, H. R.; Hems, R.; Rowsell, D. G.; Spring, D. J. New compounds with the menthol cooling effect. *J. Soc. Cosmetic Chemists* **1978**, 29 (4), 185–200. (d) Erman, M. B., P. J. Whelan, P. J. Physiological cooling compositions containing highly purified ethyl ester of N-[[5-methyl-2-(1-methylethyl) cyclohexyl]carbonyl]glycine. US Patent 7189760 B2, 2007.
- (70) (a) Leffingwell, J. C.; Rowsell, D. G. Wilkinson Sword Cooling Compounds: From the Beginning to Now. *Perfum. Flavor.* **2014**, 39, 34–44. (b) http://www.leffingwell.com/cooler_than_menthol.htm (accessed July 5, 2016). (c) Leffingwell, J. *Cooling Ingredients and Their Mechanism of Action. Handbook of Cosmetic Science and Technology*, 3rd ed.; Barel, A. O., Paye, M., Maibach, H. I., Eds.; Informa Healthcare: New York, 2009; pp 661–675; DOI: 10.1201/b15273-66. (d) Bharate, S. S.; Bharate, S. B. Modulation of Thermoreceptor TRPM8 by Cooling Compounds. *ACS Chem. Neurosci.* **2012**, 3 (4), 248–267.
- (71) We used *p*-MeO-C₆H₄-OCD₃ as internal standard for 1H and 2H NMR measurements from the same reaction mixture.
- (72) (a) Wolf, C. *Dynamic Stereochemistry of Chiral Compounds*; RSC Publishing: London, 2007; DOI: 10.1039/9781847558091. (b) Renzetti, A.; Di Crescenzo, A.; Nie, F.; Bond, A. D.; Gérard, S.; Sapi, J.; Fontana, A.; Villani, C. Diastereomer Interconversion via Enolization: A Case Study. *Chirality* **2015**, 27 (11), 779–783.
- (73) The values of $t_{1/2}$ refer to the epimerization process which is dominated by $(k_1 + k_2)$ (see ref 72). The extrapolated epimerization half-lives in dependence of temperature were derived using the Eyring equation.
- (74) (a) Walborsky, H. M.; Topolski, M. The surface nature of Grignard reagent formation. *J. Am. Chem. Soc.* **1992**, 114 (9), 3455–3459. (b) Morrison, J. D.; Lambert, G. Mechanism of benzophenone reduction with the 2-norbornyl Grignard reagent. *J. Org. Chem.* **1972**, 37 (7), 1034–1037.
- (75) (a) Beckmann, J.; Schüttrumpf, A. Reactions of the Bornyl and Fenchyl Grignard Reagent with Chlorophosphanes – Diastereoselectivity and Mechanistic Implications. *Eur. J. Org. Chem.* **2010**, 2010 (2), 363–369. (b) Beckmann, J.; Schüttrumpf, A. Thermal epimerization of diastereomeric Grignard reagents. *Org. Biomol. Chem.* **2009**, 7 (1), 41–42.
- (76) Hill, E. A. Nuclear Magnetic Resonance Spectra of the Bornyl and Norbornyl Grignard Reagents I. *J. Org. Chem.* **1966**, 31 (1), 20–23.
- (77) (a) Whitesides, G. M.; Roberts, J. D. Nuclear Magnetic Resonance Spectroscopy. The Configurational Stability of Primary Grignard Reagents. Structure and Medium Effects. *J. Am. Chem. Soc.* **1965**, 87 (21), 4878–4888. (b) Fraenkel, G.; Dix, D. T.; Adams, D. G. Inversion rate in a primary Grignard reagent. *Tetrahedron Lett.* **1964**, 5 (43), 3155–3158.
- (78) (a) Jensen, F. R.; Nakamaye, K. L. Preparation of Geometrically Isomeric Grignard Reagents and the Stereochemical Courses of Their Reactions. *J. Am. Chem. Soc.* **1966**, 88 (14), 3437–3438. (b) Davies, A. G.; Roberts, B. P. Peroxides of elements other than carbon. Part XVI. Autoxidation of the epimeric norbornylmagnesium halides. *J. Chem. Soc. B* **1969**, 317–321.
- (79) (a) Hoffmann, R. W.; Hölzer, B. Concerted and stepwise Grignard additions, probed with a chiral Grignard reagent. *Chem. Commun.* **2001**, 5, 491–492. (b) Hoffmann, R. W.; Hölzer, B.; Knopff, O.; Harms, K. Asymmetric Synthesis of a Chiral Secondary Grignard Reagent. *Angew. Chem., Int. Ed.* **2000**, 39 (17), 3072–3074.

(80) Cannon, K., Krow, G. *The Composition of Grignard Reagents in Solution: The Schlenk Equilibrium and Its Effect on Reactivity. Handbook of Grignard Reagents*; Silverman, G. S., Rakita, P. E., Eds.; Dekker: New York 1996; Chapter 13, pp 271–289; DOI: 10.1201/b16932-14.

(81) The *A* values of Grignard compounds are positive (+0.8 kcal/mol for CyMgBr in Et₂O, +0.5 kcal/mol for Cy₂Mg in Et₂O); Jensen, F. R.; Nakamaye, K. L. Conformational preferences of cyclohexyl Grignard reagents. *J. Am. Chem. Soc.* **1968**, *90* (12), 3248–3250.

(82) Negative *A* values have been reported for polarizable mercuric derivatives: (a) Jensen, F. R.; Gale, L. H. Organomercurials. V. The Conformational Preference of the Bromomercuri Group. *J. Am. Chem. Soc.* **1959**, *81* (23), 6337–6338. (b) Anet, F. A. L.; Krane, J.; Kitching, W.; Dodderel, D.; Praeger, D. A re-examination of the conformational equilibria in cyclohexylmercuric derivatives. *Tetrahedron Lett.* **1974**, *15* (37), 3255–3258.

(83) Assignment of NmnPO₂H₂ (**25b**) is based on observation of a minor ³¹P NMR signal (δ 36.5) besides the major signal of **25a** (δ 41.0), but its identity is not strictly proved.

(84) Kharasch, M. S., Reinmuth, O. *Grignard Reactions of Nonmetallic Substances*; Prentice-Hall: New York, 1954; p 7.

(85) Gilman, H.; Zoellner, E. A. A Study of the Optimal Conditions for the Preparation of Tertiary Butylmagnesium Chloride. *J. Am. Chem. Soc.* **1928**, *50* (2), 425–428.

(86) Walborsky, H. M.; Young, A. E. Cyclopropanes. XVI. An Optically Active Grignard Reagent and the Mechanism of Grignard Formation. *J. Am. Chem. Soc.* **1964**, *86* (16), 3288–3296.

(87) (a) Watanabe, Y.; Oae, S.; Iyanagi, T. Mechanisms of Enzymatic S-Oxygenation of Thioanisole Derivatives and O-Demethylation of Anisole Derivatives Promoted by Both Microsomes and a Reconstituted System with Purified Cytochrome P-450. *Bull. Chem. Soc. Jpn.* **1982**, *55* (1), 188–195. (b) Foster, A. B.; Jarman, M.; Stevens, J. D.; Thomas, P.; Westwood, J. H. Isotope effects in O- and N-demethylations mediated by rat liver microsomes: An application of direct insertion electron impact mass spectrometry. *Chem.-Biol. Interact.* **1974**, *9* (5), 327–340. (c) Tolnai, G. L.; Pethő, B.; Králl, P.; Novák, Z. Palladium-Catalyzed Methoxylation of Aromatic Chlorides with Borate Salts. *Adv. Synth. Catal.* **2014**, *356* (1), 125–129.

(88) Dillner, D. K.; Traficante, D. D. Complete ¹H and ¹³C NMR assignments of the epimeric menthane-1-carboxylic acids. *Magn. Reson. Chem.* **2007**, *45* (3), 193–197.

(89) Pedersen, D. S.; Rosenbohm, C. Dry Column Vacuum Chromatography. *Synthesis* **2001**, DOI: 10.1055/s-2001-18722.

Stereochemistry of the Menthyl Grignard Reagent: Generation, Composition, Dynamics, and Reactions with Electrophiles

Sebastian Koller,[†] Julia Gatzka,[†] Kit Ming Wong,[†] Philipp J. Altmann,[‡] Alexander Pöthig,[‡]

and Lukas Hintermann*[†]

[†]Technische Universität München, Department of Chemistry, and Catalysis Research Center, Lichtenbergstr. 4, 85748 Garching bei München

[‡]Technische Universität München, Chair of Inorganic Chemistry, and Catalysis Research Center, Ernst-Otto-Fischer Strasse 1, 85747 Garching bei München

Corresponding Author

*Email: lukas.hintermann@tum.de

Table of Contents

1 GENERAL INFORMATION	S3
1.1 Notes on the NMR data tables in the supporting information	S3
1.2 Compound numbering scheme	S3
2 NMR SPECTROSCOPY OF MENTHYL GRIGNARD REAGENT	S4
2.1 ¹ H NMR spectrum of menthyl Grignard reagent	S4
2.2 ¹ H NMR spectral shape of the menthyl CHMg-region	S4
2.3 HSQC spectrum of menthyl Grignard reagent in (D ₅)-THF (sample B)	S5
2.4 ¹³ C NMR spectra of menthyl Grignard reagents	S5
3 NMR OR OTHER DATA OF COMPONENTS IN MENTHYL GRIGNARD REAGENT	S8
3.1 NMR data for organomagnesium compounds	S8
3.2 NMR data for alkene components	S12
3.3 NMR data for saturated hydrocarbon components	S16
3.4 GC-MS analysis of the hydrocarbon fraction of Grignard reagent 1	S22
3.5 NMR data of bimenthyl hydrocarbons	S25
4 COMPONENT QUANTIFICATION IN MENTHYL GRIGNARD REAGENT	S33
5 CARBOXYLATION OF MENTHYL GRIGNARD REAGENT	S34
5.1 Carboxylation of 1 under different addition modes (Scheme 4)	S34
6 REACTIONS OF MENTHYL GRIGNARD REAGENT WITH ELECTROPHILES	S35
7 EPIMERIZATION STUDIES OF MENTHYL GRIGNARD REAGENT	S36
7.1 Kinetic equilibration studies of neomenthylmagnesium menthylcarboxylate	S36
7.2 Epimer equilibration after addition of carboxylates to 1	S37
8 PHYSIOLOGICAL COOLANT COMPOUND WS-5 (22)	S38
8.1 NMR Data for WS-5 (22)	S38
8.2 X-ray crystal structure of WS-5	S39
9 SYNTHESIS OF DIMENTHYLPHOSPHINE OXIDE (7)	S41
9.1 Details of the dry column chromatography purification	S41
9.2 NMR data of dimethylphosphine oxide (7)	S42
10 CRYSTALLOGRAPHY	S44
10.1 ORTEP Plots	S45
11 NMR SPECTRA	S49

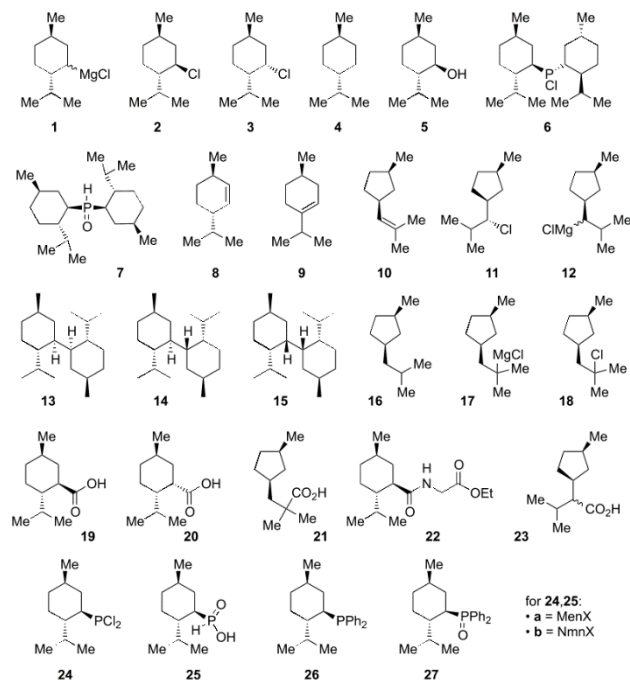
1 General Information

1.1 Notes on the NMR data tables in the supporting information

The substance NMR data tables list ^{13}C NMR peak chemical shifts together with peak area integration data (arbitrary units). The values were obtained by deconvolutive peak fitting ($\int(d)$). Peak area is also provided as "CH-index" value, i.e., as a dimensionless number relative to the average peak area of all CH-signals (set to 1.000). The index numbers are close to 1 for CH, CH₂ and CH₃ peaks, but <1 for quaternary carbons. The CH-index data is useful for assigning individual peaks to peak sets of specific components (at variable abundance) in complex mixtures such as Grignard reagent 1.

1.2 Compound numbering scheme

Figure S1. Compound numbering scheme (as used in the main text)

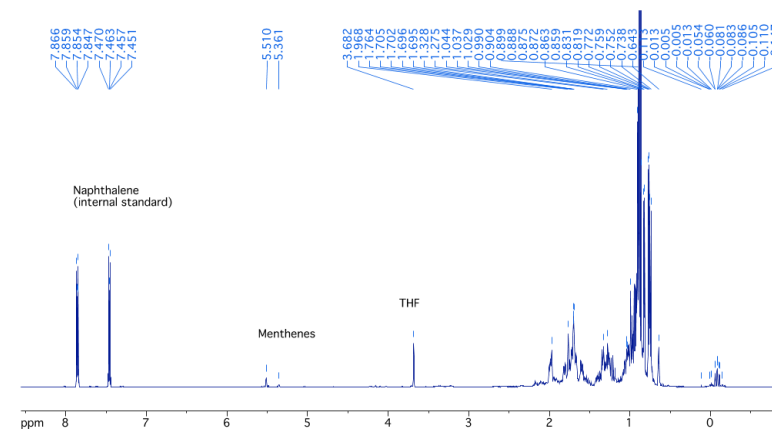


- S3 -

2 NMR spectroscopy of menthyl Grignard reagent

2.1 ^1H NMR spectrum of menthyl Grignard reagent

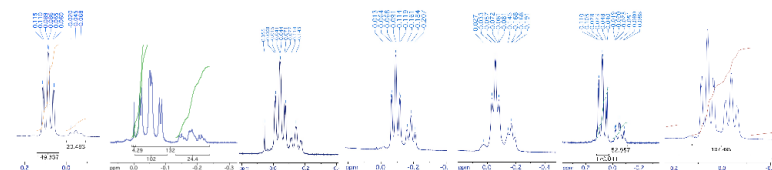
Figure S2. Full range 500 MHz ^1H NMR spectrum of 1 in (D₂)-THF (sample B)



2.2 ^1H NMR spectral shape of the menthyl CHMg-region

The following represents a selection of spectral shapes of the low frequency region of the ^1H NMR spectrum representing CHMg signals of MenMg-species. The major signal (δ -0.08) is due to MenMgCl (solvated), the higher field signal (δ -0.15) to Men₂Mg. Samples were externally referenced. All samples were recorded in THF solution with C₆D₆ added for locking (0.5 mL or 0.3 mL Grignard reagent in THF + 0.2 mL or 0.3 mL C₆D₆). Conditions used to prepare each Grignard reagent are not listed since the spectral appearance mainly depends on secondary factors such as total concentration, standing time, amount of activator used (i.e., halide composition and concentration), and others. As such, the figure intends to give an overview of the variability of possible results.

Figure S3. Shape variability of the ^1H NMR menthyl CHMg-signal region



- S4 -

Table S1. Assignment of ¹H NMR data for menthylmagnesium chloride (1a) from 2D NMR

Pos.	Type	$\delta^{13}\text{C}$ ^a	$\delta^1\text{H}$ by HSQC ^b	HMBC ^b	1D $\delta^1\text{H}$ ^{b,c}
syst.	DEPT	(D ₆)-THF	(mult, J/Hz)	$\delta^1\text{H}$	(mult, J/Hz)
2	CH	49.50	1.27 (t, 12)	0.89 (CH ₃), 0.74 (CH ₃) > 1.98 > 1.73, 1.60, 1.22, 0.97–0.92, -0.08	
6	CH ₂	44.93	1.98 (d, 14), 1.22 (q, 14)	0.766, -0.08 > 1.23, 1.60	
4	CH ₂	37.66	1.76 (d, 14), 0.92 (d, 14)		
5	CH	37.41	1.06, 0.77 (?)	-0.08	
1'	CH	35.92	1.70 > 0.89, 0.72	0.74	
1	CH(Mg)	30.57	-0.08 (t, 14)		-0.08 (ddd, 13.3, 11.9, 2.9)
3	CH ₂	29.40	1.59, 0.88		
Me-5	CH ₃	23.14	0.766 (d, 6)		0.766 (d, 6.4)
(S)-Me-1'	CH ₃	22.51	0.89 (d, 6)		
(R)-Me-1'	CH ₃	16.59	0.744 (d, 6.9)	0.90	

a) Grignard reagent (sample B) prepared and measured in (D₆)-THF at 101 MHz. (lr) = long-range. b) Grignard reagent (sample B) in (D₆)-THF at 500 MHz. c) Values from ¹H NMR spectrum. * Interchangeable assignments.

Table S2. ¹³C NMR data for menthylmagnesium chloride (1a) in menthyl Grignard reagent

Pos.	Type	$\delta^{13}\text{C}$ ^a	$\int(d)^{a,b}$	Idx ^{a,c}	$\delta^{13}\text{C}$ ^d	$\int(d)^{b,d}$	Idx ^{c,d}	$\delta^{13}\text{C}$ ^e	$\int(d)^{b,f}$	Idx ^{c,f}
	DEPT	(D ₆)-THF			THF			Et ₂ O		
2	CH	49.50	88.1	1.068	49.58	92.8	1.020	49.15	86.43	0.968
6	CH ₂	44.93	83.3	1.010	44.96	93.3	1.026	44.14	87.14*	0.976
4	CH ₂	37.66	84.3	1.022	37.72	*	*	37.39	91.46	1.025
5	CH	37.41	83.1	1.007	37.45	95.7	1.052	37.13	97.81	1.096
1'	CH	35.92	79.6	0.965	36.16	88.05	0.968	36.69	86.15	0.965
1	CH(Mg)	30.57	79.2	0.960	30.52	87.2	0.959	30.71	86.58	0.970
3	CH ₂	29.40	79.2	0.960	29.55	94.25	1.036	29.29	87.68	0.982
Me-5	CH ₃	23.14	88.7	1.075	23.46	100.6	1.106	23.16	91.51	1.025
^S Me-1'	CH ₃	22.51	78.0	0.945	22.74	105.5	1.160	22.44	*	*
^R Me-1'	CH ₃	16.59	80.6	0.977	16.90	95.0	1.045	16.69	91.24	1.022
	CH		1.000		CH	1.000		CH	1.000	
	CH ₂		0.997		CH ₂	1.031		CH ₂	0.995*	
	CH ₃		0.999		CH ₃	1.104		CH ₃	1.024*	

a) Grignard reagent prepared and measured in (D₆)-THF at 101 MHz. b) Peak integration by deconvolutive fitting ("d"); arbitrary units. c) "CH-Index", peak integral relative to the average of all CH-signals. d) Grignard reagent (sample A) prepared in THF, measured with addition of C₆D₆ and naphthalene (int. standard) at 101 MHz. f) Grignard reagent (sample D) prepared in Et₂O, measured with added C₆D₆. * Data not accessible or less accurate due to peak overlap.

- S9 -

3.1.2 Neomenthylmagnesium chloride (1b)

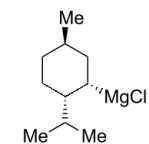


Figure S7. $\delta^1\text{H}$ and $\delta^{13}\text{C}$ assignments for neomenthylmagnesium chloride (1b)

$\delta^{13}\text{C}$ in (D ₆)-THF (systematic numbering)	$\delta^1\text{H}$ from 2D NMR (500 MHz, (D ₆)-THF)
Data from sample B in (D ₆)-THF. * Interchangeable assignments.	

Table S3. Assignment of ¹H NMR data for neomenthylmagnesium chloride (1b)

Pos.	Type	$\delta^{13}\text{C}$ ^a	$\delta^1\text{H}$ by HSQC ^b	HMBC ^b	1D $\delta^1\text{H}$ and COSY ^b
	DEPT	THF	(mult, J/Hz)		
2	CH	52.81	1.02	0.88 > 1.97 > 1.81, 1.69, 1.35, 1.27, 1.09-1.01, 0.64	
6	CH ₂	44.49	1.97, 1.33		
4	CH ₂	37.70	1.68 (d, 14), 0.83 (d, 12)		
1'	CH	35.45	1.26 (sept?) > 0.89 (lr)		
5	CH	35.30	1.32 > 0.82 (lr), 1.68 (lr)		
3	CH ₂	33.43	0.80, 1.03	1.67 > 1.94, 1.67, 0.64, 1.27, 0.69	
1	CH(Mg)	30.92	0.64	H→C: 5.2, 33.4 > 44.5, 52.8	0.64 (m); COSY to: 1.98, 1.81, 1.35, 1.03
Me-5	CH ₃	23.27	0.824 (d, 6)		0.824
^R Me-1'	CH ₃	22.05 [#]	0.89 (d, 6)		
^S Me-1'	CH ₃	21.14 [#]	0.88 (d, 6)		

a) Grignard reagent (sample B) prepared and measured in (D₆)-THF at 101 MHz. (lr) = long-range. b) Grignard reagent (sample B) prepared and measured in (D₆)-THF at 500 MHz. [#] Exchangeable assignments.

- S10 -

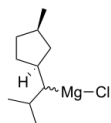
Table S4. ¹³C NMR data for neomenthylmagnesium chloride (1b)

Pos.	Type	$\alpha^{13}\text{C}^{\text{a}}$	$f(\text{d})^{\text{a,b}}$	$\text{Idx}^{\text{a,c}}$	$\alpha^{13}\text{C}^{\text{d}}$	$f(\text{d})^{\text{b,d}}$	$\text{Idx}^{\text{c,d}}$	$\alpha^{13}\text{C}^{\text{e}}$	$f(\text{d})^{\text{b,e}}$	$\text{Idx}^{\text{c,e}}$
	DEPT	(D ₆)-THF			THF			Et ₂ O		
2	CH	52.81	100	0.941	52.71	100	0.954	51.78	99.9	1.001
6	CH ₂	44.49	107.2	1.009	44.53	104.4	0.996	43.37	98.60	0.988
4	CH ₂	37.70	100.9	0.949	37.72	*	*	37.25	103.74	1.039
1'	CH	35.45	108.9	1.025	35.68	106.2	1.013	36.13	98.23	0.984
5	CH	35.30	108.7	1.023	35.46	108.4	1.034	35.60	102.38	1.026
3	CH ₂	33.43	111.9	1.053	33.74	106.2	1.013	34.10	99.74	0.999
1	CH(Mg)	30.92	107.5	1.012	31.02	108.5	1.035	31.54	98.79	0.990
Me-5	CH ₃	23.27	120.1	1.130	23.58	114.2	1.089	23.26	102.35	1.025
⁵ Me-1'	CH ₃	22.05	107.0	1.007	22.26	108.9	1.038	21.95	104.03*	1.042
⁶ Me-1'	CH ₃	21.14	111.0	1.044	21.43	117.3	1.119	21.24	102.61*	1.028
			CH	1.000		CH	1.000		CH	1.000
			CH ₂	1.004		CH ₂	1.004*		CH ₂	1.009
			CH ₃	1.060		CH ₃	1.082		CH ₃	1.032

a) Grignard reagent prepared and measured in (D₆)-THF at 101 MHz. b) Peak integral by deconvolutive peak fitting ("d"); arbitrary units. c) "CH-Index", peak integral relative to the average of all CH-signals. d) Grignard reagent (sample A) prepared in THF, C₆D₆ added for locking, 101 MHz; ref (H₂)-THF peak = 25.3 ppm. e) Grignard reagent (sample D) prepared in Et₂O, C₆D₆ added for locking, measured at 101 MHz. * Data not accessible or less accurate due to peak overlap.

3.1.3 ψ -Menthylmagnesium chloride (12)

The species is present in Grignard reagent **1** prepared from menthyl chloride (**2**) containing *sec*- ψ -menthyl chloride (**11**; 2–3 mol %) as impurity. Its presence was deduced through the following observations:



- HSQC analysis of menthyl Grignard reagent (THF–C₆D₆): $\alpha^1\text{H}$ –0.02 (dd, $J \approx 8, 4$ Hz) and 0.00 (dd, $J \approx 8, 4$ Hz), corresponding to $\alpha^{13}\text{C}$ 45.38 ppm (sharp) and $\alpha^{13}\text{C}$ 45.63 ppm (broadened), respectively. These are two sets of signals for a diastereomeric CHMgX unit. Extensive overlap and low abundance did not allow for a more complete 2D NMR analysis.

- after D₂O quenching, a peak at $\alpha^2\text{H} \approx 1.10$ ppm (2–3% of all Grignard species) was found which agrees (considering variations in referencing) with H-1' in ψ -menthane centered at $\alpha^1\text{H}$ 1.18 ppm. The signal was absent in D₂O-quenched Grignard reagents prepared from **3**, or from **2** purified by crystallization.

- after CO₂-quenching of menthyl Grignard reagents, the crude carboxylic acid mixture displayed signals for menthylcarboxylic acid (**19**), neomenthyl-carboxylic acid (**20**) and a minor, double set of signals (combined 6% relative to menthylcarboxylic acid, which would correspond to ca 3 mol% of the initial Grignard reagent) for the C-1'-diastereomeric ψ -menthancarboxylic acids **23** (*vide infra*).

- S11 -

3.2 NMR data for alkene components

Figure S8. Menthene positional numbering and selected characteristic signals.

Δ^2 -Menthene (8)	Δ^3 -Menthene (9) (<i>p</i> -Menthane numbering)
$\alpha^1\text{H}$, selected peaks: 5.48–5.57 (m, 2 H) $\alpha^{13}\text{C}$, selected signals: 133.99 (C-3), 129.91	$\alpha^1\text{H}$, selected peaks: 5.36 (m, 1 H) $\alpha^{13}\text{C}$, selected signals: 143.18 (C-4), 117.87 (C-3)

3.2.1 Δ^2 -Menthene (**8**)

Figure S9. Overview of $\alpha^1\text{H}$ and $\alpha^{13}\text{C}$ assignments for Δ^2 -menthene (**8**)

$\alpha^{13}\text{C}$ in CDCl ₃ , 101 MHz (menthane numbering)	$\alpha^1\text{H}$ (400 MHz, CDCl ₃)
* Interchangeable assignments.	

Table S5. NMR data for Δ^2 -menthene (**8**)

Pos.	Type	$\alpha^{13}\text{C}$ Lit. ^a	$\alpha^{13}\text{C}^{\text{b}}$	$f(\text{d})^{\text{b,c}}$	$\text{Idx}^{\text{b,d}}$	$\Delta\delta^{\text{e}}$	$\alpha^{13}\text{C}^{\text{f}}$	$\alpha^1\text{H}$ by HSQC ^f	$\alpha^1\text{H}^{\text{g}}$
		CDCl ₃	CDCl ₃				(D ₆)-THF	(D ₆)-THF	CDCl ₃
2	CH	134.09	133.99	99.9	0.949	0.23	133.86	5.51	5.52 (m)
3	CH	130.01	129.91	100.0	0.950	0.26	129.75	5.51	5.52 (m)
4	CH	42.01	41.94	106.4	1.011	-0.11	42.12	1.93 (sext)	1.92 (m)
8	CH	32.27	32.20	105.3	1.000	-0.07	32.34	1.56 (sext)	1.56 (sext)
6	CH ₂	31.93	32.00	120.9	1.148	-0.22	32.15	1.84 (m), 1.10 (q)	1.83 (m), 1.12 (ddd)

- S12 -

1	CH	31.03	30.97	104.1	0.989	-0.08	31.11	2.10 (m)	2.11 (m)
5	CH ₂	25.71	25.64	114.6	1.089	0.02	25.69	1.71 (m), 1.27 (q)	1.70 (m), 1.24 (ddd)
7	CH ₃	22.08	22.00	118.8	1.129	0.40	21.68	0.94 (d)	0.95 (d, 7.1)
9/10	CH ₃	19.65	19.59	120.1	1.141	0.41	19.24	0.89 (d)	0.89 (d)
9/10	CH ₃	19.33	19.28	120.5	1.145	0.44	18.89	0.87 (d)	0.86 (d)
				CH(sp ³)	1.000				
				CH(sp ²)	0.949				
				CH ₂	1.119				
				CH ₃	1.138				

a) Reference data (in CDCl₃) and assignment from Gorobetz *et al.*^[2] b) Sample in CDCl₃ at 400/101 MHz (mixture of 2-menthene and NmnCl). c) Peak integral by deconvolutive peak fitting ("d"); arbitrary units. d) "CH-Index", peak integral relative to the average of all CH(sp³)-signals. e) Difference in peak shifts between literature values (CDCl₃) and values measured in the Grignard solution (THF). f) Grignard reagent (sample B) in (D₆)-THF at 101 MHz.

Table S6. Additional ¹³C NMR Data of Δ²-menthene (8) as component in various samples

Pos.	Type	$\bar{\alpha}^{13C}$ ^a	$f(d)^{a,b}$	$\bar{\alpha}^{13C}$ ^c	$f(d)^{b,c}$	Idx ^{c,d}	$\bar{\alpha}^{13C}$ ^e	$f(d)^{d,e}$	$\bar{\alpha}^{13C}$ ^f	$f(d)^{d,f}$	Idx ^{c,f}
		THF-C ₆ D ₆		Et ₂ O-C ₆ D ₆			THF (Et ₂ O)		28.41	CDCl ₃	
2	CH	133.80	19.3	133.70	17.11	0.981	133.70	27.1	134.00	2.96	1.104
3	CH	129.71	19.4	129.61	15.42	0.885	129.61	25.3	129.91	2.75	1.026
4	CH	41.91	19.0	41.83	16.60	0.952	41.82	24.13	41.95	2.6	0.970
8	CH	32.15	23.85	32.05	20.00	1.147	32.05	31.52	32.21	2.91	1.086
6	CH ₂	32.00	23.1	31.92	21.60	1.239	31.89	28.68	32.01	3.82	1.425
1	CH	30.96	19.98	30.86	16.63	0.954	30.85	29.59	30.98	2.53	0.944
5	CH ₂	25.57	22.2	25.48	19.54	1.121	*		25.65	2.9	1.082
7	CH ₃	21.79	22.5	21.66	19.96	1.145	21.93	26.89	22.01	3.06	1.142
9/10	CH ₃	19.33	21.2	19.21	19.96	1.145	*	-	19.59	3.88	1.448
9/10	CH ₃	18.98	20.8	18.85	19.88	1.140	19.18	25.1	19.28	3.35	1.250
		CH(sp ³)	1.000			1.000		1.000		1.000	
		CH(sp ²)	0.924			0.933		0.922		1.065	
		CH ₂	1.082			1.180		*		1.254	
		CH ₃	1.027			1.143		*		1.280	

a) Grignard reagent (sample A) in THF, C₆D₆ added for locking, 101 MHz; ref. (H₈)-THF peak 25.3 ppm. b) Grignard reagent (sample D) in Et₂O, C₆D₆ added for locking, measured at 101 MHz. c) Peak integral by deconvolutive peak fitting ("d"); arbitrary units. d) "CH-Index", peak integral relative to the average of all CH(sp³)-signals. e) Grignard sample in Et₂O, solvent removed in vacuum, sample dissolved in THF, measured with C₆D₆. f) Grignard sample in THF quenched with D₂O; NMR of the nonpolar phase recorded in CDCl₃ at 101 MHz. * Data not accessible or less accurate due to peak overlap.

² Gorobetz, E. V.; Kasatkin, A. N.; Kutchin, A. V.; Tolstikov, G. A. Anomalous hydroaluminum of Methyl Nopol Ether With a LiAlH₄-3AlBr₃ System. *Russ. Chem. Bull.* **1994**, *43*, 466–470.

3.2.2 Δ³-Menthene (9)

Figure S10. Overview of $\bar{\alpha}^1H$ and $\bar{\alpha}^{13C}$ assignments for Δ³-menthene (9)^a

Numbering Scheme menthane numbering	$\bar{\alpha}^1H$ from 2D NMR (500 MHz, (D ₆)-THF)	$\bar{\alpha}^{13C}$ in (D ₆)-THF (101 MHz)
Data from sample B in (D ₆)-THF. * Interchangeable assignments.		

Table S7. NMR data for Δ³-menthene (9)

Pos.	Type	$\bar{\alpha}^{13C}$ Lit. ^a	$\Delta\delta^b$	$\bar{\alpha}^{13C}$ ^c	$\Delta\delta^b$	$\bar{\alpha}^{13C}$ ^d	$f(d)^d$	$\bar{\alpha}^1H$ by HSQC ^e
				(D ₆)-THF		(D ₆)-THF		
4	C	143.2	0.54	142.66	0.32	142.88	2.7	
3	CH	117.9	0.18	117.72	-0.02	117.92	4.4	5.36 (m)
8	CH	35.0	0.11	34.89	-0.11	35.11	11.1*	2.11
2	CH ₂	33.9	0.10	33.80	-0.08	33.98	5.8	1.59, 2.06
6	CH ₂	31.5	0.12	31.38	-0.07	31.57	6.4	1.18, 1.71
1	CH	28.7	-0.01	28.71	-0.22	28.92	4.1	1.59
5	CH ₂	26.0	0.20	25.80	0.02	25.98	6.2	1.98 ^f
7/9/10	CH ₃	21.85	0.45	21.40	0.33	21.52	*	0.91 (d)
7/9/10	CH ₃	21.62	0.42	21.20	0.30	21.32	*	0.98 (d)
7/9/10	CH ₃	21.26	0.40	20.86	0.28	20.98	*	0.98 (d)

a) Reference data (in CDCl₃) from Quast.³ b) Difference in peak shifts between literature values (CDCl₃) and values measured in the Grignard solution (THF). c) Sample C from neomenthyl chloride in (D₆)-THF. d) Grignard sample D in Et₂O. e) Correlation data from sample B in (D₆)-THF. f) Only 1 cross-peak found in HSQC, in spite of the CH₂-type (by DEPT) of the signal. * Data not accessible or less accurate due to peak overlap.

³ Quast, H.; Dietz, T. Dehydration of Secondary Alcohols via Thermolysis of In Situ Generated Alkyl Diphenyl Phosphates: An Inexpensive and Environmentally Compatible Method for the Preparation of Alkenes. *Synthesis* **1995**, 1300–1304.

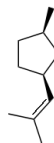
Table S8. Additional ¹³C NMR Data of Δ³-menthene (9) as component in various samples

Pos.	δ ¹³ C	Type	Δδ ^b	δ ¹³ C ^c	f(d) ^{c,d}	δ ¹³ C ^e	f(d) ^{e,e}	δ ¹³ C ^f	f(d) ^{f,f}	Idx	δ ¹³ C ^h	f(d) ^{g,h}
	Lit. ^a			CDCl ₃		CDCl ₃		THF			Et ₂ O	
4	143.2	C	-0.52	143.18	2.1	143.17	0.81	142.68	4.95	0.442	142.55	3.73
3	117.9	CH	-0.15	117.87	4.0	117.88	1.00	117.92	10.6	0.946	117.87	9.03
8	35.0	CH	-0.12	35.01	5.2	35.02	1.6	35.02	11.8	1.045	34.95	8.84
2	33.9	CH ₂	-0.09	33.94	4.7	33.95	2.3*	33.88	7.2*	*	(33.85)	*
6	31.5	CH ₂	-0.08	31.46	4.9	31.47	2.0	31.41	11.7	1.045	31.33	10.61
1	28.7	CH	-0.04	28.75	3.2	28.76	2.4	28.71	10.6	0.946	28.63	9.77
5	26.0	CH ₂	-0.23	26.03	4.0	26.04	1.4	25.93	11.8	1.054	25.84	9.57
7/9/10	21.85	CH ₃	-0.17	21.88*	*	21.87	1.8	21.62	15.8	(1.411)	21.51	11.38*
7/9/10	21.62	CH ₃	-0.24	21.64	5.2	21.64	1.8	21.39	18.6*	(1.661)	21.28*	11.77*
7/9/10	21.26	CH ₃	-0.14	21.28	4.5	21.29	1.1	21.08	11.6	1.036	20.97	11.54
								CH	1.000			
								CH ₂	1.050			
								CH ₃	*			

a) Reference data (in CDCl₃) from Quast.³ b) Peak shift difference Lit. (in CDCl₃) minus measured value in (D₆)-THF (cf.). c) Data taken from a sample in CDCl₃ at 101 MHz (mixture with NmnCl and 2-menthene). d) Peak integral from deconvolutive peak fitting ("d"); arbitrary units. e) Data from a D₂O-quenched sample of Grignard reagent (50 °C, 1 M, THF), organic phase measured in CDCl₃ at 101 MHz. f) Data from a Grignard reagent (sample A) in THF with C₆D₆ added for locking. g) Data from sample D, prepared in Et₂O and measured with C₆D₆ for locking. * Data not accessible or less accurate due to peak overlap.

3.2.3 ψ-Menthene (10)

The compound was detected by the characteristic doublet of septets for the olefinic proton at δ¹H) 5.05 ppm. Its concentrations were too low (≤0.4%) to be detected by ¹³C NMR spectroscopy of the Grignard reagents. The compound has previously been described in the literature with a ¹H NMR spectrum (δ = 5.03 (d × sept; -CH=), 2.62 [m; 3-H (cyclopentane)], 1.56 [s, 2-CH₃ (propenyl)], 1.62 [s; 2-CH₃ (propenyl)], 0.95 [1-CH₃ (cyclopentane)]).⁴

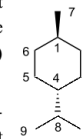


⁴ Lehmkuhl, H.; Fustero, S. (Alkenyl-η³-allyl)bis(η⁵-cyclopentadienyl)titan-Komplexe. *Liebigs Ann. Chem.* **1980**, 1353–1360.

3.3 NMR data for saturated hydrocarbon components

3.3.1 trans-para-Menthane (4)

Menthane is always present in menthyl Grignard reagent. Its generation is linked to that of 2- and 3-menthenes. Alternatively it may be formed from **1** with water traces in the reaction solvent. A sample of menthane (96 mol-% purity, with 4 mol-% of ψ-menthane) was obtained by hydrolyzing menthyl Grignard reagent as described in the main text.



Samples of 3-(D₁)-menthane, composed of diastereomers with equatorial and axial deuterium (59:41), were obtained by quenching menthyl Grignard reagent (prepared from **2** at 50 °C, 1 M in THF) with D₂O. The ratio of diastereomers depends on the mode of generation (solvent, temperature) and standing time before quenching of the Grignard reagent.

Menthane numbering is used for positional assignments.

Figure S11. Overview of δ¹H) and δ¹³C) assignments for trans-p-menthane (4)

δ ¹ H) from 2D NMR (500 MHz, CDCl ₃) menthane numbering	δ ¹³ C) in CDCl ₃ (101 MHz)	δ ¹³ C) in (D ₆)-THF in Grignard reagent

Table S9. NMR assignments for *trans-p*-menthane (4)

Pos.	Type	$\delta^{13}\text{C}^a$	$\delta^1\text{H}$ by HSQC ^b	$\delta^{13}\text{C}^c$	$\delta^1\text{H}$ by HSQC ^c	HMBC ^b	$\delta^1\text{H}^d$
		CDCl_3	CDCl_3	$(\text{D}_8)\text{-THF}$	$(\text{D}_8)\text{-THF}$	CDCl_3	CDCl_3
4	CH	43.95	0.90–0.99 (m, 1 H)	44.08	0.95–1.03 (m; 1 H)	0.855 > 1.40, 1.69	0.87–1.00 (m, 5 H)
2/6	CH ₂	35.70	1.68 (d, 12; 2 H) 0.81–0.96 (m; 2 H)	35.72	1.71 (d, 14; 2 H) 0.85–0.94 (m; 2 H)	0.865 > 1.68, 0.97	0.87–1.00 (m, 5 H) 1.62–1.69 (m, 4 H)
1	CH	33.03	1.18–1.29 (m, 1 H)	33.10	1.22–1.30 (m, 1H)	0.855 > 1.68	1.18–1.29 (m, 1 H)
8	CH	33.00	1.33–1.43 (m, 1 H)	33.08	1.36–1.43 (m, 1H)	0.855	1.38 (sept × d, 6.8, 4.2, 1 H)
3/5	CH ₂	29.89	1.61–1.70 (m, 2 H) 0.85–0.99 (m, 2 H)	29.94	1.67–1.72 (m, 2 H) 0.89–1.02 (m, 2 H)	0.855, 1.40 > 1.68	0.87–1.00 (m, 5 H) 1.62–1.69 (m, 4 H)
7	CH ₃	22.77	0.85 (d, 6; 3 H)	22.43	0.869 (d, 6; 3 H)	1.68 (w)	0.852 (d, 6.7, 3 H) ^e
9/10	CH ₃	19.90	0.84 (d, 7; 6 H)	19.56	0.865 (d, 6; 6 H)	0.855 > 1.39	0.839 (d, 6.9, 6 H) ^e

a) Sample in CDCl_3 at 101 MHz. b) Sample in CDCl_3 solution at 500 MHz. c) Grignard reagent prepared and measured in $(\text{D}_8)\text{-THF}$ at 101 MHz or 500 MHz (2D). d) Sample in CDCl_3 solution at 400 MHz. e) J extracted by deconvolution.

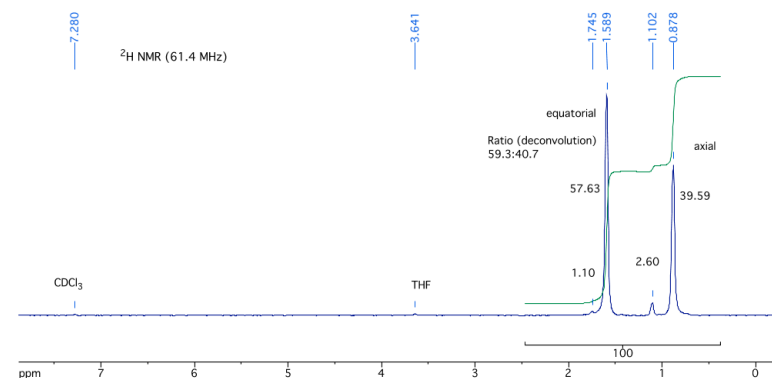
Table S10. Additional ^{13}C NMR Data for *trans-p*-menthane (4) in various samples

Pos.	Type	$\delta^{13}\text{C}$ Lit. ^a	$\Delta\delta^b$	$\delta^{13}\text{C}^c$	Idx ^{c,d}	$\delta^{13}\text{C}^e$	Idx ^{d,e}	$\delta^{13}\text{C}^f$	$f(d)^{g,a}$	Idx ^{d,f}	$\delta^{13}\text{C}^h$	$f(d)^{g,h}$
				CDCl_3		$(\text{D}_8)\text{-THF}$		THF			Et_2O	
4	CH	43.94	-0.01	43.95	0.996	44.08	0.985	43.81	94.3	1.017	43.74	31.91
2/6	CH ₂	35.71	0.01	35.70	1.132	35.72	1.096	35.56	231.7*	1.249	35.47*	69.4*
1	CH	32.94 ^d	-0.09	33.03	1.013	33.10	0.930	32.89	*	0.992	32.80 ⁱ	-
8	CH	(2 C)	-0.06	33.00	0.992	33.08	1.085	32.89	184.0	0.992	(2 C)	62.19
3/5	CH ₂	29.90	0.01	29.89	1.124	29.94	1.058	29.80	197.8	1.066	29.71	69.57
7	CH ₃	22.83	0.06	22.77	1.152	22.43	0.899*	22.56	104.8	1.130	22.44*	*
9/10	CH ₃	19.73	-0.17	19.90	1.187	19.56	1.094	19.65	200.0	1.078	19.53	71.89
				CH	1.000	CH	1.000	CH		1.000	CH av.	1.000
				CH ₂	1.128	CH ₂	1.077	CH ₂		1.157	CH ₂	1.108
				CH ₃	1.176	CH ₃	*	CH ₃		1.104	CH ₃	1.146

a) Values from Gorobetz *et al* at 75 MHz in CDCl_3 .² b) Peak shift difference Lit.^a minus measured value. c) Menthane in CDCl_3 at 101 MHz (with 5% isomenthane). d) "CH-Index", peak integral relative to the average of all CH-signals. e) Grignard prepared and measured in $(\text{D}_8)\text{-THF}$ at 101 MHz. f) Data from Grignard reagent (sample A) in THF with C_6D_6 added for locking, at 101 MHz. g) Peak integral by deconvolutive peak fitting ("d"); arbitrary units. h) Grignard reagent (sample D) prepared in Et_2O , measured with C_6D_6 added for locking, at 101 MHz. i) Signals for C-1 and C-8 may overlap by chance, depending on the solvent or medium composition. *) Value could not be extracted, or is less accurate due to peak overlap.

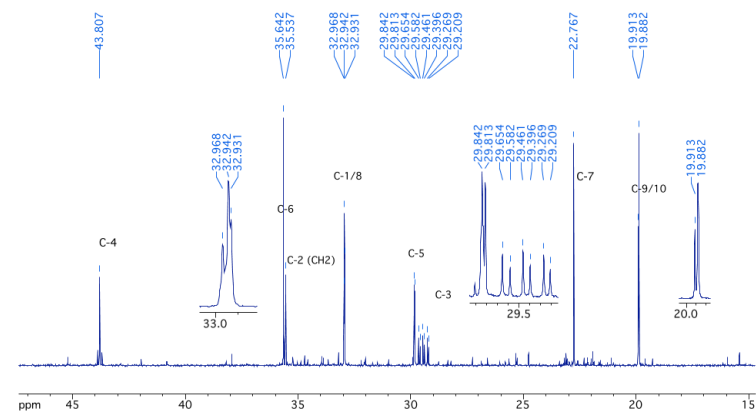
3.3.2 3-(D₁)-*trans-para*-Menthane

Figure S12. $^2\text{H}\{^1\text{H}\}$ NMR (61.4 MHz) spectrum of 3-(D₁)-menthane in $\text{CHCl}_3\text{-THF}$



Numbers next to peaks indicate peak area obtained by deconvolutive peak fitting.

Figure S13. ^{13}C NMR (101 MHz, CDCl_3) spectrum of crude 3-($^2\text{H}_1$)-menthane



Additional signals due to 2-menthene (8), 3-menthene (9) and bimenthyl isomers (13–15).

Comments on the ^{13}C NMR spectrum of (3-D₁)-menthane:

- Key points of difference are the C-3 signal with its three-line splitting $^1J(^{13}\text{C}, ^2\text{H}) = 19$ Hz, and the characteristic α - ^2H -isotope-shift that differs in the axial and equatorial (3-D₁)-menthane diastereomer.
- Due to loss of the mirror plane in *p*-menthane, the (3-D₁)-menthane diastereomers show separate signals for C-2/6, C-3/5, and partially for C-9/10 (see below).
- The major, equatorial (3-D₁)-menthane shows separate signals for methyl carbons C-9 and C-10 at δ 19.91 and δ 19.88; the latter signal overlaps with a single peak at δ 19.89 for the C-9/10 signals of the minor, axial (3-D₁)-menthane diastereomer, from which it could only be separated by deconvolution.

Table S11. ^{13}C NMR Data for (3-D₁)-*trans-p*-menthane (4)

Pos.	Type	$\alpha(^{13}\text{C})^a$ Ref.	$\alpha(^{13}\text{C})^b$	$\int(d)^{b,c}$	Idx. ^{b,d}	Notes
		CDCl ₃	CDCl ₃		90.23	
4	CH	43.87	43.89 (H) 43.81 (D ₁)	7.0 82.7	(0.994 comb.)	C-4 in unlabeled menthane C-4 in (D ₁)-menthane, β -shifted
2/6	CH ₂	35.64	35.64 35.56* 35.54*	120 36.4* 62.1*	(1.211 comb.)	C-6 (no shift) + C-2/6 unlabeled C-2 (β -shifted, axial) C-2 (β -shifted, equatorial)
1	CH	32.97	32.90–33.00	(181)	(1.003)	C-1 multiple overl. signals
8	CH	32.94	32.90–33.00	(181)	(1.003)	C-8 multiple overl. signals
3/5	CH ₂ (CHD)	29.84	29.84* ($t?$, $J_{\text{C,D}} = 1.1$) 29.81* 29.46 (t , $J_{\text{C,D}} = 19.4$) 29.40 (t , $J_{\text{C,D}} = 18.8$)	72.0* 41.3* 51.2 35.9	(1.110 comb.)	C-5 (equ. D) + unlabeled C3/5 C-5 (axial D) C-3 (equatorial D) C-3 (axial D)
7	CH ₃	22.76	22.77	109	1.208	
9/10	CH ₃	19.88	19.91 19.89* 19.88*	61,2 101.5* ^d 58.6* ^d	(1.226 comb.)	C-9 or C-10 in (D ₁)-eq. C9/10 in (D ₁)-ax. C-10 or C-9 in (D ₁)-eq
		CH CH ₂ CH ₃	CH CH ₂ CH ₃		1.000 1.161 1.220	

a) Unlabeled reference sample of *trans-p*-menthane in CDCl₃ at 101 Mhz. b) Sample of D₂O-quenched Grignard reagent worked up for neutral hydrocarbon fraction. c) Peak integral by deconvolutive peak fitting ("d"); arbitrary units. d) "CH-Index", peak integral relative to the average of all CH-signals. *) Overlapping signals, peak area (and δ) determined by deconvolutive peak fitting analysis.

3.3.3 ψ -Menthane or (1*R*,3*R*)-1-isobutyl-3-methylcyclopentane (16)

The compound was present as minor component (4 mol%) in the distilled and acid-washed menthane fraction of a hydrolyzed menthyl Grignard reagent that had been prepared from crude menthyl chloride. The ^1H NMR data agree with a spectrum reproduced in the literature.⁵

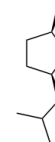


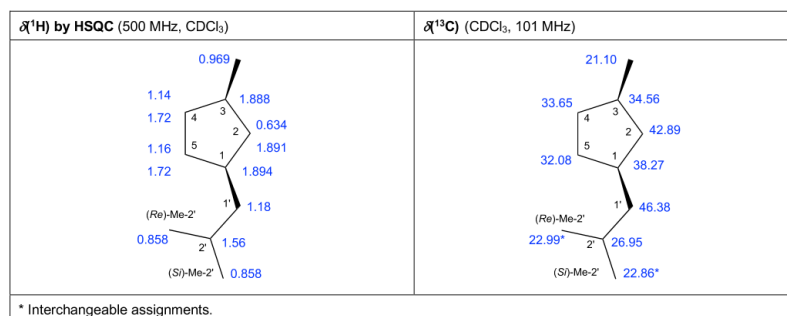
Table S12. NMR data for ψ -menthane (16)

Pos.	Type	$\alpha(^{13}\text{C})^a$	$\int(d)^{b,b}$	Idx. ^{a,c}	$\alpha(^{13}\text{C})^d$	$\int(d)^{b,d}$	Idx. ^{e,d}	$\alpha(^1\text{H})$ by HSQC ^e	HMBC
	APT	CDCl ₃							
1'	CH ₂	46.38	4.96	1.119	46.39	4.47	1.030	1.18 (m) (1.15–1.21)	0.863 (vs), 1.56, 1.30, 1.06 > 0.634
2	CH ₂	42.89	5.65	1.275	42.90	4.86	1.120	1.891 (m) (1.85–1.93) 0.634 (m) (0.58–0.68)	0.970 (vs), 1.19 > 1.73
1	CH	38.27	4.53	1.022	38.28	4.20	0.968	1.894 (m) (1.84–1.95)	1.18 > 1.58, 1.89, 0.634
3	CH	34.56	4.30	0.970	34.57	4.27	0.984	1.888 (m) (1.83–1.95)	0.970 (vs) > 0.634
4	CH ₂	33.65	4.55	1.026	33.66	4.00	0.922	1.72 (m) (1.67–1.77) 1.14 (m) (1.09–1.18)	0.970 (vs)
5	CH ₂	32.08	5.04	1.137	32.09	4.71	1.085	1.72 (m) (1.69–1.77) 1.16 (m) (1.12–1.21)	1.19 > 1.89
2'	CH	26.95	4.47	1.008	26.95	4.55	1.048	1.56 (m) (1.51–1.61)	0.862 (vs) > 1.183
Me-2 st	CH ₃	22.99	5.90	1.331	23.00	4.80	1.106	0.858 (d)	*
Me-2 nd	CH ₃	22.86	5.24	1.182	22.86	5.75	1.325	0.858 (d)	*
Me-3	CH ₃	21.10	5.07	1.144	21.10	5.32	1.226	0.969 (d)	1.09, 0.843 > 0.634
			CH CH ₂ CH ₃	1.000 1.146 1.219		1.000 1.039 1.219			

a) Sample measured in CDCl₃ at 101 MHz. b) Peak integral by deconvolutive peak fitting ("d"); arbitrary units. c) "CH-Index", peak integral relative to the average of all CH-signals. d) Alternative sample in CDCl₃ at 101 MHz. e) Data collected in CDCl₃ at 500 MHz. *) Interchangeable assignments. *) Value could not be extracted or is less accurate due to peak overlap.

⁵ Nagai, K. The Action of Boron Trifluoride Etherate on l-Menthol. *Bull. Chem. Soc. Japan* **1970**, *43*, 2628–2630.

Figure S14. Overview of $\delta(^1\text{H})$ and $\delta(^{13}\text{C})$ assignments for ψ -menthane (16)

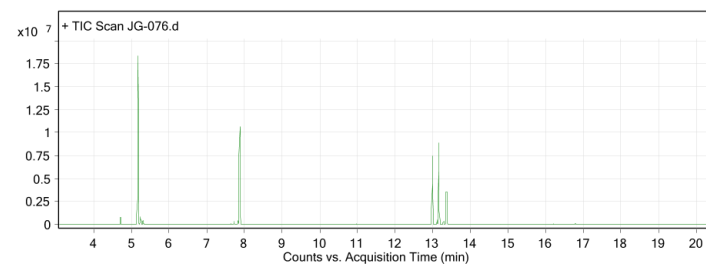


3.4 GC-MS analysis of the hydrocarbon fraction of Grignard reagent 1

A sample of Grignard reagent 1, containing naphthalene, was quenched by addition of D_2O . The organic phase was washed with water and a sample removed for GC-MS analysis.

3.4.1 Total ion count GC trace

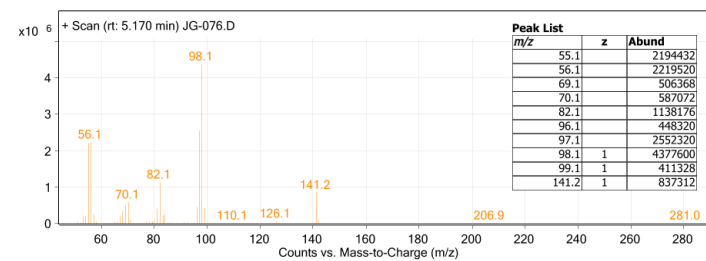
Figure S15. TIC GC trace of hydrocarbon fraction after D_2O quenching of Grignard reagent 1.



t_R : 5.17 min (D_1 -menthane), 7.88 min (naphthalene), 12.98/13.16/13.36 min (bimenthyls 13–15)

3.4.2 EI-MS of *trans-p*-(3- D_1)-menthane

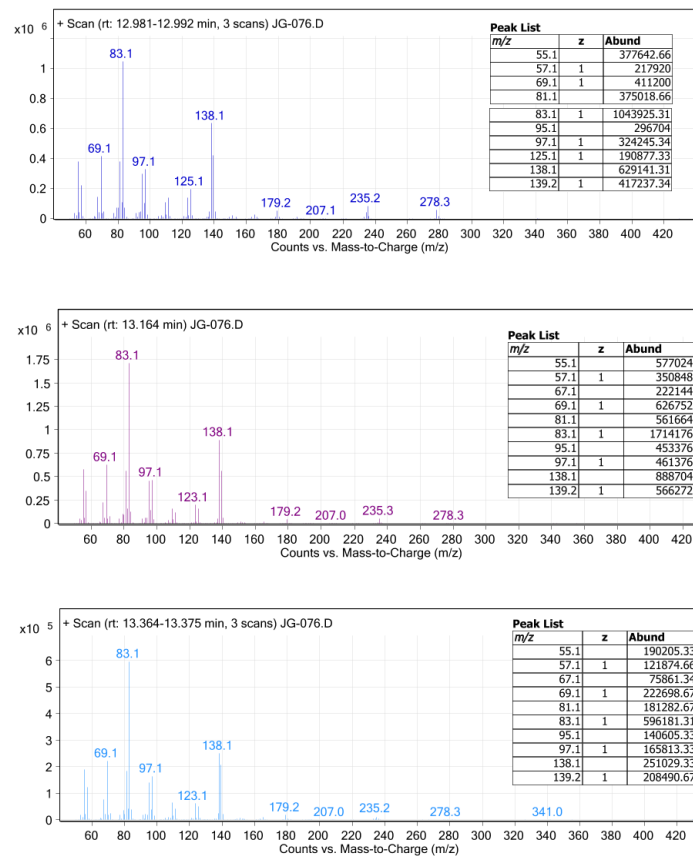
Figure S16. EI-MS spectrum of (D_1)-menthane



3.4.3 EI-MS of bimethyl hydrocarbons

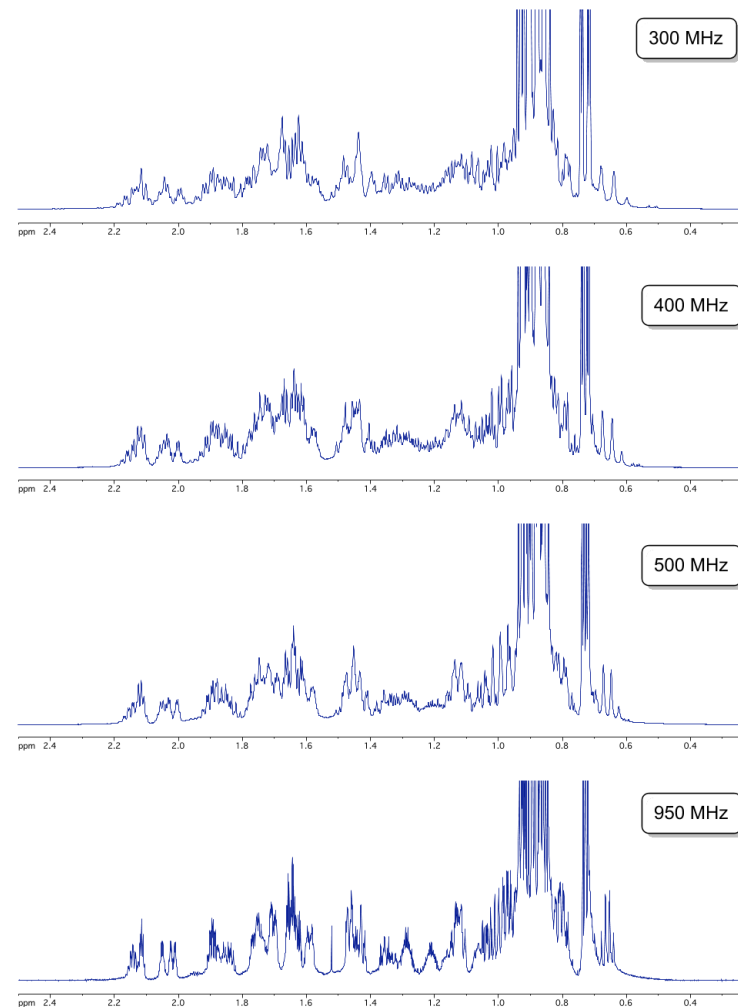
The individual isomers have not been assigned, although from the peak intensity it would appear that the elution order is: **Men₂** (13) < **Men-Nmn** (14) < **Nmn₂** (15).

Figure S17. EI-MS spectra of bimethyl hydrocarbons



- S23 -

Figure S18 Bimethyl isomer mixture (13–15): ¹H NMR spectra (CDCl₃) at various field strengths



- S24 -

3.5 NMR data of bimethyl hydrocarbons

For the ^1H NMR spectrum of the distilled, high-boiling hydrocarbon mixture at various MHz, see Figure S18 (previous page).

See the main text, experimental part, for isolation of the bimethyl mixture and crystallization of bimethyl (**13**). The distilled isomer mixture showed the composition: **13**:**14**:**15** = 38.6% : 45.1% : 16.3% (calculated based on relative CH-index values from ^{13}C NMR peak integrals).

After crystallization of **13**, the ratio of hydrocarbons in the mother liquor amounted to **13**:**14**:**15** = 23.5% : 56.1% : 20.4%. NMR data for all isomers were extracted from the 950 MHz spectrum of the isomer mixture, and in case of symmetrical bimethyl (**13**) also from spectra of crystallized material.

3.5.1 Bimethyl (**13**)

Systematic name: (1*R*,1'*R*,2*S*,5*R*,5'*R*)-2,2'-diisopropyl-5,5'-dimethyl-1,1'-bi(cyclohexane)

Table S13. NMR data for bimethyl (**13**)

Pos.	Type	$\delta(^{13}\text{C})^a$	$f(\text{d})^{a,b}$	Idx. ^{a,c}	HSQC ^d	$\delta(^1\text{H})$ by HSQC ^e	$\delta(^1\text{H})^f$	$j(^1\text{H})^g$
							400 MHz, CDCl_3	
C-2	CH	43.68	100.0	0.984	1.117	1.115 (tt, 11.5, 2.6)	1.116 (ddt, 11.6, 9.9, 2.6)	2 H
C-1	CH	37.92	101.1	0.994	1.432	1.429 (tt, 11.4, 3.1)	1.38-1.49 (m)	2 H
C-6	CH_2	35.65	105.9	1.042	0.803 ax, 1.703 eq	0.805 (qd, 12.5, 3.5) 1.702 (m)	0.70-0.85 (m) 1.66-1.74 (m)	2 H 2 H
C-4	CH_2	34.70	102.8	1.011	0.659 ax, 1.466 eq	0.659 (q, 12.5) 1.464 (dm, 12.9)	0.656 (q, \approx 12.5) 1.42-1.50 (m)	2 H 2 H
C-5	CH	33.19	103.2	1.015	1.286	1.285 (m)	1.287 (m)	2 H
C-1'	CH	25.31	102.4	1.007	1.894	1.892 (sext-d, 6.9, 2.5)	1.893 (sept \times d, 6.9, 2.7)	2 H
C-3	CH_2	24.76	102.5	1.008	0.980 ax, 1.650 eq	0.973 (qd, 12.5, 3.5) 1.649 (q, 13.1, 3.1)	0.975 (qd, 12.0, 3.1) 1.648 (dq, 12.2, 3.0)	2 H 2 H
Me-5	CH_3	23.10	101.7	1.000	0.865	0.866 (d, 6.5)	0.866 (d, 6.7)	6 H
$^{\text{Si}}\text{Me-1}'$	CH_3	21.92	106.4	1.046	0.888	0.888 (d, 7.0)	0.889 (d, 7.1)	6 H
$^{\text{Re}}\text{Me-1}'$	CH_3	15.41	100.7	0.990	0.725	0.725 (d, 7.3)	0.724 (d, 6.9)	6 H
	CH			1.000				
	CH_2			1.020				
	CH_3			1.012				

a) Bimethyl isomer mixture in CDCl_3 at 101 MHz. b) Peak integral by deconvolutive peak fitting ("d"); arbitrary units. c) "CH-Index", peak integral relative to the average of all CH-signals. d) Bimethyl isomer mixture in CDCl_3 at 500 MHz. e) ^1H NMR peak data by HSQC at 950 MHz in CDCl_3 . f) Data for pure compound in CDCl_3 at 400 MHz. g) Number of protons derived from integration, including 2D spectra, and analysis of coupling. ax = axial position; eq = equatorial position.

Figure S19. Overview of $\delta(^1\text{H})$ and $\delta(^{13}\text{C})$ assignments for symmetrical bimethyl (**13**)

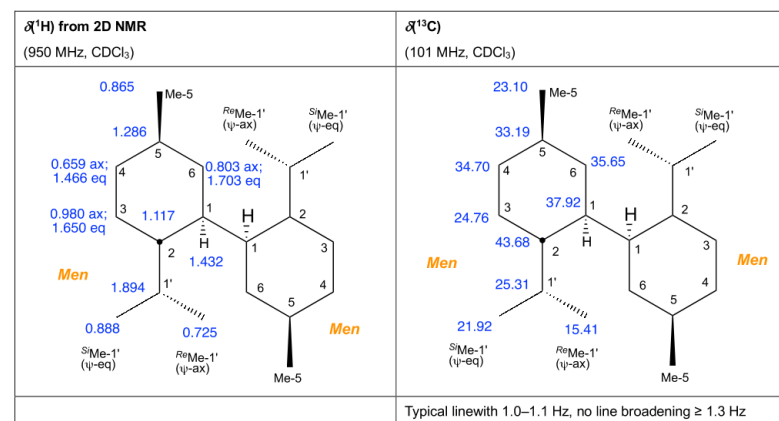


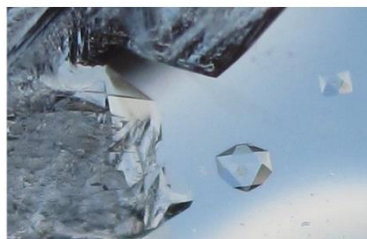
Figure S20. Crystallization of bimenthyl (13)



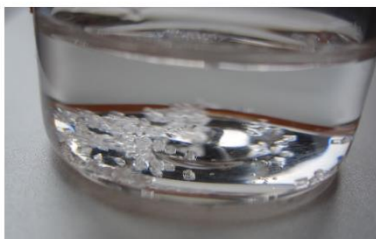
a) Distilled bimenthyl fraction (neat); early stage of crystallization, ca. 2 x original size.



b) Crystallization continued for several days.



c) Detail.



d) Crystals of **13** after recrystallization from EtOH-toluene.



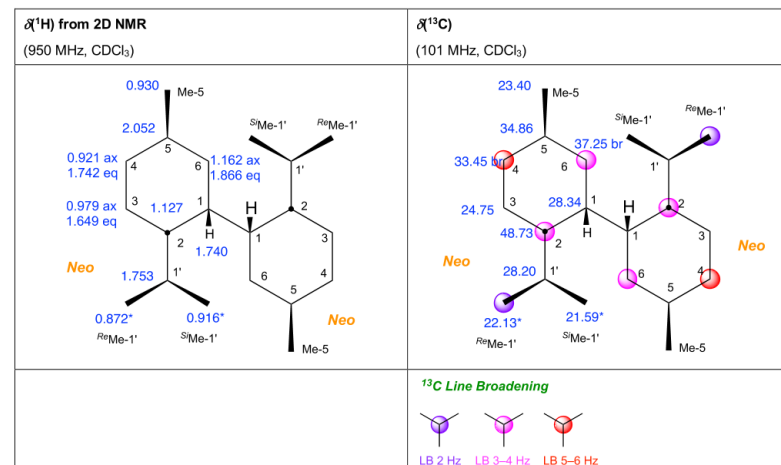
e) Crystals of **13** in EtOH mother liquor.

- S27 -

3.5.2 Bineomenthyl (15)

Systematic name: (1*S*,1'*S*,2*S*,2'*S*,5*R*,5'*R*)-2,2'-Diisopropyl-5,5'-dimethyl-1,1'-bi(cyclohexane)

Figure S21. Overview of $\delta(^1\text{H})$ and $\delta(^{13}\text{C})$ assignments for bineomenthyl (15)^a



- S28 -

Table S14. NMR data for bineomenthyl (15)

Pos.	Type	$\delta(^{13}\text{C})^a$	$J(\text{d})^{a,b}$	Idx. ^{a,c}	HSQC ^d	$\delta(^1\text{H})$ from HSQC ^e	$\delta(^1\text{H})^f$	$J(^1\text{H})^g$
						CDCl ₃ , 950 MHz	CDCl ₃ , 950 MHz	
C-2	CH	48.73	41.3*	0.957	1.127	1.124 (m)	*	2 H
C-6	CH ₂	37.25 br	44.6	1.034	1.162;	1.159 (m)	*	2 H
					1.866	1.866 (dt, \approx 14.6, 5)	*	2 H
C-5	CH	34.86	44.5	1.031	2.052	2.049 (quint, \approx 4.5)	2.051 (d-quint, 4.4, 4.0)	2 H
C-4	CH ₂	33.45 br.	46.7*	1.082	0.921	0.919 (m)	*	2 H
					1.742	1.740 (m)	*	2 H
C-1	CH	28.34	42.9	0.994	1.740	1.747 (m)	*	2 H
C-1'	CH	28.20	43.9	1.017	1.753	1.747 (m)	*	2 H
C-3	CH ₂	24.75	40.9	0.948	0.979,	0.977 (qd, 12.6, 3.3)	*	2 H
					1.649	1.648 (dq, \approx 13.1, 3.3)	1.649*	2 H
Me-5	CH ₃	23.40	44.7	1.036	0.929 (d, 6.4)	0.929 (d, 6.7)	0.930 (d, 6.6)	6 H
Me-1'	CH ₃	22.13 [#]	40.9*	0.948*	0.872 (d, 6.4)	0.871 (d, 6.6)	*	6 H
Me-1'	CH ₃	21.59 [#]	45.9	1.064	0.916 (d, 6.4)	0.916 (d, 6.8)	*	6 H
	CH			1.000				
	CH ₂			1.021				
	CH ₃			1.015*				

a) Bimenthyl isomer mixture in CDCl₃ at 101 MHz. b) Peak integral from deconvolutive peak fitting ("d"); arbitrary units. c) "CH-Index", peak integral relative to the average area of all CH-signals. d) Bimenthyl isomer mixture in CDCl₃ at 500 MHz. e) ¹H NMR peak data by HSQC at 950 MHz in CDCl₃. f) Data from bimenthyl isomer mixture in CDCl₃ at 950 MHz. g) Number of protons derived from integration, including 2D spectra, and analysis of coupling. *) Peak overlap, less accurate or extraction not possible. #) Interchangeable assignments.

3.5.3 "Menthyl-neomenthyl" or (1*R*,1'*S*,2*S*,2'*S*,5*R*,5'*R*)-2,2'-Diisopropyl-5,5'-dimethyl-1,1'-bi(cyclohexane) (14)

Table S15. NMR data for menthyl-neomenthyl (14)

Pos. ^a	Type	$\delta(^{13}\text{C})^b$	$f(\text{d})^{b,c}$	Idx. ^{b,d}	HSQC correl. ^e	$\delta(^1\text{H})$ from HSQC ^f	$\delta(^1\text{H})^g$	$J(^1\text{H})^h$	HMBC ^e
	DEPT								
N-2	CH	49.24 br	58.1	0.977	1.067	1.062 (m)	1.062 (m)	1 H	0.906 > 2.115, 1.844, 1.766, 1.634, 1.454, 1.361, 1.037,
M-2	CH	47.48	57.8	0.972	1.136	1.135 (ddt, 14.0, 11.3, ≈ 3)	overl.	1 H	0.732, 0.911 > 1.645, 2.018, 2.12, 1.356, 1.268w
M-1	CH	45.20	57.6	0.969	1.357	1.354 (tt, 12.2, 3.5)	1.355 (ddt, 12.4, 11.1, 3.6)	1 H	1.03, 1.624 > 2.118, 2.017, 0.867, 1.135w
N-6	CH ₂	44.21 br	64.2	1.080	1.035 1.594	1.034 (ddd, 13.2, 11.0, 4.5) 1.589 (d-m, ≈ 13.5)	overl. 1.589 (d × m, 13.5)	1 H 1 H	0.851 > 2.116w, 1.765, 1.359, 0.976
M-6	CH ₂	40.80	62.2	1.046	1.005 2.016	1.004 (q, ≈ 12.4) 2.017 (d-m, ≈ 13)	overl. 2.017 (dtd, 12.7, 3.1, 2.5)	1 H 1 H	0.867 > 2.116, 1.657, 1.360, 1.212, 1.135, 0.804
N-4	CH ₂	35.23	62.7	1.055	0.902 1.762	0.900 (sext-d, ≈ 12, 4.5) 1.772 (m)	* *	1 H 1 H	0.858? > 1.630, 1.453, 2.019, 1.715w, 1.212w, 1.037
M-4	CH ₂	35.22	60.5	1.018	0.815 1.654	0.819 (td, ≈ 12.6, 3.5) 1.653 (= d-quint, ≈ 12.8, 2.9)	* *	1 H 1 H	0.862 > 1.464, 1.629, 2.019, 1.212w
M-5	CH	33.93	59.6	1.003	1.211	1.209 (m)		1 H	1.635, 0.867 > 2.014, 1.009, 0.813
N-1	CH	33.86	60.3	1.014	2.116	2.114 (quint, 4.2)	2.115 (quint, 4.2)	1 H	1.034 > 1.355, 1.711?, 1.842, 2.014?
N-1'	CH	29.89	60.6	1.020	1.842	1.842 (d-quint, 9.6, 6.6)	1.840 (d-quint, 9.4, 6.6)	1 H	0.892, 0.921 > 1.068, 1.455, 1.634, 2.116
N-5	CH	27.24	60.7	1.021	1.712	1.710 (m)		1 H	0.850 > 1.036, 1.626, 1.764, 2.116, 1.459, 0.900
M-1'	CH	26.58	60.8	1.023	2.141	2.140 (sext-d, 7.0, 2.0)	2.142 (sept × d, 6.9, 2.4)	1 H	0.732, 0.909 > 1.135, 0.960?, 1.356, 1.629

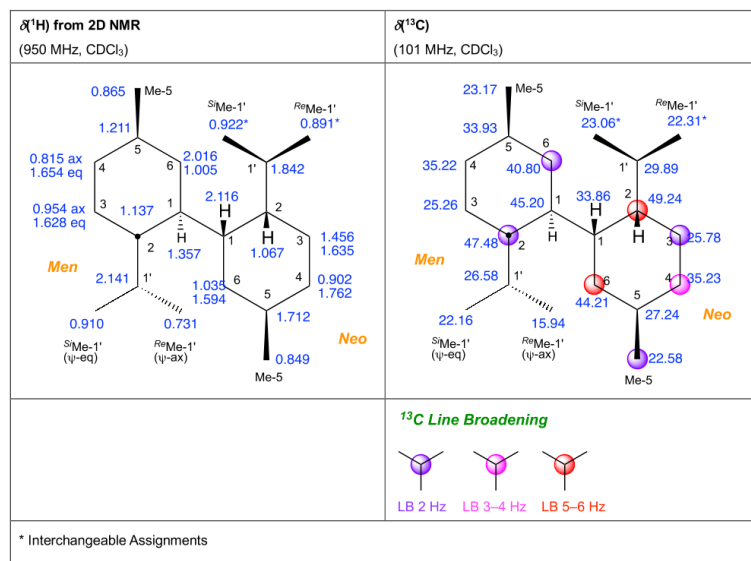
- S30 -

N-3	CH ₂	25.78	60.7	1.021	1.456 1.635	1.460 (qd, ≈ 12.5, 4.2) 1.637 (dq, 13.6, 4.1)	* *	1 H 1 H	0.850, 1.843, 1.764, 2.115, > 1.069, 0.908, 1.508, 1.706, 1.328
M-3	CH ₂	25.26	60.4	1.016	0.954 1.628	0.953 (qd, 12.7, 3.6) 1.627 (dd, 13.2, 3.5)	* *	1 H 1 H	1.650 ? (or 25.32) > 1.764? 2.142, 1.487, 1.358, 1.061?
Me-N-5	CH ₃	23.17	60.8	1.023	0.865	0.866 (d, 6.7)	*	3 H	2.017 > 1.210?, 1.646?
^S Me-N-1'	CH ₃	23.06 [#]	63.3	1.065	0.921	0.920 (d, 6.6)	0.920 (d, 6.6)*	3 H	0.921 > 1.848, 1.478?
Me-N-5	CH ₃	22.58	64.2	1.080	0.849	0.849 (d, 6.6)	0.849 (d, 6.6)*	3 H	1.712 > 1.035, 1.594, 1.771
^R Me-N-1'	CH ₃	22.31 [#]	61.0	1.026	0.891	0.890 (d, 6.7)	0.889 (d, 7.0)*	3 H	0.922 > 1.844
^S Me-M-1'	CH ₃	22.16	55.9*	0.940*	0.910	0.909 (d, 7.2)	0.910 (d, 6.9)*	3 H	0.732 > 1.14, 1.034, 2.141
^R Me-M-1'	CH ₃	15.94	59.3	0.998	0.731	0.732 (d, 7.0)	0.731 (d, 7.2)	3 H	0.910 > 2.141, 1.137
	CH			1.000					
	CH ₂			1.039					
	CH ₃			1.022					

Positional numbering system: "M" - carbon in menthyl part; "N" - carbon in neomenthyl part. a) Bimethyl isomer mixture in CDCl₃ at 101 MHz. b) Peak integral by deconvolutive peak fitting; arbitrary units. c) "CH-Index", peak integral relative to the average of all CH-signals. d) Bimethyl isomer mixture in CDCl₃ at 500 MHz. e) ¹H/¹³C NMR peak correlation by HSQC (or HMBC; correlations with "?" are weak/insecure) at 500 MHz in CDCl₃. f) ¹H NMR peak data extracted from HSQC of bimethyl isomer mixture in CDCl₃ at 950 MHz. g) ¹H NMR peak data visible in the 950 MHz 1D spectrum. h) Number of protons derived from integration, including 2D spectra, and analysis of coupling. *) Peak overlap, less accurate or extraction not possible. #) Interchangeable assignments. "quint" is quintet (5-line splitting); analysis is based on the discernible signal shape; the true splitting should be a septet.

- S31 -

Figure S22. Overview of $\delta^1\text{H}$ and $\delta^{13}\text{C}$ assignments for menthyl-neomenthyl (**14**)^a



4 Component quantification in menthyl Grignard reagent

See the main text for a description of the procedure. The following correction factors were determined in reference measurements and used in the calculation:

Table S16. Parameters used for calculating composition

Compound	menthyl units	Signal (carbon number)	CH-index	Substance ^{13}C response ^a
Naphthalene	-	δ 125.6 (4 C)	-	1.0000
Menthane (4)	1	δ 19.5 (6 C) δ 43.7 (1 C)	(1.187) 1.017	0.9944 ^b
Men ₂ (13)	2	δ 43.6 (2 C) δ 37.9 (2 C)	0.984 0.994	0.9073 ^c
Men-Neo (14)	2	δ 45.2 (1 C) δ 47.6 (1 C)	0.969 0.972	0.9073 ^c
Nmn ₂ (15)	2	δ 48.7 (2 C) δ 28.3 (2 C)	0.957 0.994	0.9073 ^c
MenMgX	1	δ 48-51 (1 C)	-	1.230 ^d
NmnMgX	1	δ 51-54 (1 C)	-	1.230 ^d

a) Relative ^{13}C NMR peak intensity responses (calculated for CH-index value) relative to equal molar quantity of naphthalene (δ 125.6 ppm). b) Relative response of menthane (CH-index) vs. naphthalene (δ 125.6) derived from reference measurement with known amounts of menthane and naphthalene. c) Relative response of bimenthyls (CH-index) vs. naphthalene (δ 125.6) derived from reference measurements with known amounts of substances. It was assumed that **13**, **14** and **15** show equal response relative to their CH-index. d) The response for **MenMgX/NmnMgX** was estimated from values of **MenOH** and **MenCl** vs **NapH**; the factor includes any corrections due to differences in the CH-index. No separate CH-index correction was applied since the CH-index data for **1a/b** cannot be reliably determined.

5 Carboxylation of menthyl Grignard reagent

5.1 Carboxylation of 1 under different addition modes (Scheme 4)

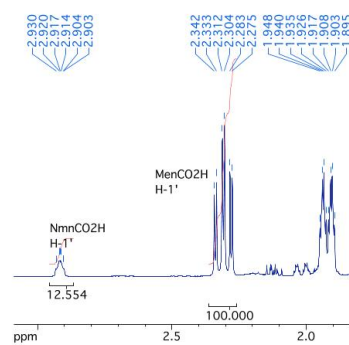


Figure S23. ¹H NMR analysis of *dr* of **19/20** (6.1.1)

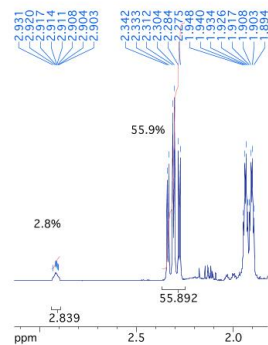
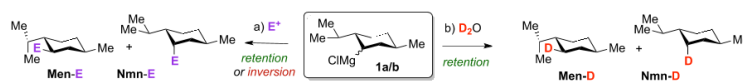


Figure S24. ¹H NMR analysis of **19/20** (6.1.2)

6 Reactions of menthyl Grignard reagent with electrophiles

Table S17. Conditions for and analyses of reactions of Grignard reagent **1** with various electrophiles (D₂O, CO₂, PCl₃).^a



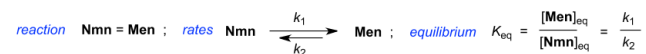
entry	RMgX [μmol] ^{b,c}	Temp. ^d	Electrophile ^e	Time [h]	Quench	MenD ^f [μmol]	Nmnd ^f [μmol]	<i>dr</i> (D ₁ - 4)	RMgX [μmol]	Products ^g (μmol)
1	3000 (1694:1219)	-78 °C	CO ₂ (xs)	1	D ₂ O	17.3 (-1677)	1181.6 (-37)	1.45:98.55		19 (1728.1); 20 (0.0); 16 (30.7)
2	1000 (565:406)	-78 °C to rt	H ₂ O (250)	1+0.5	D ₂ O	359.1 (-205.9)	406.5 (\pm 0)	46.9:53.1	780	RMgX (780), 16 (14.4)
3	1000 (565:406)	-78 °C to rt	H ₂ O (500)	1+0.5	D ₂ O	52.4 (-512.6)	279.2 (-126.8)	15.8:84.2	340	RMgX (340)
4	1000 (565:406)	-78 °C to rt	MeOH (500)	1+0.5	D ₂ O	331.3 (-233.7)	320.1 (-85.9)	50.9:49.1	660	
5	1000 (565:406)	-78 °C to rt	MenOH (500)	1+0.5	D ₂ O	317.3 (-247.7)	296.8 (-109.2)	51.7:48.3	622	
6	1000 (565:406)	-78 °C to rt ^h	PCl ₃ (2000)	3+12	H ₂ O	n.d.	n.d.	n.d.	n.d.	MenPO ₂ H ₂ (25b ; 925); NmndPO ₂ H ₂ (25b ; 65); <i>dr</i> 93.4:6.6
7	3000 (1694:1219)	0 °C, rt, 50 °C	PCl ₃ (1000)	0.2+1+2	D ₂ O	252	335	43.0:57.0	595	Men ₂ POH (7 ; 60.8%)
8a ⁱ	3000 (1694:1219)	0 °C	PCl ₃ (1000)	2	D ₂ O	408	491	45.4:54.6	917.9	Men ₂ POH (7 ; 74.8%)
8b ⁱ	3000 (1694:1219)	0 °C	PCl ₃ (1000)	2	D ₂ O	438	476	47.9:52.1	933.8	Men ₂ POH (7 ; 72.7%)
9	1000 (565:406)	0 °C to rt	Ph ₂ PCl (1000)	3	D ₂ O	82.0 (-483)	207.4 (-198.6)	28.3:71.7	295.4	MenPOPh ₂ (27 ; 723)

a) General conditions: **1** was added to electrophile in THF at -78 or 0 °C. After stirring for 1–3 h, reactions were quenched with D₂O and warmed to rt. b) Reactant quantities and analytical composition are given in μmol , whereas the main text gives rounded values in mol-%. c) RMgX composition: 2.94 mL = 3.00 mmol (titration); ²H qNMR: 1694 μmol **1a** + 1219 μmol **1b** + 45 μmol ψ -MenMgX (**12**), total 2958 μmol ; the composition of **1** varies from **1a/b** = 57.43 to 58.42, with ca. 1–1.5 mol % of ψ -MenMgCl (**12**) present. d) Room temperature (rt) is ca 22 °C. e) Electrophile = E⁺, quantity in μmol . f) Number in brackets indicates change (loss) of organometallic reagent as difference of initial and final value based on D₂O-quenching and quantification as (D₁)-**4** by ²H{¹H} NMR. g) Quantity given in μmol , or mol-% (for Men₂POH). h) Reaction for 3 h at -78 °C, followed by warming to rt with stirring overnight. i) Entry 8b is a repetition of 8a.

7 Epimerization studies of menthyl Grignard reagent

7.1 Kinetic equilibration studies of neomenthylmagnesium menthylcarboxylate

The kinetics have been analyzed for a reversible diastereomerization with two rate constants $k_1 \neq k_2$:⁹



for which holds:⁹

$$\ln \left(\frac{[\text{Nmn}]_0 - [\text{Nmn}]_{\text{eq}}}{[\text{Nmn}]_t - [\text{Nmn}]_{\text{eq}}} \right) = (k_1 + k_2) \cdot t ; \quad \text{simplified to } \ln([\text{Nmn}]_t - [\text{Nmn}]_{\text{eq}}) = -(k_1 + k_2) \cdot t + C'$$

$$\text{or further to } \ln((\% \text{Nmn})_t - (\% \text{Nmn})_{\text{eq}}) = -(k_1 + k_2) \cdot t + C'$$

where $(\% \text{Nmn})_t$ denotes mol-% of neomenthyl-species at time t , and C/C' are constant values. The data was fitted to the last equation above, and the term $(k_1 + k_2)$ was converted to k_1 and k_2 by means of the measured equilibrium constant K_{eq} at each temperature. Use of the Eyring equation for k_1 or k_2 led to the individual ΔG^\ddagger , and by fitting over the temperature range to the ΔH^\ddagger and ΔS^\ddagger values.

Table S18. Kinetic data for epimerization of NmnMgX with MenMgX

Experiment at 0 °C ^a			Experiment at 30 °C		
Time (min)	Men (mol%)	Nmn (mol%)	Time (min)	Men (mol%)	Nmn (mol%)
0	0,0	100,0	0	0,7	99,3
30	0,0	100,0	60	2,4	97,6
60	0,0	100,0	120	4,8	95,2
120	0,0	100,0	180	6,1	93,9
180	0,3	99,7	240	6,8	93,2
300 ^b	0,5	99,5	300	9,1	90,9
Experiment at 50 °C			Experiment at 70 °C		
Time (min)	Men (mol%)	Nmn (mol%)	Time (min)	Men (mol%)	Nmn (mol%)
0	0,4	99,6	0	0,3	99,7
30	7,6	92,4	15	25,2	74,8
60	13,6	86,4	30	34,5	65,5
120	24,1	75,9	45	38,9	61,1
180	31,7	68,3	60	39,3	60,7
240	35,6	64,4	90	39,6	60,4
4320	38,0	62,0			
8640 ^c	38,3	61,7			

a) The values at 0 °C were not included in the kinetic analysis, since the conversion was too low. b) The value at 300 min was extrapolated from the 180 min value for graphical reasons (drawing of the guideline). c) Equilibrium value was measured in a separate experiment.

⁹ Wolf, C. *Dynamic Stereochemistry of Chiral Compounds*; RSC Publishing: London, 2007.

Figure S25. $\ln([\text{NmnMg}]_t - [\text{NmnMg}]_{\text{eq}})$ vs time (slope = $-(k_1 + k_2)$)

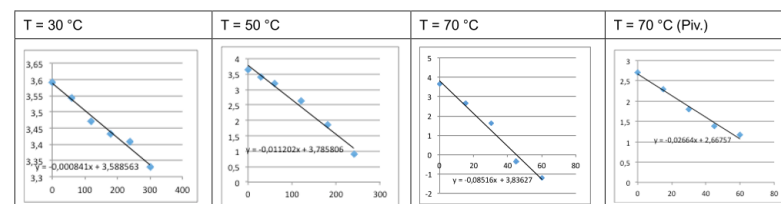


Table S19. Analysis of epimerization data for 1bⁱ

Temp. [°C]	[Nmn] _{eq} [mol %]	$K_{\text{eq}} = k_1/k_2$	$(k_1 + k_2)^a$ [min ⁻¹]	k_1 [min ⁻¹]	k_2 [min ⁻¹]	$t_{1/2}^b$ [min]	$\Delta G^\ddagger (k_1)$ [J/mol]	$\Delta G^\ddagger (k_2)$ [J/mol]
30 °C	63	0,587301587	0,000841	0,00031117	0,00052983	824,2	64338	62996,6
50 °C	61,9	0,615508885	0,011202	0,004267962	0,006934038	61,9	61719	60415
70 °C	60,4	0,655629139	0,08516	0,03372336	0,05143664	8,1	59812	58608
70 °C (piv)	57,1	0,751313485	0,02664	0,01142856	0,01521144	26,0	62900	62084

a) Value from linear regression, see Figure S25. b) Half-life to epimerization.

$[\text{Nmn}]$ denotes the concentration of any neomenthyl-Mg-species. From the temperature dependence of ΔG^\ddagger , a fit for $\Delta G^\ddagger = \Delta H^\ddagger - T \cdot \Delta S^\ddagger$ provides the values 98521 J/mol – $T \cdot 113,2$ J/mol·K ($\mathbf{1b}^i \rightarrow \mathbf{1a}^i$); and $\Delta G^\ddagger = 96128$ J/mol – $T \cdot 109,7$ J/mol·K ($\mathbf{1a}^i \rightarrow \mathbf{1b}^i$).

7.2 Epimer equilibration after addition of carboxylates to 1

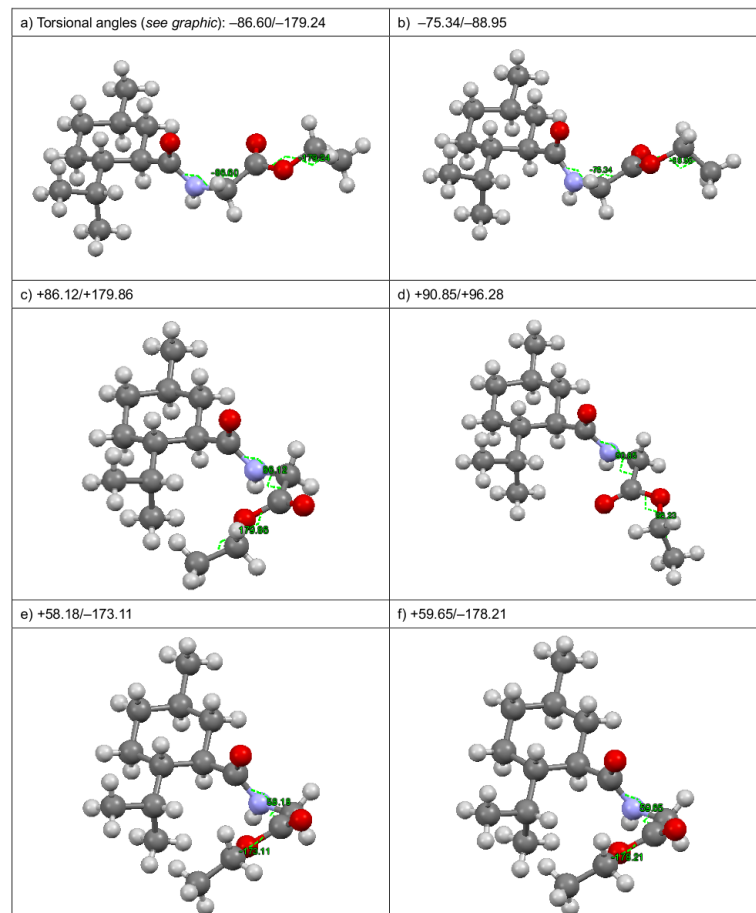
Table S20. Kinetic data for equilibration of neomenthylmagnesium pivalate ($\mathbf{1b}^{iii}$)

Experiment at 70 °C		
Time (min)	Men (%)	Nmn (%)
0	57,9	42,1
15	52,8	47,2
30	48,9	51,1
45	46,9	53,1
60	46,1	53,9
90	44,9	55,1
69 h	42,9	57,1

See Figure S25 and Table S19 for analysis of the data (entries: 70 °C (piv)).

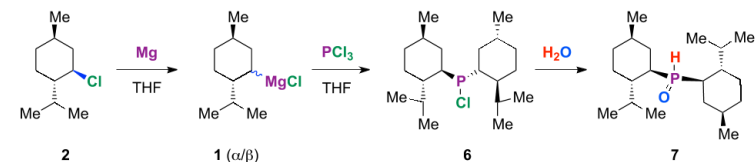
8.2.1 Ball and Stick depictions for all conformers in the X-ray structure of WS-5 (22)

Figure S28. Crystallographically independent conformers in the unit cell of WS-5 (22).



- S40 -

9 Synthesis of Dimethylphosphine oxide (7)



9.1 Details of the dry column chromatography purification

The following exemplifies a dry column vacuum chromatography purification¹⁰: Crude product was absorbed on SiO₂ and vacuum filtered through SiO₂ in two separate runs. The eluent was *t*-BuOMe–hexanes 1:5 with incremental increases of HOAc.

Table S23. Dry column chromatography fractionation of crude 7

Batch 1				Batch 2			
Fraction	HOAc [%]	Volume [mL]	combined to	Fractions	HOAc [%]	Volume [mL]	combined to
1	0	150	-	1	0	450	-
2	0.50	100	-	2	0.25	100	-
3	0.75	100	-	3	0.5	100	-
4	1.00	100	-	4	0.75	100	-
5	1.25	100	-	5	1.00	100	-
6	1.50	100	-	6	1.25	100	Fraction 2-1
7	2.00	100	Fraction 1-1	7	1.50	100	-
8	2.50	100	Fraction 1-2	8	2.00	100	-
9	3.00	100	-	9	2.50	100	Fraction 2-2
10	3.00	100	-	10	3.00	100	-
11	3.00	100	Fraction 1-3	11	3.00	100	-
12	3.00	100	-	12	3.00	100	-
13	3.00	100	-				

¹⁰ For dry column vacuum chromatography, see: Pedersen, D. S.; Rosenbohm, C. Dry Column Vacuum Chromatography. *Synthesis* **2001**, 2431–2434.

- S41 -

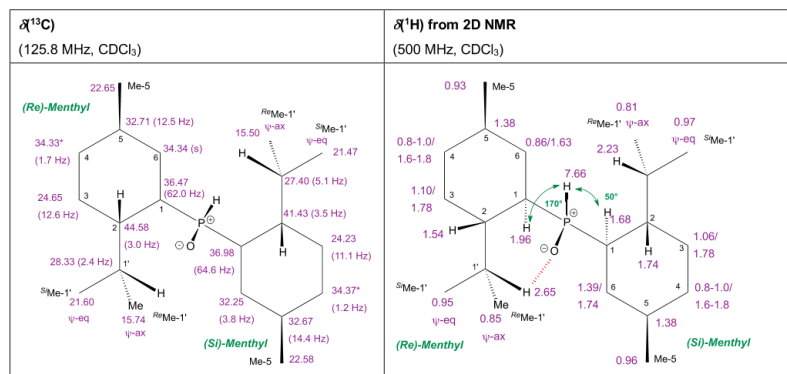
Table S24. Data for purified fractions of dimethylphosphine oxide 7.

Combined fractions	Purity (³¹ P-NMR area integration)	Yield
Fraction 1-1	90%	3.2 g
Fraction 1-2	97%	1.8 g
Fraction 1-3	97%	3.4 g
Fraction 2-1	84%	0.9 g
Fraction 2-2	93%	6.0 g
Total		15.3 g (50%)
Recrystallized sample	97%	

9.2 NMR data of dimethylphosphine oxide (7)

The assignment of the *Re*- and *Si*-menthyl groups is based on the H-C(1')-P-H coupling constant by comparing the calculated torsion angles (Karplus equation) with those observed in the X-ray structure.

Figure S29. Overview of $\delta^1\text{H}$ and $\delta^{13}\text{C}$ assignments for dimethylphosphine oxide (7)



* Interchangeable assignment.

Table S25. NMR assignments for dimethylphosphine oxide (7)

Pos. ^a	Type (2D)	$\delta^{13}\text{C}$ ^b (CDCl ₃)	mult. ^c	$J_{\text{P/C}}$	$J(\text{d})$ ^d	Idx ^e	$\delta^1\text{H}$ (HSQC)	$\delta^1\text{H}$ (500 MHz, CDCl ₃)
					Hz			
2- <i>Re</i>	CH	44.58	d	3.0	99.74	0.990	1.54	1.53 (m, 1 H)
2- <i>Si</i>	CH	41.43	d	3.5	100.41	0.997	1.74	1.61–1.82 (m, 8 H)
1- <i>Si</i>	CH	36.98	d	64.4	99.73	0.990	1.68	1.61–1.82 (m, 8 H)
1- <i>Re</i>	CH	36.47	d	62.0	99.38	0.986	1.96	1.96 (m, 1 H)
4- <i>S</i> [#]	CH ₂	34.37	d	1.2	98.9 [*]		0.8–1.0/ 1.6–1.8	0.8–1.2 (m, 5 H) 1.61–1.82 (m, 8 H)
6- <i>Re</i>	CH ₂	34.34	s		106 [*]	1.010 (avg.)	0.86/ 1.63	0.8–1.2 (m, 5 H) 1.61–1.82 (m, 8 H)
4- <i>Re</i> [#]	CH ₂	34.33	d	1.7	100.4 [*]		0.8–1.0/ 1.6–1.8	0.8–1.2 (m, 5 H) 1.61–1.82 (m, 8 H)
5- <i>Si</i>	CH	32.67	d	14.4	100.55	0.998	1.38	1.33–1.46 (m, 3 H)
5- <i>Re</i>	CH	32.71	d	12.5	102.2	1.014	1.38	1.33–1.46 (m, 3 H)
6- <i>Si</i>	CH ₂	32.25	d	3.8	102.09	1.013	1.39 1.74	0.33–1.46 (m, 3 H) 1.61–1.82 (m, 8 H)
1'- <i>Re</i>	CH	28.33	d	2.4	100.39	0.996	2.65	2.64 (sept × d, ³ J = 6.9, 2.8 Hz, 1 H),
1'- <i>Si</i>	CH	27.40	d	5.1	103.70	1.029	2.23	2.22 (sept × d, ³ J = 6.9, 2.5 Hz, 1 H)
3- <i>Re</i>	CH ₂	24.65	d	12.6	102.54	1.018	1.10/ 1.78	0.8–1.2 (m, 5 H) 1.61–1.82 (m, 8 H)
3- <i>Si</i>	CH ₂	24.23	d	11.1	101.89		1.06/ 1.78	0.8–1.2 (m, 5 H) 1.61–1.82 (m, 8 H)
Me-5- <i>Re</i>	CH ₃	22.65	s		103.06	1.023	0.93	0.93 (d, J = 6.6 Hz, 3 H)
Me-5- <i>Si</i>	CH ₃	22.58	s		104.46	1.037	0.96	0.95 (d, J = 6.1 Hz, 3 H)
^S Me-1'- <i>Re</i>	CH ₃	21.60	s		104.70	1.039	0.95	0.94 (d, J = 7.0 Hz, 3 H)
^S Me-1'- <i>Si</i>	CH ₃	21.47	s		102.22	1.014	0.97	0.97 (d, J = 6.8 Hz, 3 H)
^R Me-1'- <i>Re</i>	CH ₃	15.74	s		103.88	1.031	0.85	0.85 (d, J = 6.8 Hz, 3 H)
^R Me-1'- <i>Si</i>	CH ₃	15.50	s		103.69	1.029	0.81	0.81 (d, J = 6.9 Hz, 3 H)
	CH						1.000	
	CH ₂						1.012	
	CH ₃						1.029	

a) Positional numbering systematic; *Re* and *Si* suffix refers to assignment of the diastereotopic menthyl groups; ^{R/S}Me refers to the diastereotopic methyl groups attached to C-1'. b) ¹³C NMR at 125.8 MHz in CDCl₃, cryo-probe. c) Multiplicity of signal due to ³¹P-¹³C-splitting. d) Peak integral by deconvolutive peak fitting ("d"); arbitrary units. e) "CH-Index", peak integral relative to the average of all CH-signals. * Value inaccurate due to signal overlap. # Interchangeable assignment.

10 Crystallography

For compounds **13** and **27** the X-ray intensity data were collected on an X-ray single crystal diffractometer (Bruker D8 Venture Duo IMS) equipped with a CMOS detector (Bruker Photon-100), a Mo K α microsource with MoK α radiation ($\lambda = 0.71073 \text{ \AA}$) and a Helios optic monochromator by using the APEX 3 software package.¹¹ For compounds **7** and **22** the X-ray intensity data were collected on an X-ray single crystal diffractometer (Bruker D8) equipped with a CCD detector (APEX II, κ -CCD), a fine-focused sealed tube with MoK α radiation ($\lambda = 0.71073 \text{ \AA}$) and a graphite monochromator by using the APEX 2 software package.¹² The measurement was performed on single crystals coated with perfluorinated ether. The crystal was fixed on the top of a microsampler, transferred to the diffractometer and frozen under a stream of cold nitrogen. A matrix scan was used to determine the initial lattice parameters. Reflections were merged and corrected for Lorentz and polarization effects, scan speed, and background using SAINT.¹³ Absorption corrections, including odd and even ordered spherical harmonics were performed using SADABS.¹³ Space group assignments were based upon systematic absences, E statistics, and successful refinement of the structures. Structures were solved by direct methods with the aid of successive difference Fourier maps, and were refined against all data using the APEX 3 software¹¹ in conjunction with SHELXL-2014¹⁴ and SHELXLE.¹⁵ Methyl hydrogen atoms were refined as part of rigid rotating groups, with a C–H distance of 0.98 \AA and $U_{\text{iso(H)}} = 1.5 \cdot U_{\text{eq(C)}}$. Other H atoms were placed in calculated positions and refined using a riding model, with methylene and aromatic C–H distances of 0.99 and 0.95 \AA , respectively, and $U_{\text{iso(H)}} = 1.2 \cdot U_{\text{eq(C)}}$. For compound **7** the P-bound hydrogen atoms were located in the Fourier map and allowed to refine freely with an $U_{\text{iso(H)}} = 1.5 \cdot U_{\text{eq(P)}}$. For H3P a DFIX restraint was used. For compound **22** the N-bound hydrogen atoms were located in the Fourier maps and allowed to refine freely with N–H distances of 0.91 \AA and $U_{\text{iso(H)}} = 1.5 \cdot U_{\text{eq(N)}}$. If not mentioned otherwise, non-hydrogen atoms were refined with anisotropic displacement parameters. Full-matrix least-squares refinements were carried out by minimizing $\Delta w(F_o^2 - F_c^2)^2$ with SHELXL-97¹⁶ weighting scheme. Neutral atom scattering factors for all atoms and anomalous dispersion corrections for the non-hydrogen atoms were taken from the International Tables for Crystallography.¹⁷

¹¹ APEX suite of crystallographic software. APEX 3, version 2015.5-2, Bruker AXS Inc., Madison, Wisconsin, USA, 2015.

¹² APEX suite of crystallographic software. APEX 2, version 2008.4, Bruker AXS Inc., Madison, Wisconsin, USA, 2008.

¹³ SAINT, Version 7.56a and SADABS Version 2008/1, Bruker AXS Inc., Madison, Wisconsin, USA, 2008.

¹⁴ Sheldrick, G. M. SHELXL-2014, University of Göttingen, Göttingen, Germany, 2014.

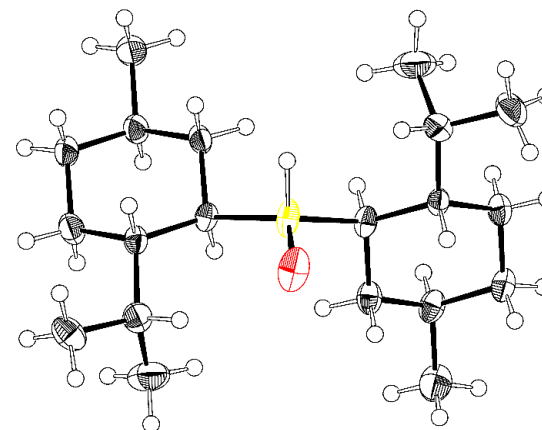
¹⁵ Huebschle, C. B.; Sheldrick, G. M.; Dittrich, B. ShelXle: A Qt Graphical User Interface for SHELXL. *J. Appl. Cryst.* **2011**, *44*, 1281–1284.

¹⁶ Sheldrick, G. M. SHELXL-97, University of Göttingen, Göttingen, Germany, 1998.

¹⁷ Wilson, A. J. C. *International Tables for Crystallography*, Vol. C, Tables 6.1.1.4 (pp. 500-502), 4.2.6.8 (pp. 219-222), and 4.2.4.2 (pp. 193-199); Kluwer Academic Publishers: Dordrecht, The Netherlands, 1992.

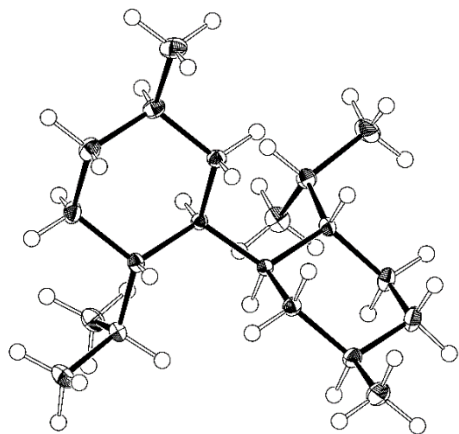
10.1 ORTEP Plots

Figure S30. Solid state molecular structure of dimethylphosphine P-oxide (**7**).



Oxygen is colored red, phosphorus purple. Ellipsoids are shown at 50 % probability. The unit cell contains three independent molecules of very similar geometry, of which one is displayed.

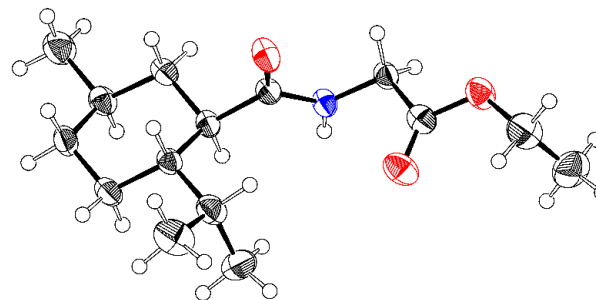
Figure S31. X-ray solid-state molecular structure of bimenthyl (13).



50 % probability level ellipsoids.

- S46 -

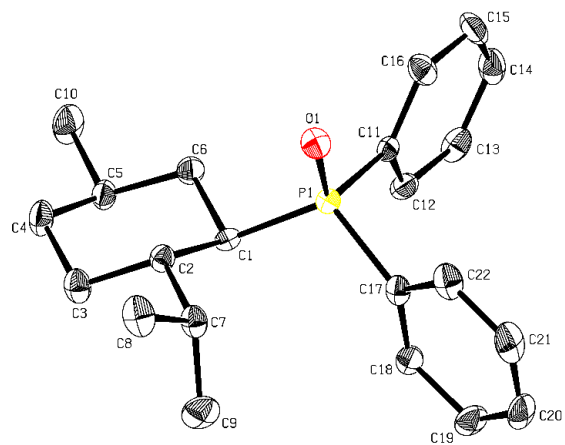
Fig. S32. Solid state molecular structure of WS-5 (22).



Ellipsoids are shown at 50 % probability level. Oxygen is red, nitrogen blue. Selected conformer, see Figure S28 for depictions of all conformers

- S47 -

Figure S33. Solid-state X-ray molecular structure of dimethylphenylphosphine P-oxide (27).



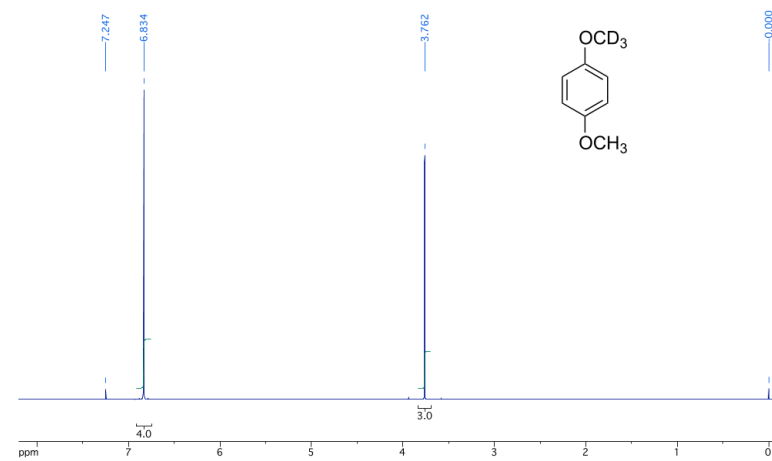
Ellipsoids are shown at 50 % probability level. Hydrogens are omitted for clarity. Oxygen is red, phosphorus purple.

- S48 -

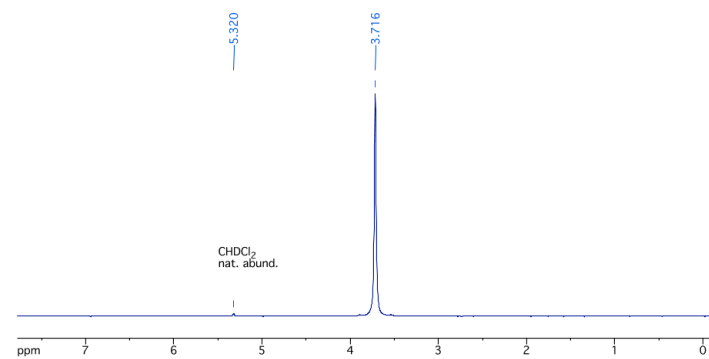
11 NMR spectra

11.1.1 1-Methoxy-4-(D₃-methoxy)-benzene (deuterated standard for ²H qNMR)

¹H NMR (400 MHz, CDCl₃)

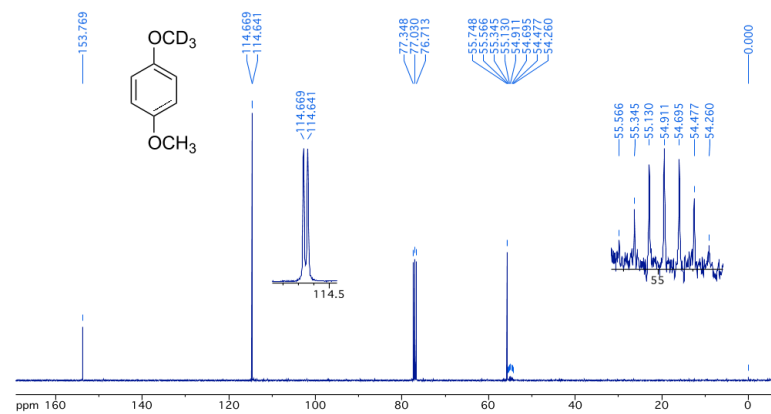


²H NMR (61.4 MHz, CH₂Cl₂)



- S49 -

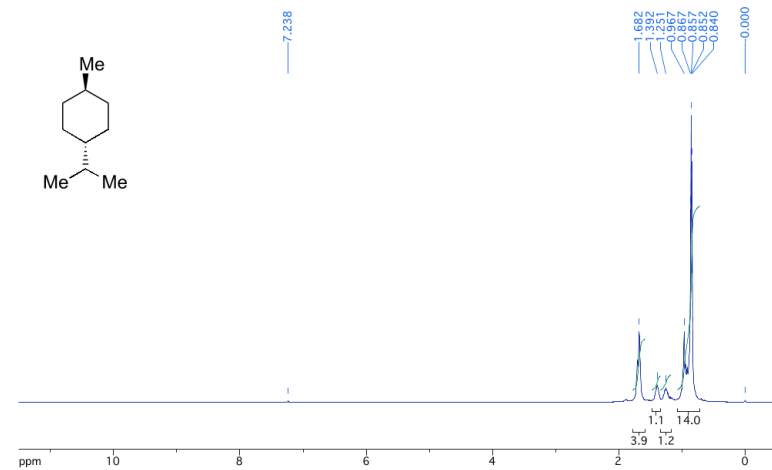
¹³C NMR (100.6 MHz, CDCl₃)



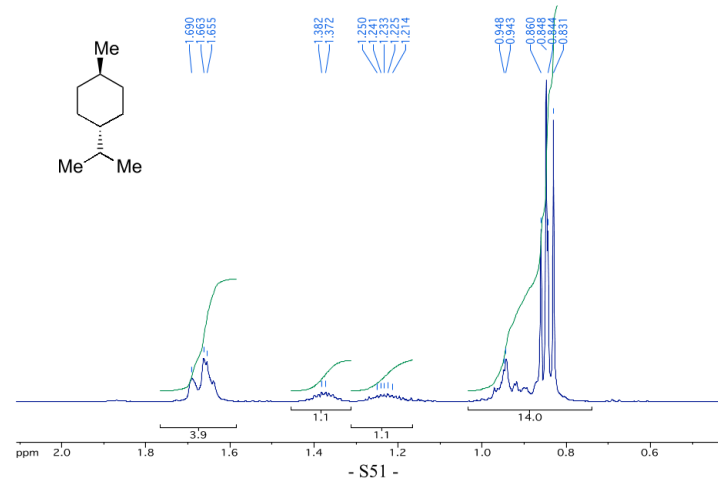
- S50 -

11.1.2 *trans-para*-Menthane (4)

¹H NMR (400 MHz, CDCl₃) - full range spectrum

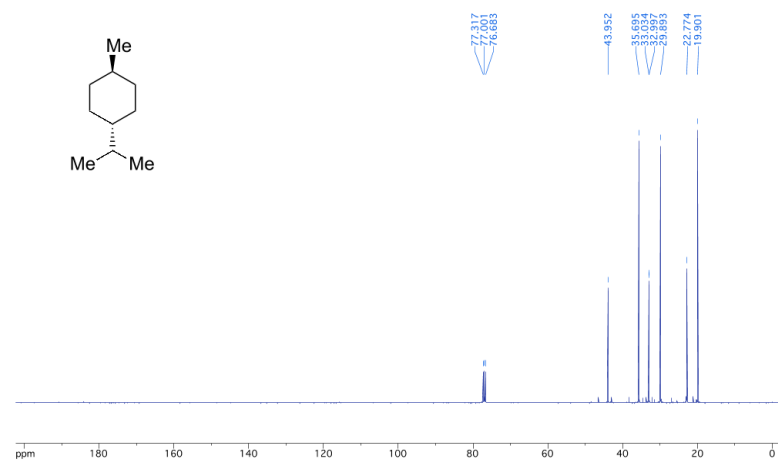


¹H NMR (400 MHz, CDCl₃) - expansion δ 0.5–2.1 ppm - different sample

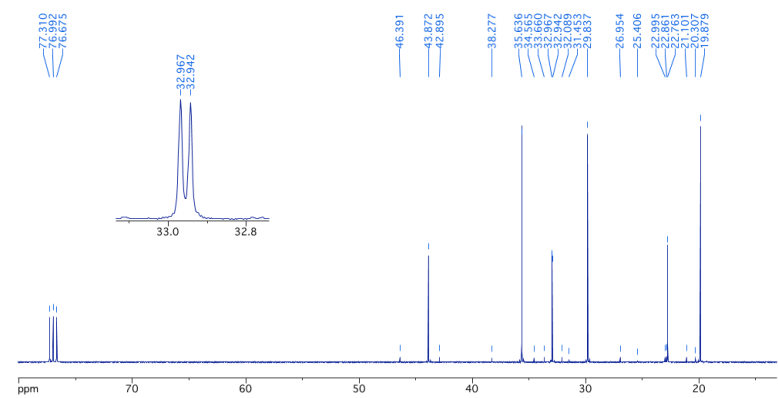


- S51 -

^{13}C NMR (101 MHz, CDCl_3), minor signals due to ψ -menthane (**16**) - full range



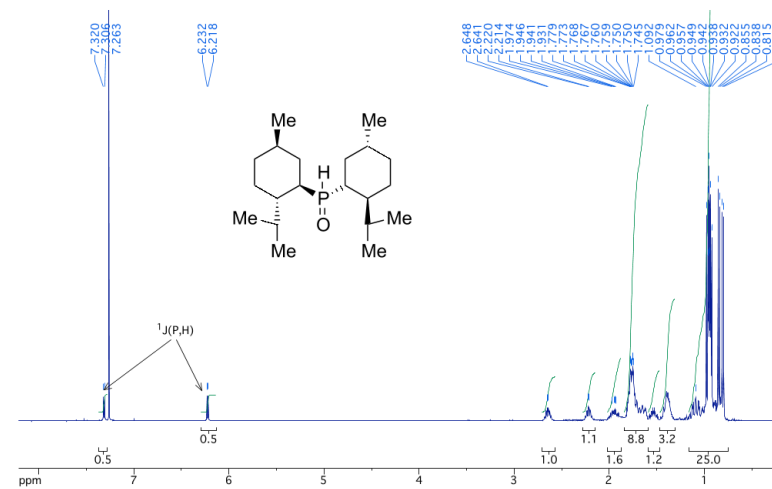
^{13}C NMR (101 MHz, CDCl_3), minor signals due to ψ -menthane (**16**) - expansion, different sample



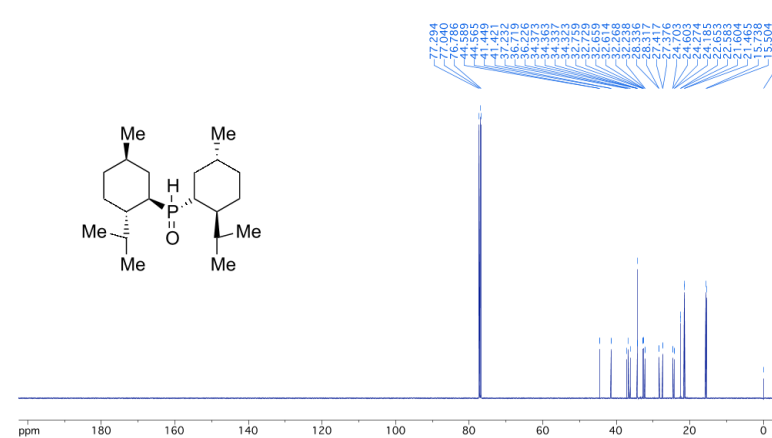
- S52 -

11.1.3 Dimethylphosphine *P*-oxide (**7**)

^1H NMR (400 MHz, CDCl_3) -

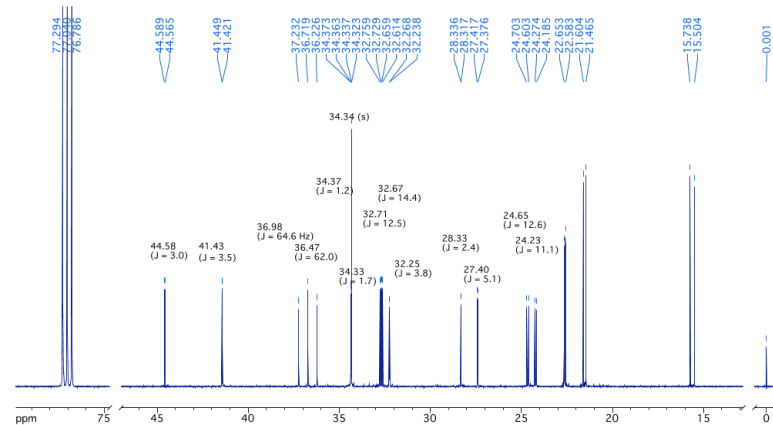


^{13}C NMR (125.8 MHz, CDCl_3) - full range

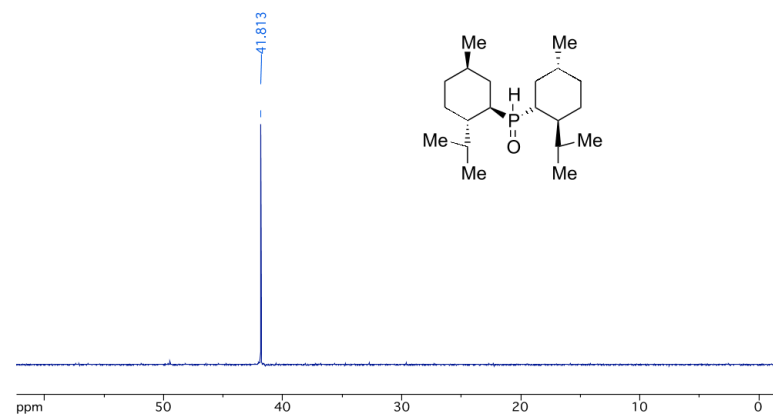


- S53 -

¹³C NMR (125.8 MHz, CDCl₃) - expansion



³¹P NMR (162 MHz, CDCl₃)

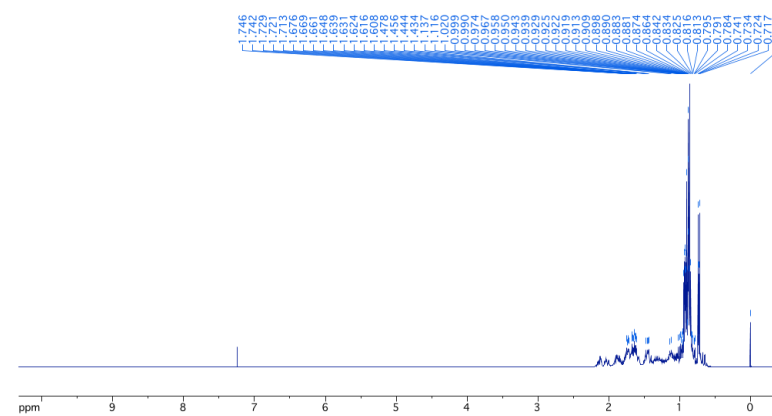


- S54 -

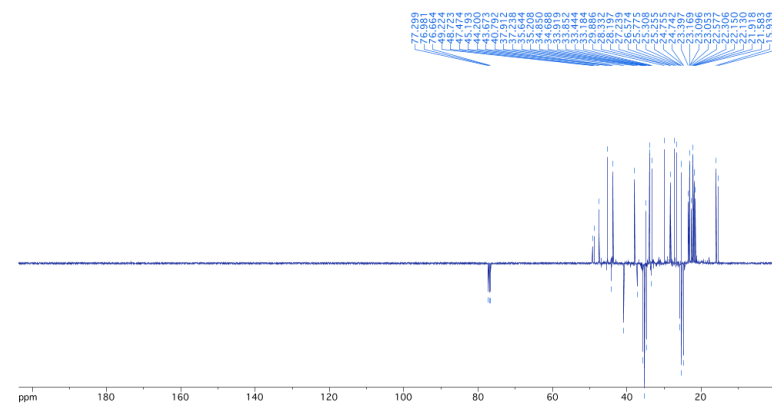
11.1.4 Bimenthyl isomer mixture (13–15) – full range spectra and ¹³C NMR expansions

Vacuum distilled mixture of bimenthyl hydrocarbons. Men₂ = 13; Men/Neo = 14; Neo₂ = 15

¹H NMR (400 MHz, CDCl₃) of bimenthyl isomer mixture, full range

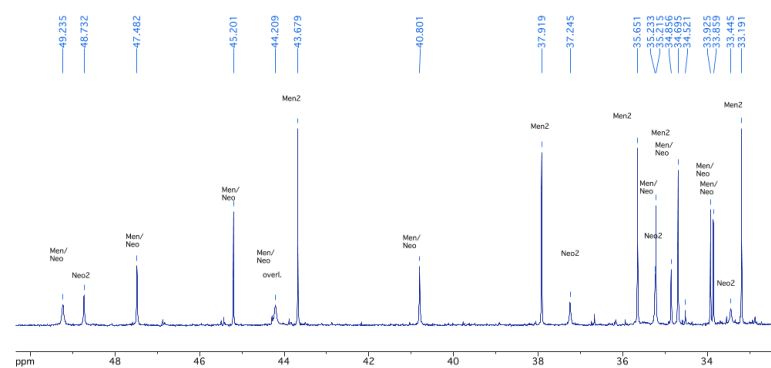


¹³C NMR APT (101 MHz, CDCl₃) of bimenthyl isomer mixture, full range

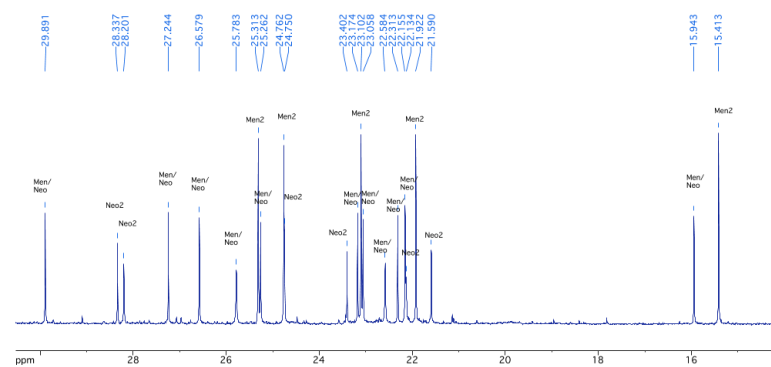


- S55 -

¹³C NMR (101 MHz, CDCl₃) of bimenthyl isomer mixture, 50–32 ppm range



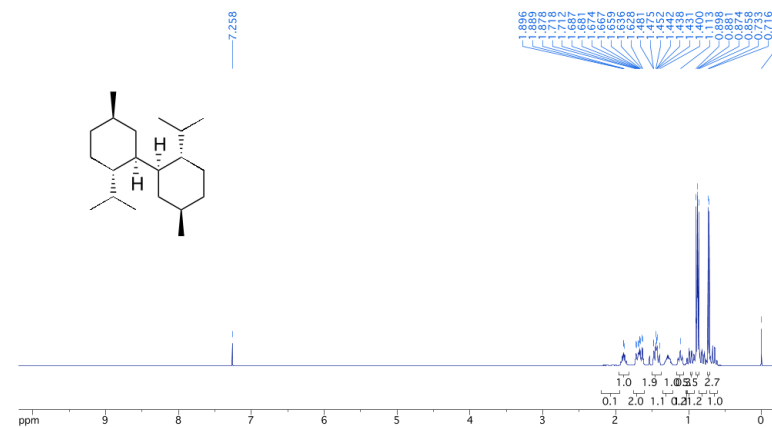
¹³C NMR (101 MHz, CDCl₃) of bimenthyl isomer mixture, 30–15 ppm range



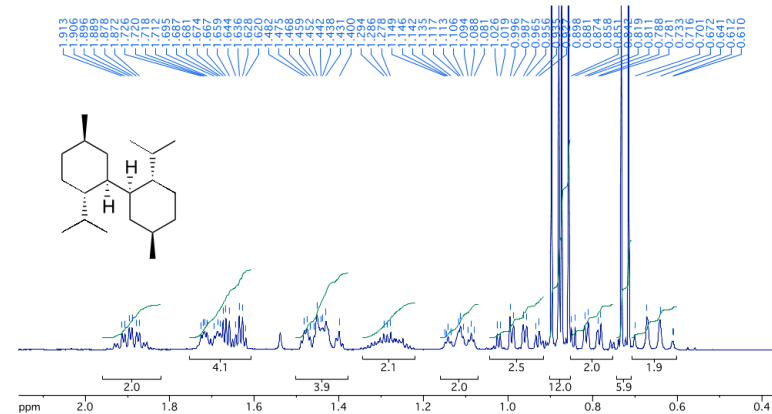
- S56 -

11.1.5 Bimenthyl (symmetric), crystalline (13)

¹H NMR (400 MHz, CDCl₃) - full range spectrum

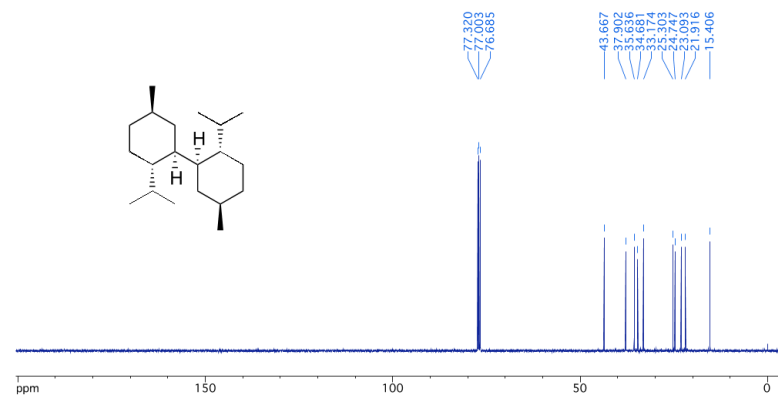


¹H NMR (400 MHz, CDCl₃) - expansion

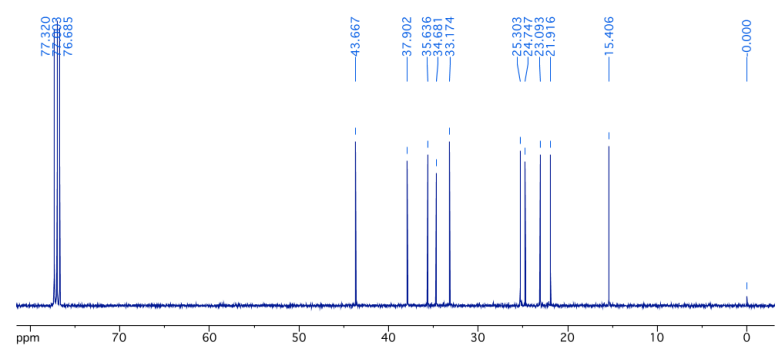


- S57 -

¹³C NMR (101 MHz, CDCl₃) - full range spectrum



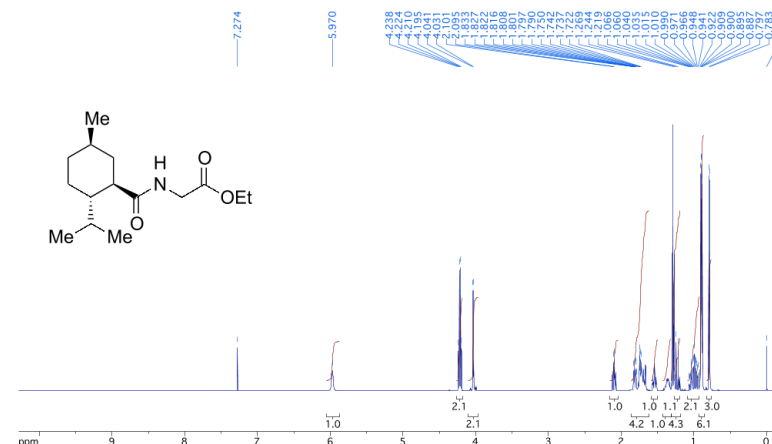
¹³C NMR (101 MHz, CDCl₃) - expansion



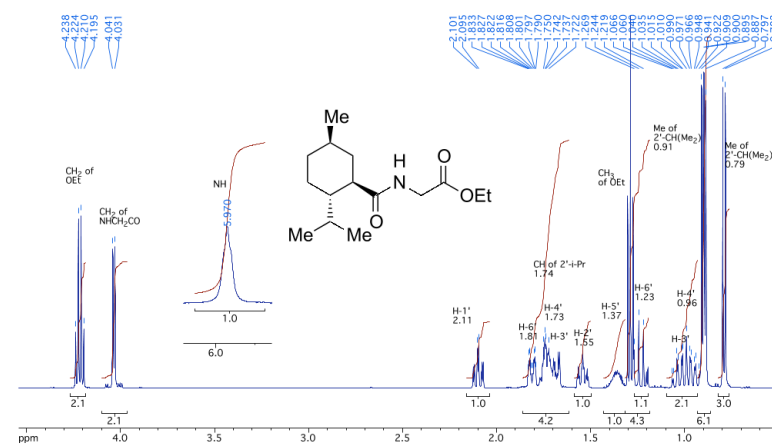
- S58 -

11.1.6 Ethyl 2-((1R,2S,5R)-2-isopropyl-5-methylcyclohexanecarboxamido)acetate (WS-5; 22)

¹H NMR (500 MHz, CDCl₃) - full range

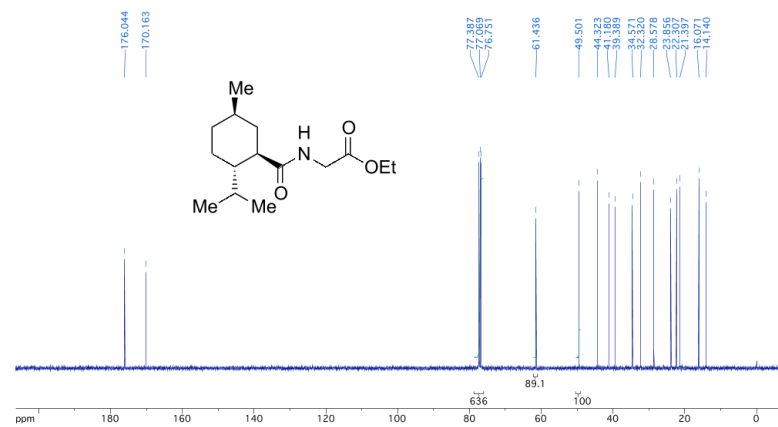


¹H NMR (500 MHz, CDCl₃) - expansion

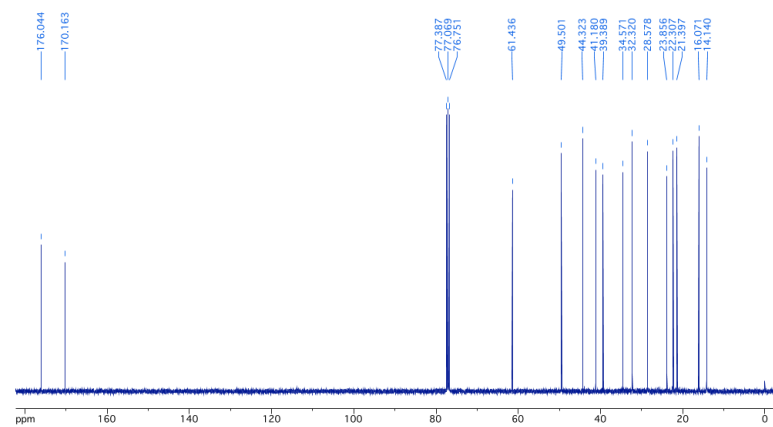


- S59 -

¹³C NMR (101 MHz, CDCl₃) - full range spectrum



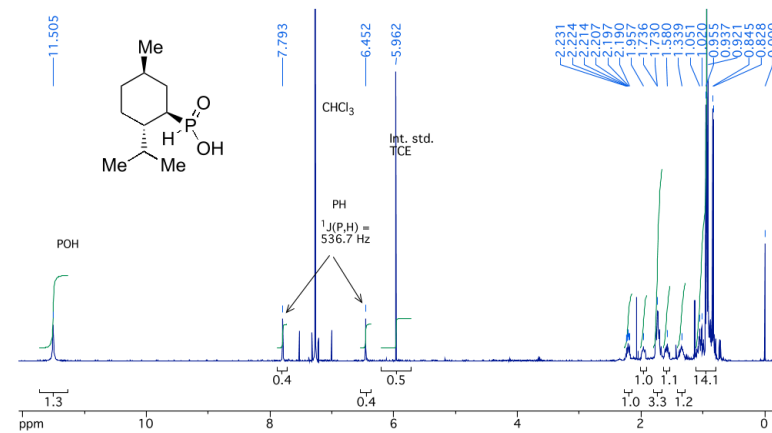
¹³C NMR (101 MHz, CDCl₃) - expansion



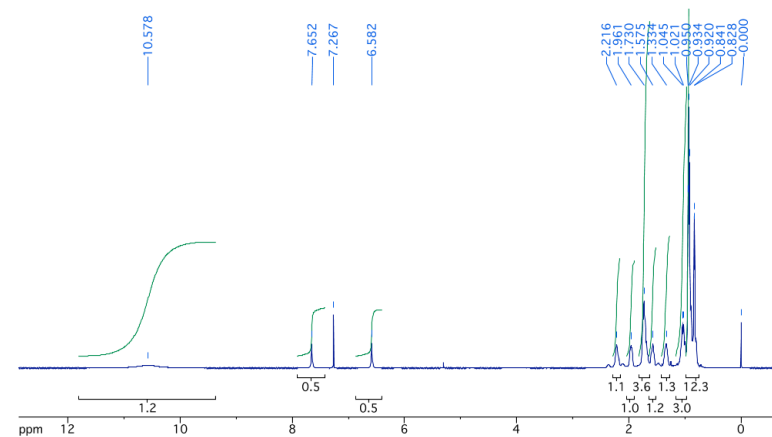
- S60 -

11.1.7 Menthylphosphinic acid (25)

¹H NMR (400 MHz, CDCl₃) - crude product w. internal standard

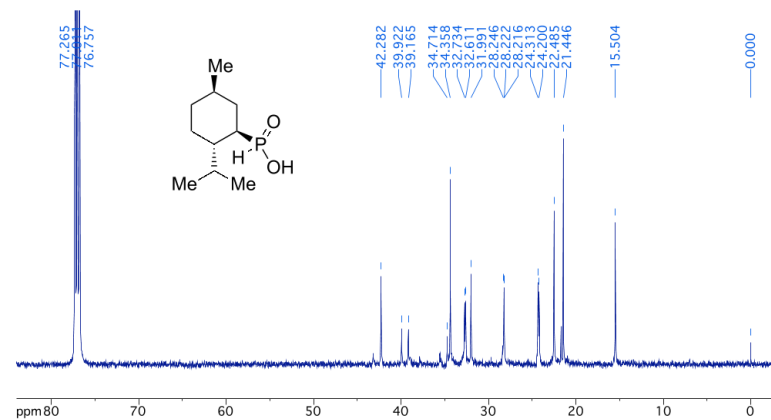


¹H NMR (500 MHz, CDCl₃) - product after SiO₂ chromatography

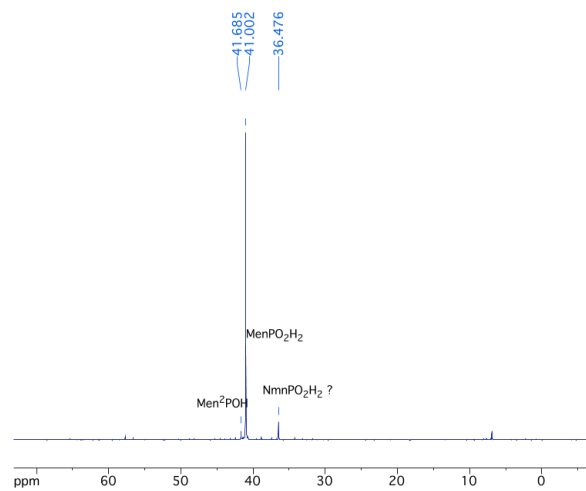


- S61 -

¹³C NMR (126 MHz, CDCl₃) - after SiO₂-chromatography



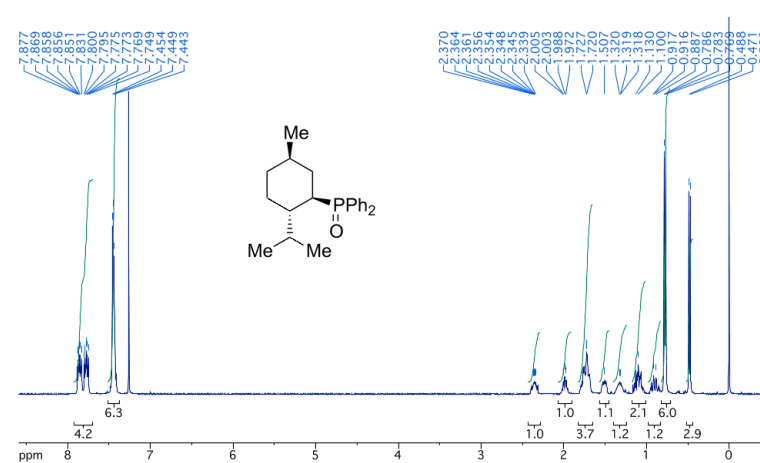
³¹P NMR (162 MHz, CDCl₃) - crude product w. internal standard



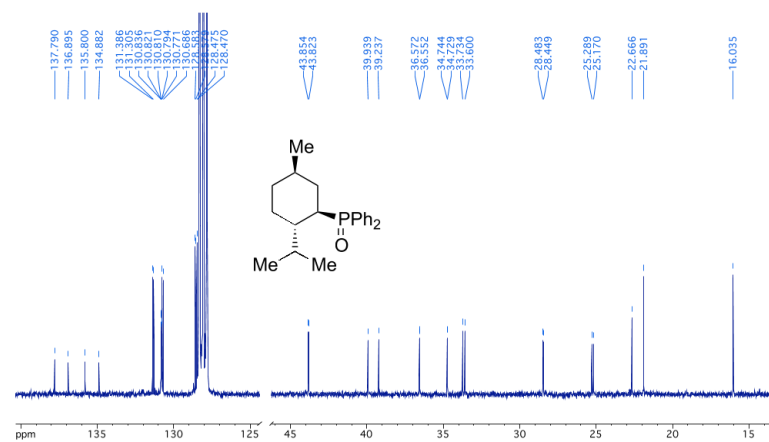
- S62 -

11.1.8 Menthylidiphenylphosphine P-oxide (27)

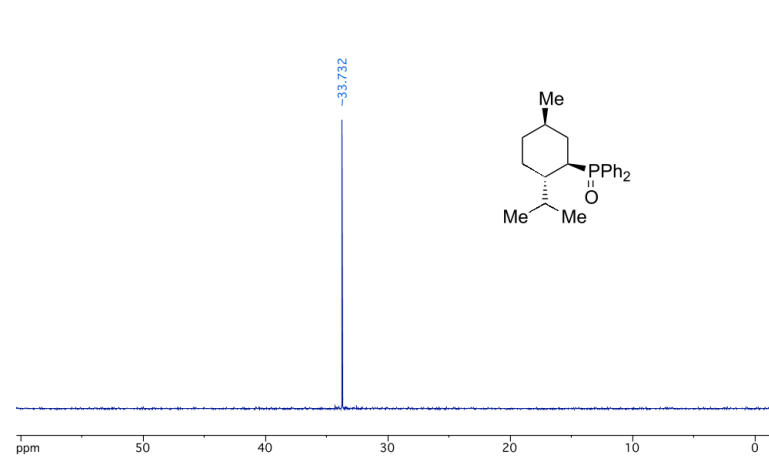
¹H NMR (400 MHz, CDCl₃)



¹³C NMR (100.6 MHz, C₆D₆) - expansion



³¹P NMR (162 MHz, CDCl₃)



Synthesis of Acceptor-Substituted Pyrroles by Ruthenium-Catalyzed Acceptorless Dehydrogenative Condensation with Amino Alcohols

Sebastian Koller, Lukas P. Ochmann, and Lukas Hintermann*

Technische Universität München, Department Chemie, Lichtenbergstr. 4, 85748 Garching bei München and TUM Catalysis Research Center, Ernst-Otto-Fischer-Str. 1, 85748 Garching bei München

KEYWORDS. dehydrogenation, homogenous catalysis, ruthenium, pyrrole

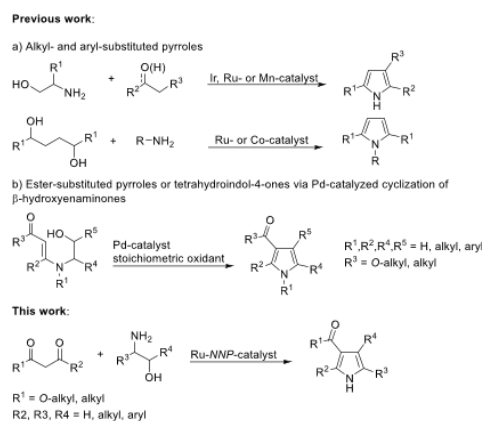
ABSTRACT: A new approach towards acceptor-substituted pyrroles is described. Starting from simple amino alcohols the acceptorless dehydrogenative condensation is conducted as a stepwise one-pot synthesis with a ruthenium *NNP*-pincer complex in the presence of weak base. Hydrogen and water are evolved as byproducts during this process.

In modern chemistry, the development of atom-economic and environmental benign synthetic methods has become more important. In this context, the principle of acceptorless dehydrogenation, more precisely liberation of hydrogen gas by catalytic oxidation of C–H, N–H or O–H bonds without the use of stoichiometric oxidants, serves as a valuable strategy.¹ The initial dehydrogenation can be followed by a condensation step with a suitable nucleophile (e.g. amines) giving water as non-toxic waste product. In some cases, the intermediately formed catalyst species $[M]H_2$ additionally transfers H_2 onto the condensation product (hydrogen autotransfer/borrowing hydrogen).² Our recently published paper on the catalytic C-alkylation of pyrroles with alcohols gives an example for the latter.³

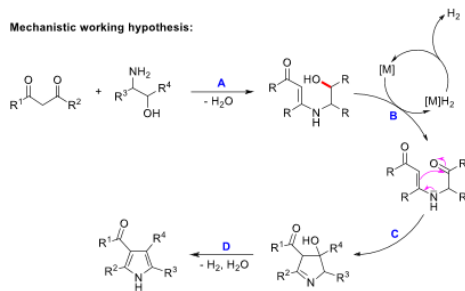
Multiple examples for the advantageous application of the dehydrogenative condensation strategy can be seen in the syntheses of *N*-heterocycles such as indoles,⁴ pyrimidines,⁵ pyrazines⁶ and pyrroles. The established Knorr pyrrole synthesis relies on the condensation of a ketone (favorably with electron-withdrawing substituents in α -position, e.g. β -keto esters or β -keto carbonyls) with unstable and not storable α -aminocarbonyl compounds, which therefore have to be prepared in situ (e.g. by reduction of nitrosocarbonyls).⁷ To circumvent this problem, Saito and coworkers used α -amino alcohols as starting material followed by in situ oxidation to α -aminocarbonyls and subsequent condensation with ketones to prepare alkyl- and aryl-substituted pyrroles.⁸ The reaction was carried out utilizing a ruthenium complex and alkali base under high temperature conditions (165 °C). Related transformations, namely reactions of α -amino alcohols with secondary alcohols⁹ or 1,4-diols with amines¹⁰ have already been realized with noble-metal based catalysts (iridium, ruthenium) as well as with systems based on cobalt or manganese (Scheme 1). However, syntheses of acceptor-substituted

pyrroles employing a dehydrogenative condensation strategy have been absent so far. A previous approach for the generation of ester-substituted pyrroles and 1,5,6,7-tetrahydroindol-4-ones followed a two-step route starting with condensation of 1,3-cyclohexadione and an α -amino alcohol.¹¹ The resulting β -hydroxyenaminone is cyclized via Pd-catalyzed oxidation with equimolar amounts of mesityl bromide as oxidant (Scheme 1). Having in mind the importance of the pyrrole scaffold in many pharmaceuticals and natural products,¹² we sought to enlarge the scope of catalytic dehydrogenative condensation onto acceptor-substituted pyrroles. We reasoned that enamine formation (**A**) from β -keto carbonyl compounds and α -amino alcohols followed by catalytic dehydrogenation (**B**), intramolecular cyclization (**C**) and a final dehydrogenation/dehydration step (**D**) would give the desired products (Scheme 1).

Scheme 1. Strategies for the dehydrogenative pyrrole synthesis.



Mechanistic working hypothesis:



At the outset, we investigated the dehydrogenative cyclization of β -hydroxyenaminone **1a** as a suitable model reaction for catalyst optimization (Table 1). Iridium or ruthenium based systems that have previously been shown to possess dehydrogenation activity all afforded the desired 1,5,6,7-tetrahydroindol-4-one **2a**. The best results at higher loadings (10 mol%) were obtained by a combination of $[\text{Ir}(\text{cod})\text{Cl}]_2$ and triazine-based *NNP*-pincer ligand **L1**¹³ or a Ru-*NNP* complex, that was introduced by Milstein (entries 7+9).¹⁴ Huang's Ir-NCP system¹⁵ and the carbene complex (Cym)Ru(IPr)Cl₂ were slightly worse (entries 4+5). At lower loadings the Ru-*NNP* system proved to be superior (entries 8+10). Reducing the amount of base to 0.5 equivalents drastically increased the yield. The milder K₃PO₄ was preferred compared to the equally active KOtBu (entries 11+12).

Table 1. Optimization of the dehydrogenative cyclization of β -hydroxyenaminone **1a.^a**

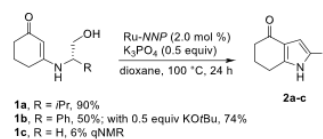
entry	catalyst (mol %)	base (equiv)	yield ^b (%)
1	$[\text{Ru}(\text{cym})\text{Cl}_2]_2$ (5.0) + DPE-Phos (10)	KOtBu (1.5)	42
2	RuHCl(CO)(PPh ₃) ₃ (10)	KOtBu (1.5)	42
3	$[\text{Cp}^*\text{IrCl}_2]_2$ (5.0)	KOtBu (1.5)	60
4	Ir-NCP (10)	KOtBu (1.5)	74
5	(Cym)Ru(IPr)Cl ₂ (10)	KOtBu (1.5)	78

6	$[\text{Ir}(\text{cod})\text{Cl}]_2$ (5.0) + PPh ₃ (15)	KOtBu (1.5)	44
7 ^c	$[\text{Ir}(\text{cod})\text{Cl}]_2$ (5.0) + L1 (10)	KOtBu (1.5)	89
8 ^c	$[\text{Ir}(\text{cod})\text{Cl}]_2$ (1.0) + L1 (2.0)	KOtBu (1.5)	43
9	Ru- <i>NNP</i> (10)	KOtBu (1.5)	86
10	Ru- <i>NNP</i> (2.0)	KOtBu (1.5)	66
11	Ru- <i>NNP</i> (2.0)	KOtBu (0.5)	92
12	Ru- <i>NNP</i> (2.0)	K ₃ PO ₄ (0.5)	96 (90)

^aAll reactions were performed with 500 μmol **1a** under argon atmosphere. ^bDetermined by quantitative ¹H-NMR against 1,1,2,2-tetrachloroethane as internal standard. Isolated yield in brackets. ^cPrecomplexation of $[\text{Ir}(\text{cod})\text{Cl}]_2$ and ligand **L1** in 0.3 mL dioxane at 50 °C for 60 min.

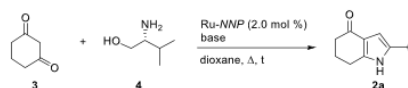
With the optimal conditions in hand, we changed the substituent R to phenyl (**1b**) finding that KOtBu is performing better in this case. Replacing it by hydrogen (**1c**) lead to nearly none of the desired product (**2a-c**) (Scheme 2).

Scheme 2. Variation of the substituent in the dehydrogenative synthesis of 1,5,6,7-tetrahydroindol-4-ones.



As the synthesis of β -hydroxyenaminones is a simple enamine formation¹¹ we next attempted to realize a one-pot protocol. 1,3-cyclohexadione (**3**) and L-valinol (**4**) were chosen as model substrates (Table 2). Mixing all reagents at the outset of the reaction led to a maximum yield of 33%, indicating that enamine formation might be suppressed under basic conditions. However, a slight excess of amino alcohol (1.2 equiv) is advisable (entries 1-4). If catalyst and base were added after 4 hours at 100 °C the yield could be improved to 82% (entry 5). Addition of molecular sieves to support the condensation step gave a negligible amount of product (entry 6), whereas later addition of catalyst and base slightly improved the yield to 88% (entries 7+8).

Table 2. Optimization of the dehydrogenative coupling of 1,3-cyclohexadione (3**) and L-valinol (**4**).^a**

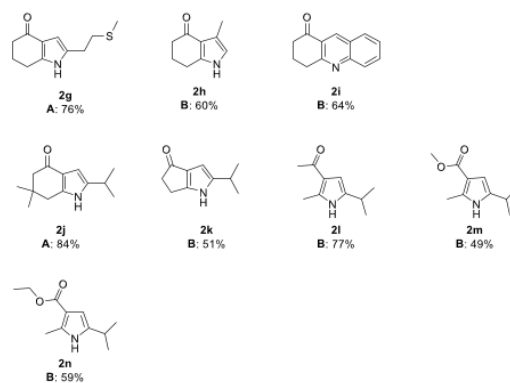
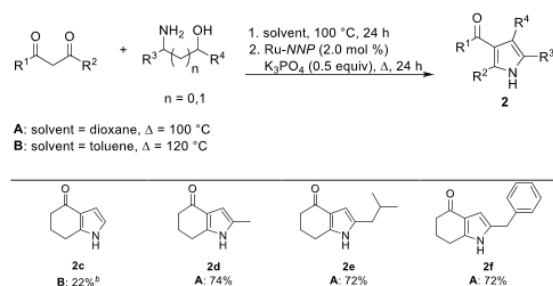


entry	4/3	base	T (°C)	t (h)	Yield ^b (%)
1	0.5	K ₃ PO ₄ (0.5)	100	24	0
2	1.2	K ₃ PO ₄ (0.5)	100	24	33
3	2.0	K ₃ PO ₄ (0.5)	100	24	16
4	1.2	KOtBu (0.1)	100	24	0
5	1.2	K ₃ PO ₄ (0.5)	100/100	4/24	82
6 ^c	1.2	K ₃ PO ₄ (0.5)	100/100	4/24	5
7	1.2	K ₃ PO ₄ (0.5)	rt/100	24/24	75
8	1.2	K ₃ PO ₄ (0.5)	100/100	24/24	88

^aAll reactions were performed with 500 μmol of the limiting compound under argon atmosphere. Catalyst and base were either directly added (entries 1-4) or after a certain time at the indicated temperature (entries 5-8). ^bDetermined by quantitative ¹H-NMR against 1,1,2,2-tetrachloroethane as internal standard. ^cWith 0.5 g molecular sieves (4 Å).

Next, the substrate scope of the synthetic protocol was investigated (Table 3; method A: 100 °C, dioxane; method B: 120 °C, toluene). The different amino alcohols were either commercially available or synthesized by simple lithium aluminium hydride reduction of the corresponding amino acids. With 1,3-cyclohexadione (**3**) as the carbonyl compound, most tetrahydroindol-4-ones were obtained in medium to good yields (≥ 60%, **2c-i**). The unsubstituted 2-aminoethanol gave only 22% product (**2c**), which is in agreement to the result of the β-hydroxyenaminone cyclization (Scheme 2). Interestingly even a thioether group was tolerated (**2g**). A γ-amino alcohol (2-aminobenzyl alcohol) afforded the respective pyridine (**2i**).¹⁶ *N*-substituted substrates like *N*-ethyl valinol did not react. Other β-keto carbonyls reacted smoothly with *L*-valinol (**2j-l**). Notably, β-keto esters were also tolerated as substrates giving the desired pyrroles in medium yields (**2m**, **2n**).

Table 3. Substrate scope of the dehydrogenative coupling of amino alcohols with β-keto carbonyl compounds.^a



^aAll reactions were performed with 500 μmol β-keto carbonyl and 600 μmol amino alcohol under argon atmosphere. Isolated yields are given. ^bDetermined by quantitative ¹H-NMR against 1,1,2,2-tetrachloroethane as internal standard after work-up.

In summary, we have developed a new reliable method for the synthesis of acceptor-substituted (carbonyl, ester) pyrroles with a special focus on tetrahydroindol-4-ones. The approach was based on a catalytic dehydrogenative condensation strategy which allows the use of easily available starting materials. Milstein's Ru-NNP complex in combination with K₃PO₄ turned out to be the most active catalyst system for the dehydrogenation of the intermediately formed β-hydroxyenaminones.

REFERENCES

- (1) For reviews: (a) Gunanathan, C.; Milstein, D. *Science* **2013**, *341*, 1229-1246. (b) R. H. Crabtree, *Chem. Rev.* **2017**, *117*, 9228-9246.
- (2) For reviews: (a) Huang, F.; Liu, Z.; Yu, Z. *Angew. Chem. Int. Ed.* **2015**, *55*, 862-875. (b) Obora, Y. *Top. Curr. Chem. (Z)* **2016**, *374*, 11. (c) Obora, Y. *ACS Catal.* **2014**, *4*, 3972-3981. (d) Corma, A.; Navas, J.; Sabater, M. J. *Chem. Rev.* **2018**, *118*, 1410-1459. (e) Nixon, T. D.; Whittlesey, M. K.; Williams, J. M. J. *Dalton Trans.* **2009**, 753-762. (f) Guillena, G.; Ramón, D. J.; Yus, M. *Angew. Chem. Int. Ed.* **2007**, *46*, 2358-2364. (g) Yamaguchi, R.; Fujita, K.; Zhu, M. *Heterocycles* **2010**, *81*, 1093-1140. (h) Obora, Y.; Ishii, Y. *Synlett* **2011**, 30-51. (i) Alonso, F.; Foubelo, F.; González-Gómez, J. C.; Martínez, R.; Ramón, D. J.; Riente, P.; Yus, M. *Mol. Divers.* **2010**, *14*, 411-424. (j) Bähn, S.; Imm, S.; Neubert, L.; Zhang, M.; Neumann, H.; Beller, M. *ChemCatChem* **2011**, *3*, 1853-1864. (k) Dobereiner, G. E.; Crabtree, R. H. *Chem. Rev.* **2010**, *110*, 681-703. (l) Guillena, G.; Ramón, D. J.; Yus, M. *Chem. Rev.* **2010**, *110*, 1611-1641. (m) Leonard, J.; Blacker, A. J.; Marsden, S. P.; Jones, M. F.; Mulholland, K. R.; Newton, R. *Org. Process Res. Dev.* **2015**, *19*, 1400-1410. (n) Ma, X.; Su, S.; Xu, Q. *Top. Curr. Chem. (Z)* **2016**, *374*, 27.
- (3) Koller, S.; Blazejak, M.; Hintermann, L. *Eur. J. Org. Chem.* **2018**, 1624-1633.
- (4) For a review: (a) Chelucci, G. *Coord. Chem. Rev.* **2017**, *331*, 37-53. For selected examples: (b) Tsuii, Y.; Huh, K.-T.; Watanabe, Y. *Tetrahedron Lett.* **1986**, *27*, 377-380. (c) Fujita, K.; Yamamoto, K.; Yamaguchi, R. *Org. Lett.* **2002**, *4*, 2691-2694. (d) Tursky, M.; Lorentz-Petersen, L. L. R.; Olsen, L. B.; Madsen, R.; *Org. Biomol. Chem.* **2010**, *8*, 5576-5582.

- (5) (a) Deibl, N.; Ament, K.; Kempe, R. *J. Am. Chem. Soc.* **2015**, *137*, 12804-12807. (b) Deibl, N.; Kempe, R. *Angew. Chem. Int. Ed.* **2017**, *56*, 1663-1666.
- (6) Gnanaprakasam, B.; Balaraman, E.; Ben-David, Y.; Milstein, D. *Angew. Chem. Int. Ed.* **2011**, *50*, 12240-12244.
- (7) (a) Knorr, L. *Ber. Dtsch. Chem. Ges.* **1884**, *17*, 1635-1642. (b) Knorr, L. *Liebigs Ann. Chem.* **1886**, *236*, 290-332. (c) Knorr, L.; Lange, H. *Ber. Dtsch. Chem. Ges.* **1902**, *35*, 2998-3008.
- (8) Iida, K.; Miura, T.; Ando, J.; Saito, S. *Org. Lett.* **2013**, *15*, 1436-1439.
- (9) (a) Michlik, S.; Kempe, R. *Nat. Chem.* **2013**, *5*, 140-144. (b) Srimani, D.; Ben-David, Y.; Milstein, D. *Angew. Chem. Int. Ed.* **2013**, *52*, 4012-4015. (c) Forberg, D.; Obenauf, J.; Friedrich, M.; Hühne, S.-M.; Mader, W.; Motz, G.; Kempe, R. *Catal. Sci. Technol.* **2014**, *4*, 4188-4192. (d) Kallmeier, F.; Dudziec, B.; Irrgang, T.; Kempe, R. *Angew. Chem. Int. Ed.* **2017**, *56*, 7261-7265.
- (10) (a) Schley, N. D.; Dobereiner, G. E.; Crabtree, R. H. *Organometallics* **2011**, *30*, 4174-4179. (b) Daw, P.; Chakraborty, S.; Garg, J. A.; Ben-David, Y.; Milstein, D. *Angew. Chem. Int. Ed.* **2016**, *55*, 14373-14377.
- (11) (a) Pita, B.; Masaguer, C. F.; Raviña, E. *Tetrahedron Lett.* **2002**, *43*, 7929-7932. (b) Aoyagi, Y.; Mizusaki, T.; Shishikura, M.; Komine, T.; Yoshinaga, T.; Inaba, H.; Ohta, A.; Takeya, K. *Tetrahedron* **2006**, *62*, 8533-8538.
- (12) For a review: Bhardwaj, V.; Gumber, D.; Abbot, V.; Dhiman, S.; Sharma, P. *RSC Adv.* **2015**, *5*, 15233-15266.
- (13) Deibl, N.; Kempe, R. *J. Am. Chem. Soc.* **2016**, *138*, 10786-10789.
- (14) Balaraman, E.; Gnanaprakasam, B.; Shimon, L. J. W.; Milstein, D. *J. Am. Chem. Soc.* **2010**, *132*, 16756-16758.
- (15) Jia, X.; Zhang, L.; Qin, C.; Leng, X.; Huang, Z. *Chem. Commun.* **2014**, *50*, 11056-11059.
- (16) Cini, E.; Petricci, E.; Truglio, G. I.; Vecchio, M.; Taddei, M. *RSC Adv.* **2016**, *6*, 31386-31390.

Supporting Information

Synthesis of Acceptor-Substituted Pyrroles by Ruthenium-Catalyzed Acceptorless Dehydrogenative Condensation with Amino Alcohols

Technische Universität München, Department Chemie, Lichtenbergstr. 4, 85748 Garching bei München and TUM Catalysis Research Center, Ernst-Otto-Fischer-Str. 1, 85748 Garching bei München

* E-mail: lukas.hintermann@tum.de

Table of contents

1	General information.....	2
2	Synthesis of β -hydroxyenaminones.....	3
3	Dehydrogenative cyclization of β -hydroxyenaminones	4
3.1	General screening procedure.....	4
3.2	Representative procedure for isolated products	6
3.3	Product characterization.....	7
4	Dehydrogenative one-pot coupling reactions.....	8
4.1	General screening procedure.....	8
4.2	Representative procedure for isolated products	9
4.3	Product characterization.....	9
5	NMR spectra	15
6	References	31

S1

1 General information

Chemicals: Unless otherwise specified, all reagents and solvents were obtained from commercial suppliers and used without further purification. Ligands **L1**^[1], Ir-*NCP* complex^[2], Ru-*NMP* complex^[3], RuHCl(CO)(PPh₃)₃^[4], (Cym)Ru(IPr)Cl₂^[5] and 3-((2-hydroxyethyl)amino)cyclohex-2-enone^[6] (**1e**) were prepared according to literature.

Solvents for water-free reactions were dried by passing through a column of Al₂O₃ and then kept over 3 Å molecular sieves under an argon atmosphere.^[7] The residual water content in dried solvents was analyzed by coulometric Karl Fischer titration.

Chromatography: Column chromatography (CC) was performed on silica gel 60 (35–70 μ m particle size), usually as a flash chromatography with 0.2 bar positive air pressure. Thin layer chromatography was performed on glass plates coated with silica gel 60 F₂₅₄ and visualized with UV light (254 nm), molybdenum stain (Mostain)¹ or anisaldehyde stain².

Analytical data: NMR spectra were recorded at 300, 400, or 500 MHz (¹H) at ambient temperature (19–25 °C). Chemical shift δ is given in ppm. ¹H NMR spectra were internally referenced to tetramethylsilane (TMS, δ_{H} 0.00) or residual solvent peaks; in CDCl₃: δ_{H} 7.26; in (D₆)-DMSO: δ_{H} 2.50. ¹³C NMR spectra were referenced to solvent peaks; CDCl₃, δ_{C} 77.16; (D₆)-DMSO, δ_{C} 39.52.

Reaction component analysis by qNMR: Yield determinations by qNMR were carried out by means of suitable internal standards and appropriate pulse sequences, typically using a pulse repetition delay d1 of ≥ 20 sec, see ref.^[8]

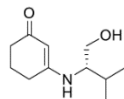
¹ Prepared from (NH₄)₆[Mo₇O₂₄]·4 H₂O (10 g), Ce(SO₄)₂·4 H₂O (0.2 g), H₂O (200 mL) and conc. H₂SO₄ (12 mL; added last with stirring).

² Prepared from acetic acid (100 mL), conc. H₂SO₄ (2 mL) and anisaldehyde (1 mL).

S2

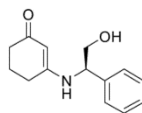
2 Synthesis of β -hydroxyenaminones

(*S*)-3-((1-hydroxy-3-methylbutan-2-yl)amino)cyclohex-2-en-1-one (**1a**)



L-valinol (3.09 g, 30.0 mmol, 1.0 eq.) was dissolved in dry THF (30 mL) and crushed molecular sieves (4 Å, 15 g) were added. A solution of 1,3-cyclohexadione (**3**) (2.80 g, 25.0 mmol, 1.2 eq.) in dry THF (15 mL) was added and the suspension was stirred for 50 h at room temperature. The reaction mixture was filtered through a pad of celite and evaporated. The crude product was purified by column chromatography (dichloromethane/methanol = 10:1) to give 4.15 g **1a** (84%) as a yellow solid. R_f 0.69 (dichloromethane/methanol = 5:1). ^1H NMR (400 MHz, CDCl_3): δ = 5.37 (bs, 1H, NH), 5.16 (s, 1H, *CHCO*), 3.96 (bs, 1H, OH), 3.73 (dd, J = 11.5, 3.8 Hz, 1H, CH_2OH), 3.67 (dd, J = 11.5, 5.1 Hz, 1H, CH_2OH), 3.28-3.20 (m, 1H, *CHNH*), 2.39 (t, J = 6.2 Hz, 2H, CH_2), 2.31-2.26 (m, 2H, CH_2), 2.03-1.90 (m, 2H, CH_2), 0.96 (d, J = 6.8 Hz, 3H, CH_3), 0.95 (d, J = 6.8 Hz, 3H, CH_3) ppm. ^{13}C NMR (101 MHz, CDCl_3): δ = 197.7, 165.9, 96.7, 61.4, 59.8, 36.4, 30.4, 29.3, 22.0, 19.3, 19.2 ppm. HRMS (EI): calcd for $\text{C}_{11}\text{H}_{19}\text{NO}_2^+$: 197.1410, found 197.1407.

(*R*)-3-((2-hydroxy-1-phenylethyl)amino)cyclohex-2-en-1-one (**1b**)



(*R*)-2-Phenylglycinol (2.47 g, 18.0 mmol, 1.2 eq.) was dissolved in dry THF (40 mL) and crushed molecular sieves (4 Å, 10.5 g) were added. A solution of 1,3-cyclohexadione (1.68 g, 15.0 mmol, 1.0 eq.) in dry THF (20 mL) was added and the suspension was stirred for 22 h at room temperature. The reaction mixture was filtered through a pad of

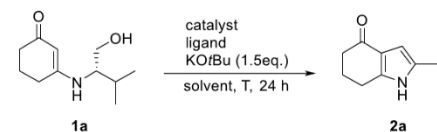
celite and evaporated. The crude product was purified by column chromatography (ethyl acetate) to give 3.23 g **1b** (93%) as a yellow crystalline solid. ^1H NMR (400 MHz, CDCl_3): δ = 7.38-7.20 (m, 5H, Ar-H), 5.57 (bs, 1H, NH), 4.95 (s, 1H, *COCH*), 4.52-4.45 (m, 1H, *CHNH*), 3.92 (dd, J = 11.6, 3.9 Hz, 1H, CH_2OH), 3.76 (dd, J = 11.6, 5.9 Hz, 1H, CH_2OH), 2.42 (t, J = 6.2 Hz, 2H, CH_2), 2.29-2.23 (m, 2H, CH_2), 1.96 (pent, J = 6.4 Hz, 2H, CH_2 , overlaps with broad OH-signal) ppm. ^{13}C NMR (75 MHz, CDCl_3): δ = 198.0, 166.0, 138.5, 128.8, 127.8, 126.5, 98.2, 66.0, 59.8, 36.1, 29.4, 21.9 ppm. Known compound, CAS 467214-80-8.

3 Dehydrogenative cyclization of β -hydroxyenaminones

3.1 General screening procedure

A 10 mL Schlenk tube was charged with metal complex, ligand, base, β -hydroxyenaminone **1a** and dry solvent under argon atmosphere. The mixture was heated at the indicated temperature for 24 h. After cooling to room temperature, a saturated solution of aq. NH_4Cl and ethyl acetate were added. The phases were separated, the organic layer was washed with water and brine and dried over Na_2SO_4 or MgSO_4 . The solvent was evaporated and 1,1,2,2-tetrachloroethane was added as internal standard for qNMR.

Table S-1. Catalyst screening.^[a]

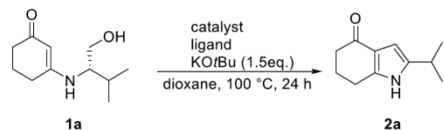


catalyst (mol%)	ligand (mol%)	solvent (mL)	temperature [°C]	yield ^[b] [%]
Pd/C (10 wt%)	-	toluene (1)	110	4
[Ir(cod)Cl] ₂ (5)	-	THF (1)	60	5

[Ir(cod)Cl] ₂ (5)	-	toluene (1)	110	15
[Ru(cym)Cl] ₂ (5)	DPE-Phos (10)	toluene (1)	110	38
[Ru(cym)Cl] ₂ (5)	DPE-Phos (10)	dioxane (2)	100	42
[Cp*IrCl] ₂ (5)	-	dioxane (2)	100	60
RuHCl(CO)(PPh ₃) ₃ (10)	-	dioxane (2)	100	42
(Cym)Ru(IPr)Cl ₂ (10)	-	dioxane (2)	100	78
CoCl ₂ (10) ^[c]	L1 (10)	dioxane (2)	100	7
Ir- <i>NCP</i> (10)	-	dioxane (2)	100	74
Ru- <i>NNP</i> (10)	-	dioxane (2)	100	86
[Ir(cod)Cl] ₂ (5)	PPh ₃ (15)	dioxane (2)	100	44
[Ir(cod)Cl] ₂ (5) ^[c]	L1 (10)	dioxane (2)	100	89
[IrOMe(cod)] ₂ (5) ^[c]	L1 (10)	dioxane (2)	100	87

[a] Reactions were performed with 500 μmol **1a**. [b] Determined by qNMR against internal standard. [c] Precomplexation of metal precursor and ligand **L1** in 0.5 mL dry dioxane for 1 h at 50 °C.

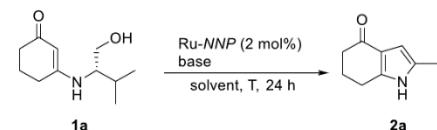
Table S-2. Loading optimization.



scale [mmol]	catalyst (mol%)	ligand (mol%)	solvent (mL)	Yield ^[a] [%]
500	Ru- <i>NNP</i> (4)	-	dioxane (2)	66
500	Ru- <i>NNP</i> (2)	-	dioxane (2)	66
1000	Ru- <i>NNP</i> (1)	-	dioxane (3)	45
500	[Ir(cod)Cl] ₂ (2) ^[b]	L1 (4)	dioxane (2)	70
500	[Ir(cod)Cl] ₂ (1) ^[b]	L1 (2)	dioxane (2)	43
1000	[Ir(cod)Cl] ₂ (0.5) ^[b]	L1 (1)	dioxane (3)	43
1000	[IrOMe(cod)] ₂ (0.5) ^[b]	L1 (1)	dioxane (3)	10

[a] Determined by qNMR against internal standard. [b] Precomplexation of metal precursor and ligand **L1** in 0.3 mL dry dioxane for 1 h at 50 °C.

Table S-3. Base/Solvent screening.^[a]



base (eq.)	solvent	temperature [°C]	yield [%]
KOtBu (2)	toluene	110	48
KOtBu (2)	dioxane	100	52
KOtBu (1)	dioxane	100	82
KOtBu (0.5)	dioxane	100	92
KOtBu (0.2)	dioxane	100	69
NaOtBu (1.5)	dioxane	100	48
K ₃ PO ₄ (1.5)	dioxane	100	97
K ₃ PO ₄ (1)	dioxane	100	96
K ₃ PO ₄ (0.5)	dioxane	100	96 (90)
K ₃ PO ₄ (0.2)	dioxane	100	33
K ₃ PO ₄ (0.5)	toluene	110	92
K ₃ PO ₄ (0.5)	THF	65	73

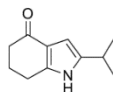
[a] Reactions were performed with 500 μmol **1a** and 2 mL solvent. [b] Determined by qNMR against internal standard. Isolated yield in parenthesis.

3.2 Representative procedure for isolated products

A 10 mL Schlenk tube was charged with Ru-*NNP* complex (4.8 mg, 2.5 μmol, 2 mol%), base (250 μmol, 0.5 eq.), β-hydroxyenaminone (500 μmol, 1.0 eq.) and dry dioxane (2 mL). The mixture was heated at 100 °C for 24 h. After cooling to room temperature, a saturated solution of aq. NH₄Cl (5 mL) and ethyl acetate (20 mL) were added. The phases were separated, the organic layer was washed with water (5 mL) and brine (5 mL) and dried over NaSO₄. The solvent was evaporated and the crude product was purified by column chromatography.

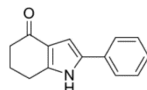
3.3 Product characterization

2-Isopropyl-1,5,6,7-tetrahydroindol-4-one (2a)



With (*S*)-3-((1-hydroxy-3-methylbutan-2-yl)amino)cyclohex-2-en-1-one (**1a**; 98.6 mg, 500 μ mol, 1.0 eq.) and K_3PO_4 (53.1 mg, 250 μ mol, 0.5 eq.). Purification by column chromatography (hexane/ethyl acetate = 1:1) gave 80.2 mg **2a** (90%) as colorless solid. R_f 0.34 (hexane/ethyl acetate = 1:2). 1H NMR (400 MHz, $CDCl_3$): δ = 8.87 (bs, 1H, NH), 6.21 (dd, J = 2.6, 1.0 Hz, 1H, Ar-H), 2.87 (heptd, J = 6.8, 1.0 Hz, 1H, $CH(CH_3)_2$), 2.79 (t, J = 6.2 Hz, 2H, CH_2), 2.48-2.43 (m, 2H, CH_2), 2.17-2.10 (m, 2H, CH_2), 1.25 (d, J = 6.8 Hz, 6H, CH_3) ppm. ^{13}C NMR (101 MHz, $CDCl_3$): δ = 194.8, 143.4, 140.4, 120.3, 100.0, 37.9, 27.1, 24.2, 22.9, 22.5 ppm. Known compound, CAS not existing, Reaxys ID 32663460.

2-Phenyl-1,5,6,7-tetrahydroindol-4-one (2b)



With (*R*)-3-((2-hydroxy-1-phenylethyl)amino)cyclohex-2-en-1-one (**1b**; 116 mg, 500 μ mol, 1.0 eq.) and $KOtBu$ (28.1 mg, 250 μ mol, 0.5 eq.). Purification by column chromatography (hexane/ethyl acetate = 1:1) gave 78.5 mg **2b** (74%) as colorless solid. R_f 0.36 (hexane/ethyl acetate = 1:2). 1H NMR (400 MHz, D_6 -DMSO): δ = 11.76 (bs, 1H, NH), 7.68-7.64 (m, 2H, Ar-H), 7.40-7.34 (m, 2H, Ar-H), 7.24-7.18 (m, 1H, Ar-H), 6.71 (d, J = 2.4 Hz, 1H, Ar-H), 2.83 (t, J = 6.1 Hz, 2H, CH_2), 2.36-2.31 (m, 2H, CH_2), 2.05 (pent, J = 6.3 Hz, 2H, CH_2). ^{13}C NMR (101 MHz, D_6 -DMSO): δ = 192.7, 145.1, 132.1, 131.8, 128.8, 126.4, 123.8, 120.8, 101.6, 37.7, 23.6, 22.2 ppm. Known compound, CAS 14006-77-0.

S7

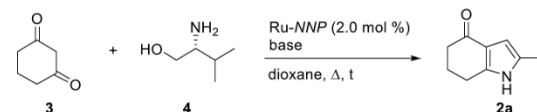
4 Dehydrogenative one-pot coupling reactions

4.1 General screening procedure

A 10 mL Schlenk tube was charged with 1,3-cyclohexadione (**3**), L-valinol (**4**), Ru-*NNP* complex (2 mol%), base and dry dioxane (2 mL) under argon atmosphere. The mixture was heated at 100 °C for 24 h. After cooling to room temperature, a saturated solution of aq. NH_4Cl and ethyl acetate were added. The phases were separated, the organic layer was washed with water and brine and dried over $NaSO_4$ or $MgSO_4$. The solvent was evaporated and 1,1,2,2-tetrachloroethane was added as internal standard for qNMR.

Note: If Ru-*NNP* complex and base were added after the condensation step, the mixture was cooled for about 5 min before addition (Table 2, entries 5-8; Table S-4, footnote [d]).

Table S-4. Screening table.



x (μ mol)	y (μ mol)	base (eq.)	temperature ^[a] [°C]	time ^[b] [h]	yield ^[c] [%]
1000	500	K_3PO_4 (0.5)	100	24	0
500	600	K_3PO_4 (0.5)	100	24	33
500	1000	K_3PO_4 (0.5)	100	24	16
500	600	$KOtBu$ (0.1)	100	24	0
500 ^[d]	600	K_3PO_4 (0.5)	100/100	4/24	82
500 ^[d,e]	600	K_3PO_4 (0.5)	100/100	4/24	5
500 ^[d]	600	K_3PO_4 (0.5)	rt/100	24/24	75
500 ^[d]	600	K_3PO_4 (0.5)	100/100	24/24	88

[a] Temperature of condensation step/temperature after addition of catalyst and base. [b] Reaction time of condensation step/reaction time after addition of catalyst and base. [c] Determined by qNMR against internal standard. [d] Catalyst and base were added after a certain time at the indicated temperature. [e] With addition of 0.5 g molecular sieves (4 Å) at the beginning.

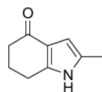
S8

4.2 Representative procedure for isolated products

A 10 mL Schlenk tube was charged with carbonyl compound (500 μmol , 1.0 eq.), amino alcohol (600 μmol , 1.2 eq.) and dry solvent (2 mL). The mixture was heated at 100 $^{\circ}\text{C}$ for 24 h. After cooling for about 5 min, Ru-*NNP* complex (4.8 mg, 2 mol%) and K_3PO_4 (53.1 mg, 250 μmol , 0.5 eq.) were added and it was heated for 24 h (100 $^{\circ}\text{C}$ for dioxane, 120 $^{\circ}\text{C}$ for toluene). It was cooled to room temperature, followed by addition of a saturated solution of aq. NH_4Cl (5 mL) and ethyl acetate (20 mL). The phases were separated, the organic layer was washed with water (5 mL) and brine (5 mL) and dried over NaSO_4 . The solvent was evaporated and the crude product was purified by column chromatography.

4.3 Product characterization

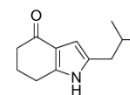
2-Methyl-1,5,6,7-tetrahydroindol-4-one (2d)



With 1,3-cyclohexadione (**3**; 56.1 mg, 500 μmol , 1.0 eq.) and DL-alaninol (48 μL , 600 μmol , 1.2 eq.) in dioxane. Purification by column chromatography (hexane/ethyl acetate = 1:2) gave 55.5 mg **2d** (74%) as colorless solid. R_f 0.30 (hexane/ethyl acetate = 1:4). ^1H NMR (400 MHz, D_6 -DMSO): δ = 11.06 (bs, 1H, NH), 5.91-5.88 (m, 1H, Ar-H), 2.68 (t, J = 6.2 Hz, 2H, CH_2), 2.26-2.22 (m, 2H, CH_2), 2.13 (d, J = 0.9 Hz, 3H, CH_3), 2.01-1.93 (m, 2H, CH_2). ^{13}C NMR (101 MHz, D_6 -DMSO): δ = 192.3, 142.9, 128.2, 119.6, 101.7, 37.6, 23.8, 22.1, 12.5 ppm. Known compound, CAS 35308-68-0.

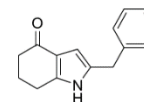
S9

2-Isobutyl-1,5,6,7-tetrahydroindol-4-one (2e)



With 1,3-cyclohexadione (**3**; 56.1 mg, 500 μmol , 1.0 eq.) and L-leucinol (77 μL , 600 μmol , 1.2 eq.) in dioxane. Purification by column chromatography (hexane/ethyl acetate = 1:2) gave 68.5 mg **2e** (72%) as colorless solid. R_f 0.47 (hexane/ethyl acetate = 1:4). ^1H NMR (400 MHz, CDCl_3): δ = 8.76 (bs, 1H, NH), 6.20-6.17 (m, 1H, Ar-H), 2.78 (t, J = 6.2 Hz, 2H, CH_2), 2.48-2.43 (m, 2H, CH_2), 2.41 (d, J = 7.9 Hz, 2H, CH_2CH), 2.13 (pent, J = 6.3 Hz, 2H, CH_2), 1.92-1.77 (m, 1H, $\text{CH}(\text{CH}_3)_2$), 0.92 (d, J = 6.6 Hz, 6H, CH_3). ^{13}C NMR (101 MHz, CDCl_3): δ = 194.8, 143.3, 133.1, 120.6, 102.9, 37.9, 37.0, 28.9, 24.2, 22.9, 22.5 ppm. HRMS (EI): calcd for $\text{C}_{12}\text{H}_{17}\text{NO}^+$: 191.1305, found 191.1305.

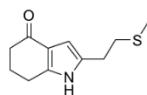
2-Benzyl-1,5,6,7-tetrahydroindol-4-one (2f)



With 1,3-cyclohexadione (**3**; 56.1 mg, 500 μmol , 1.0 eq.) and L-phenylalaninol (90.7 mg, 600 μmol , 1.2 eq.) in dioxane. Purification by column chromatography (hexane/ethyl acetate = 1:2) gave 81.5 mg **2f** (72%) as off-white solid. R_f 0.46 (hexane/ethyl acetate = 1:4). ^1H NMR (400 MHz, CDCl_3): δ = 8.53 (bs, 1H, NH), 7.32-7.26 (m, 2H, Ar-H), 7.25-7.18 (m, 3H, Ar-H), 6.27-6.24 (m, 1H, Ar-H), 3.90 (s, 2H, CH_2Ph), 2.71 (t, J = 6.2 Hz, 2H, CH_2), 2.44-2.38 (m, 2H, CH_2), 2.13-2.05 (m, 2H, Ar-H) ppm. ^{13}C NMR (101 MHz, CDCl_3): δ = 194.7, 144.0, 138.7, 132.2, 128.8, 128.8, 126.8, 120.7, 103.61, 37.8, 34.1, 24.1, 22.9 ppm. Known compound, CAS 127326-87-8.

S10

2-(2-(Methylthio)ethyl)-1,5,6,7-tetrahydroindol-4-one (2g)



With 1,3-cyclohexadione (**3**; 56.1 mg, 500 μmol , 1.0 eq.) and L-methioninol (81.1 mg, 600 μmol , 1.2 eq.) in dioxane. Purification by column chromatography (hexane/ethyl acetate = 1:2) gave 79.3 mg **2g** (76%) as colorless solid. R_f 0.37 (hexane/ethyl acetate = 1:4). ^1H NMR (400 MHz, CDCl_3): δ = 9.39 (bs, 1H, NH), 6.25-6.23 (m, 1H, Ar-H), 2.89-2.84 (m, 2H, CH_2), 2.80 (t, J = 6.2 Hz, 2H, CH_2), 2.78-2.73 (m, 2H, CH_2), 2.49-2.44 (m, 2H, CH_2), 2.18-2.10 (m, 2H, CH_2), 2.13 (s, 3H, SCH_3) ppm. ^{13}C NMR (101 MHz, CDCl_3): δ = 194.8, 143.9, 132.5, 120.4, 102.9, 37.9, 34.2, 27.2, 24.1, 23.0, 15.6 ppm. HRMS (EI): calcd for $\text{C}_{11}\text{H}_{15}\text{NOS}^+$: 209.0869, found 209.0851.

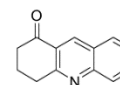
3-Methyl-1,5,6,7-tetrahydroindol-4-one (2h)



With 1,3-cyclohexadione (**3**; 56.1 mg, 500 μmol , 1.0 eq.) and amino-2-propanol (81.1 mg, 600 μmol , 1.2 eq.) in toluene. Purification by column chromatography (hexane/ethyl acetate = 1:1) gave 44.5 mg **2h** (60%) as colorless solid. R_f 0.43 (hexane/ethyl acetate = 1:2). ^1H NMR (400 MHz, $\text{D}_6\text{-DMSO}$): δ = 10.94 (bs, 1H, NH), 6.45-6.41 (m, 1H, Ar-H), 2.69 (t, J = 6.2 Hz, 2H, CH_2), 2.29-2.23 (m, 2H, CH_2), 2.13 (d, J = 1.2 Hz, 3H, CH_3), 1.97 (pent, J = 6.3 Hz, 2H, CH_2) ppm. ^{13}C NMR (101 MHz, $\text{D}_6\text{-DMSO}$): δ = 193.7, 143.3, 117.8, 116.7, 116.2, 38.4, 23.8, 22.4, 11.6 ppm. Known compound, CAS 6577-95-3.

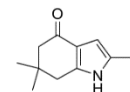
S11

3,4-Dihydroacridin-1-one (2i)



With 1,3-cyclohexadione (**3**; 56.1 mg, 500 μmol , 1.0 eq.) and 2-aminobenzyl alcohol (73.9 mg, 600 μmol , 1.2 eq.) in toluene. Purification by column chromatography (hexane/ethyl acetate = 4:1 \rightarrow 2:1) gave 63.0 mg **2i** (64%) as yellow solid. R_f 0.35 (hexane/ethyl acetate = 1:1). ^1H NMR (400 MHz, CDCl_3): δ = 8.85 (s, 1H, Ar-H), 8.07-8.02 (m, 1H, Ar-H), 7.93 (dd, J = 7.2, 5.8 Hz, 1H, Ar-H), 7.81 (ddd, J = 8.5, 6.9, 1.5 Hz, 1H, Ar-H), 7.55 (ddd, J = 8.1, 6.8, 1.2 Hz, 1H, Ar-H), 3.32 (t, J = 6.2 Hz, 2H, CH_2), 2.83-2.78 (m, 2H, CH_2), 2.32-2.24 (m, 2H, CH_2) ppm. ^{13}C NMR (101 MHz, CDCl_3): δ = 198.0, 162.1, 149.8, 137.2, 132.4, 129.8, 128.7, 126.9, 126.8, 126.4, 39.2, 33.6, 21.9 ppm. Known compound, CAS 58509-58-3.

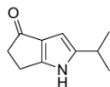
2-Isopropyl-6,6-dimethyl-1,5,6,7-tetrahydroindol-4-one (2j)



With dimedone (70.1 mg, 500 μmol , 1.0 eq.) and L-valinol (67 μL , 600 μmol , 1.2 eq.) in dioxane. Purification by column chromatography (hexane/ethyl acetate = 2:1) gave 86.1 mg **2j** (84%) as colorless solid. R_f 0.37 (hexane/ethyl acetate = 2:1). ^1H NMR (400 MHz, CDCl_3): δ = 8.75 (bs, 1H, NH), 6.19 (dd, J = 2.5, 1.0 Hz, 1H, Ar-H), 2.87 (heptd, J = 6.8, 1.0 Hz, 1H, $\text{CH}(\text{CH}_3)_2$), 2.64 (s, 2H, CH_2), 2.33 (s, 2H, CH_2), 1.24 (d, J = 6.8 Hz, 6H, $\text{CH}(\text{CH}_3)_2$), 1.11 (s, 6H, $\text{C}(\text{CH}_3)_2$) ppm. ^{13}C NMR (101 MHz, CDCl_3): δ = 194.1, 142.2, 140.5, 119.1, 99.9, 52.1, 37.0, 36.0, 28.8, 27.1, 22.4 ppm. HRMS (EI): calcd for $\text{C}_{13}\text{H}_{19}\text{NO}^+$: 205.1461, found 205.1458.

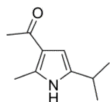
S12

2-Isopropyl-5,6-dihydro-1H-cyclopenta[b]pyrrol-4-one (**2k**)



With 1,3-cyclopentadione (49.1 mg, 500 μmol , 1.0 eq.) and L-valinol (67 μL , 600 μmol , 1.2 eq.) in toluene. Purification by column chromatography (hexane/ethyl acetate = 1:2) gave 41.3 mg **2k** (51%) as colorless solid. R_f 0.35 (hexane/ethyl acetate = 1:4). ^1H NMR (400 MHz, CDCl_3): δ = 9.30 (bs, 1H, NH), 5.96 (dd, J = 2.0, 1.0 Hz, 1H, Ar-H), 2.98-2.85 (m, 5H, CH_2 and $\text{CH}(\text{CH}_3)_2$), 1.27 (d, J = 6.9 Hz, 6H, CH_3) ppm. ^{13}C NMR (101 MHz, CDCl_3): δ = 197.4, 159.4, 147.9, 126.8, 97.1, 41.4, 27.7, 22.5, 21.3 ppm. HRMS (EI): calcd for $\text{C}_{10}\text{H}_{13}\text{NO}^+$: 163.0992, found 163.0987.

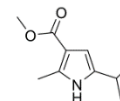
3-Acetyl-5-isopropyl-2-methylpyrrole (**2l**)



With acetylacetone (51 μL , 500 μmol , 1.0 eq.) and L-valinol (67 μL , 600 μmol , 1.2 eq.) in toluene. Purification by column chromatography (hexane/ethyl acetate = 4:1) gave 63.6 mg **2l** (77%) as colorless solid. R_f 0.31 (hexane/ethyl acetate = 2:1). ^1H NMR (400 MHz, CDCl_3): δ = 8.59 (bs, 1H, NH), 6.18 (dd, J = 2.9, 0.9 Hz, 1H, Ar-H), 2.85 (heptd, J = 6.9, 0.9 Hz, 1H, $\text{CH}(\text{CH}_3)_2$), 2.52 (s, 3H, COCH_3), 2.39 (s, 3H, CH_3), 1.25 (d, J = 6.9 Hz, 6H, $\text{CH}(\text{CH}_3)_2$) ppm. ^{13}C NMR (101 MHz, CDCl_3): δ = 195.4, 137.0, 134.1, 120.6, 105.0, 28.5, 26.9, 22.5, 14.1 ppm. Known compound, CAS 1419101-64-6.

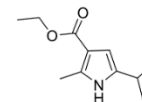
S13

Methyl 5-isopropyl-2-methyl-1H-pyrrole-3-carboxylate (**2m**)



With methyl acetoacetate (54 μL , 500 μmol , 1.0 eq.) and L-valinol (67 μL , 600 μmol , 1.2 eq.) in toluene. Purification by column chromatography (hexane/ethyl acetate = 5:1) gave 44.6 mg **2m** (49%) as yellowish viscous oil. R_f 0.62 (hexane/ethyl acetate = 2:1). ^1H NMR (400 MHz, CDCl_3): δ = 8.01 (bs, 1H, NH), 6.22 (dd, J = 3.0, 1.0 Hz, 1H, Ar-H), 3.78 (s, 3H, OCH_3), 2.83 (heptd, J = 6.9, 1.0 Hz, 1H, $\text{CH}(\text{CH}_3)_2$), 2.50 (s, 3H, CH_3), 1.23 (d, J = 6.9 Hz, 6H, $\text{CH}(\text{CH}_3)_2$) ppm. ^{13}C NMR (101 MHz, CDCl_3): δ = 166.3, 137.1, 134.3, 111.1, 104.7, 50.8, 26.9, 22.5, 13.3 ppm. HRMS (EI): calcd for $\text{C}_{10}\text{H}_{15}\text{NO}_2^+$: 181.1097, found 181.1097.

Ethyl 5-isopropyl-2-methyl-1H-pyrrole-3-carboxylate (**2n**)



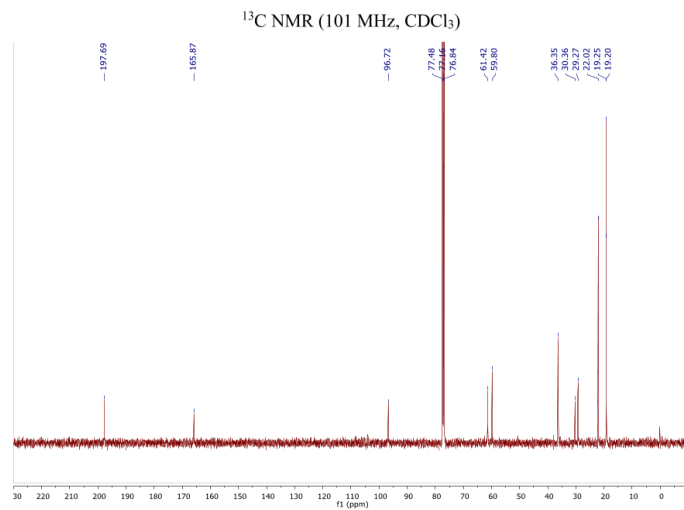
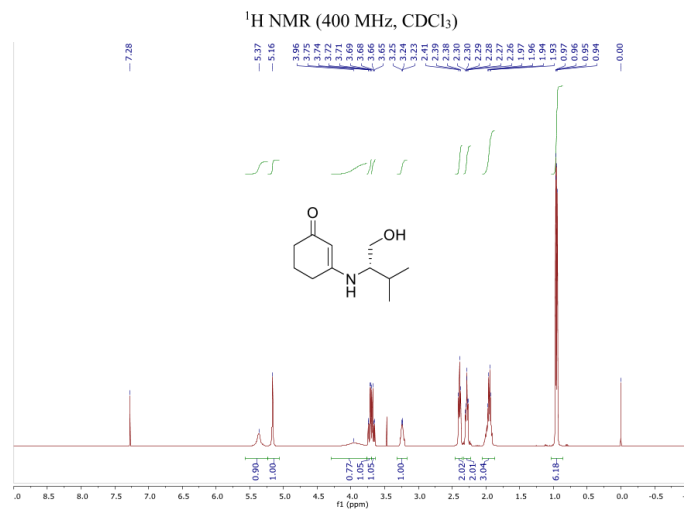
With ethyl acetoacetate (63 μL , 500 μmol , 1.0 eq.) and L-valinol (67 μL , 600 μmol , 1.2 eq.) in toluene. Purification by column chromatography (hexane/ethyl acetate = 5:1) gave 57.2 mg **2n** (59%) as yellowish solid. R_f 0.38 (hexane/ethyl acetate = 4:1). ^1H NMR (400 MHz, CDCl_3): δ = 8.04 (bs, 1H, NH), 6.23 (dd, J = 3.0, 1.0 Hz, 1H, Ar-H), 4.25 (q, J = 7.1 Hz, 2H, OCH_2CH_3), 2.83 (heptd, J = 6.9, 1.0 Hz, 1H, $\text{CH}(\text{CH}_3)_2$), 2.49 (s, 3H, CH_3), 1.33 (t, J = 7.1 Hz, 3H, OCH_2CH_3), 1.23 (d, J = 6.9 Hz, 6H, $\text{CH}(\text{CH}_3)_2$) ppm. ^{13}C NMR (101 MHz, CDCl_3): 166.0, 137.0, 134.2, 111.4, 104.7, 59.4, 26.9, 22.6, 14.7, 13.4 ppm. Known compound, CAS not existing, Reaxys ID 7634161.

S14

5 NMR spectra

Starting from the upcoming page

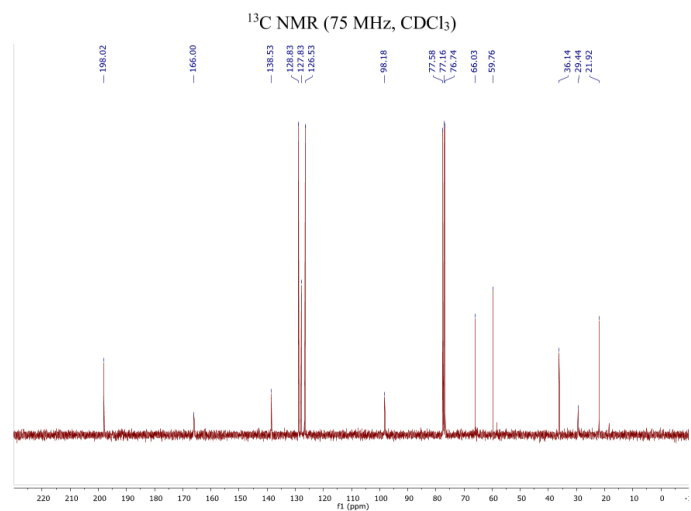
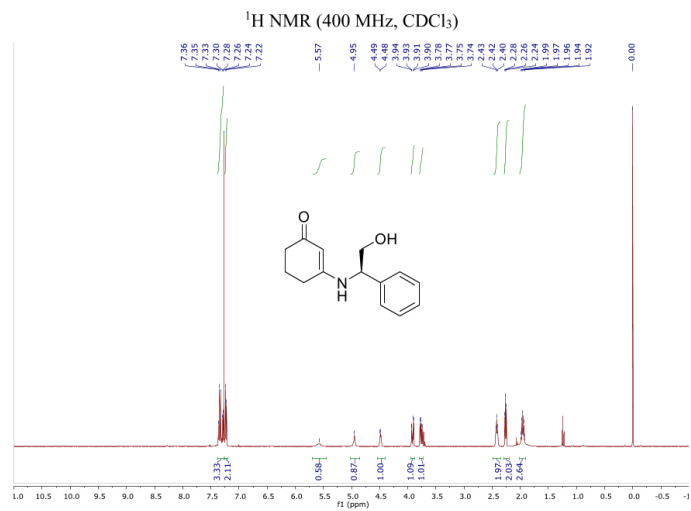
(S)-3-((1-hydroxy-3-methylbutan-2-yl)amino)cyclohex-2-en-1-one (1a)



S15

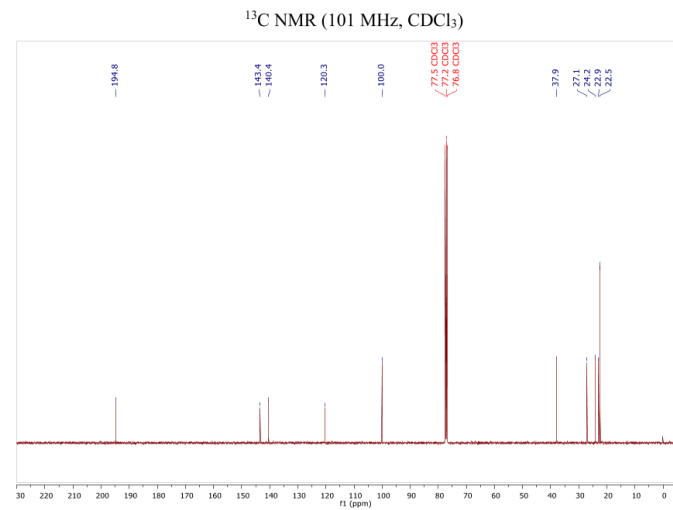
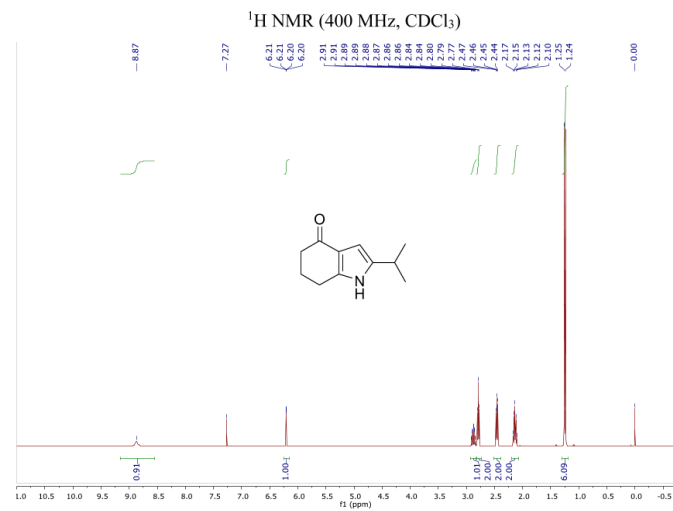
S16

(R)-3-((2-hydroxy-1-phenylethyl)amino)cyclohex-2-en-1-one (1b)



S17

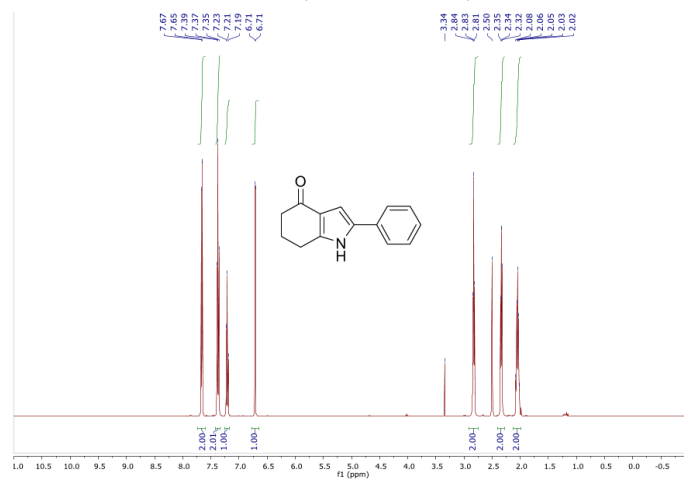
2-Isopropyl-1,5,6,7-tetrahydroindol-4-one (2a)



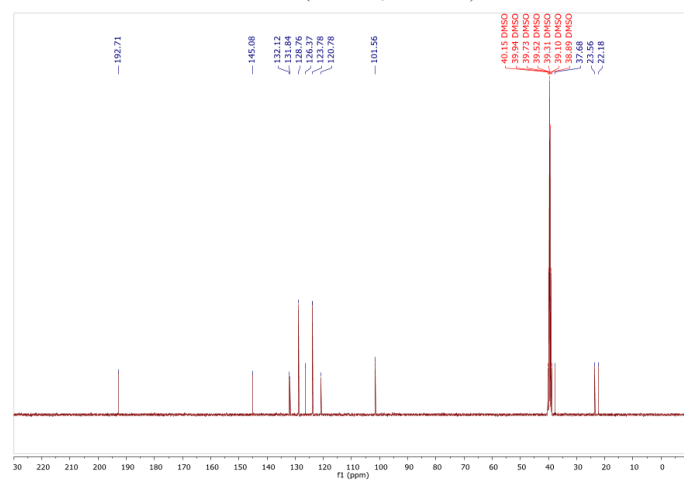
S18

2-Phenyl-1,5,6,7-tetrahydroindol-4-one (2b)

¹H NMR (400 MHz, D₆-DMSO)



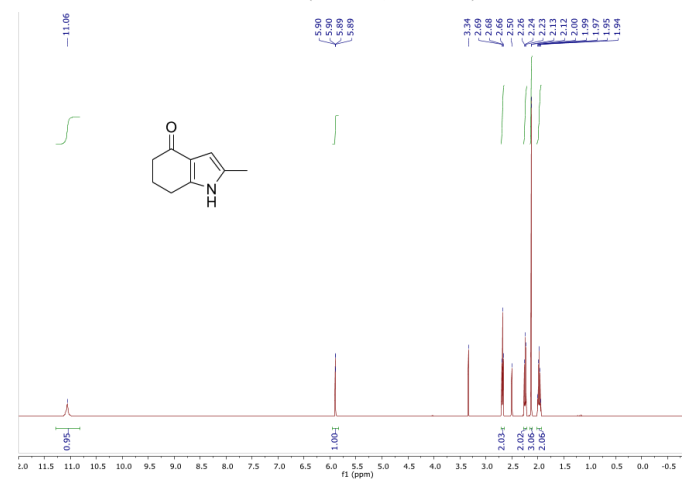
¹³C NMR (101 MHz, D₆-DMSO)



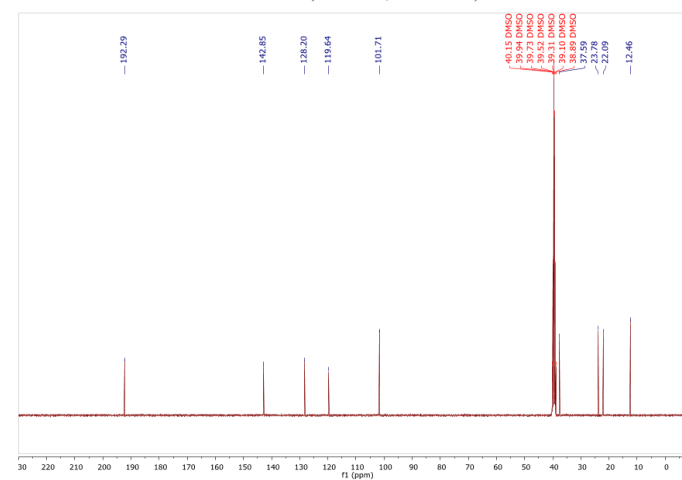
S19

2-Methyl-1,5,6,7-tetrahydroindol-4-one (2d)

¹H NMR (400 MHz, D₆-DMSO)

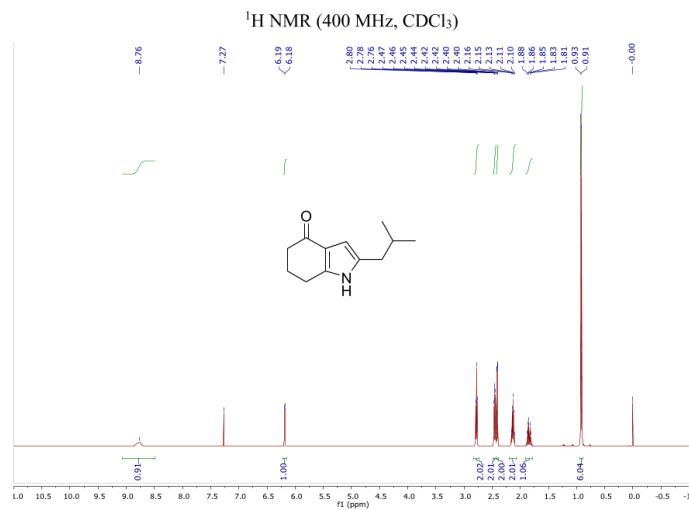


¹³C NMR (101 MHz, D₆-DMSO)

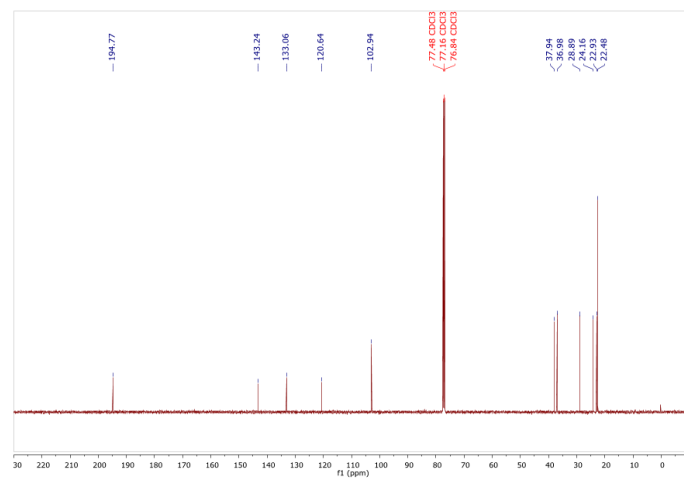


S20

2-Isobutyl-1,5,6,7-tetrahydroindol-4-one (2e)

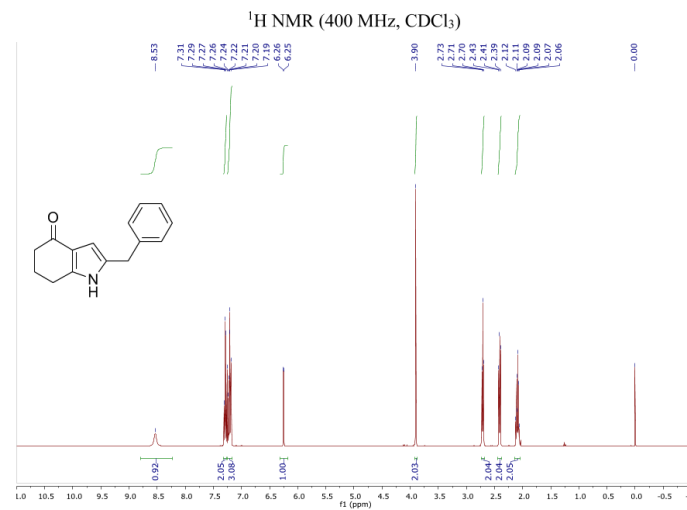


¹³C NMR (101 MHz, CDCl₃)

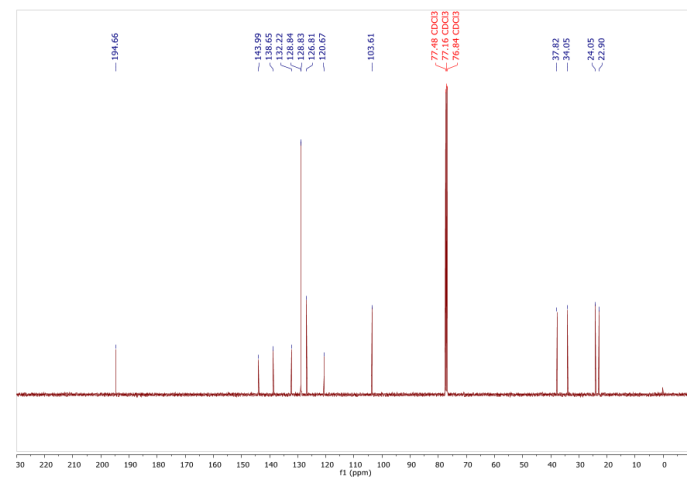


S21

2-Benzyl-1,5,6,7-tetrahydroindol-4-one (2f)

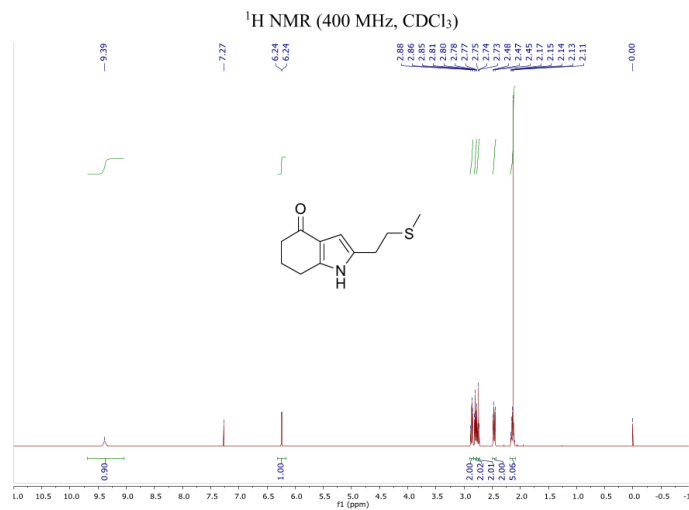


¹³C NMR (101 MHz, CDCl₃)

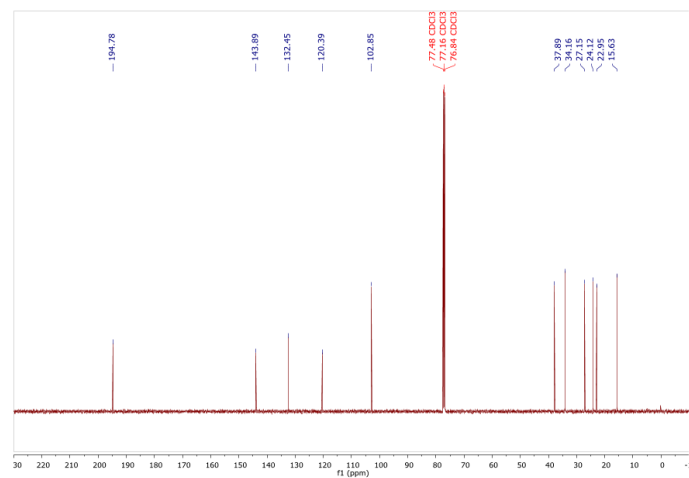


S22

2-(2-(Methylthio)ethyl)-1,5,6,7-tetrahydroindol-4-one (2g)

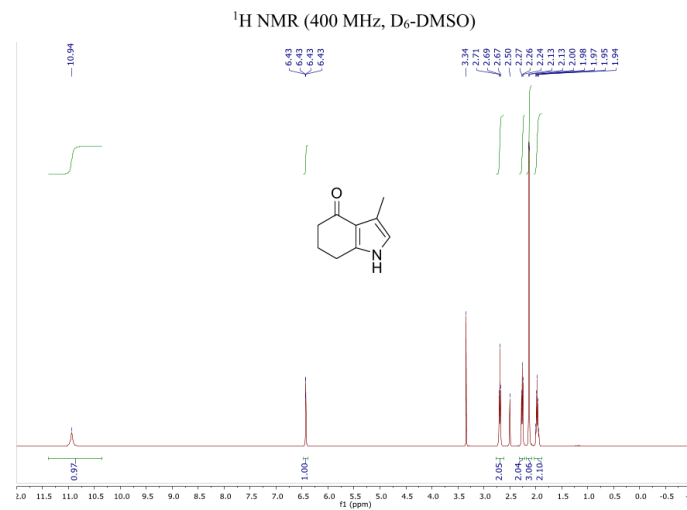


¹³C NMR (101 MHz, CDCl₃)

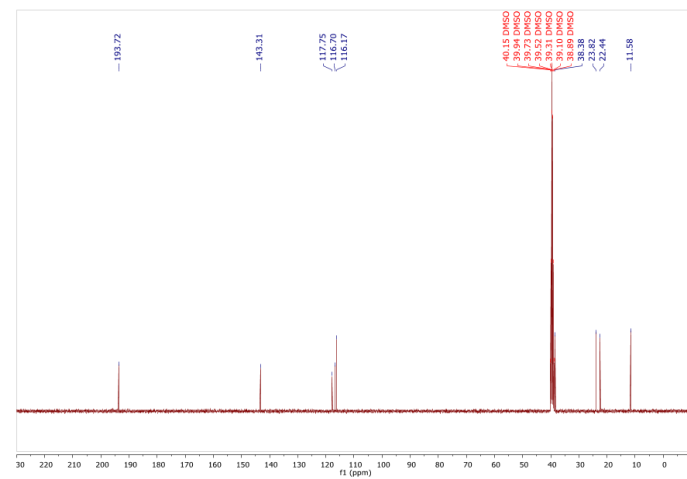


S23

3-Methyl-1,5,6,7-tetrahydroindol-4-one (2h)



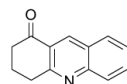
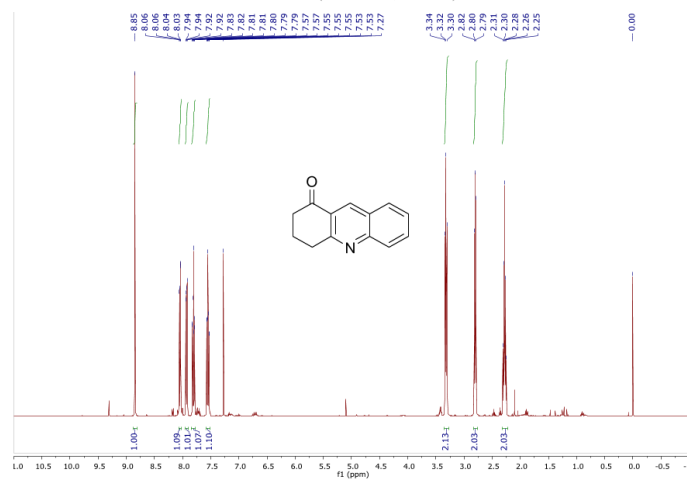
¹³C NMR (101 MHz, D₆-DMSO)



S24

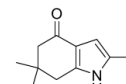
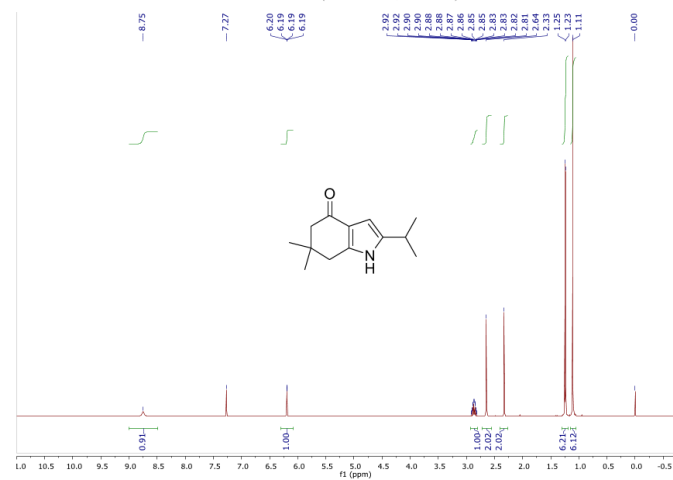
3,4-Dihydroacridin-1-one (2i)

¹H NMR (400 MHz, CDCl₃)

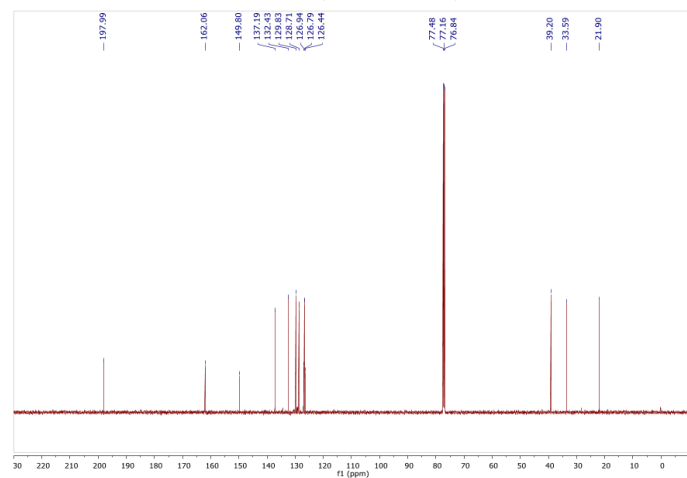


2-Isopropyl-6,6-dimethyl-1,5,6,7-tetrahydroindol-4-one (2j)

¹H NMR (400 MHz, CDCl₃)

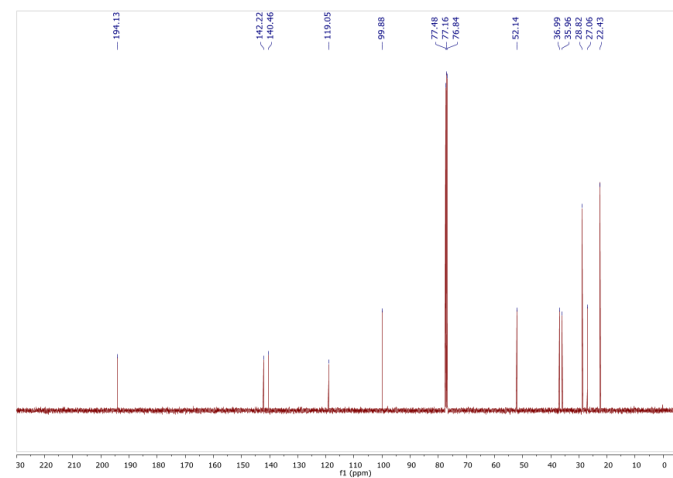


¹³C NMR (101 MHz, CDCl₃)

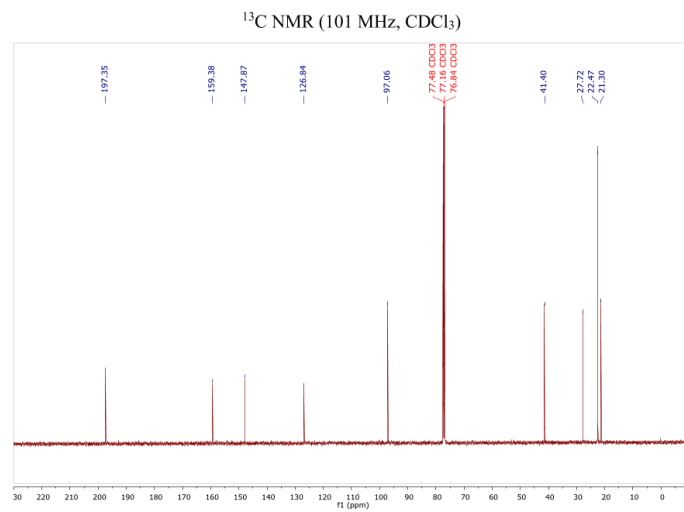
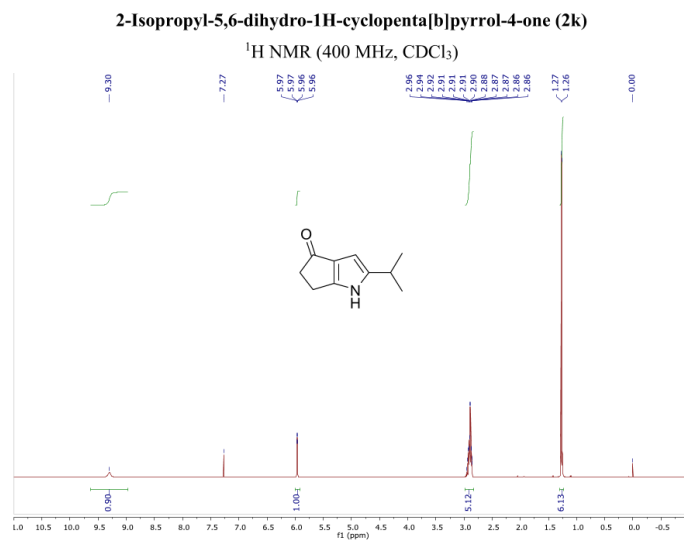


S25

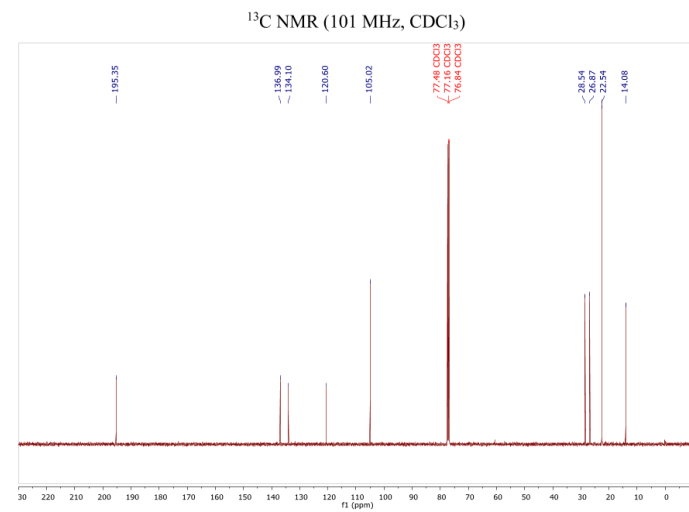
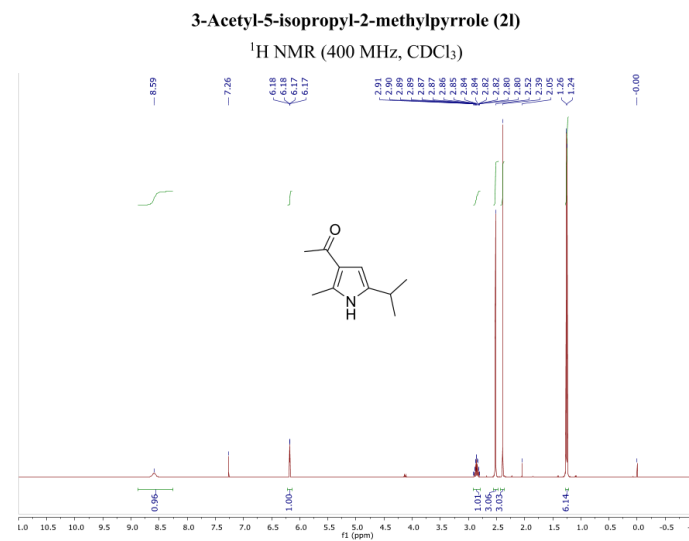
¹³C NMR (101 MHz, CDCl₃)



S26

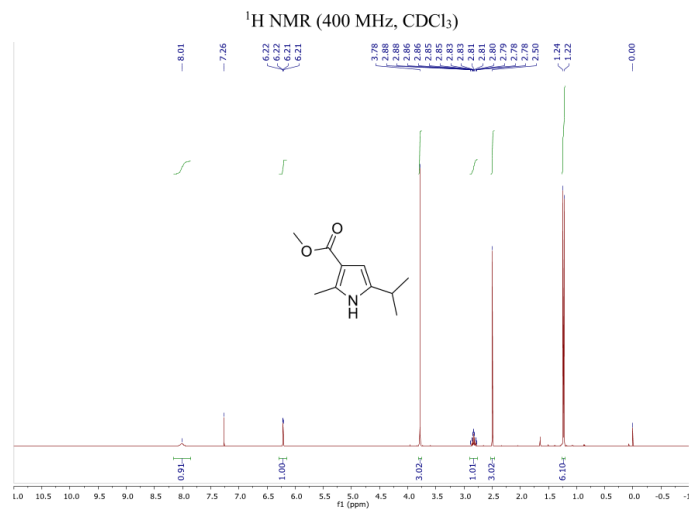


S27

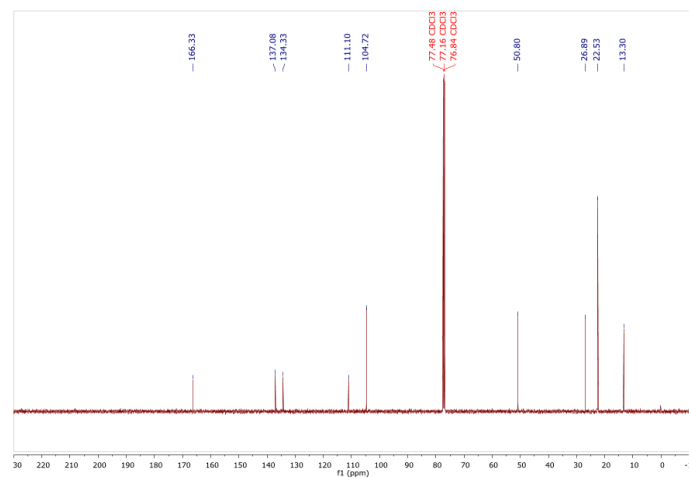


S28

Methyl 5-isopropyl-2-methyl-1*H*-pyrrole-3-carboxylate (2m)

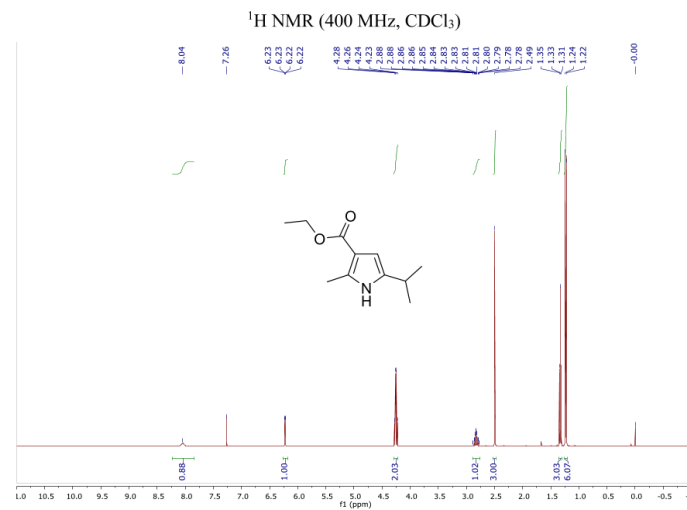


¹³C NMR (101 MHz, CDCl₃)

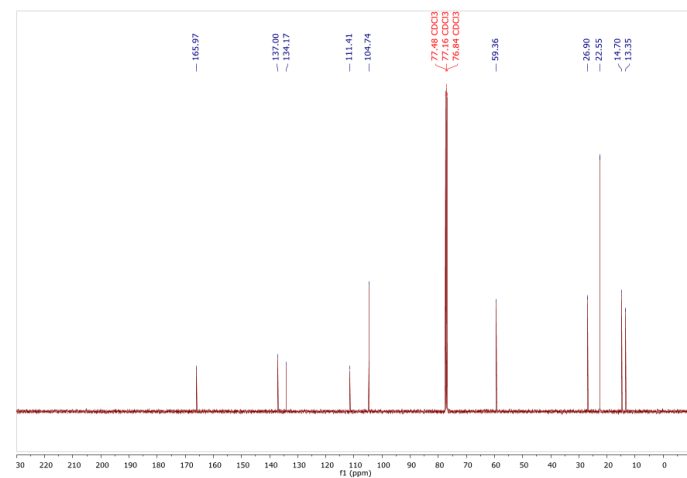


S29

Ethyl 5-isopropyl-2-methyl-1*H*-pyrrole-3-carboxylate (2n)



¹³C NMR (101 MHz, CDCl₃)



S30

6 References

- ¹ Michlik, S.; Kempe, R. *Nat. Chem.* **2013**, *5*, 140–144.
- ² Jia, X.; Zhang, L.; Qin, C.; Leng, X.; Huang, Z. *Chem. Commun.* **2014**, *50*, 11056–11059.
- ³ Balaraman, E.; Gnanaprakasam, B.; Shimon, L. J. W.; Milstein, D. *J. Am. Chem. Soc.* **2010**, *132*, 16756–16758.
- ⁴ Ahmad, N.; Levison, J. J.; Robinson, S. D.; Uttley, M. F. *Inorg. Synth.* **1974**, *15*, 45–64.
- ⁵ Dam, J. H.; Osztrovsky, G.; Nordström, L. U.; Madsen, R. *Chem. Eur. J.* **2010**, *16*, 6820–6827.
- ⁶ Aoyagi, Y.; Mizusaki, T.; Shishikura, M.; Komine, T.; Yoshinaga, T.; Inaba, H.; Ohta, A.; Takeya, K. *Tetrahedron* **2006**, *62*, 8533–8538.
- ⁷ Williams, D. B. G.; Lawton, M. *J. Org. Chem.* **2010**, *75*, 8351–8354.
- ⁸ a) Schoenberger, T. *Anal. Bioanal. Chem.* **2012**, *403*, 247–254. b) Mahajan, S.; Singh, I. P. *Magn. Reson. Chem.* **2013**, *51*, 76–81.